Lewis acid catalyst design for the transesterification of lower quality feedstock for biodiesel production

Chuck, Chris

Award date:
2007

Awarding institution:
University of Bath

LEWIS ACID CATALYST DESIGN FOR THE TRANSESTERIFICATION OF LOWER QUALITY FEEDSTOCK FOR BIODIESEL PRODUCTION

CHRISTOPHER JAMES CHUCK

A thesis submitted for the degree of Doctor of Philosophy

University of Bath

Department of Chemistry

November 2007

For Lucy

ACKNOWLEDGEMENTS

I would like to thank my supervisor Professor Matthew Davidson for his guidance and support over the three years of my PhD and for also providing many further opportunities for me beyond the laboratory.

I would also like to extend my appreciation to Johnson Matthey Catalysts for their financial support along with the Crystal Faraday Partnership. I would particularly like to thank Drs. Matthew Lunn and Bart Zwijnenburg for all their help during the project. I am also very grateful to Drs. John Lowe, Anneke Lubben and Mark Russell for all their technical support throughout the PhD. Thanks to Professor Paul Raithby, Dr. Gabriele Kociok-Kohn, Dr. Mary Mahon and Teresa Savarese for their help with X-ray structure determination.

I'm particularly grateful to Dr. Matthew Jones for all his help, constant support and sage advice throughout the entire course of this work. Likewise I would like to thank Amanda Chmura and all the other members of the Davidson group, past and present, for making my time in Bath so pleasant. Particularly Cheryl Doherty, Gillian Eade, Cathy Frankis, Carly Gilfillan, Emanuel Gullo, Andy Johnson, Charlie O'Hara, Luisa Paches Samblas, Steve Richards, Graeme Spence and Steve Wu.

I would also like to thank some great friends outside of the Department who were always there to cheer me up when it mattered most; especially Jack Dudman, Jennifer East, Christopher Heppell, Oliver Heppell, Alice Malhador and Dan Whillis among many others.

A special thanks to my close family, but especially my Mum and Dad, who have always been really supportive and encouraging in everything I have done.

But my biggest thanks goes to Lucy, without her kindness and encouragement, as well as her unerring faith, I simply wouldn't have been able to do this.

ABSTRACT

This thesis describes a range of potential Lewis acid transesterification catalysts that have been synthesised and characterised, containing a variety of benign metal centres and ligand scaffolds. Transesterification reactions, using soybean oil and model waste oils, have been initiated in order to investigate the utility of these catalysts for biodiesel production.

In the introductory chapter context is leant to this study by briefly reviewing the relevant factors involved in biodiesel production, the inherent problems with the industrial production of biodiesel from vegetable and waste oils and concludes with an extensive literature review of current research into novel catalyst design.

In Chapter 2 the synthesis and characterisation of a number of titanium diolate complexes is presented. The activity of the catalysts was compared to the original titanium alkoxide and the most promising catalyst system was then screened in the production of model waste oils. None of the titanium diolate complexes are stable to hydrolysis when water is present in the oil feedstock.

In the next chapter the synthesis and characterisation of a range of homo- and heterometallic titanium citrate complexes is presented. Unlike the titanium diolate species these complexes are stable to hydrolysis, yet none of the citrate catalysts were active in the conversion of soybean oil to FAME.

Chapter 4 details the synthesis of a range of titanium α-amino acid complexes. None of the titanium complexes screened were resistant to methanolysis. However, a synthetic modification of the amino acids was accomplished and the germanium and titanium analogues synthesised. These complexes were found to be active in the conversion of soybean oil. A range of zinc amino acid complexes were also synthesised, and screened for their activity on a laboratory scale, a scaled up process and for the conversion of model waste oils. The promising activity of zinc carboxylates as catalysts in the conversion of vegetable oils was further investigated in Chapter 5.

LIST OF ABBREVIATIONS

Ala	Alanine
Arg	Arginine
Cit	Citric acid
CMON	Covalent Metal Organic Network
Cro	Crotonic Acid
DG	Diglyceride
DMCA	1,4 Dimethyl Citric Acid
ESI-MS	Electron Spray Ionisation Mass Spectrometry
ETS-10	Titanium aluminium silicate based zeolite
FAAE	Fatty Acid Alkyl Ester
FAME	Fatty Acid Methyl Ester
FFA	Free Fatty Acid
FP	Flash Point
FT-IR	Fourier Transform Infra-Red spectroscopy
Gly	Glycine
HC	Hydrocarbon (pollutant)
HEMA	2-Hydroxyethyl Methacrylate
His	Histidine
HPLC	High Performance Liquid Chromatography
IPA	Isopropyl alcohol
MG	Monoglyceride
NMR	Nuclear Magnetic Resonance
PAH	Poly Aromatic Hydrocarbon
Phe	Phenylalanine
Pro	Proline
RSO	Rapeseed Oil
Ser	Serine
TG	Triglyceride
TPA	12 –Tungstophosphoric Acid based catalyst
Tryp	Tryptophan

TABLE OF CONTENTS

Chapter 1: Introduction

1.1 Opening Remarks **1**

1.2 History **1**

1.3 Unmodified Vegetable Oil as a Diesel Fuel Substitute **3**

1.4 Synthesis of Biodiesel by Transesterification **5**

1.5 Present Industrial Practice **9**

1.6 Conversion of Lower Quality Feedstock **11**

1.7 Physical Properties of Biodiesel **15**

1.8 Research in Novel Homogeneous Catalyst Design **17**

1.8.1 Homogeneous Tin Catalysts **17**

1.8.2 Divalent Metal Carboxylates **21**

1.8.3 Titanium Alkoxides **21**

1.8.4 Lewis Bases **22**

1.9 Research into Novel Heterogeneous Catalyst Design **25**

1.9.1 Zeolites **26**

1.9.2 Supported Alkali Metal Catalysts **28**

1.9.3 Oxide, Methoxides and Hydroxides of Group II Metals **30**

1.9.4 Hydrotalcite Catalysts **31**

1.9.5 Nafion Exchange Resin **31**

1.9.6 Functionalised Amorphous Carbon **34**

1.9.7 Zirconia / Alumina Supported Catalysts **35**

1.9.8 Group IV Oxides **38**

1.9.9 Heterogeneous Zinc Catalysts **38**

1.9.10 The Reactor Material **39**

1.10 Enzymatic Catalysis **40**

1.11 Analytical Techniques **45**

1.12 Closing Remarks **50**

1.13 References **51**

Chapter 2: Methanol Stable Titanium Diolate Complexes

2.1 Introduction **62**
2.2 Results and Discussion **70**
2.2.1 Synthesis and Characterisation of Catalysts **1-3** **70**
2.2.2 Catalytic Activity of **1-3** in the Conversion of Soybean Oil **76**
2.2.3 Optimisation of 1,3-Propanediol as a Stabilising Ligand **78**
2.2.4 Catalytic Activity in the Conversion of Model Waste Oils **80**
2.3 Summary **83**
2.4 References **84**

Chapter 3: Citric Acid Derived Ligands and Complexes

3.1 Introduction **88**
3.2 Results and Discussion **94**
3.2.1 Homometallic Titanium Citrate Synthesis and Characterisation **94**
3.2.2 Heterometallic Titanium Citrate Synthesis and Characterisation **97**
3.2.3 Homometallic Citrates of Divalent Metal Ions **106**
3.2.4 Catalytic Activity in the Conversion of Soybean Oil **109**
3.3 Summary **112**
3.4 References **113**

Chapter 4: Metal Complexes Based on α-Amino Acids

4.1 Introduction **117**

4.2 Results and Discussion **125**

4.2.1 Synthesis of α-Amino Acid Titanium Complexes **125**

4.2.2 Catalytic Activity of **14**-**17** in the Conversion of Soybean Oil **129**

4.2.3 Synthesis of Amino Acid 2,4-Dimethyl Phenolates **130**

4.2.4 Catalytic Activity of **18**-**22** in the Conversion of Soybean Oil **137**

4.2.5 Synthesis of Zinc Amino Acid Complexes **138**

4.2.6 Catalytic Activity of **23**-**29** in the Conversion of Soybean Oil **144**

4.2.7 Catalytic Activity of Various Zinc Based Systems on a Pilot Industrial Scale **146**

4.2.8 Catalytic Activity in the Conversion of Model Waste Oils **148**

4.3 Summary **152**

4.4 References **153**

Chapter 5: Homogeneous Zinc Carboxylate Catalysts

5.1 Introduction **159**

5.2 Results and Discussion **164**

5.2.1 Catalytic Conversion of Soybean Oil **164**

5.2.2 Catalytic Conversion on a Pilot Industrial Scale **171**

5.2.3 Catalytic Conversion of Model Waste Oil **175**

5.2.4 Proposed Model for Vegetable Oil Transesterification Using Zinc Crotonate **177**

5.3 Summary **180**

5.4 References **181**

Chapter 6: Conclusions and Further Research

6.1 Conclusions **183**
6.2 Further Research **184**

Chapter 7: Experimental Data

7.1 General Experimental Techniques **186**
7.2 Experimental Procedures for Chapter 2 **191**
7.3 Experimental Procedures for Chapter 3 **194**
7.4 Experimental Procedures for Chapter 4 **201**
7.5 Experimental Procedures for Chapter 5 **211**
7.6 References **214**

Appendix I: Tabulated Catalysis Results **215**

Appendix CD: Further X-Ray Crystallographic Data **CD**

CHAPTER 1

INTRODUCTION

1.1 OPENING REMARKS

In this thesis, a number of Lewis acidic, environmentally benign metal catalyst systems have been synthesised. These catalysts have then been investigated for their activity in the production of biodiesel from virgin soybean oil and eventually model waste oils. In this chapter an overview of the synthesis of biodiesel from vegetable and waste oil feedstocks is presented and will predominantly be focussed on the industrial and recent developments in catalysis technology. A more detailed exploration into the structural and coordination chemistry, relevant to the catalysts presented, is given at the start of every chapter.

1.2 HISTORY

Rudolf Diesel (1858-1913) invented the diesel engine at the end of the 19th century. He sought to improve the thermodynamic efficiency of combustion over that of a steam engine. It is often asserted that Rudolf Diesel designed his engine with vegetable oil in mind, but this does not seem to have been the case. Although he developed an interest in the practical development of vegetable oil as a fuel later on, his early designs had little to do with naturally derived oils.

The diesel engine was one of many technologically advanced exhibits showcased at the 1900 Paris World Fair. There were five diesel engines in total running at the exhibition, one of which ran on peanut oil for the whole event with no noticeable negative affects. Diesel noted afterwards '*at the Paris Exhibition in 1900 there was shown by the Otto Company a small Diesel engine, which, at the request of the French government, ran on Arachide oil, and worked so smoothly that only a few people were aware of it.*' This seemed to inspire the French government into conducting research

into the use of vegetable oils as a fuel, with Diesel himself even running tests for them later on in his life.

Up until the 1940s many papers were published, originating from England, France, Spain, Portugal and Germany noting the suitability of vegetable oils for fuel. It was thought that oil production might become the main source of energy in colonies where oil producing crops were grown; this could potentially give those colonies a massive economic advantage over colonies which had to import almost all their energy.

World War II increased the interest of vegetable oils as fuels, with many countries banning the export of vegetable oils and using the oil as a substitute for diesel. China started producing kerosene type fuels by catalytically cracking tung and other vegetable oils, and a Japanese battleship was reported to use refined soybean oil as a bunker fuel. In the United States 'duel-fuel' projects were set up to investigate whether blends of vegetable oil and diesel fuels could replace petroleum in the event of fuel shortages. It was energy security issues, not pollution issues, which were driving these and other projects around the world. After World War II, crude oil markets stabilised and a cheap and reliable source of petroleum and diesel was available. Very little research was invested in biofuel at this point and it was only after the 1970s oil crisis that research started again in this area.

Historically research focussed on using the oil itself as a fuel, and not the fatty acid alkyl esters (FAAE) which are now referred to as biodiesel. The first recognized literature on the production of FAAEs from vegetable oils for use as a fuel was a patent applied for by G. Chavanne in 1937. It described the production of ethyl esters of palm oils as a diesel fuel, using an acid catalyst. A bus route in Belgium was supplied with this new fuel, running through the summer of 1938, making it the first biodiesel run bus in history. A report written afterwards on this research commented on the vast improvements in cetane number, viscosity and other important factors that the fatty acid esters had over straight vegetable oils. It was around 1980 when the transesterification of vegetable oils was re-examined and the production of what is now termed biodiesel was first reported. [1]

The consumption of petroleum based fuels was roughly 4,200,000,000 tonnes y^{-1} worldwide by the end of 2006, of which less than 1,000,000,000 tonnes was diesel fuel. [2] Roughly 7,500,000 tonnes of diesel fuel derived from crops were produced; the three main producers of biodiesel are currently the EU (6,070,000 tonnes y^{-1}), [3] the USA

(900,000 tonnes y^{-1}) and Brazil (200,000 tonnes y^{-1}). Almost all the biodiesel produced by the EU is derived from rapeseed oil, where the US produces most of their biodiesel from soybean oil. In Brazil the feedstock used for biodiesel is area specific, for example in the north, palm oils and soybean oils are used, in the south, rapeseed and sunflower oils tend to be the main feedstocks. [4] Waste oils make up a very small percentage of global biodiesel production.

Around 75% of all biodiesel is produced in the EU but this is likely to diminish with the emergence of large scale production facilities in Asia. It is estimated that Around 1,500,000 tonnes y^{-1} will be produced in Indonesia and Malaysia by 2008. China, who presently produces 200,000 tonnes y^{-1} mainly from waste oil, plans to increase production to 11,000,000 tonnes y^{-1} by 2010. European production is estimated to be rise to this level by 2010, despite tax exemptions on biodiesel being reviewed in all the major producing countries. [5]

With such a large increase in production predicted a large amount of research has been undertaken and consequently many reviews involving the production, use and economics relating to biodiesel are available. These reviews range from specific biodiesel studies, [4, 6, 7] energy studies, [8] technical reviews, [9, 10] reviews focusing on the catalytic chemistry, [11-13] on the life cycle analysis, [14-16] feedstock's, [17] on the economics and technical development of production [18, 19] and on the general conversion of biomass to industrial grade products. [20-23]

1.3 UNMODIFIED VEGETABLE OIL AS A DIESEL FUEL SUBSTITUTE

It is possible to use the pure vegetable oil or filtered waste oil starting material as opposed to biodiesel in a diesel engine, however, especially with the modern direct injection diesel engines, this has many drawbacks that make it impractical as a long term fuel. Unmodified engines can only run up to a few hundred hours on unblended oil without damaging the vehicle; this is mainly due to the high viscosity of vegetable oils. It is this increased viscosity that leads to the incomplete burning of the triglyceride molecule, resulting in carbonization and resin formation. The formation of these sediments on injectors, valves and pistons leads to component failure and engine damage. [24]

The viscosity of vegetable oils is around 10 times that of diesel fuel but it is possible to adapt the injector and hydraulic systems for the new fuel. However, this solution is expensive, reduces performance and causes problems with the lubrication of the engine. These problems can be alleviated by lowering the viscosity of the oil. This is achievable by heating the vegetable oil prior to injection in the engine, blending the oil, making an alcoholic emulsion, pyrolysis of the oil or the chemical alteration of the vegetable oil to FAAEs.

The heating of the oil prior to injection into the engine relies on the special adaptation of the vehicle. An extra fuel tank can be installed and filled with straight vegetable oil (SVO) or waste vegetable oil (WVO). The engine is then run on normal diesel fuel until the SVO is sufficiently heated (~ 70 °C) to lower the viscosity to useable levels. A manual switch placed on the dash board is the usual method for switching between fuel sources. It is also possible to mix SVO with diesel oil but even in low concentrations of vegetable oil this can cause similar problems to using the oil unblended. [25, 26] Creating micro-emulsions is another way of lowering the viscosity of the vegetable oil but these emulsions tend to be unstable at low temperatures. The creation of an emulsion does not prevent carbonization of the triglyceride molecule. [27]

Pyrolysis of vegetable oils is achieved at high temperatures (350 – 800 °C) and gives a mixture of aldehydes, alkanes, alkenes, carboxylic acids, ketones and aromatic compounds. [28] The precise ratio, size and chain length of these compounds depends on the temperature, method and source of the vegetable oil used. The thermal decomposition of the triglyceride molecules is very complex, with many side reactions including possible free radical, carbonium ion, cleavage and elimination reaction pathways. The pyrolysis process is catalytic, where traditional catalytic systems (based on iron) have been replaced by zeolite technology. [29] No alcohol is needed to form diesel grade fuels from this process, however the selectivity in producing usable liquid fuels is not as high as that in the transesterification reaction. In addition, the temperatures needed far exceed those used for the production of FAAEs.

The catalytic transesterification of vegetable oil to produce FAAEs is the most efficient method of producing a substitute for mineral diesel fuel, which can be used in the current unmodified diesel engines.

1.4 SYNTHESIS OF BIODIESEL BY TRANSESTERIFICATION

Generally the term biodiesel is used to refer to the FAAEs derived from vegetable or animal oil feedstocks. The triglyceride molecule is the main constituent of vegetable oils, and can be transesterified with an alcohol over a basic or acidic catalyst to give FAAEs (Fig. 1.1). Methanol is most commonly used to make biodiesel as it is the least expensive and most widely available alcohol. The chain length and level of saturation of the FAAEs produced depends solely on the feedstock used.

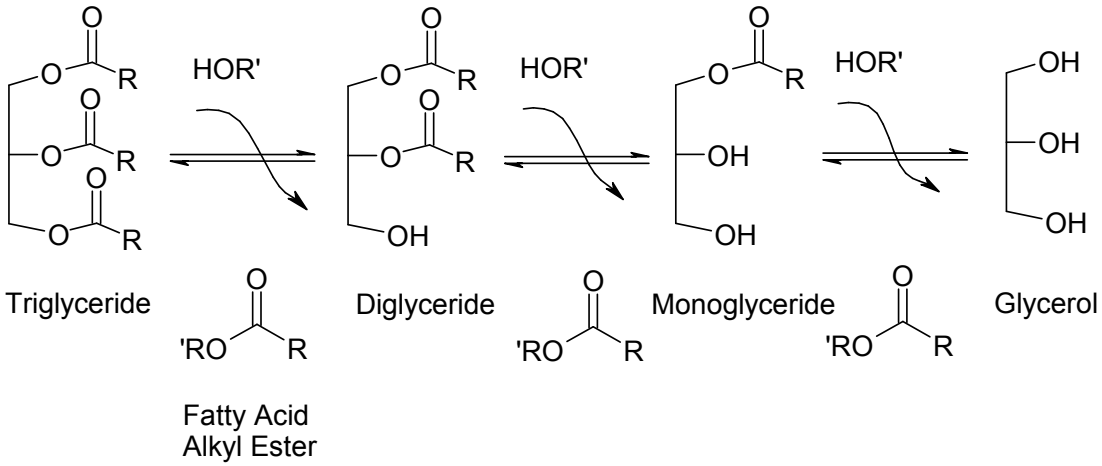

Figure 1.1 The equilibrium reaction that occurs in the transesterification of the triglyceride molecule for the production of fatty acid alkyl esters

The production of biodiesel involves a number of steps which are all in equilibrium. An excess of alcohol is used to drive the reaction to completion which is further aided by the alkyl esters separating out of the alcohol/ catalyst phase. Using this process around 99.7% conversion of vegetable oil to alkyl esters can be achieved with optimised conditions. [13, 30] The general transesterification reaction mechanism, involving a basic catalyst, is given below in Fig. 1.2.

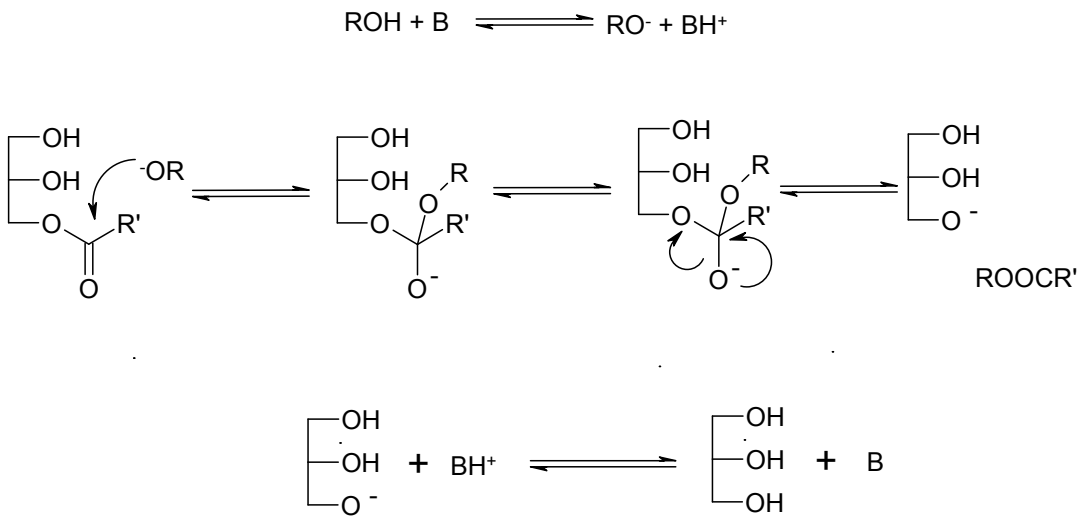

Figure 1.2 A proposed general mechanism for the base catalysed transesterification of a monoglyceride

The base deprotonates the alcohol to create an alkoxide species. The highly reactive alkoxide then goes onto react with the glyceride molecule, creating a four co-ordinate intermediate. This intermediate rapidly reacts further to form the anionic glyceride and the alkyl ester. The resulting di- and monoglycerides also react in this manner. The protonated base can then donate the proton to the partially transesterified glyceride or glycerol anion to form the glyceride or glycerol and the regenerated base.[31]

Alkali alkoxides have been identified as catalysts for cross esterification since the 1920s.[32] These alkali catalysts are almost always high yielding under mild conditions.[33,34] More recent research into alkoxides of the alkali metals suggests that the metal alkoxides aggregate into three different types of clusters depending on the size of the metal and alkoxide moiety; it is these clusters which then catalyse the reaction. [35,36] The size of the cation is very important, the reactivity increases in the order ($Li^+ < Na^+ < K^+ < Rb^+ < Cs^+$). In the ester interchange reaction of t-butoxide and methyl benzoate Stanton *et al.* demonstrated that the tetrameric clusters are the primary reactants.[35] The suggested mechanistic scheme is shown below in Fig. 1.3.

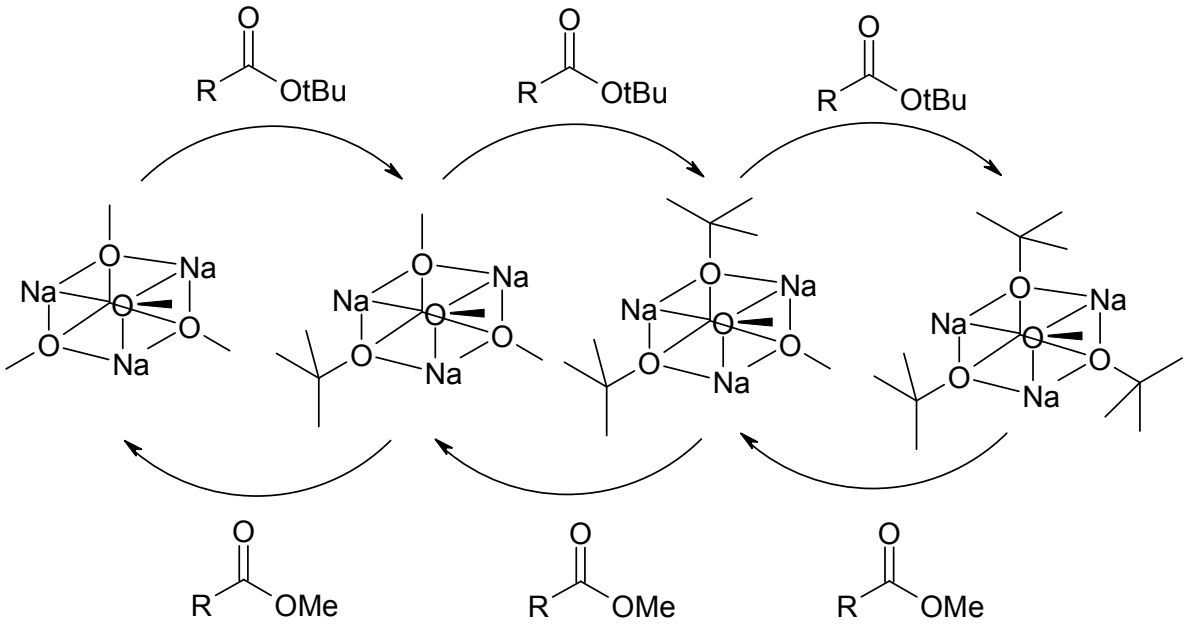

Figure 1.3 An alternative mechanism proposed for the reaction of NaOMe, with a t-butyl ester

The kinetics of the biodiesel transesterification are complicated and can vary depending on the catalyst, starting material and reaction conditions. Generally the base catalysed reaction follows three distinct sections, each defined by the production of one equivalent of fatty acid methyl esters (FAME) and a differing reaction rate. These are all reversible reactions and follow second order kinetics. [37] The first section, the reaction of the triglyceride, is slow and is related to the mass transfer. If the reaction agitation is maximised, however, the poor solubility of the triglyceride in methanol can be overcome and the rate maximised. The following two sections are kinetically controlled and can be described as pseudo-homogeneously catalyzed. The rate determining step is the production of the monoglyceride from the diglyceride. This can be manipulated by the addition of more catalyst, and the rate increases linearly with an increase in catalyst. [38]

Addition of another solvent will increase the solubility of the glycerides in methanol. It has been shown that tetrahydrofuran can significantly increase the rate of reaction due to this effect. [39] The kinetics and reaction mechanism of this base catalysed process have by no means definitively been characterized, and other mechanisms have been suggested in the literature. [6, 40]

One disadvantage of the base catalysed process is the inability to esterify free fatty acids (FFA) to FAAE. The amount of FFA in pure vegetable oils varies. In waste triglyceride oils such as cooking oils, 2-7 wt % FFA is normal, and in animal fats 5-30 wt % is found. Significant amounts of FFA can cause problems such as catalyst deactivation, soap formation, downstream gel formation and an increase in viscosity. A recommended concentration of FFA in the oil should be less than 0.5 wt %, otherwise, the FFA will react with base catalysts to form soap and water. [41] Transesterification of vegetable oil with a Brønsted acid catalyst has also been investigated. Fig. 1.4, shown below, demonstrates a possible mechanism for the transesterification. [42]

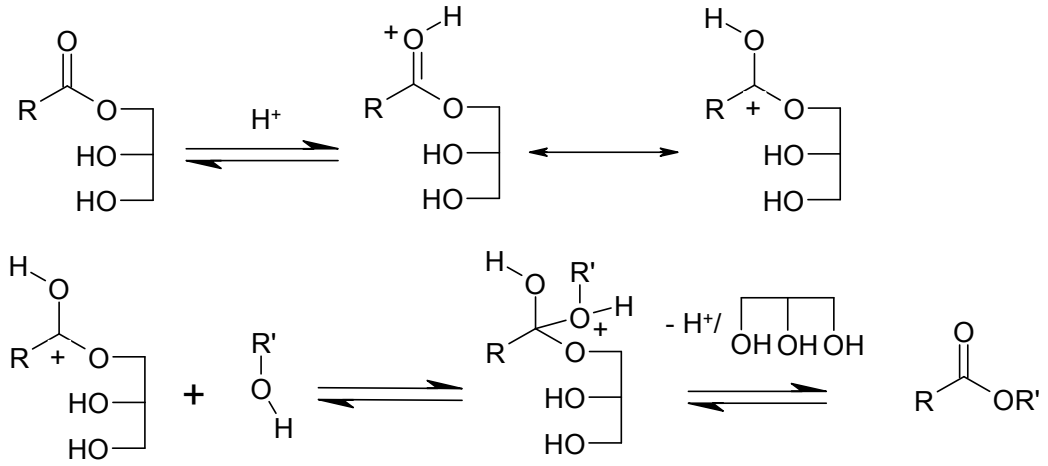

Figure 1.4 A proposed mechanism for the protonic catalysed transesterification of a monoglyceride

Methyl ester yields of 98 wt% can be achieved using 2% H_2SO_4 and an excess of alcohol over a reaction time of 24 hours. The reaction temperature used to affect this varies from 65 °C – 120 °C. [40, 43-45]

Acid catalysts have the advantage of producing purer products, especially when the FFA content is above 1%. Quicker reaction times can be achieved if transesterifying with a higher boiling point alcohol like butanol (bpt. 117 °C). [42] Nitric, acetic, formic and hydrochloric acids have all been examined for their activity, but were shown to be far less active than H_2SO_4 demonstrating that the catalytic ability of the acid is not dependent on its pKa. High water concentrations also deplete the reaction yield when using sulphuric acid, due to the competing reaction to produce FFA from the

triglycerides and the creation of a water phase which reduces the contact of the catalyst and reactants. [42]

1.5 PRESENT INDUSTRIAL PRACTICE

Biodiesel is currently processed industrially using either a homogeneous alkaline metal based catalyst, or a mineral acid as shown above. The alkaline catalysts used are alkali metal (usually Na, K) hydroxides, or methoxides. These catalysts are extremely alkaline and require stainless steel technology to avoid corrosion, but they are over 4000 times more active and are easier to handle than mineral acids. Mineral acids (such as sulphuric [13] or sulphonic acids [46]) are used in the biodiesel process, but generally only to esterify the FFA present in the oil before the transesterification step where the alkaline catalyst is used. Sodium methoxide is the most widely used catalyst in the world (over 60% of processes use it); although it costs more than the hydroxide it shows a higher activity and does not generate water on reaction with methanol. [1] An additional neutralisation step is needed when using these homogeneous systems to neutralise both the resulting biodiesel and glycerol streams. A flow diagram (Fig. 1.5) demonstrating the typical production of methyl ester using an alkaline catalyst.

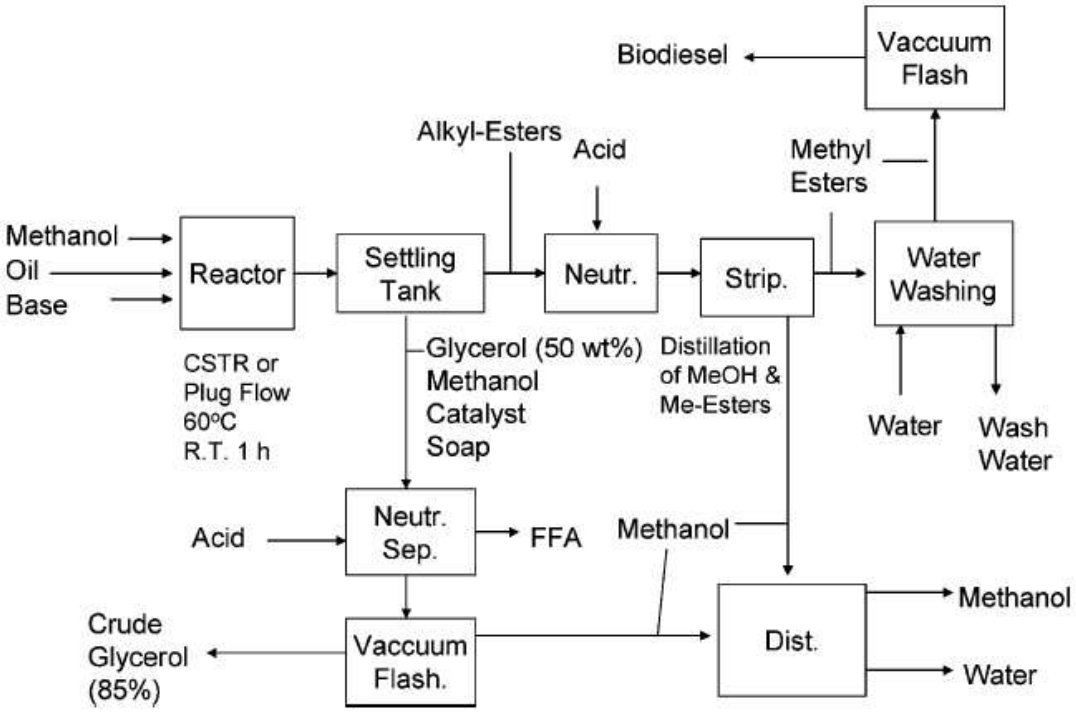

Figure 1.5 Flow diagram for biodiesel production using an alkaline catalyst originally published by Knothe and Van Gerpen [47-49]

The first step needed in the production of biodiesel is to recover the oil from the crop. Once the pure vegetable oil is obtained it is fed into a reactor with methanol and the basic catalyst. The reactors vary, but tend to be either a batch reactor or a continuous stirred-tank reactor. A plug flow type reactor is also appropriate for biodiesel production. The temperature is then set between 45 - 60 °C, approximately 1 atm of pressure and a methanol/oil molar ratio of between 6-12:1 is used. Reaction times vary between 45-120 min. The reaction can be carried out in one or a combination of these reactors.

After the reaction is complete the products from the reactor separate into two phases the glycerol phase (containing any water and most of the methanol which has not been esterified) and the alkyl ester phase (containing any remaining glycerides). A settling tank and/ or centrifuge are used to separate the two phases. Research is on going to develop a 'dry' removal technique of glycerol that selectively adsorbs the glycerol on to a silica surface. [1, 6, 20, 50-55]

The glycerol stream contains approximately 50 wt % glycerol, most of the remaining base catalyst, and a quantity of the soap. This fraction is then neutralized with acid (usually HCl) and the remaining soap forms FFAs which are mostly solids and can be separated from the liquid glycerol phase. These FFAs are not usually reused, but can be entered into the start of the process to be esterified by the mineral acid.

A vacuum flash process separates the methanol and glycerol phases, with an 85 wt % glycerol product, which can then be sold. The methyl ester-rich stream, which also contains a small portion of methanol, a small amount of base, and amounts of tri-, di- and monoglycerides, is neutralized prior to methanol removal. Again the HCl removes any remaining catalyst or soap as NaCl. The methanol in the methyl ester stream is then stripped by vacuum flash or a falling film evaporator. Water washing of the methyl ester stream removes salts and FFA. Finally any remaining water in the biodiesel is removed during a final drying step in a vacuum flash process. Water is also removed from the methanol stream, and the remaining methanol can be recycled back into the process. [14]

It should be noted that biodiesel can be produced without a catalyst at temperatures exceeding 350°C and pressures of over 120 atm. Despite the large capital and running costs involved in this method some producers around Europe use this technology. It is attractive because of the short reaction times (5-300 s) and the lack of pre- and after- treatment steps necessary to produce grade fuel. [56]

1.6 CONVERSION OF LOWER QUALITY FEEDSTOCK

The major barriers in the commercialization of biodiesel are the cost of the feedstock, application of the glycerine product and the problems involved with plant size. The eventual cost of biodiesel could be made competitive with diesel fuel if the cost of the feedstock could be reduced significantly. [57] Waste cooking oils and animal tallow products are a far less expensive alternative. Currently the largest use of waste oils around the world is the production of animal feed. The EU has banned this practice, citing fears of cross contamination, and that the harmful products produced during frying could enter the food chain. [58, 59]

The amount of waste cooking oil collectable in any one country varies and depends on the culture, the ease of collection and legislation dealing with the above factors. It is estimated that the EU alone produces 1,000,000 tonnes yr^{-1} of waste oil that

is potentially collectable and usable. [55] The US produces at least five times this amount.[60]

In Europe the standard nomenclature is to describe waste oils by whether they are vegetable based or animal based (WVO or WAO) and by their FFA content. In the United States the term Waste Frying Grease (WFG) is commonly used and it is described as being yellow (FFA <15 wt%) or brown (FFA > 15 wt%). If this amount of waste oil could be collected in the EU alone, it could produce between 600,000,000 – 750,000,000 litres of biodiesel which would become a significant percentage of the total biodiesel produced in the EU. [61]

In the frying process, the major process for the production of waste oils, oil is heated up to 200 ºC in the presence of organic matter and light. In public restaurants the oil will be maintained at this temperature over relatively long times, and will be continually cooled and reheated until replaced. During this time three basic reactions occur, the thermolytic, the oxidative and the hydrolytic. [62-64]

1.6.1 THERMOLYTIC

The thermolytic process occurs in the absence of oxygen, where the temperatures are at least 180 ºC or higher. The triglycerides that contain saturated fatty acids will produce a series of alkanes, alkenes, smaller FFA, ketones and oxo- esters, CO and CO_2 are also produced.

The unsaturated compounds will form dimeric structures, saturated dimers and unsaturated dehydro-dimers. Polycyclic and polymeric compounds are also commonly formed via a Diels Alder reaction between unsaturated FFA.

1.6.2 OXIDATIVE REACTIONS

The heating of triglycerides with air also forms oxidative products. In the environment of the frying process oils react with atmospheric oxygen via a free radical mechanism, to produce hydrogen peroxides. A scission of the O-O bond will create alkoxy radicals which then may lose or gain hydrogen atoms to form the hydroxyl or ketone derivatives. Aldehydes, hydrocarbons and acids are made by decomposition of the

alkoxy radicals. Dimerisation or oligomerisation are also possible when an excess of oxygen is present.

1.6.3 HYDROLYTIC REACTIONS

Steam is produced in the preparation of foods, and this can affect the composition of the FFA and triglycerides in the oil. The steam causes hydrolysis of the triglycerides to produce a higher level of FFA, monoglycerides and diglycerides. This is the major transformation of vegetable oils observed in the cooking process and as a result all waste oils have increased levels of FFA.

1.6.4 ANALYTICAL SPECIFICATION

All of these reactions occur competitively and there are two commonly used methods to determine the extent of degradation of the waste oils; measuring the polarity and using High Performance Size Exclusion Chromatography (HPSEC). With the formation of these products, the general polarity of the solution increases and can be measured. The EU legislation on edible oils states that if the polar fraction of waste oils is above 25% then the waste oil can no longer be used for the preparation of food.

HPSEC is a more involved analytical technique but (much like HPLC) can determine the amount and identity of separate products from the reaction mixture. This type of analysis is important as waste oils collected from many different sources when pooled together will have a vast array of different contaminants and this will affect the transesterification process as well as the potential fuel properties.

Generally the larger amount of polymeric material present in the waste oil, the less suitable the resulting biodiesel produced will be for use as a fuel. This is due to the elevated carbon residues that are generated by the incomplete burning of these compounds. [65]

1.6.5 CATALYSIS OF WASTE OILS

The normal industrial methods for the production of FAAE are hindered by their sensitivity to water, FFA and any solid organic matter. In the catalysis of virgin

vegetable oils this does not represent a large problem as there is very little water and a FFA concentration of below 1 wt%. Waste oils all have large FFA contents, higher moisture residues and varying amounts of solid suspensions.

Waste oils are subjected to a filtration or centrifugation step to remove the organic matter, then the removal of all the FFA and water is achieved by a neutralisation step and heat treatment. This must be completed before the addition of the alkali catalyst used to synthesise the biodiesel product.

Current industrial practice is to treat the solid matter with either citric acid or steam. This step releases trapped solid particulates and melts any solid fats, helping to release moisture and sub-particulate matter. The resulting oils are then filtered through a selection of fine sieves. [55] The waste oil stream is then esterified with the FFA being turned into FAAE with either an H_2SO_4 or a $Fe_2(SO_4)_3$ solid catalyst. With high loadings of both acid catalyst and alcohol the transesterification of vegetable oil can also be achieved with these acid catalysts without the need for an alkali-metal transesterification step. The step approach is more common however as it negates the need for large amounts of H_2SO_4 that would require special reactor technology. [66-69]

As discussed above the vegetable oil feedstock has already undergone chemical and physical changes aside from the production of FFA previous to use as a feedstock. Even though the majority of triglycerides in the vegetable oil feedstock are unchanged by the time they are transesterified, there is a proportion of dimeric and oligomeric compounds present. In the catalytic process these compounds will also be transformed. The dimeric fatty acids are tranesterified and the alkyl esters formed. The oligomeric and polymeric compounds are generally cleaved to form novel dimeric and monomeric esters. These dimeric and oligmeric esters increase the flash point of the biodiesel and an increase in the viscosity is also observed. [63]

The resulting emissions from using the waste alkyl esters were tested on a variety of test rigs. All tests showed no difference in the levels of pollution run on waste oil alkyl esters than those observed for virgin oil alkyl esters. [67] This was also true of animal tallow methyl esters. [70, 71]

The use of waste oil as a feedstock could make up a significant proportion of biodiesel produced. However, out of the four practical methods for producing biodiesel based on technology used presently (alkaline transesterification, acid transesterification, a two step esterification with acid followed by an alkaline transesterification and using

supercritical fluids) only the acid esterification and transesterification is deemed economic. [18, 19] This is not to imply that a solid base / acid catalyst can not be developed which reduces a large amount of the problems with using waste oils as fuels and research in this area is ongoing. Two reviews in using these techniques have been written detailing the industrial advantages and disadvantages associated with this approach. [72, 73] FFA tend to interfere with the catalytic process by promoting either competing acidification reactions or reducing the amount of active sites for solid acids and bases. [74]

1.7 PHYSICAL PROPERTIES OF BIODIESEL

When biodiesel is burned it produces around three times the amount of energy that is used to create it, and has a carbon cycle which reduces carbon emissions from between 70-79 %. Biodiesel is a lot less viscous than the vegetable oils it is synthesised from. Resistance to flow is an important factor in the fuels efficiency in the engine. If the fuel viscosity is too low, a substantial amount of liquid will leak past the plunger and result in power loss. If the viscosity is too high, the injection pump will not be able to fill the chamber again resulting in power loss. If the viscosity is much higher, as in vegetable oils, the degradation of the spray will lead to poor atomization, and coke formation in the engine. The viscosity of biodiesel is normally between 3.5 – 5.0 $mm^2\ s^{-1}$, comparable to diesel fuel (2.5-4.5 $mm^2\ s^{-1}$) and not vegetable oils (38 $mm^2\ s^{-1}$).

The density of biodiesel is typically around 0.88 g cm^{-3}, which is greater than diesel (0.83 g cm^{-3}) but less than vegetable oils (0.92 g cm^{-3}). Another important physical property is the flash point (FP), defined as the lowest temperature at which the vapour makes a flammable mixture with air. Diesel fuel has a low FP, typically between 52-66ºC, whereas biodiesel has a FP of over 150ºC comparable to that of vegetable oils that have a flash point of around 220ºC. The composition of the biodiesel, particularly the alcohol moiety, chain length and saturation, are the predominant factors which determine these physical properties.

The two main physical disadvantages of biodiesel are the poor cold-flow characteristics and oxidative stability. To reduce cold weather performance issues biodiesel must contain a high proportion of low melting point alkyl esters, namely unsaturated long chain FAAEs. Problems with storage are due to the auto-oxidation of

FAAE with atmospheric air over a period of time. Unsaturated esters have a much greater reactivity towards oxidation than the saturated counterparts, where polyunsaturated esters are the most. Oxidation products of biodiesel vary depending on the feedstock. Initially hydroperoxides are formed, which then break down into aldehydes, acids and other soluble oxygenates. Soluble and insoluble polymeric compounds are also created. [75-78]

The creation of the oxidised products affects the physical properties of the fuel in many ways. Oxidation leads to a change in colour from yellow to brown and usually a pungent smell is also given off. A slight increase in the cetane number (CN), and a large change in the kinematic viscosity (ν) is observed bringing it to above the levels stipulated by ASTM D6751. [79] The peroxide value (PV) and acid value (AV) are methods used to test the level of oxidation, and the values thereof form a part of the specification parameters for biodiesel.

All diesel fuels are susceptible to performance problems in cold weather. This is in part due to the crystallisation of higher melting point molecules such as FFA, high weight paraffins or certain FAAEs. The temperature at which these crystals appear to the naked eye is termed the cloud point (CP). At temperatures below the CP, crystals can fuse together and cause large agglomerates, which can prevent the free pouring of the liquid, this is termed the pour point (PP). There are other tests relating to these two factors, namely the wax appearance point (WAP), resulting in the wax precipitation index (WPI) for the prediction of the minimum operating temperature. The Cold Filter Plugging Point (CFPP) is another method used (ASTM D6371) whereby a sample is drawn through a wire mesh filter under vacuum; this is closely related to the low temperature flow test (LTFT). Biodiesel can also gel at low temperatures. This temperature varies significantly, and depends upon the feedstock used to produce the biodiesel. The temperature range is roughly between -10 °C and 16 °C.

When compared with mineral diesel, biodiesel has been shown to have higher combustion efficiency and a generally improved emission profile when used in a diesel engine. [80, 81] Biodiesel and fuel blends have been shown to reduce emissions of particulate material (also described as the smoke capacity), the hydrocarbon emissions (HC), carbon monoxide (CO) and sulphoxides (SO_x). Although a general rise in NO_x emissions is observed, there is a lowering of carcinogenic PAH particles. [82-85] Studies have also shown that even though there is an increase in contamination by micro-

organisms in diesel grade fuel (much like in water), methyl soyate acts as an inhibitor in the growth of such species even at low concentration blends with diesel fuel. [86]

1.8 RESEARCH IN NOVEL HOMOGENEOUS CATALYST DESIGN

Sodium and potassium alkoxides are the most effective transesterification catalysts for the conversion of triglycerides to FAAE. Due to the competing saponification reaction all FFA and most of the H_2O must be removed from the process before the reaction takes place. After the reaction is complete the soap must be separated out and the base catalyst neutralised. The resulting salt must also be removed from the reaction products. This increases the production costs and makes the use of low quality oil as a feedstock practically impossible. These alkali metal catalysts have faster reaction times, require milder conditions and involve much cheaper handling costs than Brønsted acid catalysed systems, although Brønsted acid catalysed systems do not result in saponification. The Brønsted acid systems are also homogeneous and require removal from the glycerol and FAAE products. Current research design is focused on creating systems, which do not saponify the reaction mixture, are easier to handle than the Brønsted acid counterparts, and have a degree of water and acid tolerance. This would allow the transesterification of lower quality feedstock such as waste oils, whilst reducing the amount of steps in the production process making the industrial synthesis of biodiesel more economical.

In terms of the biodiesel reaction a homogeneous catalyst is one that is soluble in either the methanol or the lipid reactants. Methanol soluble catalysts, such as NaOMe, are easier to introduce in to the reaction and generally are easier to recycle. Lipid soluble catalysts, such as zinc stearate, tend to have a higher activity.

1.8.1 HOMOGENEOUS TIN CATALYSTS

Sn (IV) based systems, and in particular stannoxane catalysts, have been investigated as efficient catalysts since before the 1980s. [33, 87] In industry Sn (IV) based compounds are used as homogeneous and heterogeneous catalysts for a variety of reactions, including polycondensations and esterifications. In 1967 Okawara *et al.* had shown that the partial

hydrolysis of any diorganotin dihalides leads to formation of an air-stable rigid tin ladder structure, as shown in Fig. 1.6 below.[88]

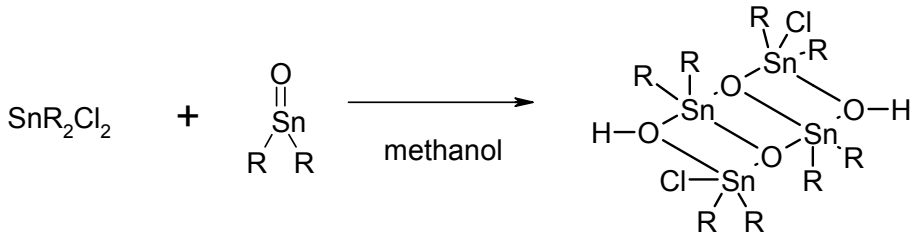

Figure 1.6 The reaction of dibutyl tin chloride and dibutyl tin oxide to form a stable tin ladder

Otera, who wrote a comprehensive review on transesterification catalysts,[33] speculated that these rigid ladders would give rise to various properties beneficial to catalysing the transesterification reaction.[89] One aspect of these properties is their high solubility in chlorinated and non-chlorinated solvents. Despite the metalloxane core, the compound forms a double-layered structure where the alkyl groups shield this core from the organic solvent. Otera described the solution state of these compounds as forming polar 'islands', made up of stannoxane cores, dispersed in an 'ocean' of less-polar, reversed micelles.

There are two geometrically different Sn centres in these compounds, both are bonded to two alkyl groups, where Sn(1) binds to a Y and two oxygen atoms, Sn(2) is bonded to an X, a Y and one oxygen atom. This leads to a second unusual property where the two Sn atoms are in differing environments and yet have a very close proximity to each other. His research showed that the identity of the substituents made no real difference to the reactivity of the catalyst, when screened for the reaction between methyl butyrate and benzyl alcohol. The stannoxane clusters were remarkably active, for such a stable complex, yielding 100% conversions in just a few hours when as little as 0.05 molar % of catalyst was used.[90] Otera suggested the following reaction mechanism, shown in Fig. 1.7 below.

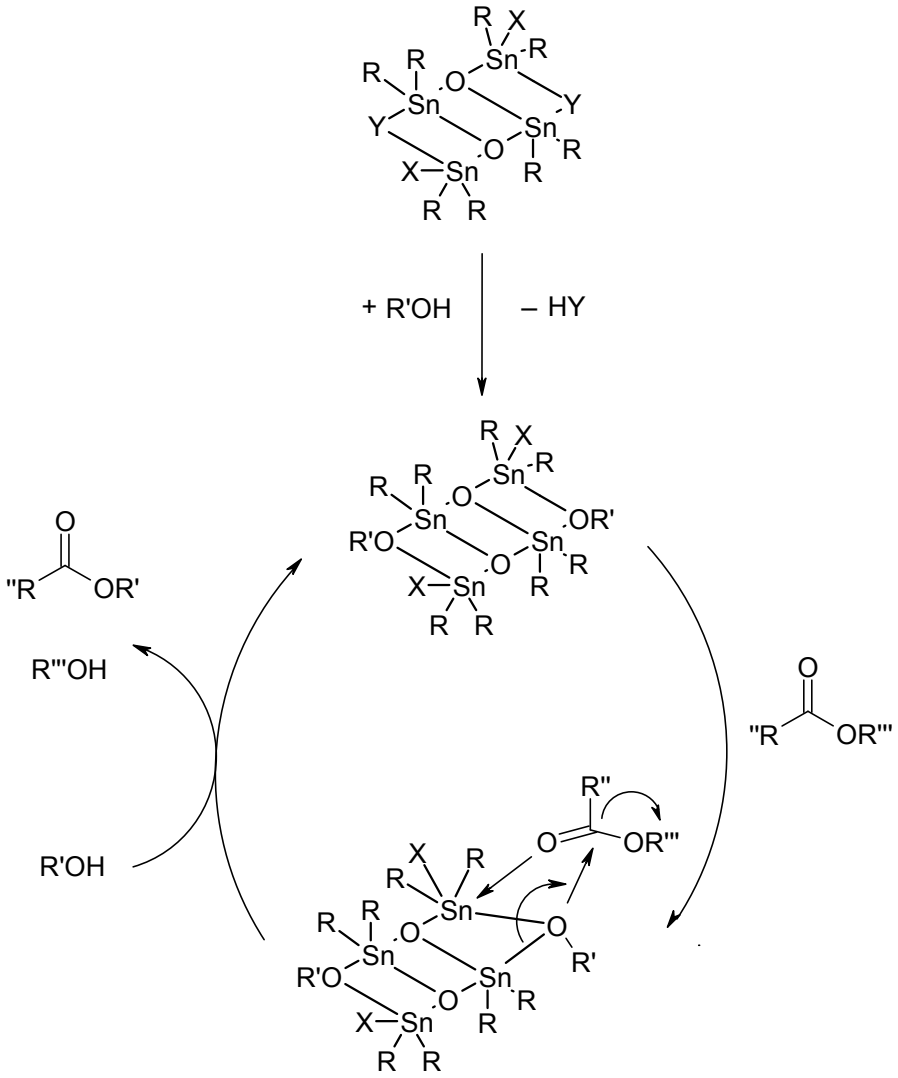

Figure 1.7 The reaction mechanism showing a general transesterification, catalysed by two Sn(IV) atoms in differing environments

One large problem with these compounds is the low yields achieved when reacting bulky ester groups with smaller alcohols. Research to increase the size of the spacer group while retaining the catalytic activity has been performed [91, 92] however these problems, with the undesirability of the metal, mean these compounds are unattractive for the industrial production of bio-diesel.

Alkyl stannoxanes are simple to make and are generally stable to the air and moisture, Meneghetti et al. investigated the methanol and vegetable oil soluble dibutyltin dilaureate complex for the methanolysis of soybean oil. This homogeneous system was compared to similar Sn (IV) heterogeneous catalysts (di-n-butyl-oxo-stannane and butylstannoic acid); the homogeneous system was found to be more active

than the heterogeneous catalysts at any time over the ten hour reaction period, at 80 °C with a loading of 1%. An increase in the temperature of the reaction to 120 °C led to the homogeneous system giving a higher percentage increase than the nearest heterogeneous system. An increase in the loading and stirring rate improved the homogeneous and heterogeneous by roughly the same percentage. [93]

Sn (IV) complexes are active for a lot of reactions and previously had a wide range of industrial uses. However, alkyl derivatives of Sn (IV) are highly toxic and where they are used for large scale applications, alternative catalyst systems are being sort. Suarez et al. investigated the activity of a less toxic Sn (II) complex (using 3-hydroxy-2-methyl-4-pyrone as the ligand), and compared the activity in the transesterification of vegetable oils to other divalent heavy metals and zinc. [94]

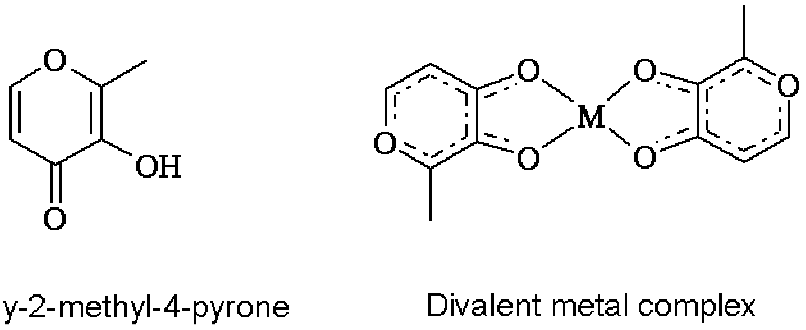

Figure 1.8 Novel ligand system for the homogeneous transesterification of vegetable oil with methanol

The tin complex was a very good transesterification catalyst and converted 37% of the vegetable oil to methyl ester after one hour at refluxing temperature. The order of activity can be described as follows: Sn(II) > Zn(II) > Pb(II) ~ Hg(II). These catalysts were tested for activity in the transesterification of different vegetable oils as well. The results indicated that both saturation and chain length of the fatty acid arms are important in determining the activity of a catalyst. The researchers note that the shorter, less saturated oils are more open to methanolysis. These catalysts also gave optimum results when using methanol, an increase in the size of the alcohol group gave a sharp decrease in the amount of FAAE formed. [95] Mechanistically they believe that the formation of a trivalent metal intermediate, involving one ligand and a deprotonated methanol molecule occurs. The carboxylate group of the glyceride molecule then

donates electrons into the empty metal orbital and then goes on to further react with the bound (or a co-ordinated) methanol to form the FAME. These pyrone complexes are costly while active, and Sn (II) complexes are still considered to be too toxic for 21st century industrial use.

1.8.2 Divalent Metal Carboxylates

One of the main problems with using alkaline catalysts is the sensitivity to FFA. Basu and Norris proposed a barium acetate/calcium acetate homogeneous system which could tranesterify the triglycerides and esterify the FFA in a one pot reaction. [96] The reactions conditions reported were a temperature of up to 250 ºC with high alcohol and catalyst loadings. Di Serio et al., further investigated the use of metal carboxylate catalysts, choosing a range of methanol soluble, divalent metal acetates and comparing the activity against the oil soluble stearate complexes.

Barium, calcium and magnesium acetate showed very little activity at 150 ºC or 200 ºC (using a standard 600:100:1 loading of methanol, vegetable oil and catalyst over 2 hours.) The stearates showed a much higher activity of around 60% conversion. Cobalt and nickel complexes were almost inactive, regardless of which ligand was present. However the acetates and stearate salts of cadmium, manganese, lead and zinc were highly active at 200 ºC, converting an average of more than 80% of the triglyceride to FAME. The researchers reasoned that the high activity of the stearates was mainly due to the increased solubility in the vegetable oil layer, where the trend in activity across a series was solely dependent on the Lewis acidic strength of the metal ion. [97]

1.8.3 Titanium Alkoxides

Titanium is also highly Lewis acidic, and complexes of titanium tend to be benign. Titanium alkoxides have a high solubility in alcohols, however when dissolved in methanol the production of titanium methoxide (an insoluble white powder) is favoured. Some mixed titanium alkoxide, alkyl and halogenated catalysts have been suggested in the patent literature but high temperatures, loadings and pressures are needed to achieve high conversions of the triglycerides to FAAE. [98, 99]

1.8.4 LEWIS BASES

Certain Lewis bases have also been shown to be active in the transesterification of vegetable oils. [13] A series of guanidine and other similar organic bases were reported for their activity in the transesterification of vegetable oils by Vargas et al. The bases used, their abbreviations, structure and activity in the biodiesel reaction are summarized in Table 1.1.

Catalyst	Structure	Relative Basicity	pKa (CH_3CN)	Yield %
TBD	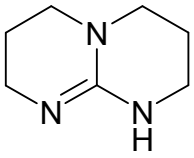	150	25.9	91
BEMP	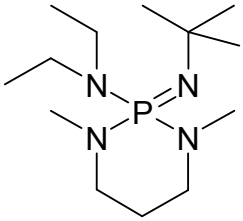	6873		66
Me_7N_4P	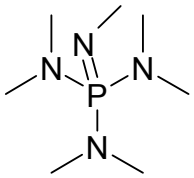	4762	27.52	63
MTBD		44	25.43	47
DBU	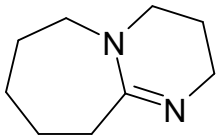	3	24.32	32
DBN	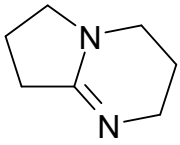	1	23.79	4.5

Table 1.1 Comparison of the catalytic activity of some organic bases for the transesterification of rapeseed oil (8.00 g) with methanol (2.00 g); 1 mol% catalyst, 70°C after 1 hour

The activity of the bases is not directly attributable to the strength of the base but is more closely linked to kinetic factors. The lone pair of electrons on the sp^2 hybridized nitrogen atom, as shown below in Fig. 1.9, is assumed to be the active site. The more active catalysts have less steric hindrance around this reactive centre.

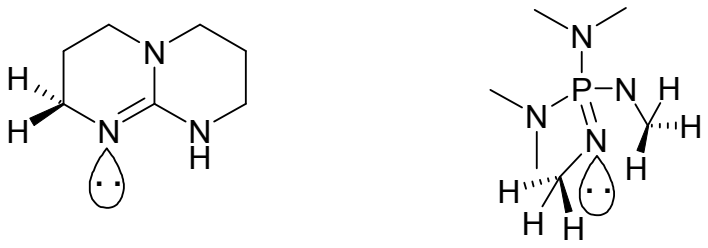

Figure 1.9 Lone pair arrangements of two basic organic transesterification catalysts

These amino bases compare favourably to alkali hydroxides, converting the triglyceride molecule in similar yields with no saponification, albeit over 2 to 3 times longer. Triethylamine, quinoline and pyridine were also tested but were not active under these conditions.

Guanadines can also be easily heterogenised onto organic frameworks. [100] Schuchardt et al. used cellulose and poly(styrene/divinylbenzene) to incorporate the guanidine catalyst. The guanidine can be anchored to microcrystalline cellulose, if the sugar has been activated by cyanuric chloride first, this process is shown in Fig. 1.10.

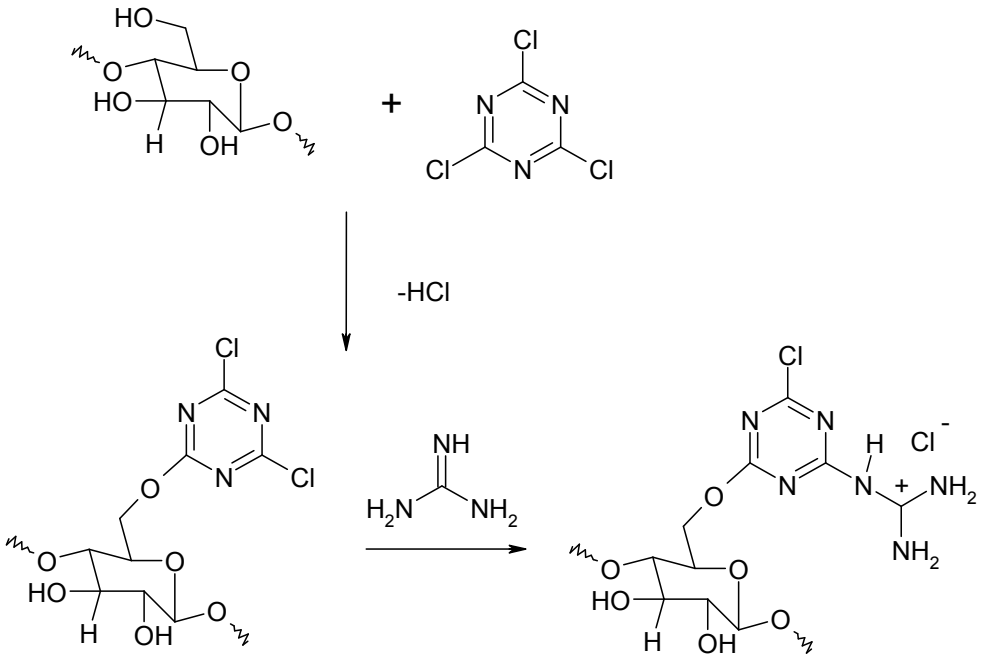

Figure 1.10 Guanidine derivative heterogeneised on cellulose for the production of FAME from vegetable oil

Guanidine was also heterogeneised on other anchors (e.g. polystyrene) but it was generally observed that the heterogeneised base catalysts were less active than the base in the homogeneous phase. Leaching of the base into the reaction medium was also observed for most of the heterogeneous catalysts after a relatively short time. [101]

1.9 RESEARCH INTO NOVEL HETEROGENEOUS CATALYST DESIGN

The majority of research into biodiesel production is in producing heterogeneous systems to affect the transesterification of vegetable and waste oils. Heterogeneous systems are attractive for biodiesel production mainly due to the ease of separation from the resulting products as well as their applicability in more efficient chemical plant design.

1.9.1 ZEOLITES

Zeolites were tested for the esterification of FFA with methanol by A.A. Kiss et al. [72, 73]. They concluded that zeolites were poor catalysts for this reaction due to the size of the reactants and poor diffusion through the pores. Zeolites are crystalline aluminosilicates that contain open structures with apertures of molecular dimensions, cations are trapped within the cages and tunnels of the aluminosilicate framework. These counterions are usually alkali metals such as sodium or cesium. When catalysing the transesterification of vegetable oils zeolites can be thought of holding an alkali metal catalyst within a rigid framework, which inhibits soap formation. The main limiting factor is the rate of diffusion into the pores where the reaction can take place.

NaX zeolite structures have been investigated by two groups. Moreau et al. investigated the activity of NaX faujasite type zeolites with varying amounts of cesium, to establish the optimum conditions of the transesterification reaction. In this they found that at refluxing temperatures they needed 2 g of catalyst (with 30% of the cationic sites filled by cesium ions), 22 hours of reaction time and 63 ml of methanol to convert 5 g of vegetable oil to FAME. [102] A more detailed study was under taken by Suppes et al. [103] They tested a range of zeolite catalysts which have been summarised below in Table 1.2.

Parent Zeolite	NaX	NaX	ETS-10
Description	Basic $Na_{82.8}K_{1.8}Al_{85.8}Si_{106.2}O_{384}$	Occulded with excess Na species	TiO_6SiO_4 structure $Na_{21.9}K_{7.5}Ti_{16.5}Si_{77.5}O_{208}$
Surface Area	591 $m^2 g^{-1}$		326 $m^2 g^{-1}$
Pore Volume	0.299 $cm^3 g^{-1}$		0.159 $cm^3 g^{-1}$
Catalyst types	KX	1 (NaO_x / NaX*)	K- ETS-10
	CsX	3 (NaO_x / NaX*)	Cs-ETS-10
	(Cs, K)X	4 (NaO_x / NaX*)	(Cs, K)ETS-10
		0.25 (NaO_x / NaX)	
		1 (NaO_x / NaX)	
		3 (NaO_x / NaX)	

Table 1.2 A range of zeolite types tested for activity in the biodiesel reaction. All NaX species were occluded with sodium acetate apart from NaX which were occluded with sodium azide*

NaX is a faujasite aluminosilicate zeolite with a relatively low charge. The rigid framework is remarkably stable and contains the largest void space of any known zeolite. It was this type of zeolite that was tested by Moreu et al. (see above). ETS-10 is a new microporous zeolite which consists of 12-ring pore structure consisting of interlocking chains of TiO_6^{8-} and tetrahedral SiO_4^{4-} atoms. Despite having a smaller pore size this zeolite carries a large charge, and therefore exhibits a very high cation-exchange capacity. NaX type zeolites were also prepared with a large excess of sodium species.

To prepare a zeolite catalyst for catalysis, it must be calcined (by heating the zeolite to high temperatures under an O_2 enriched atmosphere.) This is used to burn off the organic framework used to prepare the catalyst and in some cases oxygenate the framework. Suppes found that calcination was vital to create an active zeolite, as the catalysts showed very little activity without this step. The reactions were completed over 24 hours, with a catalyst loading of 10 wt % (This would roughly equate to between 40-60 mol% in respect to the alkali ions present). The results are summarised below in Table 1.3.

Catalyst	Percentage of Esters at 150 ºC	Percentage of Esters at 120 ºC	Percentage of Esters at 60 ºC
NaX – K	31.5	22.7	10.3
ETS-10	95.8	94.6	80.7
ETS-10 (Cs, K)	88.1	83.9	67.4
1 (NaO_x / NaX*)	79.1	72.4	-
3 (NaO_x / NaX*)	94.0	93.2	84.2
0.25 (NaO_x / NaX)	58.4	45.5	-
3 (NaO_x / NaX)	95.6	94.1	82.0

Table 1.3 A range of zeolite catalysts tested by Suppes et al. for the conversion of vegetable oils with methanol

Suppes et al. confirmed that faujasite aluminosilicate zeolite, despite the increased pore sizes, is not an ideal catalyst for the transesterification of vegetable oils. This is not reliant on the identity of the cation. It should be noted that recently published results show that high conversions of FAME can be achieved by increasing the basicity of the NaX zeolite substantially with KOH (as opposed to occulsion with an excess of sodium azide) under similar conditions. [104]

The activity of these catalysts can be extended by the (costly) occulsion process, no data was given as to the level of saponification this caused. The ETS-10 zeolite gave high conversions, proving that it is not directly pore size that enhances a catalyst's activity, but the amount of active sites. In the conversion of waste oils large amounts of FFA (up to 25%) inactivated the catalysts used this is presumably due to soap formation blocking the cavities. [103]

1.9.2 Supported Alkali Metal Catalysts

To avoid the problems inherent with using the zeolite catalysts, alkali metals can be anchored on to materials with a high surface area, with the catalysis reaction taking place on that surface. Xie et al. investigated loading different potassium salts onto an Al_2O_3 support. Al_2O_3 is acidic and can be reacted with KNO_3, after calcination this

KNO_3 is converted into K_2O sites. The following reaction also will take place where KNO_3 reacts with the isolated aluminium hydroxide groups on the surface. The calcinations temperature is around 773 K.

It is these two basic sites which are thought to be active for the transesterification reaction. The amount of KNO_3 used is important, as is the calcination temperature. The optimum conditions for the synthesis of these catalysts are to use 35 wt% KNO_3 and then calcining between 723-823 K.

Conversion of 90% of the soybean oil to FAME was achieved at reflux when using a reaction time of 8 hours, a methanol to oil ratio of 14:1, and a loading of 6 wt% catalyst; highly comparable to the zeolite type catalysts used. [105] Xie et al. tested other potassium salts on the same support. KI, KF and KOH anchored catalysts showed slightly higher activity than the KNO_3 prepared catalyst. The same optimum conditions applied to all the aluminum oxide supported catalysts. The researchers compared their results to a KF loaded NaX zeolite, which they found to be inactive under their conditions. They found a strong correlation across the series that an increasing activity is observed with an increasing amount of basic sites. [106] A similar series of catalysts were synthesised using sodium instead of potassium by Lee et al. They found similar activities to the potassium counterparts at reflux when using lower catalyst loadings (1 wt%) and a co-solvent (THF, n-hexane). [107]

Xie et al. also experimented in using different supports for their potassium solid base catalysts, notably using ZnO instead of Al_2O_3, with KF as the potassium source. The most notable advantage is the need for less KF, only around 15 wt%, and less supported catalyst in the reaction mixture (4 wt%). The alumina supported potassium catalysts are highly dependent on the calcination temperature and this factor was also studied for the ZnO species. To create the largest amount of basic sites on the surface of the catalyst a temperature of 873 K is optimum over a reaction time of five hours. [108] ZnO can also act as a catalyst; Suppes et al. found its activity as a catalyst comparable to the ETS-10 zeolites under the conditions described above. [103]

CaO can also be used as a support for alkali metals. Meher et al. used these supported heterogeneous catalysts in the transesterification of karanja oil. [74] The catalysts were not calcined but laboratory grade CaO was wet-impregnated with 1.25% of the metal nitrate, the water was then removed at 100 ºC over 24 hours. The researchers found that the Li doped CaO catalyst at refluxing temperature and 2 wt%

converted 95% of the vegetable oil to FAME over 8 hours, the optimal methanol ratio was 12:1. The Na and K doped complexes also achieved this conversion but showed a lower initial rate of reaction. The amount of FFA in the oil (up to ~6%) had little effect on the activity of the catalyst.

Calcium carbonate was also investigated, as a possible catalyst, for the transesterification of soybean oil by Suppes et al. However, temperatures exceeding 200 ºC are needed to activate the limestone catalyst. [109] This was also shown to be true for magnesium oxides. [110] In the patent literature Nakayama et al. highlight the use of hydroxides, oxides and carbonates based on alkali earth metals, but in particular highlight a $CaTiO_3$ species for use as a catalyst at refluxing temperatures: the implication is that the perovskite structure may be critical. [111]

1.9.3 Oxides, Methoxides and Hydroxides of Group II Metals

These basic compounds have been extensively investigated as potential biodiesel catalysts. The bascity of the alkaline earth metals increases going down the group. For any one particular metal the methoxide tends to be more basic than the oxide which in turn is more basic than the hydroxide salt.

Gryglewicz demonstrated that these compounds were active in the methanolysis of rapeseed oil, the activity followed this trend of basicity. And despite being slightly less active catalysts than NaOH, with optimum conditions (a methanol oil, to catalyst ratio of 60:15:1) at reflux over 2 hours gave 90% conversions of FAME. [38]

Repeated experimentation found that using soluble $Ba(OH)_2$, a similar activity was observed as published, but using calcium oxide and calcium methoxide as catalysts (bought from Aldrich Chemicals) under the conditions reported gave lower yields than stated. Reddy et al. also found laboratory grade CaO to be completely inactive in the conversion of vegetable oils to FAME, however when using nanocrystalline (a crystalline size of 20 nm, a surface area of 90 $m^2\ g^{-1}$) particles the activity increased dramatically. The complete conversion of soybean oil could be achieved after 12 hours at room temperature with a methanol, rapeseed oil to catalyst molar ratio of 150:5:1. Nanocrystalline particles of other metal oxides (Mg, Ti, Zn, Ce and Cs) were found to be inactive under these conditions.

Reddy et al. discovered that a large amount of Calcium methoxide was being formed on the surface of the CaO and also that any hydroxyl groups on the surface were efficiently converting methanol into the methoxide anion. After 8 cycles the catalyst became deactivated, SEM pictures show the loss of edges and large amounts of polycrystallite formation they observed that this was consistent with catalyst deactivation. [112]

1.9.4 HYDROTALCITE CATALYSTS

Hydrotalcites have similar structures to perovskite amalgamations, where the general formula for a hydrotalcite mineral is $[M^{2+}_{(1-x)} M^{3+}_{x} (OH)_2]^{x+} (A_{x/n})^{n-} \cdot y\ H_2O$. Wilson et al. prepared as series of Al Mg hydrotalcites with varying levels of magnesium and tested their activity in the transesterification of glyceryl tributyrate with methanol. A conversion of 75% was observed with high Mg loadings at 60 ºC. This was a vast improvement on the MgO and Al_2O_3 supports used without doping for comparison. [113]

1.9.5 NAFION EXCHANGE RESINS

Solid acid catalysts have also been extensively researched for their utility in the biodiesel reaction. Nafion exchange resins are acidic solid resins, which, much like imbedded alkali metals in the zeolite pores, contain a large amount of H^+ per gram of substance. Nafion resins are sulphonic resins, which are part of a group of catalysts that are classified according to their polymer backbone. Polystyrene based sulphonic resins (Amberlyst®) and perfluorinated (Nafion®) are the most commonly used. These resins have very low surface areas until a solvent is used to swell the polymer and expose the internal acidic sites, this can also be achieved with out a solvent by anchorage onto a high surface area silica or metal oxide (Al_2O_3, ZnO etc.) support.

Goodwin Jr. et al. investigated the use of Nafion NR50 and the silica supported SAC-13 (see below) for the transesterification reaction of triacetin. In doing this model biodiesel reaction they were able to compare the solid acids to sulphuric acid kinetically.

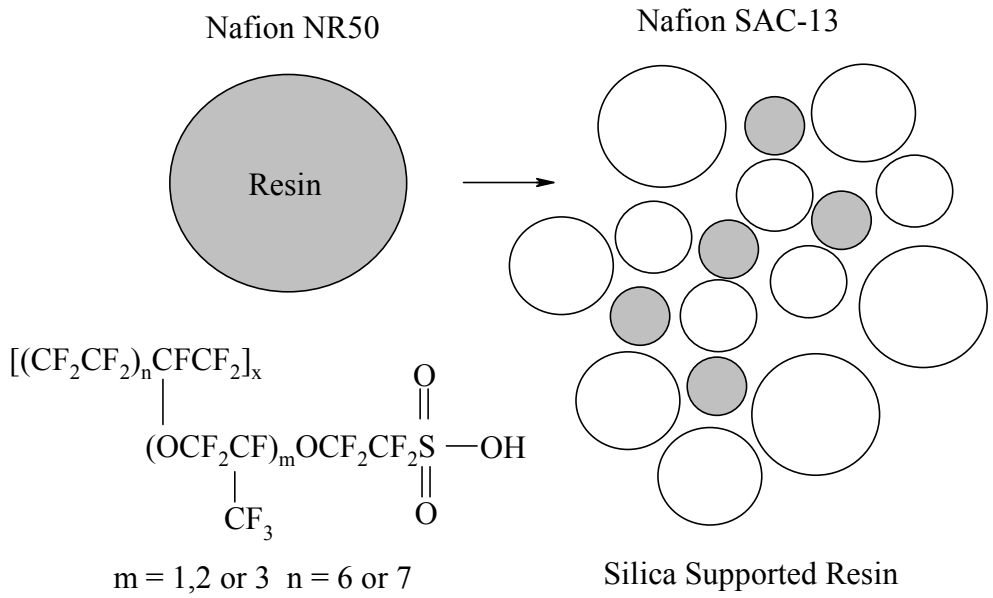

Figure 1.11 Schematic demonstrating the Nafion NR50 catalytic site and the same resin supported on a silica anchor.

The activity of the Nafion catalysts strongly depends on the accessibility of the reactants to the acidic sites. For the non-supported resin, soaking for 12 hours in methanol prior to use was deemed sufficient. Even with this pre-treatment the supported resin showed a higher degree of activity. The researchers found that the catalyst was as active on multiple cycles as the first, indicating no leaching of the heterogeneous protons. They proposed that the mechanism is remarkably similar to that of the homogeneous catalysed reaction. Where the triglyceride is protonated a surface reaction takes place between this positive triglyceride and the liquid phase alcohol. After this rate determining step the product is then taken up into the liquid phase. The Nafion resins were active in this model reaction but less so than the H_2SO_4. [114]

The researchers also investigated the effect the chain length would have on the kinetics of this reaction using the supported Nafion and H_2SO_4 by esterifying fatty acids of a known chain length with methanol. They found the reactivity was strongly dependent on the size of the alkyl chain: as the chain grew lower yields of FAME were observed. For the largest chain lengths the resin showed a continual loss of activity, probably due to the accumulation of carboxylic acids at the Brønsted acid sites by irreversible adsorption. Effective regeneration is needed to improve the applicability of the SAC-13, if it is to be used for the esterifcation of large FFA. [115]

Yonemoto et al. tested triolein with ethanol using a range of cationic and anionic exchange resins. They found that no cationic exchange resin was active in ethanolysis, at 50 °C, with a ratio of ethanol to vegetable oil of 10:1. They reported that the anionic exchange resins (using OH^- as the anion) demonstrated a much higher activity. For all the Amberlyst anionic exchange resins, the conversion of over 90% of the triglyceride was achieved over 2 hours under the conditions mentioned above. The resin tended to demonstrate a higher activity with a lower cross linking density and a smaller particle size. This technology was then adapted to a fixed bed continuous reactor packed with the resin allowing a successful high through-put production process. [116]

The transesterification of actual vegetable oil by acidic (cationic exchange) membranes was investigated by Vital et al. A range of resins where chosen for the reactions including two Nafion types (112, 115) Dowex (50X8, X4 and X2) and poly(vinyl alcohol) membranes (5, 20 and SS20), see below.

Sample	**Brønsted acid sites (mmol g^{-1})**	**Thickness of the membrane (mm)**	**Percentage Swelling (methanol)**	**Percentage Swelling (soybean oil)**
Nafion 112	0.9	0.05	-	-
Nafion 115	1.0	0.13	116	negligible
PVA 20	3.8	0.13	negligible	2.9
PVA 5	0.8	0.02	8.1	6.9
PVA S20	9.0	0.14	negligible	18.9
Dowex 2	5.0	-	-	-
Dowex 4	4.3	-	-	-
Dowex 8	4.4	-	-	-

Table 1.4 A range of cationic membranes used as catalysts in the biodiesel reaction.

All these resins were used in a membrane reactor, shown in Fig. 1.12.

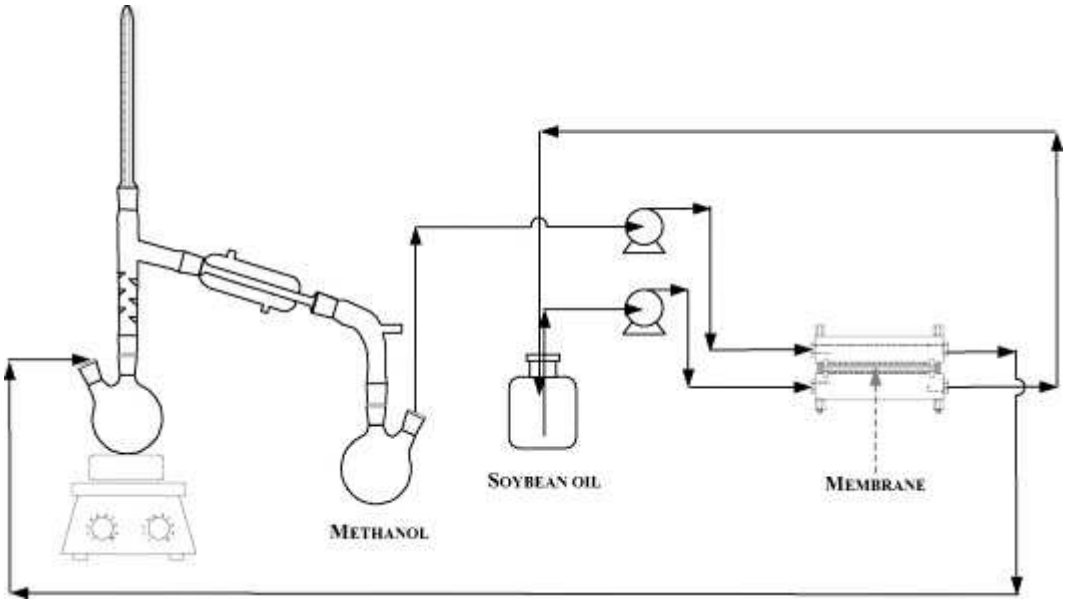

Figure 1.12 Membrane reactor apparatus used in the transesterification of soybean oil with methanol taken from Guerreio et al. [117]

The catalyst was soaked in methanol for 24 hours prior to use and fitted to the reactor, which was heated to 60 °C. The methanol was distilled prior to use and the reactants were then passed through from the relevant reservoirs at a fixed rate.

All the resins were found to be active but the PVA polymer crosslinked with sulfosuccinic acid was more active than the Nafion or Dowex membranes. The researchers concluded this was not only due to the greater extent of Brønsted acid sites but due to its higher swelling properties. [117]

1.9.6 FUNCTIONALISED AMORPHOUS CARBON

One factor that reduces the yield of ester when using cationic exchange resins is the diffusion through the polymer. Hara et al. synthesised a functionalised amorphous carbon material (from glucose) with acidic catalytic activity. The material contains phenolic hydroxyl, carboxylic acid and sulphonic acid groups; it has a catalytic activity akin to the homogeneous sulphuric acid.

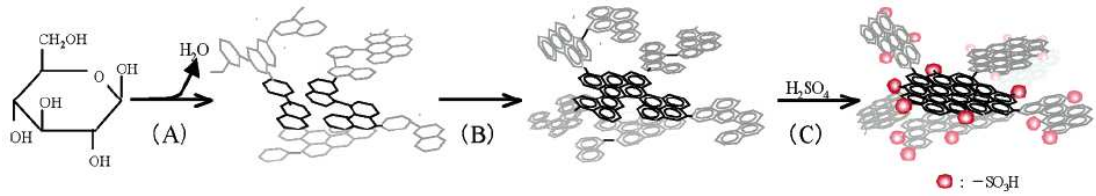

Figure 1.13 Schematic showing the functionalisation of an amorphous carbon material from glucose, taken from Hara et al. [118]

Synthesis of the catalyst takes three stages: A) pyrolysis, B) carbonization and C) sulphonation. D-glucose is taken and heated to temperatures of up to 823 K under N_2 gas. This leads to dehydration and dissociation of the C-O-C bonds, formation of polycyclic aromatic carbon rings at higher temperature, and eventually the amorphous carbon structure. Concentrated H_2SO_4 is then added and the catalyst heated to 423 K. The product is washed with water to remove all impurities from the surface, such as sulphate ions.

The researchers then tested this solid acid catalyst in the esterification of FFA (stearic and oleic); they observed that the activity was roughly half that of H_2SO_4. On further catalytic cycles no leaching or deactivation was observed, unlike in the use of ion exchange resins. [118, 119]

Further research on this type catalyst has been undertaken with one research team demonstrating the applicability of this type catalyst for the conversion of waste oils, noting a yield of just below 90% FAME after 12 hrs using 5.0 g waste oil (27.8% FFA content); 5.54 g methanol; 0.5 g catalyst at 80 °C. [120]

1.9.7 Zirconia / Alumina Supported Catalysts

Futura et al. investigated a number of Lewis acidic heterogeneous systems using zirconia/ alumina supports. Tungsten, zirconia and alumina were mixed together at 130 °C to create the supported catalyst (WZA), this was then calcinated at 800 °C. This catalyst was compared to a sulfated tin oxide complex and sulfated zirconia. All catalysts were set into a flow bed reactor and soybean oil and methanol (1:40) were passed over the bed at a flow rate of 3.0 g h^{-1} and 4.4 g h^{-1} respectively. None of the catalysts were active until around 200 °C. By 250 °C the tungsten based catalyst

converted over 90% of the soybean oil. The esterification of octanoic acid was also examined, to test the suitability of the catalysts to convert waste oils into biodiesel. In a similar reactor all the catalysts had converted the acid completely at 200 °C. [121]

This supported catalyst was then tested under the same conditions against TiO_2 / ZrO_2 (11 wt% Ti) and Al_2O_3 / ZrO_2 (2.6 wt% Al) amorphous materials, both of which calcined at 400 °C over 2 hours. These two catalysts demonstrated a comparable activity to WZA. [122] Zirconia catalysts have been used for the conversion of vegetable oils previously, but only for the production of gasoline type fuels from the cracking of waste oils at 400 °C. [123]

Dalai et al. tested the more acidic 12 –tungstophosphoric acid (TPA) as a solid acid catalyst by anchoring the tungsten onto four different supports, these are shown in Table 1.5.

Catalysts	TPA wt%	Surface area $m^2 g^{-1}$	Average pore volume $cc\ g^{-1}$	Average pore diameter Å
Pure TPA	-	8	-	20.7
Hydrous zirconia (HZ)	-	221	0.12	23.0
TPA/ HZ	10	146	0.08	21.8
	20	143	0.07	21.8
SiO_2	-	218	0.21	29.0
TPA / SiO_2	10	177	0.17	28.0
	20	137	0.12	27.4
Alumina	-	223	0.72	118.0
TPA/ Al_2O_3	10	207	0.59	107.0
	20	193	0.46	95.7
Activated Carbon (AC)	-	1003	0.46	14
TPA / AC	10	990	0.53	14.3
	20	997	0.59	14.0

Table 1.5 The physical attributes of various supported TPA catalysts, taken from Dalai et al. [124]

The catalysts were screened for activity during the transesterification of low quality soybean oil at 200 ºC, with a molar ratio of methanol of 6:1 and 3 wt % catalyst. The 10% TPA / HZ converted the oil to over 70% ester over 5 hours; the highest conversion achieved with the other catalysts was below 50%. A much better conversion was achieved using 3 wt % than 1 wt % catalyst, but there was little difference in conversion when larger amounts of catalyst were used. The catalyst was largely inactive at temperatures lower than 150 ºC, but a rise to 225 ºC converted over 90% of the triglycerides. The optimum conversion was achieved with 9 parts of methanol, more than that made little difference to the conversion. Surprisingly, raising the amount of FFA in the soybean oil (from 10% to 20%) increased the conversion, suggesting that

this catalyst system could be used for the conversion of animal tallow and other waste oils that contain large amount of FFA. [124]

Wang et al. synthesized the related catalyst, $Cs_{2.5}H_{0.5}PW_{12}O_{40}$, and used it in the conversion of waste oils. Despite being an excellent catalyst for the conversion of high FFA feedstocks, just a small amount of water completely deactivated the system. [125]

1.9.8 GROUP IV OXIDES

Group IV oxides have also been investigated for their activity in the conversion of vegetable oils. Generally these oxides are mixed with bismuth oxide, zinc oxide or alumina. Delfort et al. patented the use of these catalysts to transesterify vegetable oils with a large FFA content between 150 and 200 °C, under a pressure of up to 100 bar. They claim these catalysts are suitable for use in batch and continuous flow reactors, with fixed bed or decanter technology. [126] Zinc spinel/ aluminates are also active under these conditions. [127]

1.9.9 HETEROGENEOUS ZINC CATALYSTS

Srinivas et al. synthesised a mixed metal solid acidic, zinc-iron cyanide acid catalysts, shown below in Fig. 1.14.

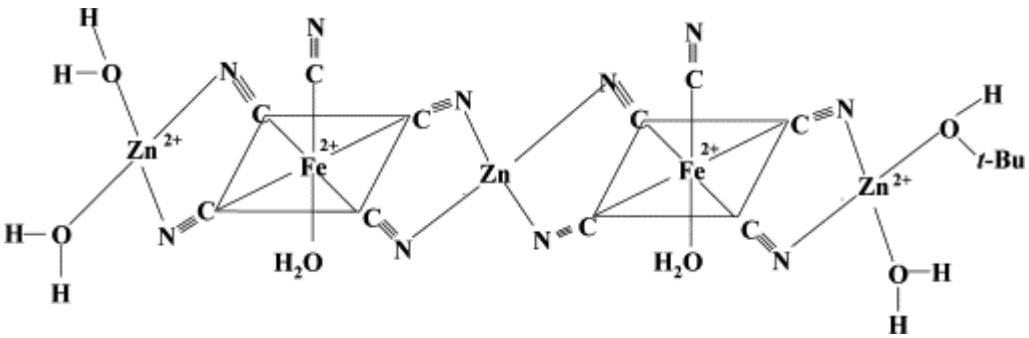

Figure 1.14 The tentative structure of the FeZn cyanide catalyst, used to convert rapeseed oil, taken from Srinivas et al. [128]

These compounds aggregate to form zeolite-like cage structures. The researchers showed that there were no basic or Brønsted acidic sites on the surface. They then

screened the catalyst for activity against similar Fe divalent cyanides, and found the zinc catalyst to be by far the most active. In optimising the conditions the loading of catalyst was found not to influence the course of the reaction significantly when more than 2 wt% was added. Where temperatures of over 400 K were needed, 8 hours and an alcohol to oil ratio of 14:1 proved to be the most effective. This catalyst is water tolerant and an increase of water does not affect the yield significantly. The catalyst is active in the esterification of FFA and any amount of these in the reaction solution does not deactivate it. [129]

Peters et al. tested a range of metal arginine salts for the methanolysis of de-acidified palm oil. In this study the zinc argininate salt was found to be the most active. Arginine is a naturally occurring amino acid, with a strong quaternary basic guandine group. A 70% conversion was achieved over 3 hours using 6 parts methanol at 75 °C. The catalyst was deactivated by the addition of FFA, but this effect could be offset by raising the temperature of reaction to 135 °C and the pressure to 0.5 MPa. [130] Peters et al. proposed that the basicity of the amino acid side chain was directly affecting the yield of FAME. [97, 130]

1.9.10 THE REACTOR MATERIAL

The metal walls of the reactor can also be used to catalyse the reaction. Suppes et al. investigated the effect of different metals which can be used to make up the inside of a reactor. [103] The reactions were carried out at 120 ºC over a 24 hour period with a 6:1 molar ratio of methanol and 10 wt% catalyst.

Catalyst	% Conversion of FAME
Nickel	53
Palladium	29
Stainless steel	3.9
ZnO	80
Cast iron	3.1

Table 1.6 The effect on FAME yield of using various base metals (10 wt%) as catalysts

The researchers suggested that future reactor technology could incorporate a nickel / steel framework that would be beneficial to producing faster reaction rates.

1.10 ENZYMATIC CATALYSIS

A large proportion of organisms have the ability to catalyse the production of FFA from triglyceride oils. This is achieved by an enzyme called a lipase, which is the general term for any water-soluble enzyme which can bring about the hydrolysis of lipid substrates. For example, the main enzyme (HPL) responsible for breaking down fats in the pancreas converts the triglycerides into two equivalents of FFA leaving the resulting monoglyceride molecule. Lipase substrates function best between 30-40 º C, and are present in almost all living organisms including bacteria and even certain viruses.

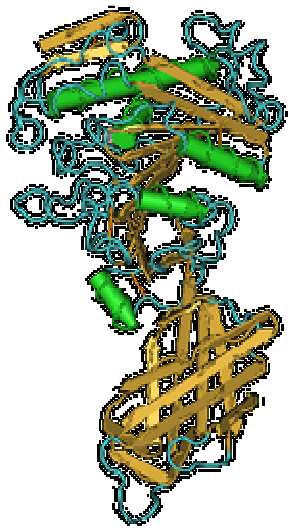

Figure 1.15 Computer generated image of the lipase enzyme PLRP2, a common lipase

Lipases do not only catalyse hydrolysis reactions but can also, in the presence of alcohol cause the esterification and transesterification of vegetable and animal oils. In general lipases catalyse the reaction of longer chain alcohols (i.e. butanol) more efficiently than with shorter chain alcohols, an excess of methanol can even inactivate the catalyst. Lipases catalyse reactions more efficiently when the substrates are miscible, in the case of methanol and ethanol, this is not the case. The short chain alcohol (<3 carbon atoms) form droplets in solution, and will destabalise the protein catalyst if present in large quantities. Using a co-solvent (larger chain alcohol, hexane, tetrahydrofuran etc.) can

dissolve the alcohol preventing the formation of large droplets, however this can be costly and decrease the theoretical yield of FAAEs. Enzymes can also be regenerated after deactivation by submersion in a long chain alcohol. The addition of one equivalent (the stoichiometry needed for complete reaction is at least three) of methanol does not destabilise the catalyst and within 5-10 hours in a fixed bed reactor has completely reacted. Two other equivalents can then be added together, as the presence of glycerol from the first reaction stops the formation of large droplets on the surface of the protein, and within 24-48 hours the vegetable oil has been completely converted to FAME, as shown below. [131]

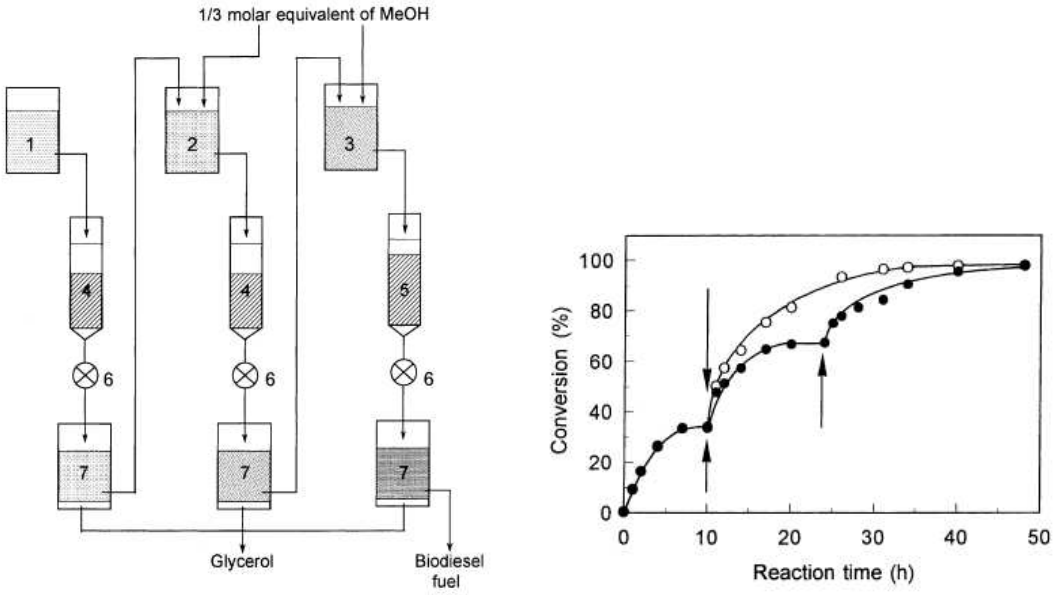

Figure 1.16 Flow diagram and reaction conversion for the sequential addition of methanol to avoid catalyst poisoning, taken from Schimada et al. [131]

Lipase catalysed FAAE reactions have been extensively researched, with lipases being developed which can perform both esterification and transesterification reactions of waste oils [132] However, the rates of reaction can be severely diminished by the presence of water and gumming oligomeric compounds. [131]

There are two reviews on the use of enzymes for esterifications and other industrial synthesis. [133, 134] Kinetic measurement and mathematical modelling have also been undertaken for the transesterification reaction. [135, 136]

The lipase can be used with no modification (water soluble), with the whole cell that it was created in, or anchored on to an insoluble substrate (immobilisation). The

lipase solubility can create problems when reusing the catalyst, it is also highly expensive to refine certain lipases, it is thus more favourable for the whole cell to be used. Lipases are most commonly immobilised for the production of biodiesel, where the particle size of the surface and the surface area play important roles in the activity.[137] The typical catalyst loading for an enzymatic reaction is similar to that of the heterogeneous catalysed reaction, and most enzymes display a higher reactivity towards the esterification of unsaturated cis-fatty acids than the saturated counterparts. Counterintuitively, the presence of water in the oil can assist the production of FAME due to the increased miscibility of the reactants.

Candida Antarctica is a strain of yeast which belongs to the Candida genus. It is easy to grow under laboratory conditions and produces a lipase that when supported is commercially available as Novozym 435. By far the most commonly used enzyme for biodiesel production is Novozym 435 produced from this yeast strain [138-152] The two most commonly associated problems with using lipases as the catalyst in this reaction is their cost and the poisoning of the enzymes by an excess of alcohol or glycerol. The table presented below summarizes the research being undertaken to alleviate these problems.

Lipase	Feedstock	Solvents	Conditions			Notes	Ref
			Time (Hrs)	MeOH: Oil	Wt %		
Burkholderias cepacia (IM BS-30)	Grease (high FFA)	Ethanol	8-48	4:1		Continuous reactor technology	[153]
Candida Antartica (Novozyme 435)	Vegetable oil / waste oils	t-butanol, THF, methanol, methyl acetate [144]	7-24	4-12:1	2-30	Continuous reactor [138] In silica aerogel [139] On acrylic resin [140] Water tolerance [141, 142] Glycerol removal [146]	[152]
Candida cylindracea	Waste oil	n hexane / primary alcohols	8			Waste stream containing some triglycerides	[154]
Chromobacterium viscosum (immobilised on celite)	Jatropha	Methanol, ethanol	8				
Lipase PS from Pseudomonas cepacia (immobilised)	Madhuca indica Soybean oil	Water / methanol ethanol, methyl acetate	0.5-6	7-15:1	5	The conversion of a high FFA content oil, using protein coats	[132] [155] [156]

Lipase	Feedstock	Solvents	Conditions			Notes	Ref
			Time (Hrs)	MeOH: Oil	Wt %		
Psychrophilic lipase			3				[157]
Rhizomucor miehei	Refined soybean oil	n hexane / methanol	0.5	2.4:1	9	Surface studies also carried out.	[158] [159]
Rhizopus oryzae (IFO 4697), whole cell	Soybean oil	Methanol	10-30	1:1		Sequential addition of methanol	[160] [161]
Thermomyces lanuginose Novozym 435 (combined)	Soybean oil deodorizer distillate (SODD)	t-Butanol / methanol	8-25	3.9:1	3 & 2 (Tl : N435)	Highly reusauable (over 120 cycles), water removed by mol. sieves	[162]
Thermomyces lanuginosus (Lipozyme TL –IM)	Soybean oil	methanol	12	3:2	4-10	Continuous reactor technology	[163, 164] [165]

Table 1.7 Summary of a range of lipases utilised as catalysts in the production of biodiesel

1.11 ANALYTICAL TECHNIQUES

A range of chromatographic and spectroscopic techniques are available to determine the purity and composition of samples of biodiesel. All techniques have both positive and negative qualities in determining biodiesel content and are usefully employed at some point in the production chain. The ideal analytical method would be both fast, up to on-line sampling speeds, and be able to detect trace amounts of all the contaminants legislated for. An analytical technique must be able to determine the ratios of different levels of saturation, variable chain length and isomerization of the resulting FAAE also. For a complete quantitative analysis of a sample of biodiesel two or more techniques are normally used. [166]

1.11.1 CHROMATOGRAPHIC TECHNIQUES

Chromatographic analysis is a series of closely related techniques which separate components in a mixture. This is made possible by the distribution of components across a mobile (liquid or gas) and stationary phase (high surface area solid). It is the varying strength of interactions with these phases that different components display which allows the separation. After separation a range of techniques can be used to further investigate the different components including mass spectrometry and infra red spectroscopy.

1.11.1.1 Thin Layer Chromatography (TLC)

TLC is the easiest chromatographic technique to use, and involves an adsorbent stationary phase (usually silica gel or cellulose) which is supported on an inert sheet. The liquid phase consists of a solution of solvent and the biodiesel analyte. The solution is then drawn up the plate via a capillary action and the products separate out according to the solubility in the solvent and attraction to the stationary phase. An example of a TLC analysis of an incomplete biodiesel reaction is shown below. The spots from left to right are 100% soybean oil (0.56% FFA content), 100% soybean methyl ester, Barium hydroxide catalysed mixture and calcium methoxide catalysed mixture.

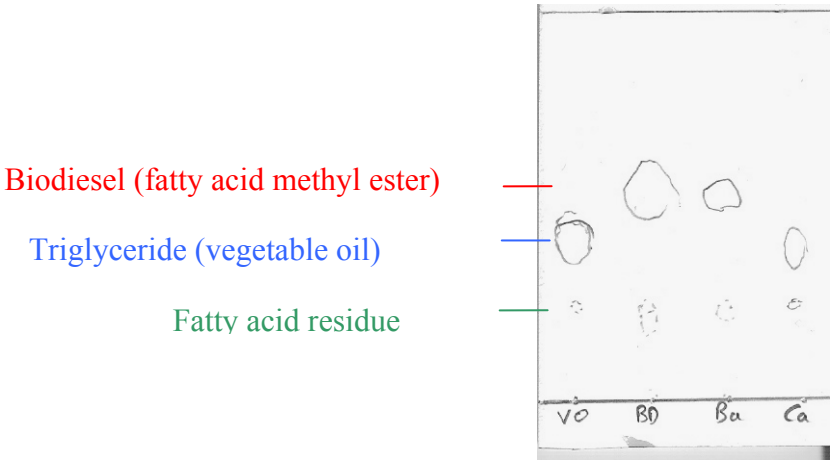

Figure 1.17 A TLC plate, showing the separation of biodiesel and vegetable oil using a solvent mixture of petroleum ether, diethyl ether and acetic acid in a ratio of 85:15:1

TLC is an easy to use and quick method of analysis however it is a qualitative measure only and provides no structural data on the resulting FAAE. [167]

1.11.1.2 Gas Chromatography (GC)

Is the type of chromatography the mobile phase is a carrier gas (usually helium, nitrogen or hydrogen) and the stationary phase is either a layer of liquid or a supported polymer. The stationary phase will interact with the components in the gaseous phase causing each component to adsorb at a different rate and therefore exit the end of the column separately (retention time), the flow rate of the gas and temperature can be altered to achieve acceptable resolutions. GC standards are necessary to be able to quantify the data however it is probably the most widely used technique in determining the composition of biodiesel samples.

GC is widely used in the determination of biodiesel samples as the techniques can be used for the quantification of esters in a sample as well as glycerol and methanol contaminants. [29, 168, 169] The determination of glycerol, methanol and the acylglycerides can be achieved simultaneously by GC. [170] Typically fused-silica capillary columns coated with a 0.1 µm film of (5%-phenyl)-methylpolysiloxane of up to 15m length are used. [171]

Two types of detectors are used for biodiesel analysis, the flame ionisation detector (FID) [172] and mass spectrometric detectors (MSD). [169, 173] The flame ionisation technique is easier and cheaper to implement however ambiguities in the eluting materials cannot be verified, though the ambiguities can be decreased by using a liquid chromatographic technique first (LC-GC). [174] Using a GC-MS technique has the major advantage of being able to determine the varying molecular weights of the sample being eluted. Therefore the structure of the FAAE can be examined also. Other Contaminants such as sterols and sterol esters can also be detected. With the GC-MS technique a sample of biodiesel can be assessed for most known contaminants and structural information (chain length, saturation and alcohol moiety) can be obtained for the FAAE.

1.11.1.3 High Performance Liquid Chromatography (HPLC)

HPLC is a form of liquid chromatography where the components of the mixture are separated by their chemical interactions with the chromatographic column. In HPLC analysis the mobile phase can be non polar, with the stationary phase being polar (Normal Phase HPLC). Alternatively Reversed Phase HPLC (RP-HPLC) can be used where the mobile phase is polar and the stationary phase is non polar. RP-HPLC separates components based on polarity, the lower the polarity the longer the retention time. This retention time can then be increased by adding a more polar solvent to the liquid phase or decreased by the addition of a non-polar solvent.

HPLC is a powerful technique in determining the yields of separate components in the biodiesel mixture. One advantage over GC is that an HPLC analysis is a lot less time consuming and only needs a fraction of the amount of sample. HPLC is used mainly for the quantification of various degrees of conversion during the biodiesel reaction, yet can be adapted for the measurement of alcohol and glycerol contaminants. A series of detectors have been examined for their use in RP-HPLC of biodiesel samples. Atmospheric Pressure Chemical Ionization Mass Spectrometry (APCI-MS) was found to be the most accurate and suitable detection method when coupled with HPLC. Like GC, to return quantifiable results the machine must be calibrated with known amounts of the reaction constituents.

1.11.1.4 Gel Permeation Chromatography (GPC)

Molecules can also be separated by their relative sizes. Size exclusion chromatography is normally used for polymers and other very large molecules, when using an organic solvent to transport the analyte, the technique is termed Gel Permeation Chromatography (GPC). GPC is normally used to analyze the molecular weight distribution of soluble polymers such as polylactide. The stationary gel medium, which the molecule is forced through, can be made from a range of compounds such as dextrin or polystyrene. The column consists of tightly packed extremely porous polymer beads. The pores have depressions and channels running from the surface and as the solution travels down the column particles enter into the pores, the larger the molecules cannot enter so many pores, and the smaller the overall volume to traverse is and the faster the elution time.

GPC can be applied to biodiesel analysis and is very similar to HPLC in instrumentation and what can be inferred from the resulting chromatograph. [175] The reproducibility of the chromatograph is very good, however it can be difficult to get exact values for the triglyceride and diglyceride peaks as there is almost always an amount of overlap. [176]

1.11.2 SPECTROSCOPIC TECHNIQUES

1.11.2.1 Nuclear Magnetic Resonance (NMR)

The most useful technique is ^{1}H NMR, [177] but ^{13}C NMR can be used in limited circumstances and ^{31}P NMR can be used for detecting traces of phosphorous containing compounds in a sample. For a ^{1}H NMR sample the glycerol needs to be separated out from the reaction mixture and the remaining oils dissolved in deuterated chloroform. The amount of glyceride (the sum of tri, di and mono), FAAE and methanol can be quantified. The level of saturation and the orientation of the double bonds can also be quantified. [178] An example of a spectrum is given below.

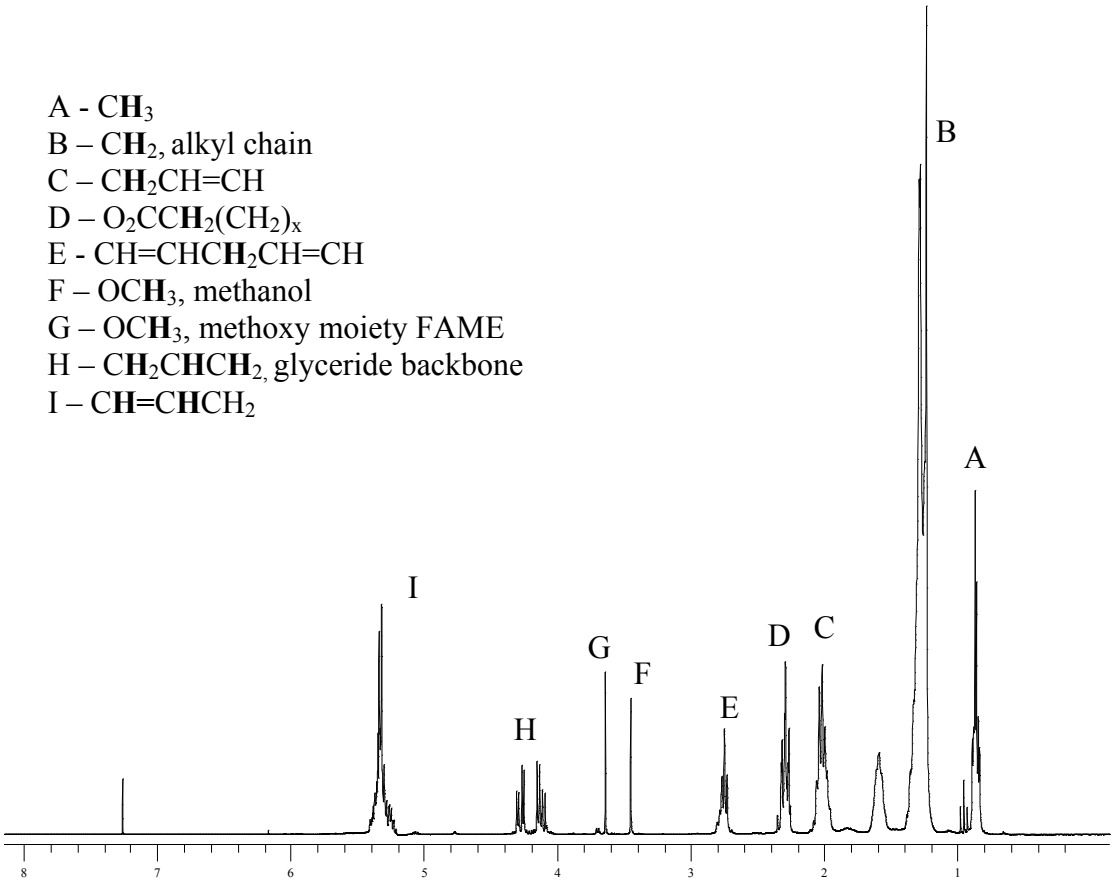

Figure 1.18 ^{1}H NMR spectrum of a blend of FAME and soybean oil the relevant peaks are labelled A-I

1.11.2.2 Fourier Transform-Infra Red Spectroscopy (FT-IR)

FT-IR is used to determine relative amounts of biodiesel to acylglycerides, the results of which show a close correlation to results derived from other techniques. [178] The methyl esters display peaks at 6005 cm^{-1} and 4425-4430 cm^{-1}, where the acyl glycerides only exhibit shoulders. Contaminants, in the levels stipulated by legal specifications, cannot be detected by IR spectroscopy. Using other techniques however combined with IR can cut the cost and time of the analysis than just using the first technique alone.

1.11.3 MISCELLANEOUS TECHNIQUES

1.11.3.1 Viscosity

The viscosity of vegetable oil and the pure alkyl esters is an order of magnitude apart. The viscosity difference can then be used as an analytical tool to determine the level of vegetable oil remaining in the methyl ester. This method was found to be suitable in determining biodiesel samples of up to 98% purity. [179]

1.12 CLOSING REMARKS

In the search to reduce dependence on foreign oil imports, reduce global greenhouse emissions and replace depleting oil feedstocks a viable replacement technology for transport fuels is being sort. Currently biodiesel is produced from virgin vegetable oils however these feedstocks are both expensive and in the case of rapeseed or soybean oil, are in direct competition with food produce. Waste oils from commercial and industrial sources avoid both of these problems, however, this low quality feedstock also contains FFA and water both of which cause processing issues due to the inactivation of the alkali catalyst and the formation of soaps.

Previous work researching the catalysis of low quality feedstocks have focussed on heterogeneous basic catalysts with very few homogeneous systems being researched at all. Few hetero- or homogeneous systems have been reported that are not deactivated by water. Kiss et al. showed that it is possible to esterify the FFA with an acidic catalyst and then (after a separation step) affect a transesterification with a second basic catalyst to produce biodiesel from the triglyceride molecule. However, this two step approach negates the low cost of the feedstock. There is a subsequently a need for a catalyst which can convert both feedstocks in a step reaction and is not deactivated by the presence of water, as well as other organic molecules present in waste oil.

The following chapters will chart the attempts to design such a catalytic system, by investigating a number of titanium alkoxides and zinc carboxylate systems for their catalytic prowess and the effect that water and FFA have on this activity.

1.13 REFERENCES

1. G. Knothe, J. Van Gerpen and J. Krahl., *The Biodiesel Handbook*, AOCS Press, Campaign, IL, 2005.
2. *US Department of Energy*, http://www.eia.doe.gov, Accessed March 2007.
3. *The European Biodiesel Board*, www.ebb-eu.org, March 2007.
4. A. C. Pinto, L. L. N. Guarieiro, M. J. C. Rezende, N. M. Ribeiro, E. A. Torres, W. A. Lopes, P. Pereira and J. B. der Andrade, *Journal of the Brazilian Chemical Society*, 2005, **16**, 1313-1330.
5. C. S. Wassell and T. P. Dittmer, *Energy Policy*, 2006, **34**, 3993-4001.
6. F. Ma and M. A. Hanna, *Bioresource Technology*, 1999, **70**, 1-15.
7. A. Demirbas, *International Journal of Green Energy*, 2007, **4**, 15-26.
8. K. Scharmer, *Biodiesel: Energy and Environmental Evaluation Rapeseed-Oil-Methyl-Ester*, Gesellschaft fur Entwicklungstechnologie mbH, Aldenhoven, 2001.
9. L. C. Meher, D. Vidya Sagar and S. N. Naik, *Renewable and Sustainable Energy Reviews*, 2006, **10**, 248-268.
10. P. Q. E. Clothier, B. D. Aguda, A. Moise and H. O. Pritchard., *Chemical Society Reviews*, 1993, 101-108.
11. H. E. Hoydonckx, D. E. De Vos, S. A. Chavan and P. A. Jacobs, *Topics in Catalysis*, 2004, **27**, 83-96.
12. P. Bondoli, *Topics in Catalysis*, 2004, **27**, 77-82.
13. U. Schuchardt, R. R. Sercheli and M. Vargas, *Journal of the Brazilian Chemical Society*, 1998, **9**, 199-210.
14. J. Sheehan, V. Camobreco, J. Duffield, M. Graboski and H. Shapouri., *Final Report, Life Cycle Inventory of Biodiesel and Petroleum Diesel for Use in an Urban Bus,* NREL-SR-580-24089, National Renewable Energy Laboratory, CO, 1998.
15. A. Niedrerl and M. Narodoslawsky, *Life Cycle Assessment - study of Biodiesel from Tallow and Used Vegetable Oil*, Institute for Resource Efficient and Sustainable Systems, Graz, 2004.

16. A. E. Landis, S. A. Miller and T. L. Theis, *Environmental Science Technology*, 2007, **41**, 1457-1464.
17. M. G. Kulkarni and A. K. Dalai, *Industrial & Engineering Chemistry Research*, 2006, **45**, 2901-2913.
18. Y. Zhang, M. A. Dube, D. D. McLean and M. Kates, *Bioresource Technology*, 2003, **90**, 229-240.
19. Y. Zhang, M. A. Dube, D. D. McLean and M. Kates, *Bioresource Technology*, 2003, **89**, 1-16.
20. G. W. Huber, S. Iborra and A. Corma, *Chemical Reviews*, 2006, **106**, 4044-4098.
21. D. Mohan, C. U. Pittman and P. H. Steele, *Energy & Fuels*, 2006, **20**, 848-889.
22. S. Fernando, S. Adhikari, C. Chandrapal and N. Murali, *Energy & Fuels*, 2006, **20**, 1727-1737.
23. R. Montgomery, *Bioresource Technology*, 2004, **91**, 1-29.
24. *Straight Vegetable Oil as a Diesel Fuel*, Clean Cities Fact Sheet, The U.S. Department of Energy National Laboratory, Columbus, OH, 2006.
25. C. E. Goering and B. Fry, *Journal of the American Oil Chemists Society*, 1984, **61**, 1627-1632.
26. A. W. Schwab, H. C. Nielsen, D. D. Brooks and E. H. Pryde, *Journal of Dispersion Science and Technology*, 1983, **4**, 1-17.
27. D. G. Lima, V. C. D. Soares, E. B. Ribeiro, D. A. Carvalho, E. C. V. Cardoso, F. C. Rassi, K. C. Mundim, J. C. Rubim and P. A. Z. Suarez, *Journal of Analytical and Applied Pyrolysis*, 2004, **71**, 987-996.
28. F. A. Twaiq, N. A. M. Zabidi and S. Bhatia, *Industrial & Engineering Chemistry Research*, 1999, **38**, 3230-3237.
29. B. Freedman, W.F. Kwolek and E. H. Pryde, *Journal of the American Oil Chemists Society*, 1986, **63**, 1370-1375.
30. B. Freedman, R. O. Butterfield and E. H. Pryde, *Journal of the American Oil Chemists Society*, 1986, **63**, 1375-1380.
31. H. Noureddini and D. Zhu, *Journal of the American Oil Chemists Society*, 1997, **74**, 1457-1463.
32. M. Reimer and H. R. Downes, *Journal of the American Chemical Society*, 1921, **43**, 945-951.

33. J. Otera, *Chemical Reviews*, 1993, 1449-1470.
34. O. Meth-Cohn, *Journal of the Chemical Society, Chemical Communications*, 1986, 695-697.
35. M. G Stanton, C. B. Allen, R. M. Kissling, A. L. Lincoln and M. R. Gagne, *Journal of the American Chemical Society*, 1998, **120**, 5981-5989.
36. M. G. Stanton and M. R. Gagne, *Journal of the American Chemical Society*, 1997, **119**, 5075-5076.
37. G. Vicente, M. Martinez, J. Aracil and A. Esteban, *Industrial & Engineering Chemistry Research*, 2005, **44**, 5447-5454.
38. S. Gryglewicz, *Bioresource Technology*, 1999, **70**, 249-253.
39. L. S. Liu, *Journal of the American Oil Chemists Society*, 2004, **81**, 331-337.
40. B. Freedman, E. H. Pryde and T. L. Mounts, *Journal of the American Oil Chemists Society*, 1984, **61**, 1638-1643.
41. R. W. Taft, M. S. Newman and F. H. Verhoek, *Journal of the American Chemical Society*, 1950, **72**, 959-968.
42. M. J. Goff, N.S. Bauer, S. Lopes, W.R. Sutterlin and G. J. Suppes, *Journal of the American Oil Chemists Society*, 2004, **81**, 415-420.
43. A. W. Schwab, M. O. Bagby and B. Freedman, *Fuel*, 1987, **66**, 1372-1378.
44. M. J. Haas, P. J. Michalski, S. Runyon, A. Nunez and K. M. Scott, *Journal of the American Oil Chemists Society*, 2003, **80**, 97-102.
45. K. S. Liu, *Journal of the American Oil Chemists Society*, 1994, **71**, 1179-1187.
46. R. G. Bray, *Biodiesel Production*, http://www.sriconsulting.com, Accessed Februray, 2007.
47. D. Kusdiana and S. Saka, *Fuel*, 2001, **80**, 225-231.
48. S. Saka, D. Kusdiana and E. Minami, *Journal of Scientific & Industrial Research*, 2006, **65**, 420-425.
49. D. Kusdiana and S. Saka, *Fuel*, 2001, **80**, 693-698.
50. M. J. Haas, K. M. Scott, W. N. Marmer and T. A. Foglia, *Journal of the American Oil Chemists Society*, 2004, **81**, 83-89.
51. S. K. Karmee, P. Mahesh, R. Ravi and A. Chadha, *Journal of the American Oil Chemists Society*, 2004, **81**, 425-429.
52. S. Siler-Marinkovic and A. Tomasevic, *Fuel*, 1998, **77**, 1389-1391.

53. D. Nimcevic, R. Puntigam, M. Worgetter and J. R. Gapes, *Journal of the American Oil Chemists Society*, 2000, **77**, 275-280.
54. M. J. Haas, *Fuel Processing Technology* 2005, **86**, 1087-1096.
55. B. Supple, R. Howard-Hildige, E. Gonzalez-Gomez and J. J. Leahy, *Journal of the American Oil Chemists Society*, 2002, **79**, 175-178.
56. J. C. Yori, S. A. D'Ippolito, C. L. Pieck and C. R. Vera, *Energy Fuels*, 2007, **21**, 347-353.
57. M. Noordam and R. Withers., *Producing Biodiesel from Canola in the Inland Northwest: An Economic Feasibility Study.*, University of Idaho, The College of Agriculture, Moscow, ID, 1996.
58. *Directive 75/439/EEC on Waste Oils*, 2005.
59. J. Cvengros and Z. Cvengrosova, *Biomass & Bioenergy*, 2004, **27**, 173-181.
60. M. Canakci, *Bioresource Technology*, 2007, **98**, 183-190.
61. *Draft EU Directive on the use of Biofuels*, 2004, 1-7.
62. W. W. Nawar, *Journal of Chemical Education* 1984, **61**, 299-302.
63. M. Mittelbach and H. Enzelsberger, *Journal of the American Oil Chemists Society*, 1999, **76**, 545-550.
64. F. J. Guesta, C. Sanchex-Muniz, S. Polonio-Garrido, V. Lopez and R. Arroyo., *Journal of the American Oil Chemists Society*, 1993, **70**, 1069-1073.
65. M. Mittelbach and H. Enzelsberger, *Journal of the American Oil Chemists Society*, 1999, **76**, 545-550.
66. Y. Wang, S. Y. Ou, P. Z. Liu and Z. S. Zhang, *Energy Conversion and Management*, 2007, **48**, 184-188.
67. J. M. Encinar, J. F. Gonzalez and A. Rodriguez-Reinares, *Industrial & Engineering Chemistry Research*, 2005, **44**, 5491-5499.
68. Y. Wang, S. Y. Ou, P. Z. Liu, F. Xue and S. Z. Tang, *Journal of Molecular Catalysis A-Chemical*, 2006, **252**, 107-112.
69. M. J. Haas, K. M. Scott, T. L. Alleman and R. L. McCormick, *Energy & Fuels*, 2001, **15**, 1207-1212.
70. S. Lebedevas, A. Vaicekauskas, G. Lebedeva, V. Makareviciene, P. Janulis and K. Kazancev, *Energy & Fuels*, 2006, **20**, 2274-2280.
71. M. Cetinkaya, Y. Ulusoy, Y. Tekin and F. Karaosmanoglu, *Energy Conversion and Management*, 2005, **46**, 1279-1291.

72. A. A. Kiss, F. Omota, A. C. Dimian and G. Rothenberg, *Topics in Catalysis*, 2006, **40**, 141-150.
73. A. A. Kiss, A. C. Dimian and G. Rothenberg, *Advanced Synthesis & Catalysis*, 2006, **348**, 75-81.
74. L. C. Meher, M. G. Kulkarni, A. K. Dalai and S. N. Naik, *European Journal of Lipid Science and Technology*, 2006, **108**, 389-397.
75. R. O. Dunn, *Journal of the American Oil Chemists Society*, 2002, **79**, 915-920.
76. J. C. Thompson, C. L. Peterson, D. L. Reece and S. M. Beck, *Transactions of the Asae*, 1998, **41**, 931-939.
77. P. Bondioli, A. Gasparoli, A. Lanzani, E. Fedeli, S. Veronese and M. Sala, *Journal of the American Oil Chemists Society*, 1995, **72**, 699-702.
78. A. Monyem, M. Canakci and J. H. Van Gerpen, *Applied Engineering in Agriculture*, 2000, **16**, 373-378.
79. P. Q. E. Clothier, B. D. Aguda, A. Moise and H. O. Pritchard, *Chemical Society Reviews*, 1993, **22**, 101-108.
80. D. Altiparmak, A. Keskin, A. Koca and M. Guru, *Bioresource Technology*, 2007, **98**, 241-246.
81. M. P. Dorado, E. Ballesteros, J. M. Arnal, J. Gomez and F. J. Lopez, *Fuel*, 2003, **82**, 1311-1315.
82. Y. Ali and M. A. Hanna, *Bioresource Technology*, 1994, **50**, 153-163.
83. D. Y. Z. Chang, J. H. VanGerpen, I. Lee, L. A. Johnson, E. G. Hammond and S. J. Marley, *Journal of the American Oil Chemists Society*, 1996, **73**, 1549-1555.
84. C. Peterson and D. Reece, *Transactions of the Asae*, 1996, **39**, 805-816.
85. K. McDonnell, S. Ward, J. J. Leahy and P. McNulty, *Journal of the American Oil Chemists Society*, 1999, **76**, 539-543.
86. D. Ryu, S. K. Katta, L. B. Bullerman, M. A. Hanna and A. Gennadios, *Transactions of the Asae*, 1996, **39**, 2001-2004.
87. R. C. Poller and S. P. Retout, *Journal of Organometallic Chemistry*, 1979, **173**, c7-c8.
88. R. Okawra and M. Wada, *Advances in Organometallic Chemistry*, 1967, **5**, 137-167.
89. J. Otera, Nobuhisa Dan-oh and H. Nozaki, *Journal of Organic Chemistry*, 1991, **56**, 5307-5311.

90. J. Otera, T. Yano, A. Kawabata. and H. Nozaki, *Tetrahedron Letters*, 1986, **27**, 2383-2386.

91. D. Dakternieks, A. Duthis, B. Zobel, K. Jurkschat and M. Schurmann, *Organometallics*, 2002, **21**, 647-652.

92. M. Mehring, M. Schurmann, I. Paulus, D. Horn, K. Jurkschat, A. Orita, J. Otera, D. Dakternieks and A. Duthie, *Journal of Organometallic Chemistry*, 1999, **574**, 176-192.

93. D. A. C. Ferreira, M. R. Meneghetti, S. M. P. Meneghetti and C. R. Wolf, *Applied Catalysis a-General*, 2007, **317**, 58-61.

94. F. R. Abreu, D. G. Lima, E. H. Hamu, S. Einloft, J. C. Rubim and P. A. Z. Suarez, *Journal of the American Oil Chemists Society*, 2003, **80**, 601-604.

95. F.R. Abreu, D.G. Lima, E.H. Hamu, C. Wolf and P. A. Z. Suarez, *Journal of Molecular Catalysis A: Chemical*, 2004, **209**, 29-33.

96. *United States Pat.*, US 5525126, 1996.

97. M. Di Serio, R. Tesser, M. Dimiccoli, F. Cammarota, M. Nastasi and E. Santacesaria, *Journal of Molecular Catalysis A-Chemical*, 2005, **239**, 111-115.

98. M. Gheorghiu, *United States Pat.*, US 5532392, 1996.

99. M. Mizukami, H. Harada, *Japan Pat.*, JP 09241213, 1997.

100. U. Schuchardt, O. C. Lopes, *Brazil Pat.*, Br 82 02 429, 1984.

101. U. Schuchardt, R. M. Vargas and G. Gelbard, *Journal of Molecular Catalysis A: Chemical*, 1996, **109**, 37-44.

102. E. Leclercq, A. Finiels and C. Moreau, *Journal of the American Oil Chemists Society*, 2001, **78**, 1161-1165.

103. G. J. Suppes, A. D. Mohanprasad, E. J. Doskocil, P. J. Mankidy and M. J. Goff, *Applied Catalysis A: General*, 2004, **257**, 213-223.

104. W. L. Xie, X. M. Huang and H. T. Li, *Bioresource Technology*, 2007, **98**, 936-939.

105. W. L. Xie, H. Peng and L. G. Chen, *Applied Catalysis A-General*, 2006, **300**, 67-74.

106. W. L. Xie and H. T. Li, *Journal of Molecular Catalysis A-Chemical*, 2006, **255**, 1-9.

107. H. J. Kim, B. S. Kang, M. J. Kim, Y. M. Park, D. K. Kim, J. S. Lee and K. Y. Lee, *Catalysis Today*, 2004, **93-95**, 315-320.

108. W. L. Xie and X. M. Huang, *Catalysis Letters*, 2006, **107**, 53-59.
109. G.J. Suppes, K. Bockwinkel, S. Lucas, J.B. Botts, M.H. Mason and J. A. Heppert, *Journal of the American Oil Chemists Society*, 2001, **78**, 139-145.
110. T. F. Dossin, M. F. Reyniers, R. J. Berger and G. B. Marin, *Applied Catalysis B-Environmental*, 2006, **67**, 136-148.
111. M. Nakayama, K. Tsuto, T. Hirano, *Japan Pat.*, JP 2002294277, 2001.
112. C. Reddy, V. Reddy, R. Oshel and J. G. Verkade, *Energy & Fuels*, 2006, **20**, 1310-1314.
113. D. G. Cantrell, L. J. Gillie, A. F. Lee and K. Wilson, *Applied Catalysis A-General*, 2005, **287**, 183-190.
114. D. E. Lopez, J. G. Goodwin and D. A. Bruce, *Journal of Catalysis*, 2007, **245**, 381-391.
115. Y. J. Liu, E. Lotero and J. G. Goodwin, *Journal of Catalysis*, 2006, **243**, 221-228.
116. N. Shibasaki-Kitakawa, H. Honda, H. Kuribayashi, T. Toda, T. Fukumura and T. Yonemoto, *Bioresource Technology*, 2007, **98**, 416-421.
117. L. Guerreiro, J. E. Castanheiro, I. M. Fonseca, R. M. Martin-Aranda, A. M. Ramos and J. Vital, *Catalysis Today*, 2006, **118**, 166-171.
118. M. Okamura, A. Takagaki, M. Toda, J. N. Kondo, K. Domen, T. Tatsumi, M. Hara and S. Hayashi, *Chemistry of Materials*, 2006, **18**, 3039-3045.
119. M. Toda, A. Takagaki, M. Okamura, J. N. Kondo, S. Hayashi, K. Domen and M. Hara, *Nature*, 2005, **438**, 178-178.
120. M. Zong, Z. Duana, W. Loua, T. J. Smith and H. Wua., *Green Chemistry*, 2007, **9**, 434-437.
121. S. Furuta, H. Matsuhashi and K. Arata, *Catalysis Communications*, 2004, **5**, 721-723.
122. S. Furuta, H. Matsuhashi and K. Arata, *Biomass & Bioenergy*, 2006, **30**, 870-873.
123. W. Charusiri and T. Vitidsant, *Energy & Fuels*, 2005, **19**, 1783-1789.
124. M. G. Kulkarni, R. Gopinath, L. C. Meher and A. K. Dalai, *Green Chemistry*, 2006, **8**, 1056-1062.
125. F. Chai, F. Cao, F. Zhai, Y. Chen, X. Wang and Z. Su, *Advanced Synthesis & Catalysis*, 2007, **349**, 1057-1065.

126. B. Delfort, G. Hillion, D. Le Pennec, *United States Pat.*, US 7151187, 2006.
127. R. Stern, G. Hillion, J. Rouxel, *United States Pat.*, US 5908946, 1999.
128. R. Srivastava, D. Srinivas and P. Ratnasamy, *Journal of Catalysis*, 2006, **241**, 34-44.
129. P. S. Sreeprasanth, R. Srivastava, D. Srinivas and P. Ratnasamy, *Applied Catalysis A-General*, 2006, **314**, 148-159.
130. S. K. F. Peter, R. Ganswindt, H. Neuner and E. Weidner, *European Journal of Lipid Science and Technology*, 2002, **104**, 324-330.
131. Y Schimada, Y. Watanabe, A. Sugihara and Y. Tominaga, *Journal of Molecular Catalysis B: Enzymatic*, 2002, **17**, 133-142.
132. V. Kumari, S. Shah and M. N. Gupta, *Energy & Fuels*, 2007, **21**, 368-372.
133. F. Hasan, A. A. Shah and A. Hameed, *Enzyme and Microbial Technology*, 2006, **39**, 235-251.
134. L. Deng, X. B. Xu, G. G. Haraldsson, T. W. Tan and F. Wang, *Journal of the American Oil Chemists Society*, 2005, **82**, 341-347.
135. S. Al-Zuhair, *Journal of Chemical Technology and Biotechnology*, 2006, **81**, 299-305.
136. S. Al-Zuhair, *Biotechnology Progress*, 2005, **21**, 1442-1448.
137. E. Y. Park, M. Sato and S. Kojima, *Enzyme and Microbial Technology*, 2006, **39**, 889-896.
138. D. Royon, M. Daz, G. Ellenrieder and S. Locatelli, *Bioresource Technology*, 2007, **98**, 648-653.
139. O. Orcaire, P. Buisson and A. C. Pierre, *Journal of Molecular Catalysis B-Enzymatic*, 2006, **42**, 106-113.
140. M. Mahabubur, R. Talukder, S. M. Puah, J. C. Wu, C. J. Won and Y. Chow, *Biocatalysis and Biotransformation*, 2006, **24**, 257-262.
141. T. W. Tan, K. L. Nie and F. Wang, *Applied Biochemistry and Biotechnology*, 2006, **128**, 109-116.
142. R. Brenneis, B. Baeck and G. Kley, *European Journal of Lipid Science and Technology*, 2004, **106**, 809-814.
143. L. Deng, T. W. Tan, F. Wang and X. B. Xu, *European Journal of Lipid Science and Technology*, 2003, **105**, 727-734.

144. Y. Y. Xu, W. Du, D. H. Lui and J. Zeng, *Biotechnology Letters*, 2003, **25**, 1239-1241.

145. J. W. Chen and W. T. Wu, *Journal of Bioscience and Bioengineering*, 2003, **95**, 466-469.

146. K. Belafi-Bako, F. Kovacs, L. Gubicza and J. Hancsok., *Biocatalysis and Biotransformation*, 2002, **20**, 437-439.

147. Y. Watanabe, P. Pinsirodom, T. Nagao, T. Kobayashi, Y. Nishida, Y. Takagi and Y. Shimada, *Journal of the American Oil Chemists Society*, 2005, **82**, 825-831.

148. Y. Watanabe, Y. Shimada, A. Sugihara and Y. Tominaga, *Journal of Molecular Catalysis B-Enzymatic*, 2002, **17**, 151-155.

149. O. Kose, M. Tuter and H. A. Aksoy, *Bioresource Technology*, 2002, **83**, 125-129.

150. F. Sanchez and P. T. Vasudevan, *Applied Biochemistry and Biotechnology*, 2006, **135**, 1-14.

151. D. Wei, Y. Y. Xu, Z. Jing and D. H. Liu, *Biotechnology and Applied Biochemistry*, 2004, **40**, 187-190.

152. W. Du, Y. Y. Xu, D. H. Liu and J. Zeng, *Journal of Molecular Catalysis B-Enzymatic*, 2004, **30**, 125-129.

153. A. F. Hsu, K. C. Jones, T. A. Foglia and W. N. Marmer, *Journal of the American Oil Chemists Society*, 2004, **81**, 749-752.

154. P. V. Lara and E. Y. Park, *Enzyme and Microbial Technology*, 2004, **34**, 270-277.

155. H. Noureddini, X. Gao and R. S. Philkana, *Bioresource Technology*, 2005, **96**, 769-777.

156. A. F. Hsu, K. C. Jones, T. A. Foglia and W. N. Marmer, *Biotechnology Letters*, 2004, **26**, 917-921.

157. Y. Luo, Y. T. Zheng, Z. B. Jiang, Y. S. Ma and D. X. Wei, *Applied Microbiology and Biotechnology*, 2006, **73**, 349-355.

158. S. Demirkol, H. A. Aksoy, M. Tuter, G. Ustun and D. A. Sasmaz, *Journal of the American Oil Chemists Society*, 2006, **83**, 929-932.

159. A. C. Oliveira and M. F. Rosa, *Journal of the American Oil Chemists Society*, 2006, **83**, 21-25.

160. J. Zeng, W. Du, X. Y. Liu, D. H. Liu and L. M. Dai, *Journal of Molecular Catalysis B-Enzymatic*, 2006, **43**, 15-18.
161. S. Hama, H. Yamaji, M. Kaieda, M. Oda, A. Kondo and H. Fukuda, *Biochemical Engineering Journal*, 2004, **21**, 155-160.
162. L. Wang, W. Du, D. H. Liu, L. L. Li and N. M. Dai, *Journal of Molecular Catalysis B-Enzymatic*, 2006, **43**, 29-32.
163. W. Du, Y. Y. Xu, D. H. Liu and Z. B. Li, *Journal of Molecular Catalysis B-Enzymatic*, 2005, **37**, 68-71.
164. W. Du, Y. Y. Xu and D. H. Liu, *Biotechnology and Applied Biochemistry*, 2003, **38**, 103-106.
165. Y. Y. Xu, W. Du, J. Zeng and D. H. Liu, *Biocatalysis and Biotransformation*, 2004, **22**, 45-48.
166. G. Knothe, *Transactions of the ASAE*, 2001, **44**, 193-200.
167. P. S. Devi, *Journal of the American Oil Chemists Society*, 2003, **80**, 315-318.
168. P. C. Fourie and D. S. Basson, *Journal of the American Oil Chemists Society*, 1990, **67**, 18-20.
169. M. Mittelbach, G. Roth and A. Bergmann, *Chromatographica*, 1996, **42**, 431-434.
170. C. Plank and E. Lorbeer, *Journal of Chromatography A*, 1995, **697**, 461-468.
171. Z. Cvengrosova, J. Cvengros and M. Hronec., *Petroleum and Coal*, 1997, **39**, 36-40.
172. F. Ulberth, R. G. Gabernig and F. Schrammel, *Journal of the American Oil Chemists Society*, 1999, **76**, 263-266.
173. M. Mittelbach, *Chromatographica*, 1993, **37**, 623-626.
174. M. Lechner, C. Bauer-Plank and E. Lorbeer, *Journal of High Resolution Chromatogaphy* 1997, **20**, 581-585.
175. D. Darnoko, M. Cheryan and E. G. Perkins, *Journal of Liquid Chromatography Related Technologies*, 2000, **23**, 2327-2335.
176. M. A. Dube, S. Zheng, D. D. McLean and M. Kates, *Journal of the American Oil Chemists Society*, 2004, **81**, 599-603.
177. G. Gelbard, O. Bres, R. M. Vargas, F. Vielfaure and U. F. Schuchardt, *Journal of the American Oil Chemists Society*, 1995, **72**, 1239-1241.
178. G. Knothe, *Journal of the American Oil Chemists Society*, 2001, **78**, 1025-1028.

179. P. De Filippis, C. Giavarini, M. Scarsella and M. Sorrentino, *Journal of the American Oil Chemists Society*, 1995, **72**, 1399-1404.

CHAPTER 2

METHANOL STABLE TITANIUM DIOLATE COMPLEXES

Surprisingly few examples of homogeneous Lewis acidic systems have been investigated as biodiesel catalysts. Homoleptic titanium alkoxides are potentially attractive for the synthesis of biodiesel as they are inexpensive, benign and are known to be highly active in various esterification reactions. This chapter deals with the synthesis and application of $Ti(O^iPr)_4$ and related complexes for the transesterification of vegetable oil.

2.1 INTRODUCTION

Metal alkoxides, of the general formula $[M(OR)_x]_n$, were synthesised as early as 1846 with the discovery of a boron and silicon alkoxide complex. Today the alkoxide derivatives of almost all the metals in the periodic table have been synthesised and characterised and this area has been extensively reviewed. [1]

Primarily titanium alkoxides are used as precursors to forming metal oxide films and ceramics. These applications are achieved by both chemical vapour deposition (MOCVD) or by certain sol-gel processes. [2-5] Due to the high Lewis acidity, the relative non-toxicity and inexpense of simple titanium alkoxides, a growing amount of research has been focussed on their applicability as industrial catalysts. [6] Titanium ethoxide and isopropoxide have been successfully used as catalysts for the polymerisation of olefins,[7, 8] epoxidations, [9] Diels-Alder synthesis [10] and esterification reactions.[11-13]

Titanium alkoxides are generally volatile and are soluble in common organic solvents. However, they tend to be highly reactive and especially prone to hydrolysis, making the preparation and handling of these compounds intricate. [14-17] There are a number of other chemical and physical attributes of titanium alkoxides that also need to be considered in respect to the biodiesel reaction

Simple industrially available titanium derivatives will react with almost all the components in the reaction mixture, one facile reaction is alcohol exchange. Two

factors are important in determining the favourability of this reaction; steric accessibility to the vacant d-orbitals on the titanium centre and the degree of association present in the formed alkoxide. Verma et al. investigated the susceptibility of titanium alkoxides to undergo exchange and established the following order of substitution. [18]

$$^{-}OMe > {}^{-}OEt > {}^{-}O^{i}Pr > {}^{-}O^{t}Bu$$

Figure 2.1 Order of susceptibility of $^{-}$OR groups to exchange in a titanium alkoxide

In the case of the methanolysis of titanium alkoxides the exchange is further facilitated by the formation of titanium methoxide, a highly stable, insoluble solid. Titanium alkoxides will aggregate in solution into oligomeric forms. Soluble titanium alkoxides are present in equilibrium, and generally form the monomeric and trimeric complexes. [19] Even though this equilibrium is concentration dependent, the larger the branching of the R group the closer the molecular complexity will be to 1.[14-16, 20, 21] The difference in the physical properties of the titanium methoxide is due to extensive aggregation into a stable tetrameric species, shown below in Fig. 2.2. This large stable aggregation is facilitated by the lack of steric hinderance of the alkoxide groups.

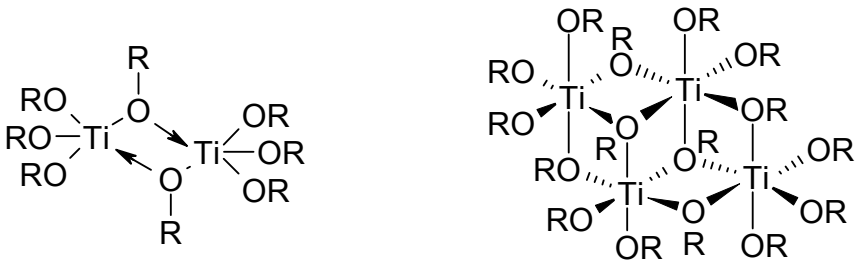

Figure 2.2 Alkoxo bridging prevalent in titanium alkoxides and the potential tetrameric titanium alkoxide aggregate

A transesterification reaction is also possible with the alkoxide being replaced by a longer chain alcohol moiety as shown below in Fig 2.3. [22] It is plausible that a similar reaction could take place between the titanium catalyst and the triglyceride molecule.

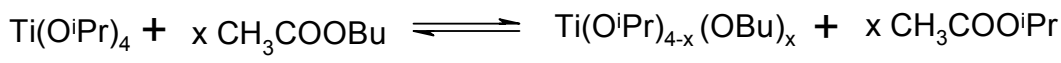

Figure 2.3 Transesterification reaction involving titanium isopropoxide and butyl acetate

In waste oils, large amounts of FFA and water are also present both of which react with titanium alkoxides. In the case of carboxylic acids a number of reactions are possible. [17, 23, 24] Primarily these reactions are thermodynamically favoured as the carboxylate moiety can bind through both the hydroxyl arm and carboxylate oxygen. Ultimately these reactions, involving the production of oxo species, yield a variety of products resulting in a higher degree of aggregation and loss of solubility. The general production of mixed carboxylate alkoxide complexes and the formation of oxo-species are shown below in Fig. 2.4.

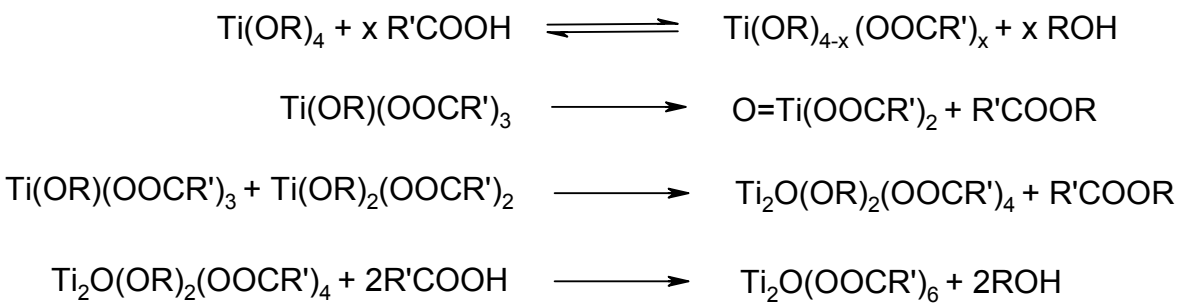

Figure 2.4 Various equations relating to the reaction of titanium alkoxides with carboxylic acids

The di-carboxylate/alkoxide titanium species is very stable but further reaction to the tri- or tetra- titanium carboxylates are unstable and are either not formed or decompose depending on the conditions. [12] All of these oxo complexes created are markedly less reactive than the original titanium alkoxide. [25, 26]

Titanium alkoxides readily undergo hydrolysis. The hydrolysis of these species is highly favourable and leads to the formation of the hydroxide and eventually the

oxide species. The water molecule will initially co-ordinate to the metal via the oxygen atom. Dealcoholation and eventual dehydration occur to form the extremely stable titanium dioxide.

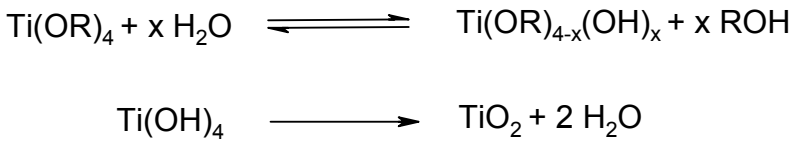

Figure 2.5 Hydrolysis products of titanium alkoxides

Despite the possible side reactions between the titanium catalyst and reactants, a number of papers have investigated their utility in both esterification and transesterification reactions. Krasik et al. prepared sterically hindered esters using titanium ethoxide as the transesterification catalyst. The researchers concluded that in reactions where the use of a strong acid or base is inappropriate, titanium ethoxide can be an efficient catalytic replacement. [11]

Blandy et al. following on from their investigations of stearic acid esterification using titanium isopropoxide and related alkoxides as catalysts, [27, 28] used these catalysts for the transesterification of methylmethacrylate with 1-dodecanol. [29] In this study they compared the homogeneous $Ti(O^iPr)_4$ with H_2SO_4 and found the titanate to be the far more efficient catalyst at temperatures exceeding 70 ºC. At much higher temperatures though, the titanium catalyst would oligomerise and a reduction in the activity was observed. To combat this effect the researchers heterogenised $TiCl(O^iPr)_3$ onto silica. This heterogeneous catalyst, while being less active than the $Ti(O^iPr)_4$, was still more efficient than either the homo- or heterogeneous (Amberlyst) Brønsted acid catalysts. Deluze et al. using similar techniques found these heterogenised titanium catalysts to be active for the esterification of saturated esters as well as vinyl esters with other alcohols. A further examination of these catalysts demonstrated that they were also active for epoxidations. [13, 30]

The mechanism of the transesterification of triglycerides using titanium alkoxide catalysts is more complicated than when using a Brønsted acid catalyst. Possible pathways to the formation of FAME are given below in Fig. 2.6.

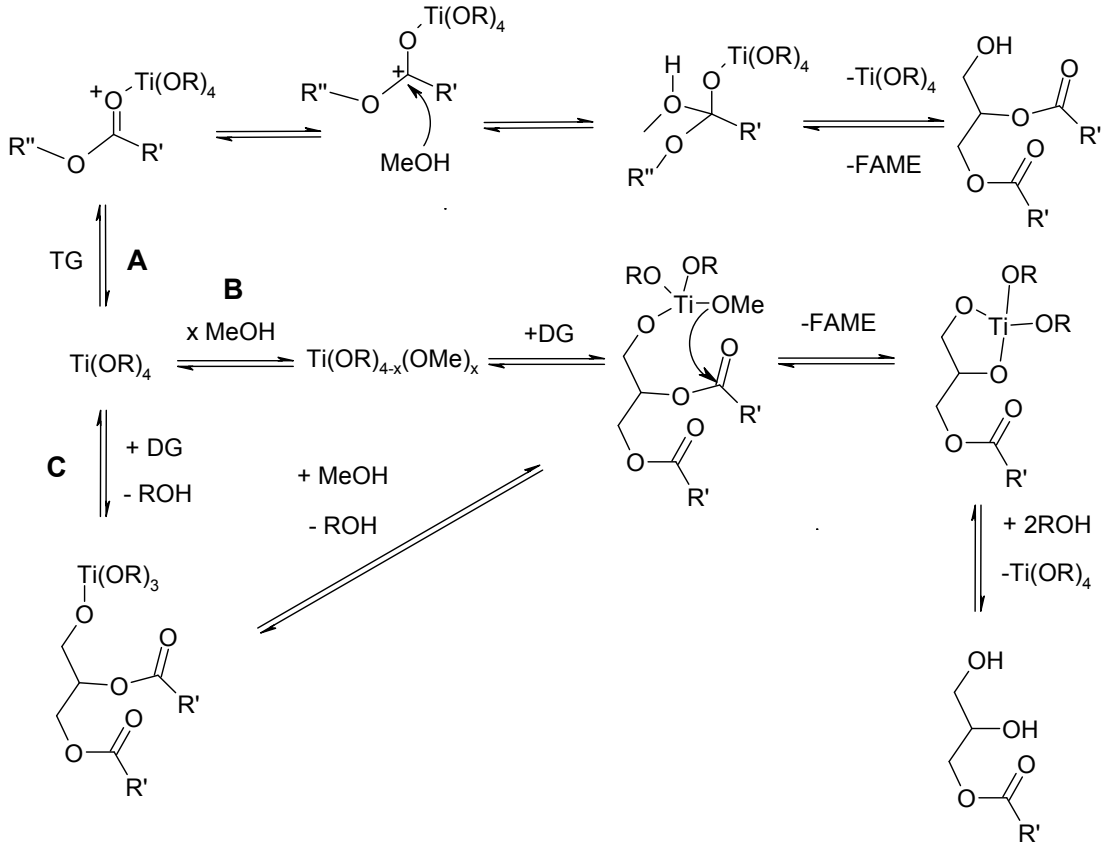

Figure 2.6 Three possible transesterification reactions catalysed by $Ti(OR)_4$, where R = Me, ^{i}Pr a glyceride or alkyl chain of the vegetable oil

The titanium species is likely to act in a similar manner to the Brønsted acid catalyst in the transesterification of the triglyceride molecule (**A**). However the titanium alkoxide catalyst can also react with methanol (**B**) or the resulting glyceride (**C**). Both of the resulting complexes can further react with the glyceride species to form FAME.

Despite the high Lewis acidity, inexpense and applicability in simpler transesterification reactions, simple titanium alkoxides are not suitable for the production of biodiesel. This is due to the competing hydrolysis and methanolysis reactions that the catalyst will undergo in the presence of these reagents. The products of these reactions, TiO_2 and $Ti(OMe)_4$, have a severely depleted catalytic activity.

A number of methods have been investigated to reduce the tendency of these metal alkoxides to react in this way. Firstly the incomplete reaction of the original titanium chloride with the alcohol (synthesised by the direct reaction between the two without a base) yields mixed halogenated alkoxide species' as shown below in Fig 2.7. The formation of one product selectively can be achieved by limiting the alcohol present or by varying the pH. [31]

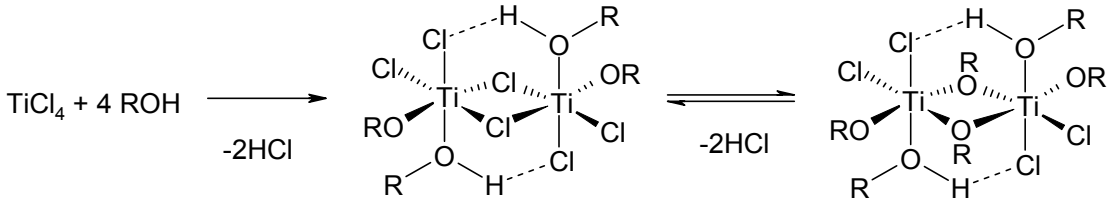

Figure 2.7 The formation of mixed alkoxide-chloride titanium species

Halogenated titanium catalysts of the type $TiX_3(OR)$ and $TiX_2(OR)_2$ have been patented as potential biodiesel catalysts. [32, 33] These species have a higher water and methanol tolerance than the tetra-alkoxides, however, the possible degradation products and general toxicity of these complexes make these titanates unattractive industrial catalysts.

Recently a number of reports have been published improving the stability of the titanium alkoxide centre by the controlled production of a mixed oxo-alkoxide species. As previously described these can be created by the addition of carboxylic acids, [34-36] but can also be achieved by including small amounts of water in the synthesis. [37, 38] These reactions create various mixed oxo-alkoxide species that tend to be water stable. These titanium complexes can range from two or three titanium centres to containing over nine unique metal centres bound into large clusters. The main application of these oxo- species comes from preparing sol-gel precursors for solid materials. The use of titanium oxo-alkoxide clusters as catalysts is much less well documented with examples of these complexes being used for oxidations [39] and as a catalyst in the reaction between a carbonyl-ene and glyoxalate. [40, 41]

One method used to stabilise metal alkoxide centres without the production of highly stable oxo complexes is to use diols as ligands which have the ability to chelate or bridge to a metal centre. The reaction of the diol with the titanium centre is usually exothermic while reducing the steric hinderance of the two alkoxide groups it has replaced. Yamamoto et al. investigated the reaction between titanium and 2-methylpentane-2,4-diol, [42] while Mehrotra et al. investigated similar complexes using 2-methylpentane-1,5-diol. [43] Three structural types of these complexes are possible, as shown in Fig. 2.8.

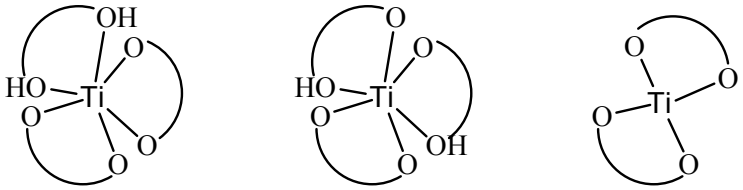

Structual Type 1 Structual Type 2 Structual Type 3

Figure 2.8 Three structural types in which titanium 2-methylpentane diolate can be isolated

Monomeric complexes of titanium are not the only possible structural types formed. Pajot et al. isolated the pentameric complex, $Ti_5(O^iPr)_{10}(OC_2H_4O)_5$, formed from reacting $Ti(O^iPr)_4$ with HEMA. This complex is one of the few examples of a seven co-ordinate titanium alkoxide in the literature. [44] Zechmann et al. using the similar ligand pinacol (2,3-dimethyl-2,3-butanediol), synthesised a range of mixed titanium-zirconium alkoxides. Despite the intricate co-ordination chemistry and steric bulk around the metal centres these complexes are not resistant to hydrolysis. [45]

A further method used to stabilise metal centres from nucleophilic attack is to synthesise a metal-coordination polymer, known as a Metal Organic Framework (MOF) or Covalent Metal Organic Network (CMON). [46] These compounds can possess well-defined arrays, which often define large pores or channels, akin to zeolites making them of interest as functional materials. [47] To date, many metal-organic coordination motifs are known, such as those based on Cd^{2+}, Zn^{2+} and Ag^{+}.[48-54] Titanium-organic frameworks are rarer, Wolczanski et al. synthesised a range of titanium polymers using aryl oxide spacers. Using 4-hydroxy phenol and quinone a 2-D network was synthesised, [55] while 3-D networks were also synthesised by the complete reaction of the ligand with titanium isopropoxide. [56, 57] Two examples of these moisture stable structures are shown below in Fig. 2.9.

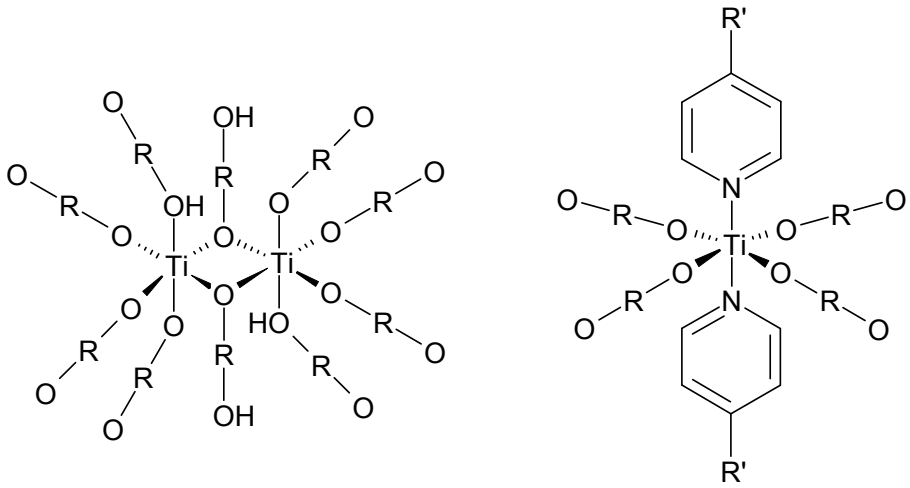

Figure 2.9 Two structural types of a titanium CMON, where R = Ph.

This final approach is the subject of this chapter where the formation of various titanium diolate complexes has been investigated. The ligands 1,4 butanediol, 2,3 butanediol and 1,3 propanediol were used with the aim of stabilising the coordination environment to methanol deactivation. These complexes were also examined for the stability in converting model waste oils.

2.2 Results And Discussion

2.2.1 Synthesis and Characterisation of Catalysts 1-3

2.2.2.1 Titanium Butanediolate, $[Ti_2(OC_4H_8O)_3(OC_4H_8OH)_2]_\infty$, 1

Complex **1**, $[Ti_2(OC_4H_8O)_3(OC_4H_8OH)_2]_\infty$, was synthesised using an excess of butanediol with $Ti(O^iPr)_4$ in hexane. The use of butanediol as a ligand is rare with only examples of sodium and aluminium complexes having been previously investigated.[58,59] On standing of the solution overnight, a substantial yield of large, clear crystals was obtained and analysed by single-crystal X-ray diffraction, shown below in Fig. 2.10.

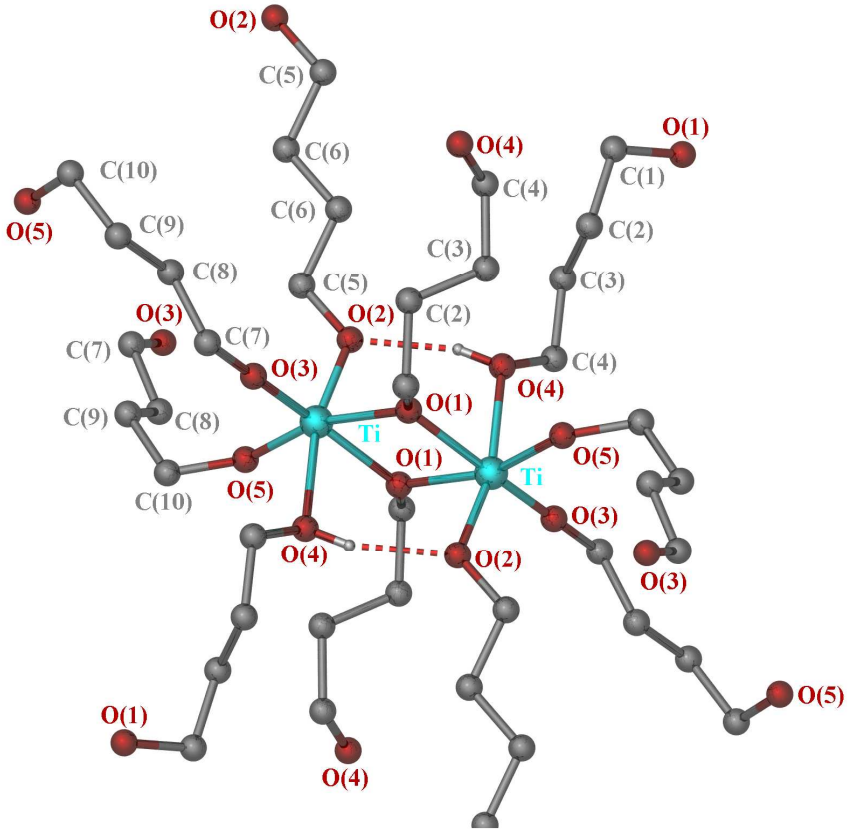

*Figure 2.10 Molecular structure of the titanium dimer structural unit of complex **1**, all alkyl hydrogen atoms have been removed for clarity*

Unlike the aryl oxides discussed in the introduction, the novel titanium based MOF is covalently bound to a flexible aliphatic alkoxide linker. The two titanium centres lie in a *pseudo* octahedral formation, typified by the angle O(4)-Ti(1)-O(1) 78.96(4)° and O(3)-Ti(1)-O(1) 163.68(5)°, linked together by one protonated and one un-protonated bridging butanediol ligand. This structure is stabilised by a hydrogen bond () similar to those observed in the aryl titanium 3-D networks published by Wolczanski et al. [56] This type of hydrogen bond is also observed in other titanium alkoxide oligomers. [60-62] The O-H hydrogen atom was located using a difference Fourier Map, and is located on O4, shown below in Fig. 2.11.

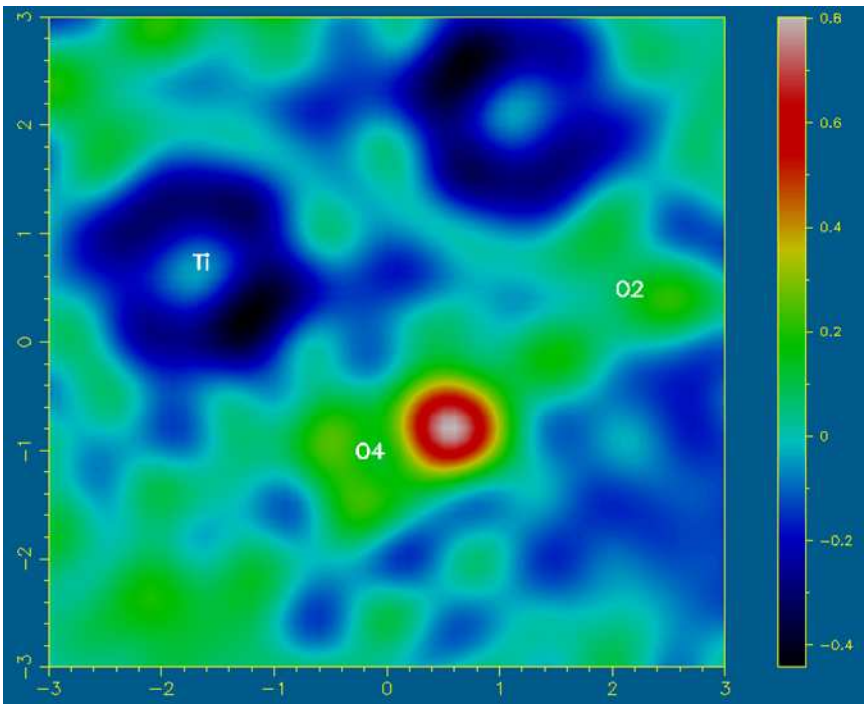

*Figure 2.11 Fourier Map of complex **1**, showing the location of the hydrogen atom on the ligand HOC_4H_8O*

The dimer, a Ti_2O_{10} bioctahedron, represents a node with ten potential connecting sites, all of these sites are occupied resulting in a complex polymeric structure displayed in Fig. 2.12.

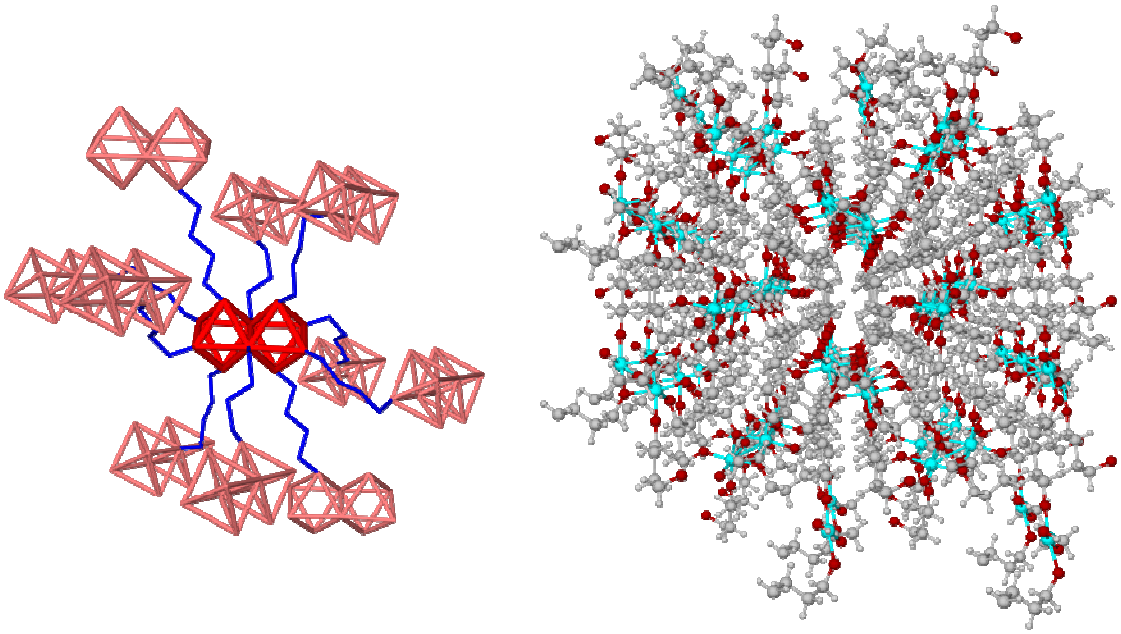

*Figure 2.12 Depiction of the ten nodal titanium bioctahedra (a) and the supramolecular structure (b) of complex **1***

This novel 3-D network is created due to the relative acidity of the 1,4-butanediol protons and the length of the linker which disfavours chelation. The occupancy of all ten sites from the titanium dimer is also unusual and contrasts with the previously reported aryloxide MOFs, which due to their rigidity and therefore less efficient packing resulted in a maximum of eight nodal species. [55-57]

Complex **1** contains highly Lewis acidic titanium centres and despite being soluble in most organic solvents is insoluble in methanol. Exposure of **1** to the atmosphere over five days resulted in no change to the FT-IR spectra and the pXRD pattern was the same as calculated for the single crystal suggesting that it is both air and moisture stable and as such is an attractive candidate for use as a biodiesel catalyst.

2.2.2.2 Titanium 2,3 Butanediolate, $Ti_3(OC_4H_8O)_4(OC_4H_8OH)_4$, 2

By reducing the length of the organic linker the synthesis of 3-D networks is no longer favoured and dimers and trimers become the most common aggregates with the dihydroxyl ligands favouring chelation. [63, 64] (2*R*, 3*R*)-2,3-Butanediol was reacted with

$Ti(O^iPr)_4$ in a similar manner to complex **1**. Small clear crystals were obtained from the resulting solution and analysed by single crystal X-ray diffraction. The solid state structure is shown below in Fig. 2.13.

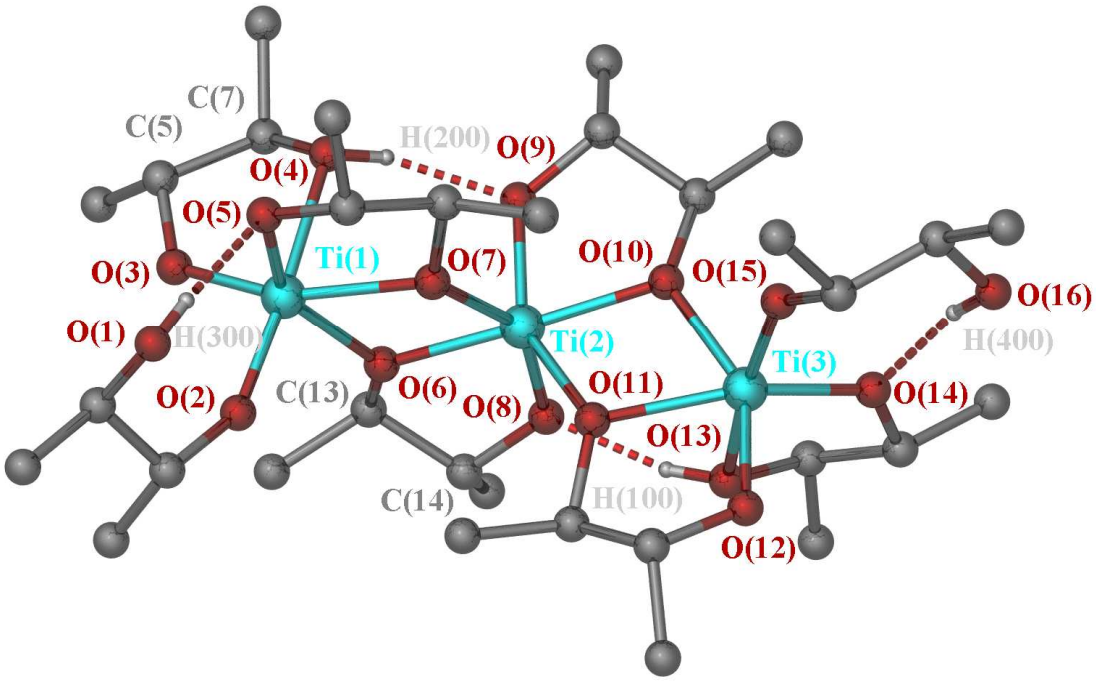

Figure 2.13 Molecular structure of the titanium 2,3 butanediol complex, ***2,*** *all alkyl hydrogen atoms have been omitted for clarity*

Much like complex **1**, the titanium centres in **2** have a distorted octahedral geometry, the -OH groups of the bound ligands participate in hydrogen bonding. The terminal titanium centres are bound to three terminal and two bridging alkoxides, coordination to the protonated ligand completes this octahedral geometry. The central titanium atom consists of four bridging and two terminal alkoxides. All but two of the ligands in complex **2** chelate to the titanium centres forming highly stable five membered rings. The ^1H NMR shows eight distinctive resonances for the methyl groups suggesting that the complex retains this trimeric structure in solution.

Wang et al. found that the reaction between $Ti(O^iPr)_4$ and ethylene glycol formed a well defined polymer with one unique titanium centre similar to the central Ti(2) atom in complex **2,** this structure is shown below in Fig. 2.14. [63]

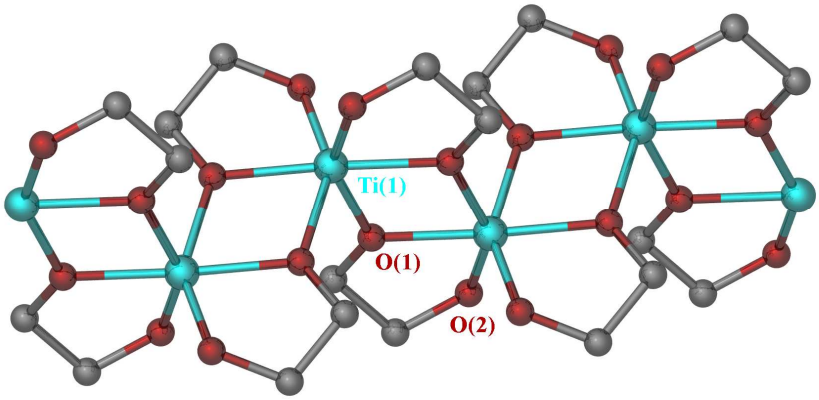

Figure 2.14 Molecular structure of titanium ethylene glycolate, taken from Wang et al.[63]

The terminal chelating ring in complex **2**, defined by the angles C(5)-O(3)-Ti(1) 127.04(13)° and C(7)-O(4)-Ti(1) 112.00(12)° is more distorted than in the ethylene glycol complex shown above. The central titanium ring is also more distorted than in the ethylene glycol complex but to a lesser extent, this is demonstrated by the angles C(14)-O(8)-Ti(2) 120.57(13)° and C(13)-O(6)-Ti(2) 116.61(11)°. The ethylene glycol complex differs to **2** presumably due to the lack of steric bulk afforded by the methyl groups as well as the lack of intramolecular hydrogen bonding.

2.2.2.3 Titanium 1,3 Propanediolate, $Ti_4(OC_3H_6O)_3(C_3H_7O)_{10}$, 3

A different synthetic approach was used for the synthesis of the mixed alkoxide **3**. The correct ratio of $Ti(O^iPr)_4$ and propanediol were mixed without a co-solvent present and the resulting alcohol removed by heating. Large clear crystals, which were recovered from this thick solution, were analysed by X-ray diffraction.

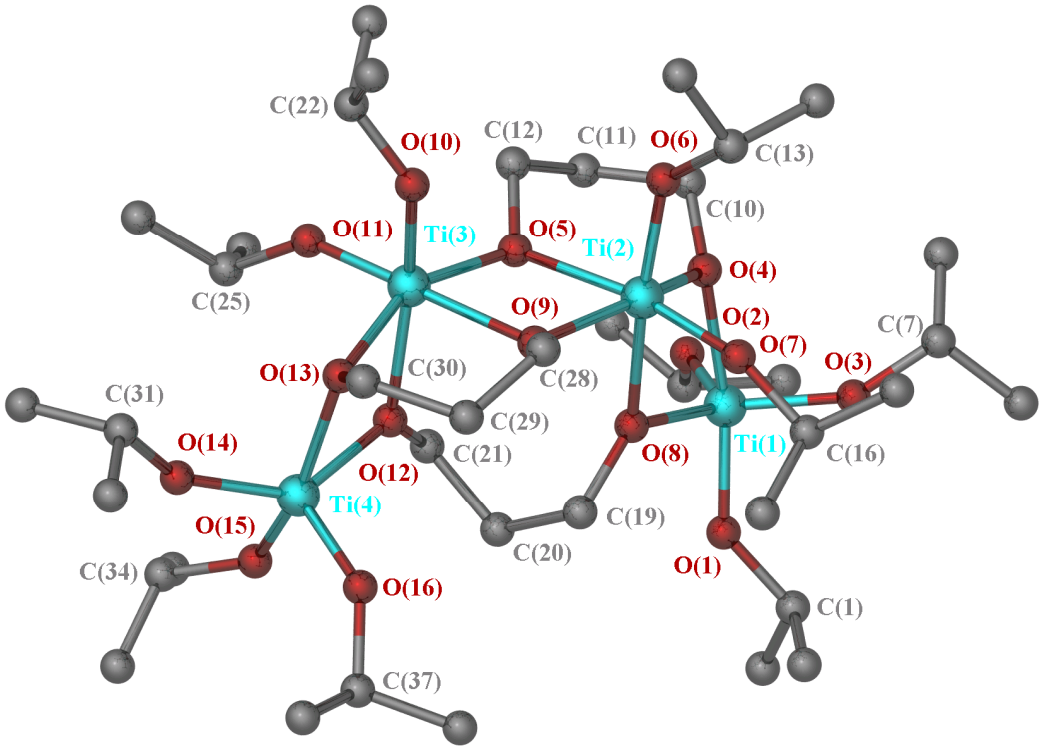

Figure 2.15 Molecular structure of the titanium 1,3 propanediol complex ***3****, all hydrogen atoms have been removed for clarity*

Complex **3** is a tetramer containing three 1,3-propanediol and ten isopropoxide ligands in the complex. One ligand is bound to all four titanium atoms and the other two ligands are bound to three titanium centres. Both of the latter ligands chelate to a central titanium atom and the two terminal titanium centres are present in a five coordinate geometry. Bound to these titanium atoms are three terminal isopropoxides and two bridging 1,3 propanediol alkoxide groups. Even though the corresponding titanium alkoxide bond lengths and angles are not identical, they are highly similar. The two central titanium atoms both lie in a distorted octahedral geometry with four bridging propanediol ligands and two terminal isopropoxides present.

The ^{1}H NMR of **3** is complex and even at 500 MHz there are no specific peaks for each of the protons. On addition of methanol to the NMR tube a sharp doublet at 1.08 ppm and septet at 3.89 ppm with coupling constants of 6Hz were observed. The integration of these peaks confirms that the methanol displaces all the isopropoxide groups on the titanium centres without the formation of $Ti(OMe)_4$.

2.2.2 CATALYTIC ACTIVITY OF 1-3 IN THE CONVERSION OF SOYBEAN OIL

Having established the molecular structures of complexes **1-3**, the catalytic activity for the transesterification of vegetable oil was investigated. Soybean Oil was purchased from a supermarket and used without further purification. The oil (36.8 ml) was then placed in a 120 ml autoclave with methanol in a 1:12 molar ratio. The catalyst (2.5 mol %) was added, the autoclave sealed and placed in a graphite bath, the mixture was then heated to temperature, t = 0 was taken when the graphite bath had reached that. After 120 minutes the autoclave was crash cooled in a water bath.

The reaction mixture was added to water and shaken vigorously. The top layer (FAME and remaining vegetable oil) was dissolved in $CDCl_3$ and analysed by ^1H NMR spectroscopy. The yield of FAME was calculated by taking the integral value of the methoxy group of the FAME against the remaining proton signals adjacent to the glycerol backbone of the triglyceride. This method was reported by G. Knothe. [65] The yields calculated by ^1H NMR showed a deviation from the values calculated by HPLC of 3%. An example of the ^1H NMR spectrum of a vegetable oil/FAME mixture is shown below in Fig. 2.16.

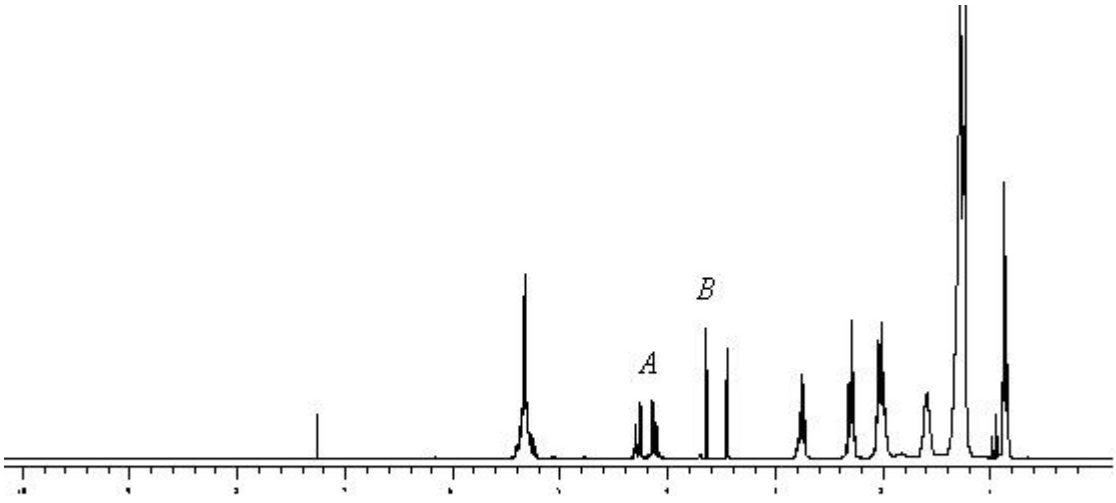

Figure 2.16 ^1H NMR spectra of the partially transesterified soybean oil. The plot shows the glyceride (A) and FAME (B) peaks

The following catalytic results were obtained at 195 ºC, the results of which are shown below in Fig. 2.17.

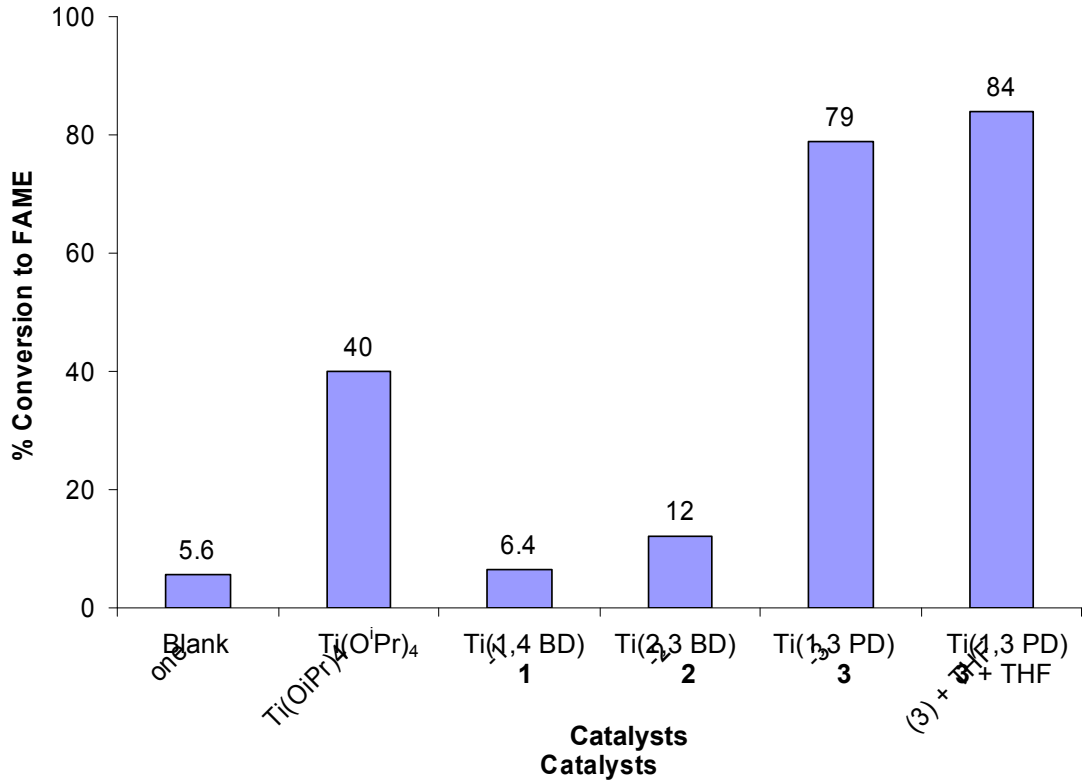

*Figure 2.17 Graph depicting the catalytic activity of $Ti(O^iPr)_4$ and complexes **1-3***

As soon as $Ti(O^iPr)_4$ was added to the reaction vessel $Ti(OMe)_4$ was formed, this heterogeneous material converted 40% of the glycerides to FAME under the reaction conditions. Complexes **1-3** are stable to this methanolysis reaction and no precipitate was observed.

Complex **1** shows a greatly reduced activity relative to the homoleptic alkoxide precursor. The diolate is stable to methanolysis and no methoxide species is formed. The titanium diolate species, while not retaining the solid structure in solution, will still form an aggregated species. The chelation effect of the diolate ligands suppress the coordination of the triglyceride hence little catalytic activity is observed.

Complex **2** is a related structure that favours chelation over polymeric bridging. The titanium centres are similar to complex **1**, as is the activity. The chelating ligands form highly stable five membered rings, for the titanium centre to be catalytically active the co-ordination number would have to be increased to seven or eight and sterically accommodate the triglyceride molecule or these chelate ring systems would need to be broken followed by insertion of the bulky reactant. Both of these reactions are

unfavourable and the equilibrium between the titanium and diol would lie towards the formation of the complex.

Structually **3** is very different to the previous complexes. Two titanium centres are in a five co-ordinate arrangement where there are ten labile isopropoxide groups and three chelating ligands. The isopropoxide groups are labile and an active species can be formed without the production of $Ti(OMe)_4$. These structural differences between all three complexes are mirrored in the catalytic activity.

Complex **3** was then added to a solution of THF (1:20 ratio to methanol) this soluble catalyst was then added to methanol and no precipitation was observed. THF is a useful co-solvent in the biodiesel reaction and helps solubilise the methanol in the oil medium due to this homogenising effect the yield of FAME is increased [66] This is observed for these catalyst systems.

2.2.3 Optimisation of 1,3 Propanediol As a Stabilising Ligand

Titanium alkoxides can be stabilised against hydrolysis by atmospheric moisture or methanolysis in the biodiesel reaction by using simple alkyl diol ligands. However, when an excess of diol ligand is used to form these complexes there are no labile ligands and the complexes themselves are too stable for catalysis. By using less than stoichiometric amounts of ligand, this activity can be increased.

2.2.3.1 Concentration of 1,3 Propanediol

Complex **3** was formed *in situ*, by adding $Ti(O^iPr)_4$ and 1,3 propanediol to THF. The amount of propanediol was varied and the optimum concentration was found, these results are shown below in Fig. 2.18. As these complexes are stable to methanol the THF solution was then blended with methanol to make a homogeneous reactant-catalyst system.

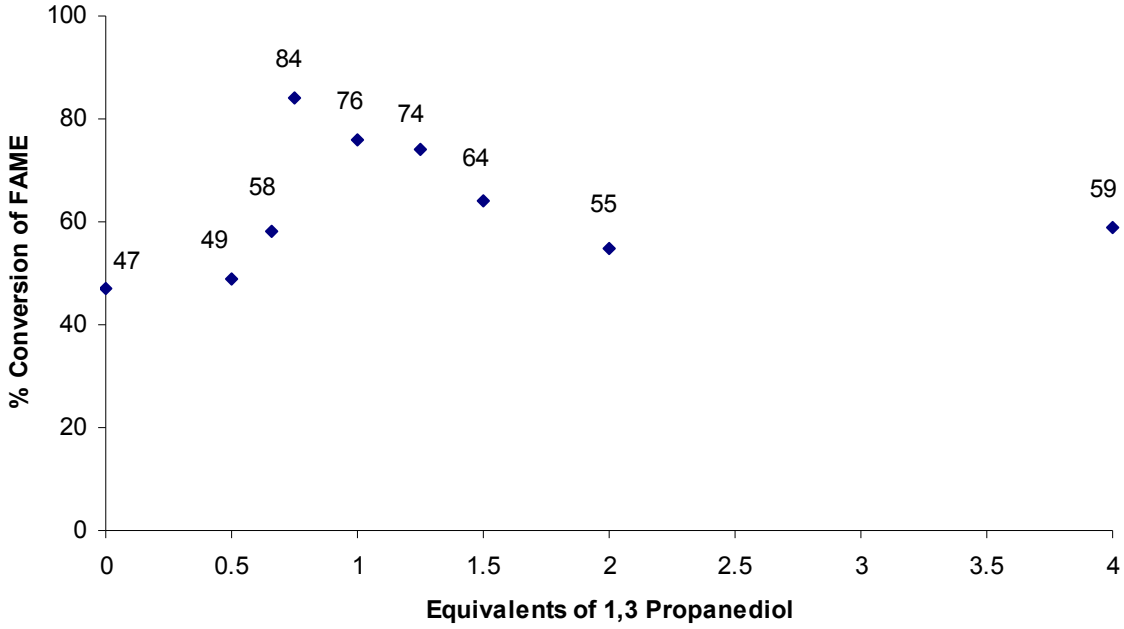

Figure 2.18 The effect of the concentration of 1,3-propanediol on the conversion of FAME from soybean oil

The solution that contained no stabilising diol ligand converted 47% of the triglycerides to FAME under the reaction conditions. Adding anywhere up to 0.5 equivalents of 1,3-propanediol does not significantly increase this conversion. On addition of methanol to the THF/Ti(O^iPr)$_4$ solution at room temperature Ti(OMe)$_4$ was precipitated, this was not the case when 0.5 equivalents of propanediol were added, however, after the biodiesel reaction had been run Ti(OMe)$_4$ was recovered. No precipitate was observed for solutions containing between 0.66 and 1 equivalents of propanediol before or after the biodiesel reaction. The catalyst solution, of complex **3** dissolved in THF was the most successful in this series. For solutions with higher amounts of 1,3-propanediol, a milky white precipitate was observed at room temperature, this was found to be an insoluble titanium propanediolate complex.

In the titanium propanediol solutions**,** an optimum amount of diol ligand needs to be added to avoid the formation of Ti(OMe)$_4$. If too much ligand is used then less active titanium diolate complexes are formed. It is suggestive that the presence of labile alkoxide groups and the chelation of the ligand are decisive factors in the activity of the catalyst. However, unlike 1,4 butandiol the insoluble complexes formed are relatively active.

2.2.3.2 Temperature Dependence

As the solution of complex **3** in THF and methanol was the most active catalyst, the dependence of the yield of FAME on temperature was investigated. The results are shown below in Fig. 2.19.

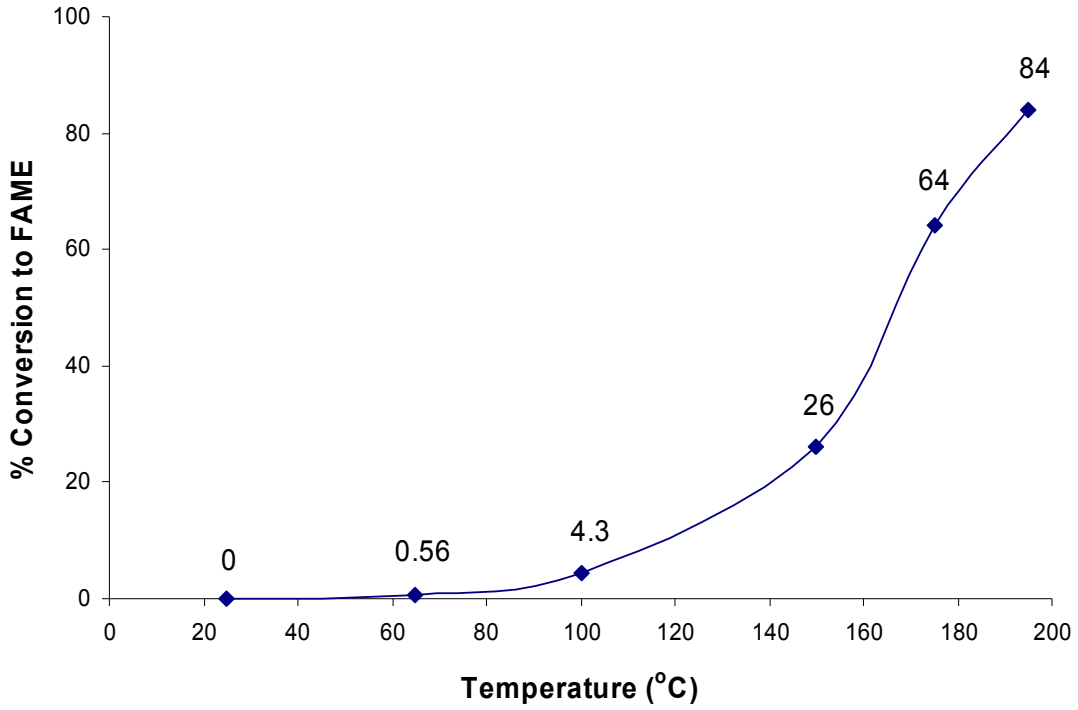

*Figure 2.19 The effect of the temperature of reaction on the conversion of FAME using a solution of **3** in THF as a catalyst*

Despite the catalyst being highly active at 195 °C, the activity decreases rapidly as the temperature is reduced. At reflux temperature it is completely inactive for the conversion of glycerides to FAME.

2.2.4 Catalytic Activity In The Conversion of Model Waste Oils

The two main differences in the production of FAME from waste oils as opposed to virgin vegetable oil is an increased FFA (between 2-30%) and water content (up to 2 wt%). The effect of these constituents was tested on the activity of the most active catalyst, complex **3** in THF.

2.2.4.1 FFA Tolerance

As a model for FFA content, stearic acid was added to the vegetable oil prior to the reaction, the catalyst-methanol solution was then added and the reaction undertaken.

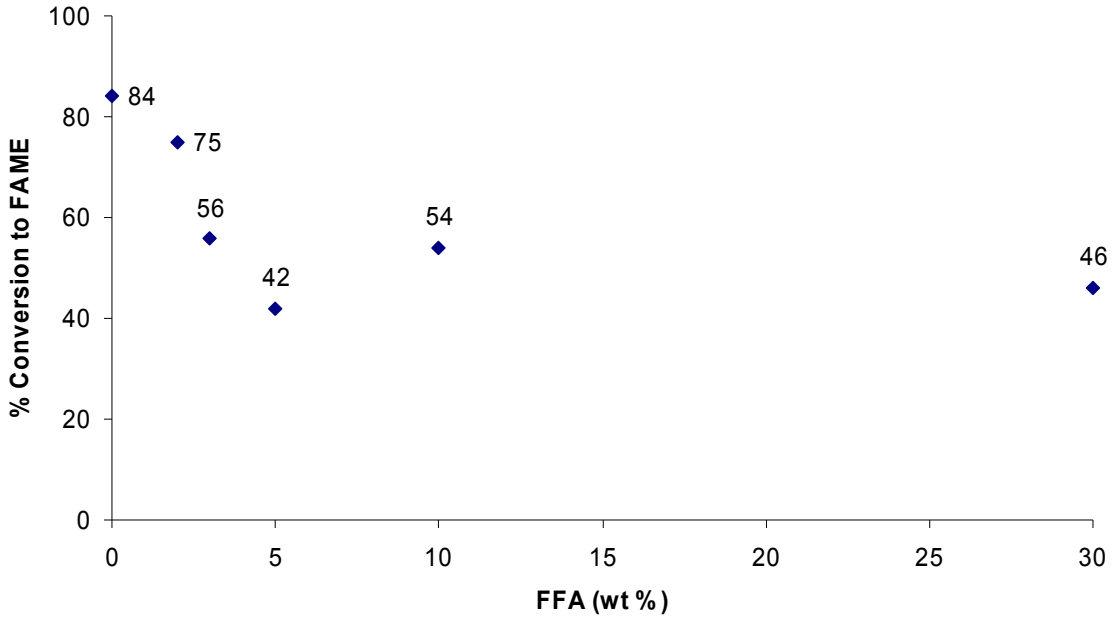

*Figure 2.20 The effect of stearic acid on the conversion of triglycerides to FAME using a solution of **3** in THF as a catalyst*

A substantial decrease in the conversion of glycerides to FAME is observed on the addition of stearic acid (a model for FFA present in waste oil). The decrease is roughly linear until 5% FFA are present where the conversion remains approximately constant. The titanium catalyst could be selectively esterifying the stearic acid, generating water and thus being deactivated. However, this scenario is unlikely as the conversion would drop more dramatically than observed at low concentrations of FFA while at high concentrations the conversion should be closer to 0.

At 2 wt% FFA content, there is already 2.5 equivalents of stearic acid to catalyst, this rises to 6 equivalents when the FFA content is increased to 5 wt%. The data supports the formation of one or more stable oxo-complexes, which have an increased water and FFA stability but in general a lower activity than the original catalyst.

2.2.4.2 Water Stability

The stability to water inherent in the waste oil was then examined, a range of 1,3 propanediol solutions were investigated. The results are shown below in Table 2.1.

Equiv. of Propanediol	% Yield Virgin Soybean Oil	% Yield + 0.5 wt% H_2O
0	47	1.5
0.5	49	6.0
0.66	58	4.2
0.75	84	7.2
1	76	1.4
1.25	74	5.4
1.5	64	4.6
2	55	8.2
4	59	13

Table 2.1 The catalytic activity of solutions containing $Ti(O^iPr)_4$, THF, MeOH and various amounts of 1,3 propanediol with and without added H_2O

None of the complexes are stable to hydrolysis under the optimum reaction conditions. The highest conversion of FAME was under 15%, when a modest amount of water was added to the virgin soybean oil.

2.3 SUMMARY

Typically current research in biodiesel technology is focussed on the replacement of homogeneous alkali metal catalysts by heterogeneous systems. Very little work has been published on the use of homogeneous Lewis acid catalysts for this reaction. In this chapter it has been shown that it is possible to use a homogeneous catalyst system, namely titanium alkoxides, for the production of biodiesel.

The most appropriate industrially available titanium alkoxide catalysts ($Ti(OEt)_4$ & $Ti(O^iPr)_4$) are prone to methanolysis and the insoluble $Ti(OMe)_4$ catalyst formed is less active. The titanium alkoxide can be stabilised against this by the judicious use of a diol ligand. However, the formation of chelate rings, six co-ordinate titanium centres and large supramolecular structures in these complexes seem to hamper the activity of the titanium catalyst.

Despite being stable to methanolysis and an active catalyst for the transesterification of virgin oil, the stabilised titanium alkoxide catalysts are not stable to the formation of less active adducts when FFA or water, two distinct components of waste oils, are present. Titanium diol/alkoxide solutions are therefore not suitable catalysts for the production of biodiesel from lower quality feedstocks.

One class of titanium alkoxides not previously discussed are the titanium complexes of α-hydroxy acids such as citric acid. These complexes are capable of forming five membered mixed carboxylate-alkoxide rings that are not only water stable but also highly water-soluble. These compounds discussed in Chapter 3, have vastly increased water stability, even up to temperatures of 200 °C.

2.4 REFERENCES

1. D.C. Bradley, R.C. Mehrotra, I.P. Rothwell and A. Singh, in *Alkoxo and Aryloxo Derivatives of Metals* Academic Press, London, Rev. Edition, 2001, pp. 229-382.
2. D. C. Bradley, *Chemical Reviews*, 1989, **89**, 1317.
3. Y. Wu, D. C. Bradley and R. M. Nix, *Applied Surface Science*, 1993, **64**, 21-28.
4. C. J. Brinker and G. W. Scherer, *Sol-Gel Science: The Physics and Chemistry of Sol-Gel Processing*, Academic Press, New York, 1990.
5. C. J. Brinker, D. E. Clark and D. R. Ulrich, *Better Ceramics Through Chemistry*, Elsevier, New York, 1984.
6. I. Marek, *Titanium and Zirconium in Organic Synthesis*, Wiley VCH, Weinheim, 2002.
7. N. R. D. Basso, P. P. Greco, C. L. P. Carone, P. R. Livotto, L. M. T. Simplicio, Z. N. da Rocha, G. B. Galland and J. H. Z. dos Santos, *Journal of Molecular Catalysis A-Chemical*, 2007, **267**, 129-136.
8. G. W. Coates, *Chemical Reviews*, 2000, **100**, 1223-1252.
9. T. Katsuki and K. B. Sharpless, *Journal of the American Chemical Society*, 1980, **102**, 5974.
10. D. J. Ramon and M. Yus, *Chemical Reviews*, 2006, **106**, 2126-2208.
11. P. Krasik, *Tetrahedron Letters*, 1998, **39**, 4223-4226.
12. D. P. Birnie, *Journal of Materials Science*, 2000, **35**, 367-374.
13. H. Deleuze, X. Schultze and D. C. Sherrington, *Journal of Molecular Catalysis A: Chemical*, 2000, **159**, 257-267.
14. D.C. Bradley, R.C. Mehrotra and W. Wardlaw, *Journal of the Chemical Society*, 1952, 5020.
15. D.C. Bradley, R.C. Mehrotra and W. Wardlaw, *Journal of the Chemical Society*, 1952, 2027.
16. D.C. Bradley, R.C. Mehrotra and W. Wardlaw, *Journal of the Chemical Society*, 1952, 4204.
17. D.C. Bradley, R.C. Mehrotra, I.P. Rothwell and A. Singh, in *Alkoxo and Aryloxo Derivatives of Metals*, Academic Press, London, Rev. Editon, 2001, pp. 3-181.

18. I. D. Verma and R. C. Mehrotra, *Journal of the Chemical Society*, 1960, 2966.
19. D. C. Bradley and C. E. Holloway, *Inorganic Chemistry*, 1964, **3**, 1163.
20. R. L. Martin and G. Winter, *Journal of the Chemical Society*, 1961, 2947.
21. C. G. Barraclough, R. L. Martin and G. Winter, *Journal of the Chemical Society*, 1964, 758.
22. R. C. Mehrotra, *Journal of the American Chemical Society*, 1954, **76**, 2266.
23. R. N. Kapoor and R. C. Mehrotra, *Journal of the American Chemical Society*, 1958, 3569.
24. S. Doeuff, Y. Dromzee, F. Taulelle and C. Sanchez, *Inorganic Chemistry*, 1989, **28**, 4439-4445.
25. C. F. Campana, Y. Chen, V. W. Day, W. G. Klemperer and R. A. Sparks, *Journal of the Chemical Society-Dalton Transactions*, 1996, 691-702.
26. F. Biechel, J. Dubuc and M. Henry., *New Journal of Chemistry*, 2004, **28**, 764-769.
27. E. Nasr, R. Guiraud, J.-L. Pellegatta and C. Blandy, *Canadian Journal of Chemical Engineering*, 1995, **73**, 129-134.
28. C. Blandy, J.-L. Pellegatta, R. Choukroun, B. Gilot and R.Guiraud, *Canadian Journal of Chemistry-Revue Canadienne De Chimie*, 1993, **71**, 34-37.
29. C. Blandy, J. Pellegatta and P. Cassoux, *Catalysis Letters*, 1997, **43**, 139-142.
30. H. Deleuze, X. Schultze and D. C. Sherrington, *Polymer*, 1998, **39**, 6109-6114.
31. Y. T. Wu, Y. C. Ho, C. C. Lin and H. M. Gau, *Inorganic Chemistry*, 1996, **35**, 5948-5952.
32. M. Gheorghiu, *United States Pat.*, US 5532392, 1996.
33. M. Mizumaki, H. Harada, *Japan Pat.*, JP 09241213, 1997.
34. N. Steunou, F. Robert, K. Boubekeur, F. Ribot and C. Sanchez, *Inorganica Chimica Acta*, 1998, **279**, 144-151.
35. P. Piszczek, A. Grodzicki, M. Richert and A. Wojtczak, *Inorganica Chimica Acta*, 2004, **357**, 2769-2775.
36. N. Steunou, R. Portal and C. Sanchez, *High Pressure Research*, 2001, **20**, 63-70.
37. M. Mehring, G. Guerrero, F. Dahan, P. H. Mutin and A. Vioux, *Inorganic Chemistry*, 2000, **39**, 3325-3332.
38. M. Mehring, V. Lafond, P. H. Mutin and A. Vioux, *Journal of Sol-Gel Science and Technology*, 2003, **26**, 99-102.

39. H. Hanawa, D. Uraguchi, S. Konishi, T. Hashimoto and K. Maruoka, *Chemistry-a European Journal*, 2003, **9**, 4405-4413.
40. M. Terada, Y. Matsumoto, Y. Nakamura and K. Mikami, *Inorganica Chimica Acta*, 1999, **296**, 267-272.
41. M. Terada and K. Mikami, *Journal of the Chemical Society-Chemical Communications*, 1994, 833-834.
42. A. Yamamoto and S. Kambara, *Journal of the American Chemical Society*, 1959, **81**, 2663-2667.
43. R. C. Mehrotra, A. Singh, M. Bhagat and J. Goghwani, *Journal of Sol-Gel Science and Technology*, 1998, **13**, 45-49.
44. N. Pajot, R. Papiernik, L. G. Hubert-Pfalzgraf, J. Vaissermannb and S. Parraudc, *Journal of the Chemical Society, Chemical Communications* 1995, 1817-1819.
45. C. A. Zechmann, J. C. Huffman, K. Folting and K. G. Caulton., *Inorganic Chemistry*, 1998, **37**, 5856-5861.
46. A. J. Blake, N. R. Champness, P. Hubberstey, W. S. Li, M. A. Withersby and M. Schroder, *Coordination Chemistry Reviews*, 1999, **183**, 117-138.
47. F. Q. Liu and T. D. Tilley, *Chemical Communications*, 1998, 103-104.
48. F. A. A. Paz and J. Klinowski, *Inorganic Chemistry*, 2004, **43**, 3882-3893.
49. F. A. A. Paz and J. Klinowski, *Inorganic Chemistry*, 2004, **43**, 3948-3954.
50. M. L. Tong, S. L. Zheng and X. M. Chen, *Chemistry-a European Journal*, 2000, **6**, 3729-3738.
51. M. A. Withersby, A. J. Blake, N. R. Champness, P. A. Cooke, P. Hubberstey, W. S. Li and M. Schröder, *Inorganic Chemistry*, 1999, **38**, 2259-2266.
52. J. Tao, J. X. Shi, M. L. Tong, X. X. Zhang and X. M. Chen, *Inorganic Chemistry*, 2001, **40**, 6328.
53. Y. G. Zhang, J. M. Li, M. Nishiura, H. Y. Hou, W. Deng and T. Imamoto, *Journal of the Chemical Society-Dalton Transactions*, 2000, 293-297.
54. A. N. Khlobystov, A. J. Blake, N. R. Champness, D. A. Lemenovskii, A. G. Majouga, N. V. Zyk and M. Schröder, *Coordination Chemistry Reviews*, 2001, **222**, 155-192.
55. J. M. Tanski, T. P. Vaid, E. B. Lobkovsky and P. T. Wolczanski, *Inorganic Chemistry*, 2000, **39**, 4756-4765.
56. T. P. Vaid, J. M. Tanski, J. M. Pette, E. B. Lobkovsky and P. T. Wolczanski, *Inorganic Chemistry*, 1999, **38**, 3394-3405.

57. T. P. Vaid, E. B. Lobkovsky and P. T. Wolczanski, *Journal of the American Chemical Society*, 1997, **119**, 8742-8743.
58. G. J. Gainsford and T. Kemmitt, *Acta Crystallographica Section C-Crystal Structure Communications*, 2005, **61**, M136-M138.
59. W. Ziemkowska, S. Kwasniewska, R. Wroblewski and R. Anulewicz-Ostrowska, *Journal of Organometallic Chemistry*, 2002, **651**, 72-79.
60. M. G. Davidson, M. D. Jones, M. D. Lunn and M. F. Mahon, *Inorganic Chemistry*, 2006, **45**, 2282-2287.
61. K. Gigant, A. Rammal and M. Henry, *Journal of the American Chemical Society*, 2001, **123**, 11632-11637.
62. Y. Wu, Y. Ho, C. Lin and H. Gau, *Inorganic Chemistry*, 1996, **35**, 5948-5952.
63. D. Wang, R. Yu, N. Kumada and N. Kinomura, *Chemistry of Materials*, 1999, **11**, 2008-2012.
64. A. Snell, G. Kehr, O. Kataeva, R. Frohlich and G. Erker, *Journal of Organometallic Chemistry*, 2003, **687**, 171-177.
65. G. Knothe, *Journal of the American Oil Chemists Society*, 2000, **77**, 489-493.
66. S. Gryglewicz, *Bioresource Technology*, 1999, **70**, 249-253.

CHAPTER 3

CITRIC ACID DERIVED LIGANDS AND COMPLEXES

In the last chapter diol ligands were used to stabilise titanium alkoxides to effect the conversion of soybean oil to FAME. However, despite preventing methanolysis the titanium diolate species were not resistant to hydrolysis. In this chapter a number of water stable titanium citrate complexes are reported, and their activity in the transesterification of soybean oil investigated.

3.1 INTRODUCTION

Citric acid is a significant organic co-factor; among its many uses is its ability to stabilise metal ions, making them available to biological tissues. It plays a vital role in many biological processes such as the Krebs cycle, an essential step in the catabolism process of turning sugars and fats into energy.[1,2] Its role in solubilising metal ions is interesting to the synthetic chemist, and has spurred research into the interactions of this molecule with many biologically active metals.

Citric acid is insoluble in almost all organic solvents and only partially soluble in lower alcohols and THF. However, it is highly soluble in water and almost all reactions are carried out, at least in part, in aqueous solutions. Citric acid has four hard donors and therefore the potential to chelate with numerous metals. As a ligand it also has the potential to form highly stable 5-membered ring systems through the hydroxyl and β-carboxylic acid arm. A range of monometallic complexes have been reported using a variety of transition metals,[3-6] Group I [7-9] and Group II metals.[10-12] Citrate salts of the lanthanides Ln, Yb and Gd [13-15] as well as main group complexes of citric acid have also been investigated.[16, 17]

A number of bimetallic complexes have been synthesised, generally of the type $AB_y(Cit)_x$ where B is normally a monovalent metal and A and B are aliovalent, these complexes are usually heavily hydrated.[18-25] There are far fewer examples of mixed

metal citrate complexes which do not contain an alkali metal. As the sodium will react with any FFA, or H_2O present in waste oils and produce soap these catalysts would not be suitable biodiesel production of lower quality feedstocks. Hartley et al. synthesised a mixed metal Ag/Sb complex, shown below in Fig. 3.1. [26]

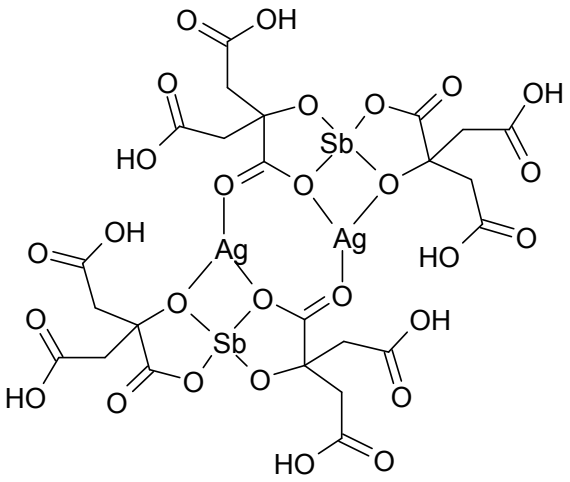

Figure 3.1 Mixed metal antimony silver citrate complex

The two citric acid molecules in Fig. 3.1 are bound to the antimony by the central hydroxyl and carboxylic acid arm, the silver is in a three coordinate binding mode. A similar structure was observed by Smith et al. using Cu(I) instead of Ag(I). [27] Antimony is a heavy metal though and is considered unsuitable as an industrial biodiesel catalyst due to the toxicity.

The majority of other mixed metal citrates are based on titanium. These titanium citrate systems have applications as precursors to oxide catalysts, [28] ceramics [29] and ionic conductors,[30-33] they have also been investigated for their biological applicability [34, 35] and as a reducing agent.[36, 37]

Citric acid behaves like a triprotic acid in aqueous solution (the pKa value of the hydroxyl atom is over 14). On addition of Ti(IV) the citric acid becomes tetraprotic and binding occurs between the hydroxyl arm and the titanium. When $Ti(O^iPr)_4$ is added to water with no citric acid available, titanium hydroxide is instantly formed. When a 1:1 ratio of the citric acid to titanium in aqueous solution is used then, even at low pH, hydroxyl titanium citrates are formed. These species have up to three hydroxides bound to the titanium along with one citric acid molecule. These hydroxide species are soluble and no precipitate is observed. Hydroxide species are also formed when a ratio of 2 citrate ligands to 1 titanium are reacted together.

Structually only a few hydroxyl titanium citrates have been published and are all made by the addition of hydrogen peroxide to a solution of titanium citrate. [38-40] Kemmitt et al. observed that these hydroxide species can be unstable and form complicated titanium-oxo citrate complexes. [41]

When three equivalents of citric acid are reacted with titanium the major products in solution are titanium tris-citrates. When the solution remains acidic these are the only products formed however at basic pH levels other titanium species such as $[Ti(OH)_2(cit)_2]^{6-}$ and $Ti(HCit)^+$ are observed alongside these products. [42] The potential titanium tris-citrate complexes are shown below in Fig 3.2.

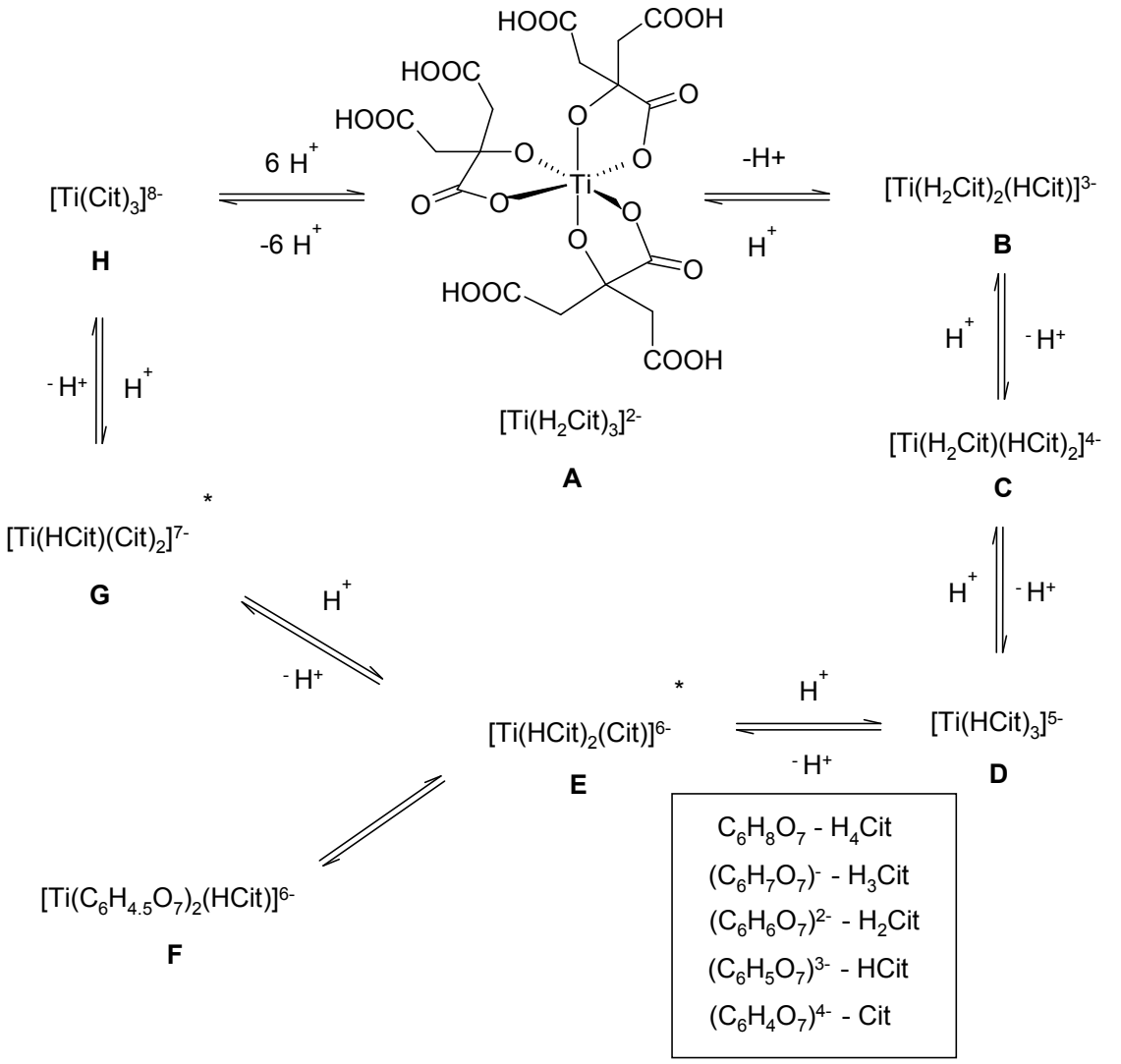

Figure 3.2 Potential variants of the Ti(IV) citrate octahedral anion at different pH levels, anions marked with an asterisk denote species which are yet to be characterised, adapted from Kefalas et al. [43]

The citrates are synthesised by a variety of methods. Collins et al. synthesised the octa-anionic species **H** by addition of a solution of $Na_3(C_6H_5O_7) \cdot 2H_2O$ to $TiCl_3$, this mixture was then air-oxidised to the Ti(IV) species. The resulting complex, $Na_8[Ti(C_6H_4O_7)_3] \cdot 17H_2O$, was characterised by X-ray crystallography. This structure contains a C_3-symmetric Ti centre resulting from three citric anions chelating to the metal *via* carboxylate and alkoxide oxygen atoms. The complex is also heavily hydrated and has the opportunity to exhibit optical isomerism.

Paradies et al. reacted $Ti(O^iPr)_4$ with monosodium citrate resulting in the trianionic complex $[TiNa_3(H_2Cit)_2(HCit)(H_2O)_{6.8}] \cdot 2H_2O$. [44] This complex was converted to a Ti(III) citrate solution on irradiation with U.V. light. These experiments highlight the interesting redox chemistry of the titanium citrate system, especially when present in biological systems.

Kefalas et al isolated the hexa-anionic species **F** by reacting citric acid with $TiCl_4$ in water and then neutralising the solution with sodium hydroxide. [43] This method of synthesising the titanium citrate anion *insitu* before neutralisation has been used to create the more complex heterometallic divalent titanium citrates such as titanium barium citrate.

Titanium barium citrate is used in the production of ceramics as a precursor to $BaTiO_3$ powder. In a process described as the Pechnini method the titanium citrate is synthesised by adding $Ti(O^iPr)_4$ to citric acid in ethylene glycol followed by the addition of barium citrate. [29] Despite various adaptations of this method the only structural information available is based on I.R. spectroscopy and solid state NMR spectroscopy measurements. [45]

Many compounds with the general formula $MTiO_3$ or $M_2Ti_2O_7$ are extremely useful in industry for their ferroelectric, piezoelectric and pyroelectric properties. The synthesis of these titanates via the Pechini method is well understood. [29] Citrate complexes from aqueous media lead to highly homogeneous, well crystallised products; Deng et al. undertook a comprehensive study into the structural and solution characteristics of a range of divalent metal titanium citrates. [46] The titanium barium citrate was synthesised in a 1:1:3 ratio by the addition of barium chloride to a solution of titanium chloride and citric acid, ammonia was used to adjust the pH of the solution. At pH 3.5 crystals of $[TiBa(H_2Cit)(HCit)_2]^{2-} \cdot 8\ H_2O$ were collected, the resulting structure is shown below in Fig. 3.3.

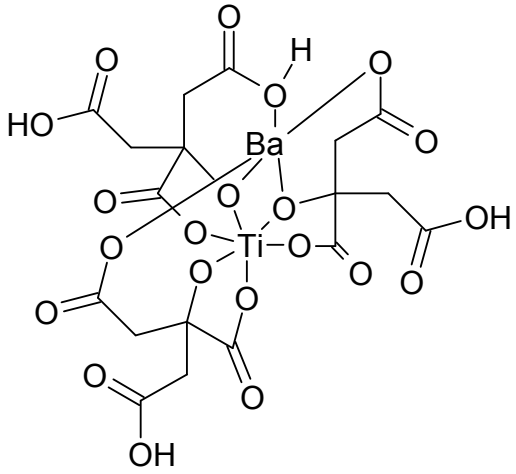

Figure 3.3 Titanium barium citrate structure (two water molecules and two intermolecular bonds with the barium cation have been left out for clarity) taken from Deng et al. [46]

The researchers also reported a Ti(IV)/Fe(III) citrate which had a similar structure to the previously reported titanium magnesium citrate, this is shown in Fig. 3.4 below.

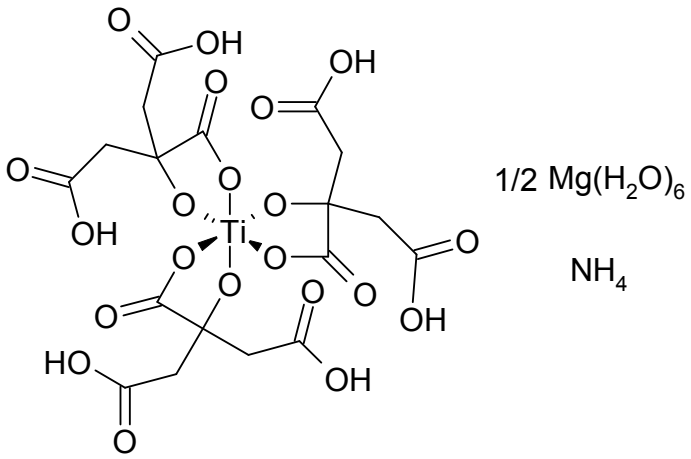

Figure 3.4 Depiction of a titanium magnesium citrate ($[NH_4Mg_{1/2}(Ti(C_6H_6O_7)_3) \cdot 6H_2O]$ taken from Zhou et al. [47]

The tendency of heterometallic titanium citrates to form homogeneous mixtures is advantageous in designing precursors for ceramics, while the stability and biological activity of the titanium citrate are of interest in developing anti-cancer drugs. [48]

Titanium citrate complexes are mainly water soluble mixed carboxylate alkoxide species which could be adapted to catalysis. Previous work at Johnson Matthey isolated the penta-anionic titanium citrate **D**, $[TiNa_5(HCit)_3] \cdot 19\ H_2O$. This was found to

catalyse the polycondensation of bishydroxyethylterphtalate and ethylene glycol to make poly(ethylene)terephtalate (PET) successfully at 250 °C. [49]

There are few examples of titanium citrates and their adducts as catalysts in the literature. This is surprising as citric acid is an attractive ligand in industrial processes because of its benign nature and the inherent stability of the complexes that are formed. Mixed metal titanium citrates have the potential to be highly active through the Lewis acidity of the titanium alkoxide centre and the possible positive synergic effects by the two metal sites.

Industrially titanium sodium citrate is undesirable for the transesterification of vegetable oils as there is the possibility of saponification, however a range of other titanium mixed metal catalysts could be active in the synthesis of biodiesel without being inactivated by the water found in waste oils. In this chapter a range of complexes derived from the titanium citrate anion are synthesised, characterised and examined for their activity in the production of biodiesel.

3.2 Results and Discussion

3.2.1 Homometallic Titanium Citrate Synthesis and Characterisation

In order to synthesise all the subsequent titanium citrate complexes, an ill-defined titanium citrate solution was prepared. This solution was synthesised by refluxing $Ti(O^iPr)_4$ with citric acid in a one to three molar ratio in water over 24 hours and removal of the resulting IPA. The ^1H and ^{13}C NMR spectra are consistent with homoleptic titanium citrate complexes, but no further information can be gained. A further insight into the possible solution chemistry was investigated by the use of Electron Spray Ionisation Mass Spectrometry (ESI-MS). These measurements were taken in water and the spectrum is shown below in Fig. 3.5.

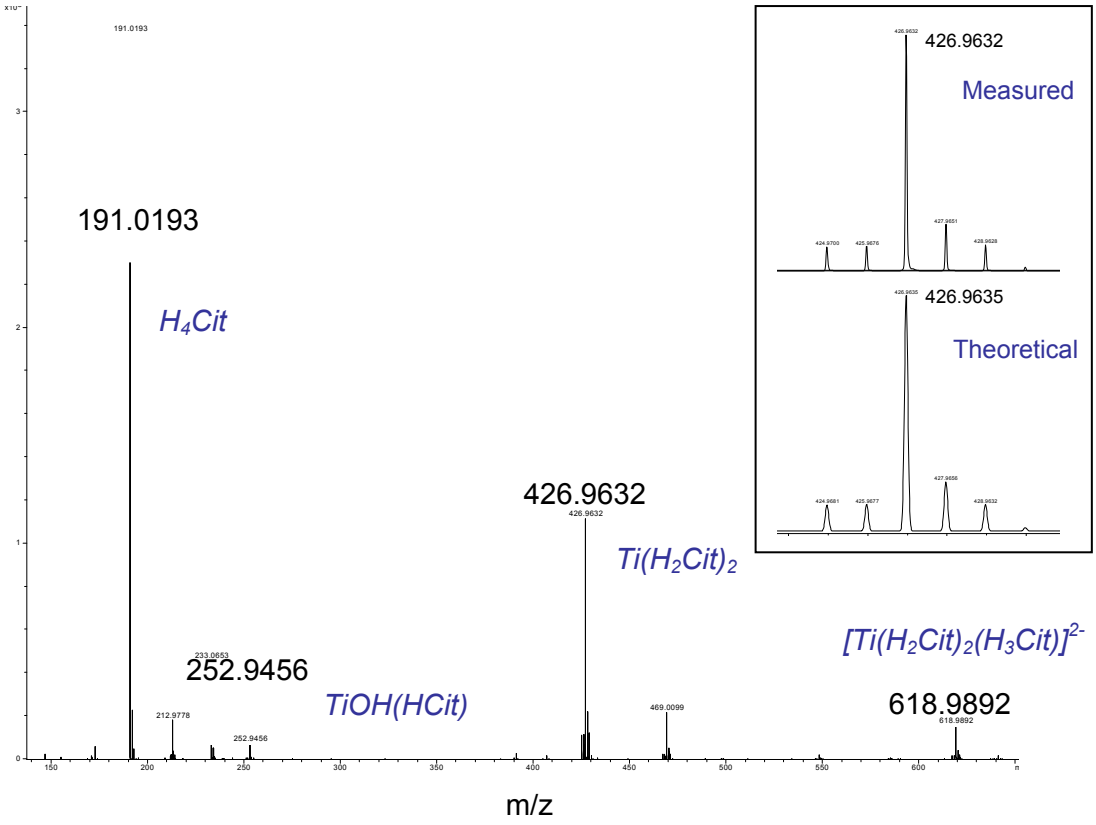

Figure 3.5 Mass spectrum of an aqueous solution of titanium citrate, all anions measured were $[M-H]^-$, the isotope pattern of $Ti(H_2Cit)_2$ is also shown

At a pH of 2, the Ti(HCit)OH and $Ti(H_2Cit)_3^{2-}$ are observed as described by Collins et al. In addition to these complexes, a titanium bis-citrate, $Ti(H_2Cit)_2$, and citric acid were also observed. An identical spectrum was obtained in methanol.

The pH was raised using a NaOH solution and the solution at each pH level was analyzed by mass spectrometry. When the pH was raised up to 5 then further anionic titanium species are observed including the penta-anionic $Ti(HCit)_3^{5-}$ as well as the tetra and tri-anionic titanium citrates. When the pH of the solution was raised further solid precipitates were observed in the acetonitrile/water mixture used for the mass spectrometry measurements.

Despite the evident solubility of the monometallic titanium citrate in methanol the reaction between titanium and citric acid must be carried out in an aqueous solution. This is to avoid the esterification of citric acid to dimethyl citrate (DMCA that can be catalysed by the titanium alkoxide present.

DMCA has been synthesised previously and the Sn(II) complex reported. The DMCA was synthesised by esterifying citric acid with methanol using a catalytic amount of H_2SO_4.[17] A further amount of DMCA was made in this way and recrystallised from methanol. The DMCA was analysed by ^1H, and ^{13}C NMR spectroscopy, elemental analysis and X-ray crystallography. The molecular structure is shown below in Fig. 3.6

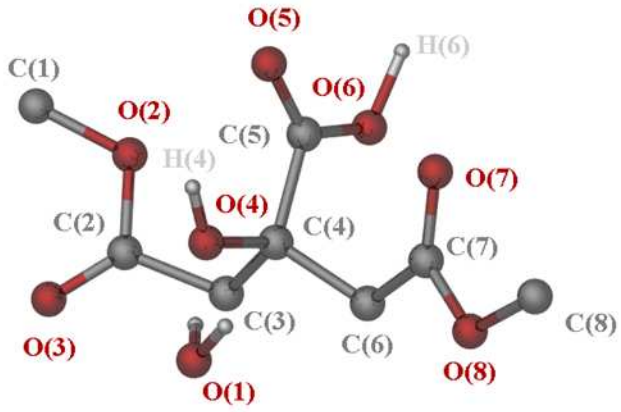

Figure 3.6 Molecular structure of dimethyl citrate monohydrate (DMCA)

The titanium tris-citrate anion is highly stable due to the steric bulk around the titanium centre, the three stable 5 membered rings formed and the strong hydrogen bonds formed between the terminal carboxylic acid groups. These factors protect the titanium centre from hydrolysis, however this stability can also reduce the catalytic

effectiveness of the titanium. By protecting the two terminal carboxylic groups there are only two possible bonding sites left for metal chelation. It has been shown that titanium selectively binds to these two sites with the unprotected citric acid. However, the diester is soluble in a range of organic solvents, and with the aim of forming stable complexes of ligand to titanium in a 1:1 and 2:1 ratio, was reacted with $Ti(O^iPr)_4$.

The complexes of DMCA with titanium were synthesised and isolated with titanium to citrate stoichiometries of 1:1 and 1:2. These complexes are labelled **4** and **5** respectively. The resulting citrate complexes contain less steric bulk around the titanium centre, no hydroxide groups and in the case of complex **4** labile isopropoxide groups. The molecular structure of **4** is shown below in Fig. 3.7.

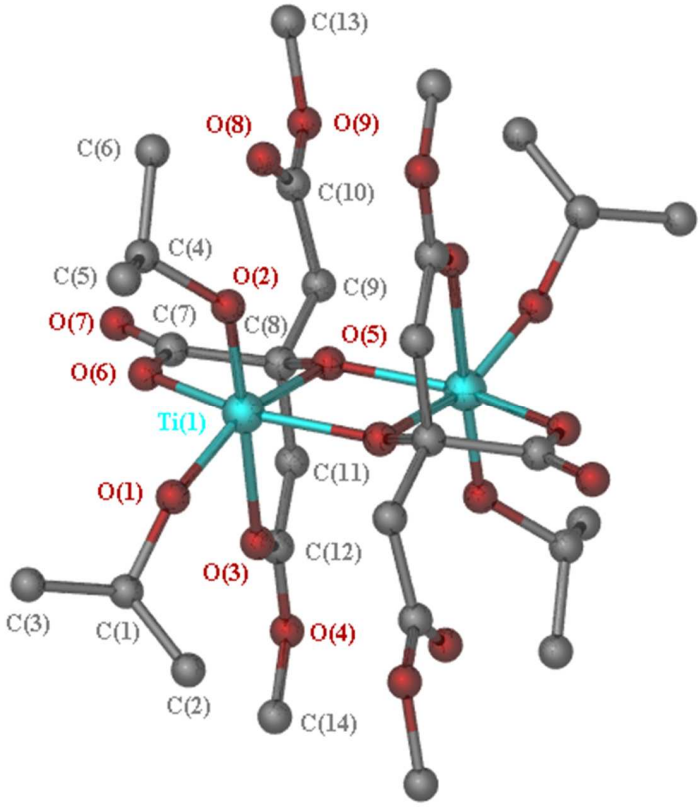

*Figure 3.7 Molecular structure of titanium DMCA complex **4***

The hydroxyl moiety on the DMCA ligand acts as a bridging group to the neighbouring titanium atom. The titanium oxygen bond distance Ti(1)-O(5) 2.066(2) Å is highly similar to Ti(1)-O(5)# 1.991(2) Å, as are the angles Ti(1)-O(5)#-Ti(1)# 106.08(4) ° and Ti(1)-O(5)-Ti(1)# 105.74(4)°.

A similar water soluble complex was synthesised with glycolic acid by Tomita et al. [50] As with complex **4,** the carboxylate and hydroxyl groups are deprotonated with the hydroxyl arm bridging between two titanium atoms. The bond distances and angles in the tetrameric complex observed by Tomita et al. are almost identical.

Mahrwald et al. synthesised a mandelic acid titanium complex which contained a similar five membered chelating ring to complex **4**, this complex also contained labile alkoxide groups.[51] The titanium alkoxide distances Ti(1)-O(1) 1.785(2) Å and Ti(1)-O(2) 1.788(2) Å are similar to the structure they reported. The five membered ring in **4** is distorted, and with the exception of the angle C(8)-O(5)-Ti(1) 113.29(13)° has similar bond lengths and angles to the tris-citrate titanium systems. This exception is due to the binding of the alkoxide with both titanium atoms. Similar binding modes using analogous ligands to DMCA were also observed for aluminium and gallium complexes.[52, 53]

Complex **5** was synthesised using similar methods and a fine microcrystalline solid was recovered on crystallisation from a toluene and hexane mixture. The complex was analyzed by NMR spectroscopy, melting point and elemental analysis. The analysis suggest the formation of $Ti(DMCA)_2$.

3.2.2 Heterometallic Titanium Citrate Synthesis and Characterisation

Having synthesised two well defined monometallic titanium citrates as well as establishing a practical synthesis for *in situ* titanium citrate, the synthesis of a number of heterometallic complexes was attempted. Heterobimetallic catalysts can often promote reactions more efficiently than their monomeric counterparts through a synergistic cooperation between two different metal centres. [54]

3.2.2.1 Titanium Sodium Citrate, $Na_2Ti(H_2Cit)_3 \cdot 10H_2O$, 6

A novel titanium sodium citrate, $Na_2Ti(H_2Cit)_3 \cdot 10H_2O$ (**6**), was recovered from a solution containing three equivalents of sodium hydroxide solution to the aqueous titanium citrate. Large colourless crystals in a 60% yield were obtained by slow evaporation of the volatiles.

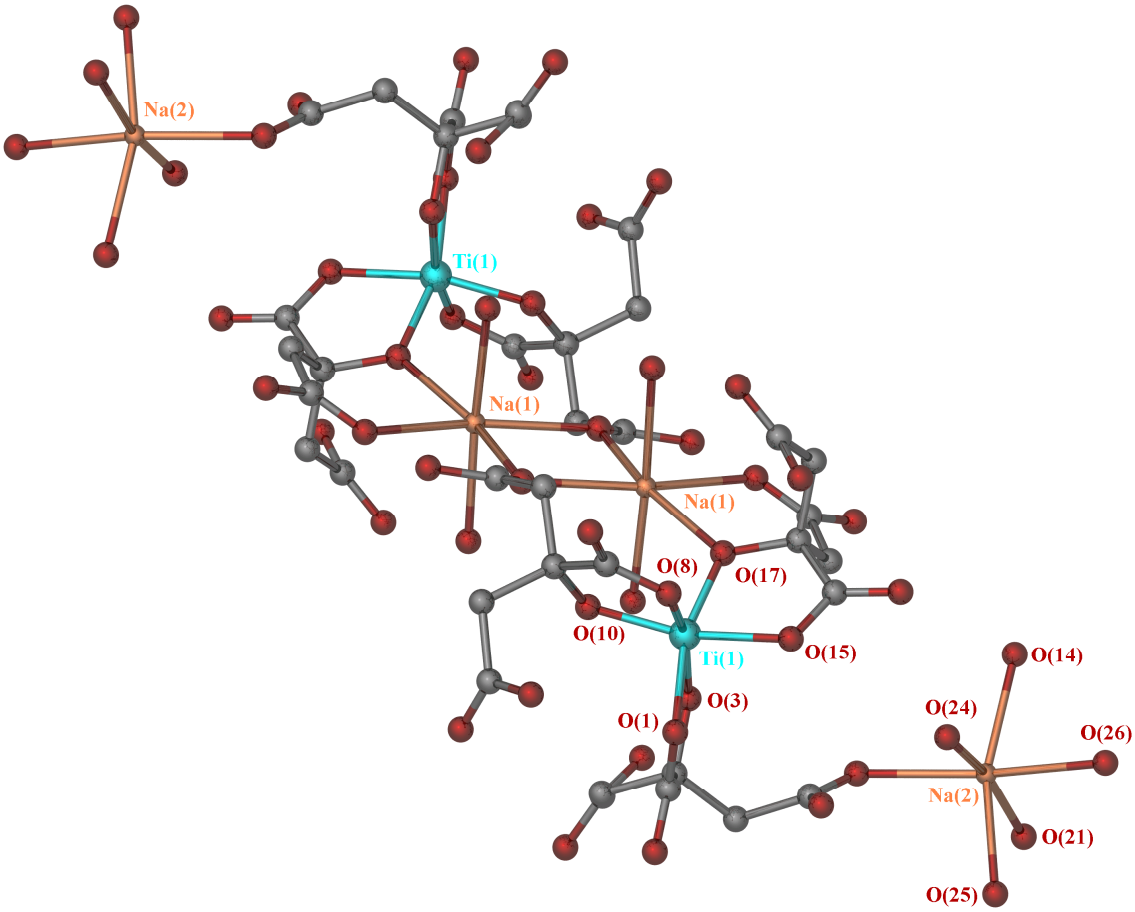

Figure 3.8 Molecular unit of the titanium citrate, $(Na_2Ti(C_6H_6O_7)_3 \cdot 10H_2O)_\infty$, **6**

Complex **6** includes a di-anionic titanium citrate and two sodium cations; similar to most titanium citrates the complex is heavily hydrated. The water in the structure was mainly disordered and was analysed using the SQUEEZE function of Platon. All hydrogen atoms on the sodium bound water have been omitted in Fig. 3.6 as it is not possible to accurately locate them.

The citric acid coordinates to the titanium through the formation of three five membered rings via the central deprotonated carboxyl and hydroxyl groups. All the terminal carboxylate groups are fully protonated leaving an overall charge of 2-, two sodium atoms then make up the crystal lattice. This bonding motif is consistent with other tris-citrate complexes published. [55]

In complex **6,** unlike in the di-anionic titanium citrate species ($NH_4Mg_{1/2}(Ti(H_2Cit)_3)$, the cations present are bound into the citrate ligand. [47] Each titanium citrate anion is bound to three sodium atoms, Na(1) that forms the dimer with two titanium citrate anions and Na(2) that binds to two other separate titanium citrate discs, exemplified by the bond lengths Na(2)-O(21) 2.424(4) Å and Na(2)-O(14) 2.365(4) Å. All the sodium atoms lie in an octahedral arrangement with the remaining coordination sphere completed by water molecules. The hydroxyl arm of one of the citrate acid ligands is distorted in **6** and binds to one of the bridging sodium atoms. giving three crystallographically unique citrate ligands around the titanium.

The titanium atom lies in a distorted octahedral formation. Paradies et al., reported an analogous tri-anionc species: $[TiNa_3(H_2Cit)_2(HCit)(H2O)_{6.8}] \cdot 2H_2O$. This complex contains hydroxyl bound sodium centres with similar bond lengths and angles to those observed in **6**. [44] Paradies et al. observed that the bite angle of the ligand was the primary reason for the distorted octahedral titanium geometry. The angles quoted, 78.89°, 78.94° and 79.27° are comparable to the angles observed in **6** of O(10)-Ti(1)-O(8) 79.00(11)°, O(17)-Ti(1)-O(15) 79.37(11)° and O(3)-Ti(1)-O(1) 78.81(11)°. Unlike the 3- anion discussed above, none of the terminal carboxylic acid arms are deprotonated and bind with the sodium atoms via a dative interaction with the carboxylate oxygen. This is the first example of the di-anionic titanium citrate being present in a sodium complex.

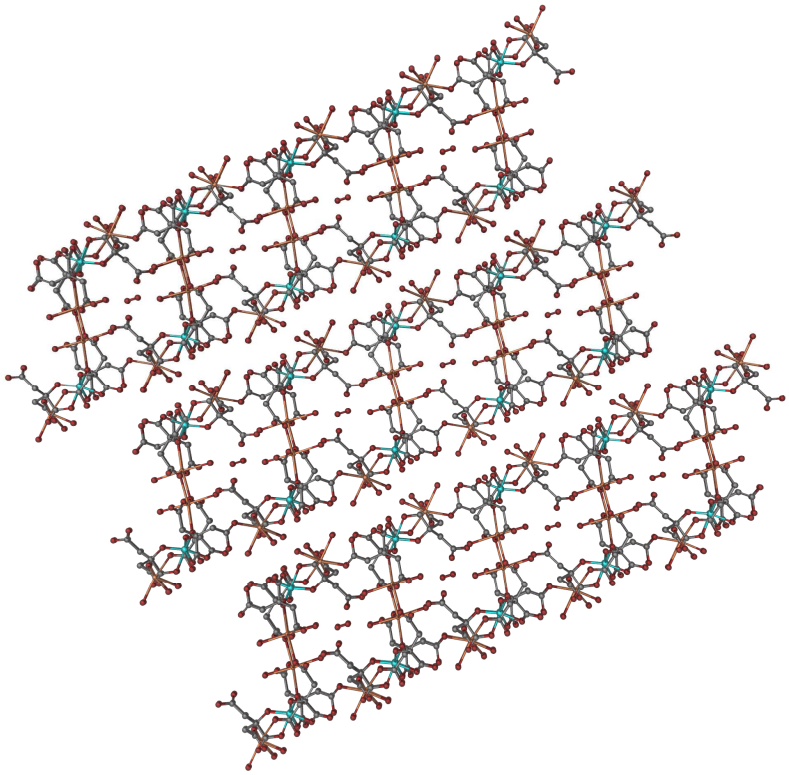

Figure 3.7 Supramolecular unit of the titanium citrate, $Na_2Ti(H_2Cit)_3 \cdot 10H_2O$, ***6***

The titanium dimers form elongated sheets bound together by the sodium atoms. These sheets align perpendicular to one another as shown in Fig. 3.7 above. The mass spectrum of the isolated complex **6** in an aqueous solution suggests that *in situ* citric acid, $NaTi(HCit)(H_2Cit)$, $HNaTi(H_2Cit)_3$ and $Na_3Ti(H_2Cit)_2(HCit)$ are all formed in solution.

3.2.2.2 Titanium Nickel Citrate, $Ni[Ti(H_2Cit)_3]_2 \cdot 13\ H_2O(H_3O^+)$, 7

On addition of 1 equivalent of $NiCO_3$ to a solution of titanium citrate, the colour of the solution changed to bright green. On refluxing overnight all the nickel carbonate had reacted and small colourless crystals suitable for X-ray crystallography were recovered on standing. Titanium nickel citrate, **7**, was also characterised by the melting point, elemental analysis and ^1H NMR spectroscopy.

The structure obtained contained the same tris-citrate di-anion, **A**, discussed in the introduction. Complex **7**, $Ni[Ti(H_2Cit)_3]_2 \cdot 13\ H_2O(H_3O^+)$ is similar to the titanium

citrate $KMg_{½}[Ti(H_2Cit)_3] \cdot 6\ H_2O$ and isomorphic with the citrate $(NH_4)Mg_{½}[Ti(H_2Cit)_3] \cdot 6\ H_2O$ published by Zhou et al. [47]

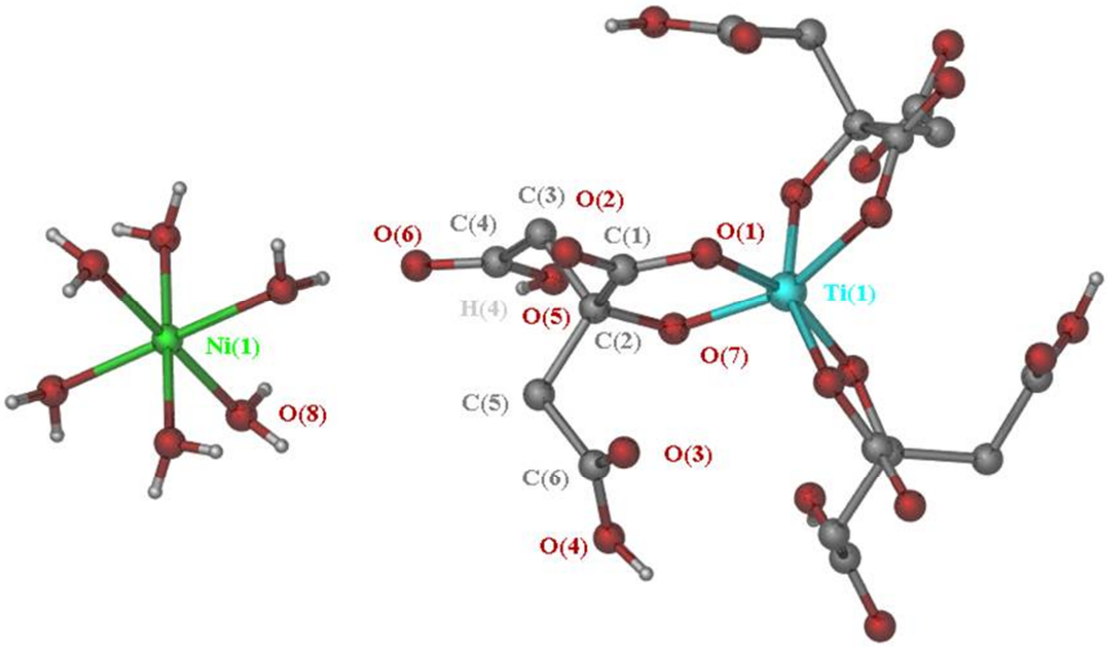

Figure 3.8 Molecular structure of the titanium nickel citrate ***7***

The citric acid binds to the titanium centre via the central deprotonated hydroxyl and carboxylic acid groups. The binding though these atoms forms a stable 5 membered ring. The bond lengths Ti(1)-O(1) 2.052(1) Å and Ti(1)-O(7) of 1.879(1) Å and the binding mode are in agreement with literature precedents. [47, 56]

The titanium citrate anions shown in Fig. 3.9 form elongated 'tubes' with a water molecule hydrogen bonded between each titanium citrate disc (Fig. 3.9). The water molecule participates in hydrogen bonding with both citrates, fixing the structure together. The distance between titanium atoms is on average 7.6 Å, where the distance of the water molecule to the first titanium centre is only 3.6 Å.

In the crystal lattice, depicted in Fig 3.10, the titanium citrate discs form hexagonal structures around the nickel cations. A large amount of water is bound through various hydrogen bonding modes into the structure, this makes the complex highly stable to nucleophilic attack.

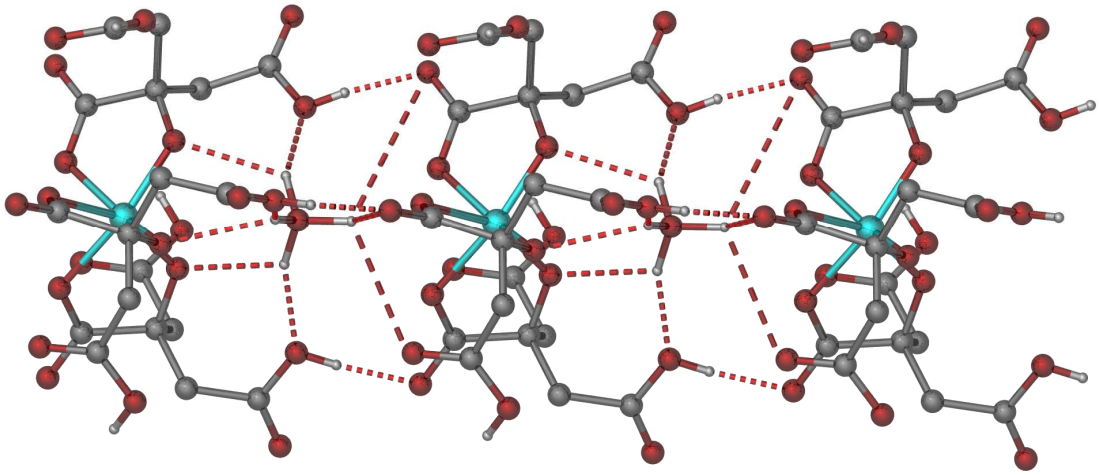

Figure 3.9 Molecular diagram showing the titanium citrate 'tube' of **7**, *joined by a trapped, hydrogen bonded, water molecule (modelled over two sites). Some water molecules and all alkyl hydrogen atoms have omitted for clarity*

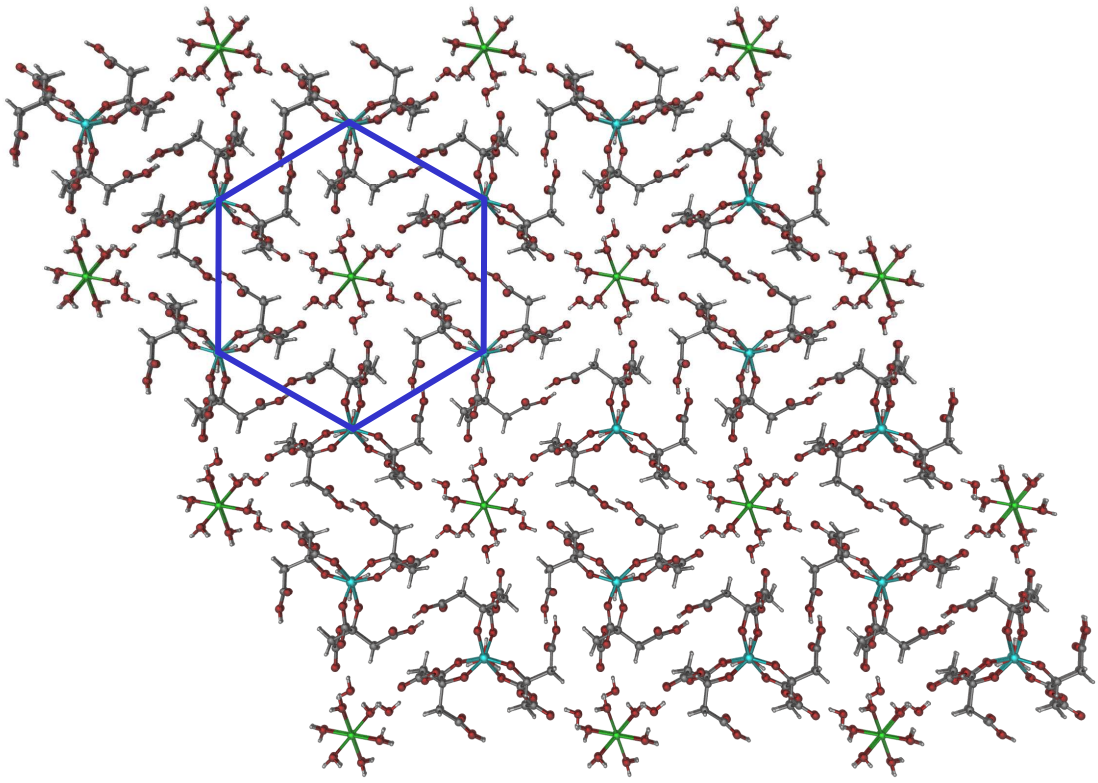

Figure 3.10 Molecular diagram showing the larger titanium citrate structure

3.2.2.3 Titanium Barium Citrate, via the Pechini method, 8

Titanium barium citrate **8** was synthesised by the method given by Tsay et al. [45] The compound was analysed by FT-IR, melting point and elemental analysis. The IR spectrum shows CO stretches at 1727, 1647 and 1377 cm^{-1}. This is comparable to the modes quoted by Tsay et al at 1730, 1637 and 1374 cm^{-1}. The melting point and elemental analysis confirm the formation of $TiBa(C_6H_6O_7)_3$. Titanium barium citrate is insoluble in all common organic solvents. Using this heterogeneous material could be advantageous in the production of biodiesel. Even though only a few citrates are soluble in methanol, their high affinity to water could lead to leaching of the catalyst if high water value waste oils are used as a feedstock.

3.2.2.4 Titanium Tin (II) Citrate, 9

$SnCl_2$ was added to an aqueous solution of titanium citrate and stirred over night. The solution went light green, the pH of the solution was found to be between 1 and 2. No observable solids were formed on evaporation. The gel was analysed by ^{1}H and ^{13}C NMR spectroscopy and showed a citrate system that is heavily hydrated. The ^{119}Sn NMR spectrum shows a single peak at –696.9 ppm which is characteristic of an octahedral Sn(II) metal ion, the spectrum is shown below in Fig. 3.11.

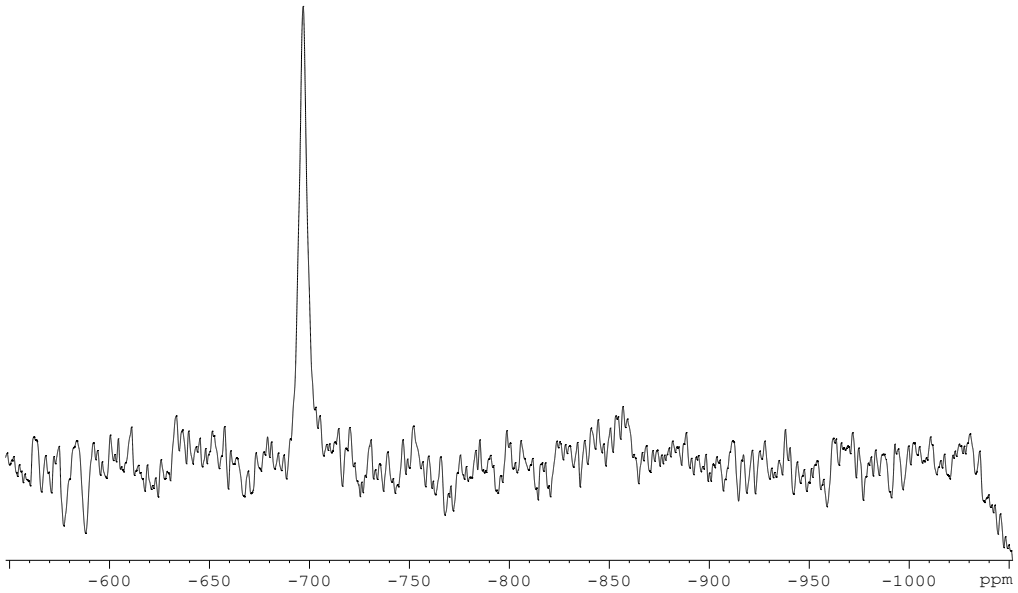

*Figure 3.11 ^{119}Sn (^{1}H) NMR spectrum of the tin titanium citrate **9***

The elemental analysis suggests that a possible empirical formula is $TiSn(H_2Cit)_3 \cdot 2HCl \cdot 3H_2O$. The structure of **9** is presumably similar to that of the titanium barium citrate discussed previously. An aqueous solution of **9** was analyzed by mass spectrometry. The mass spectrum of **9**, shown below in Fig. 3.13, demonstrates the possible solution equilibria of the system. As there is only one observable peak in the ^{119}Sn NMR spectrum it suggests that the system is in rapid equilibrium.

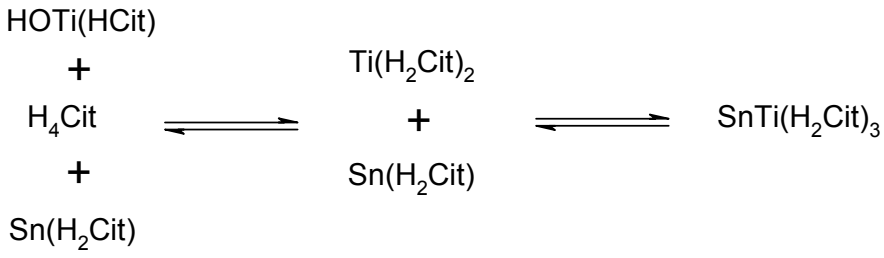

*Figure 3.12 Possible solution equilibrium of titanium tin citrate **9***

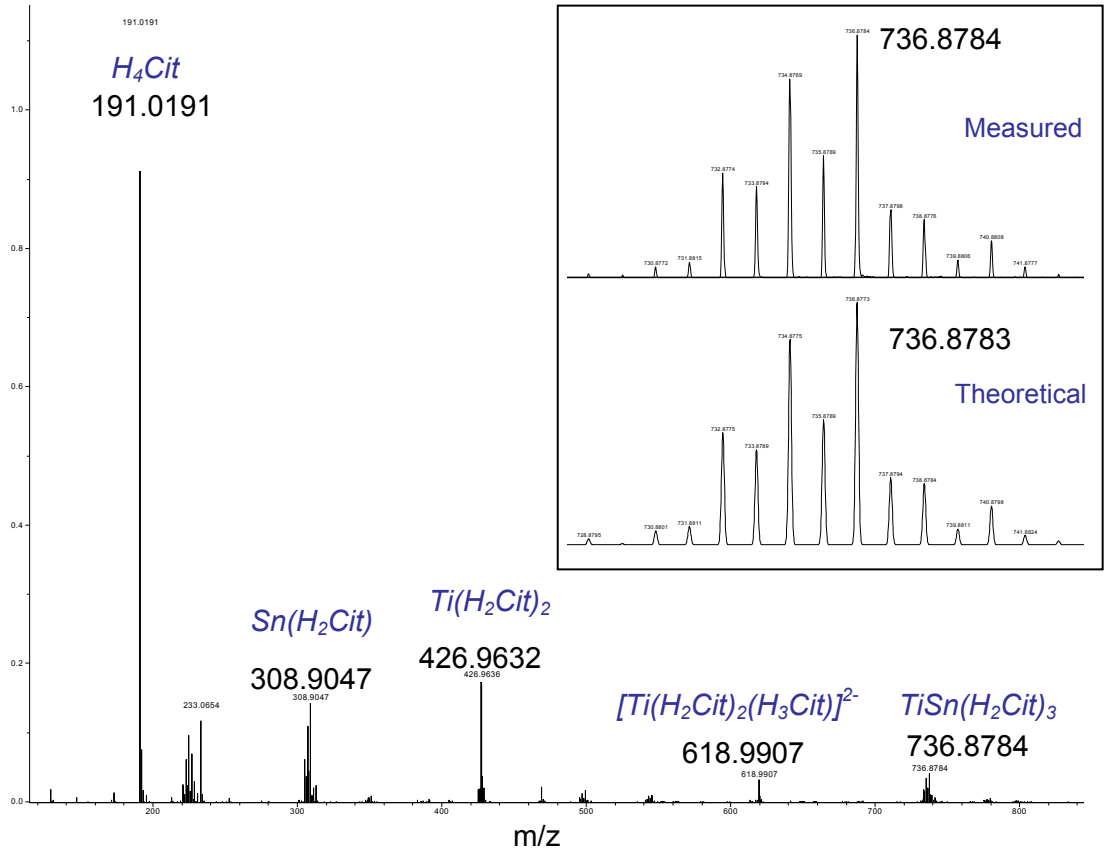

Figure 3.13 Mass spectrum of an aqueous solution of titanium tin citrate, ***9,*** *the isotope pattern of* $TiSn(H_2Cit)_3$ *is also shown, all measurements were of* $(M\text{-}H)^-$

In an attempt to make a homogeneous methanolic solution of the titanium tin citrate, the hydrated gel was dried under vacuum for 24 hours and redissolved in methanol. On standing for a further 24 hours only DMCA was recovered.

3.2.2.5 Titanium Aluminium Citrate, 10

To the aqueous solution of titanium citrate, aluminium isopropoxide was added. The solution turned gunmetal blue, and on reaction of all the solid and removal of the resulting IPA, a gel was recovered. Unlike **9** the titanium aluminium citrate is an insoluble gel in methanol. As expected the ^{1}H and ^{13}C NMR spectroscopy data reveals little structural information. The ^{27}Al NMR data, shown in Fig 3.14 below, is more revealing.

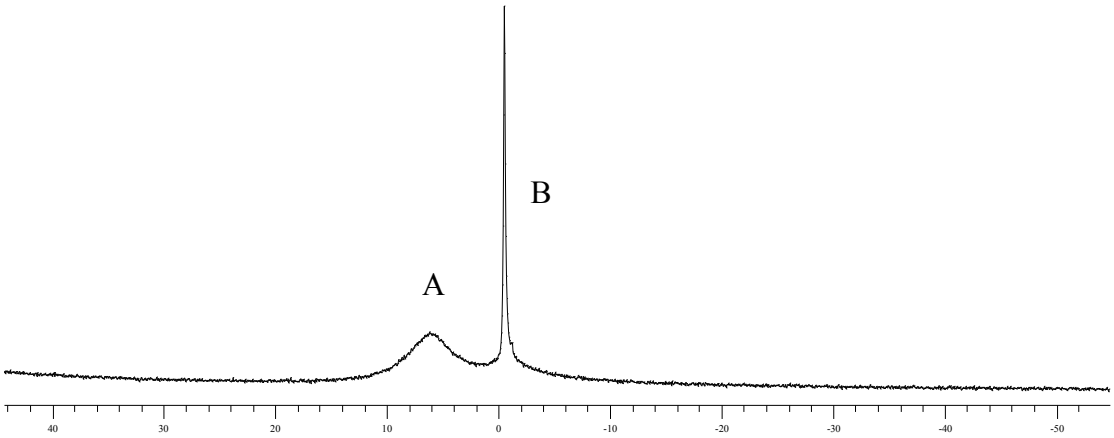

Figure 3.14. ^{27}Al (^{1}H) NMR spectrum of the aluminium titanium citrate CCCA 10.1

The NMR spectrum shows two peaks, one broad (A) and one sharp (B), at 6.03 and –0.52 ppm respectively, suggesting that there are at least two different environments occupied by aluminium. The chemical shift of (A) suggests that one aluminium is in an octahedral arrangement, the peak is very broad and suggests that the environment is distorted. The sharp peak (B) suggests that a symmetrical, octahedral aluminium is also present in solution. An aqueous solution of titanium aluminium citrate was analyzed by mass spectrometry and no evidence of a hetero metallic titanium aluminium citrate was observed. However, peaks corresponding to aluminium bis-citrate, aluminium tris-citrate, titanium bis-citrate and titanium tris-citrate were all identified. No peak relating to $Al(OH)_6^{3+}$ was observed in the spectrum. These results suggest that, at least at the stoichiometry used in the synthesis of **10**, the formation of a heterometallic complex is not favourable.

3.2.3 HOMOMETALLIC CITRATES OF DIVALENT METAL IONS

This section details a number of homometallic compounds synthesised in an attempt to make titanium based heterometallic citrate complexes. These complexes were then used as catalysts to directly compare the activity of the mixed metal titanium citrates detailed above.

The mass spectroscopic data collected for the titanium citrate in solution presented in this chapter and the previous work achieved by Collins et al. demonstrate that free citric acid is present. [42] Various divalent metal salts were added to the titanium

source, followed by the isolation of monometallic citrate species. The reaction between the salt and the free ligand seems to be kinetically favoured, and high yields are obtainable by the formation of a stable citric acid salt.

Zinc acetate was added to a solution of titanium citrate and on refluxing over 48 hours a clear solution was obtained. A zinc citrate complex, **11**, was recovered and characterised by ^{1}H, ^{13}C NMR spectroscopy and X-ray crystallography. **11** is isomorphic with a previously published manganese citrate structure. [57] A shortening of the bond distances and slight warping of the angles in comparison to the published structure was observed. This is due to the difference in the effective nuclear charge between manganese and zinc. The molecular unit of complex **11,** is shown below in Fig. 3.15

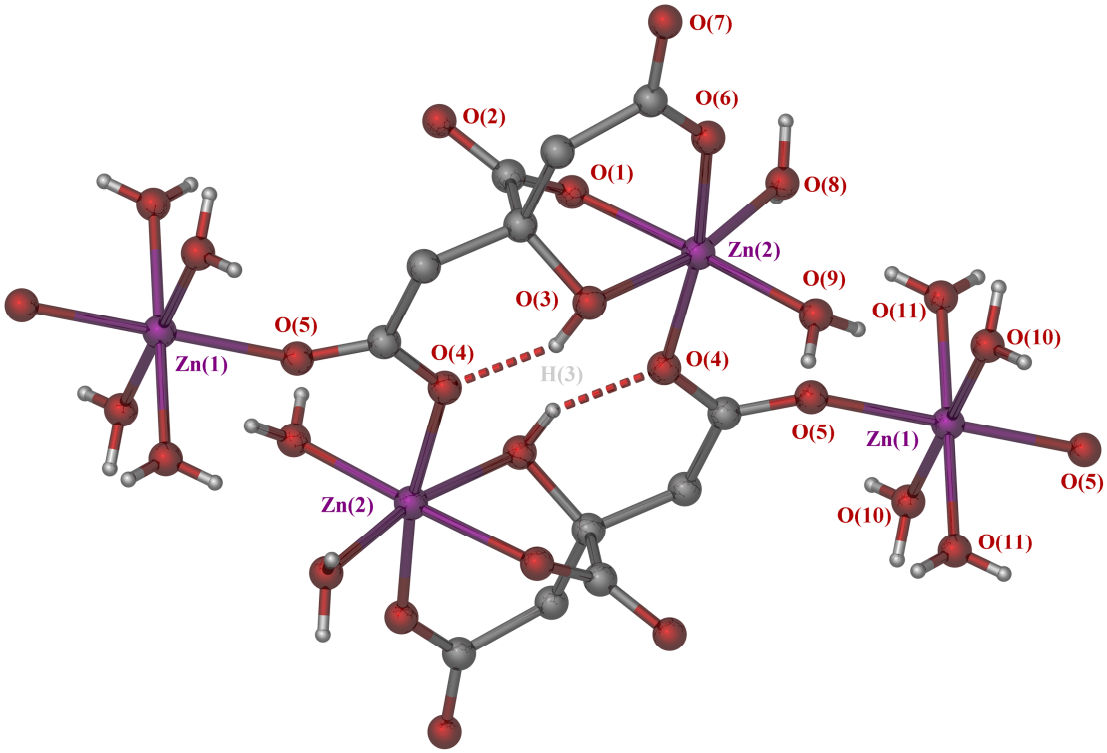

*Figure 3.15 Molecular unit of the zinc citrate complex **11**, all alkyl hydrogen atoms have been removed for clarity*

One other structural example of a zinc citrate has been reported in the literature. Hudson et al. synthesised a range of cubane like isostructural complexes using a range divalent metals, citric acid and guanidine. [3] All the complexes reported contained the $M_4(Cit)_4^{8-}$ anion and were heavily hydrated. Unlike these cubane structures **11** is

comprised of two crystallographically unique zinc centres. One in an unsymmetrical distorted octahedral arrangement, Zn(2), exemplified by the angles O(4#)-Zn(2)-O(6) 170.29(5)° and O(3)-Zn(2)-O(6) 83.11(5)°. The zinc atom is facially capped by the citric acid. Constrained ligand geometry, rather than any loss of degeneracy means an increased distortion of certain angles and bond lengths. The largest bond is that between the alcohol and the zinc, the shortest between the zinc and water molecules. This is consistent with findings of Wang et al. who reported the isomorphic manganese structure $[Mn(HCit)_2]^{4-}$. [57]

Zn (1) lies in a symmetrical octahedral arrangement exemplified by the angles O(5)-Zn(1)- O(5#) 180.00(1)° and O(5)-Zn(1)-O(11) 92.15(6) °. The unsymmetrical Zn (2) has a typical bond length with the citric oxygen atoms of 2.1 Å and with the water oxygen atoms of 2.0 Å. The symmetrical Zn atom has an average bond length of 2.1 Å with the citric oxygens and 2.0 Å with the water oxygens; this is also consistent with examples of similar systems in the literature. [3]

On addition of manganese carbonate the aqueous titanium citrate solution a bright orange solution was formed. On standing crystals of complex **12** the manganese citrate, $Mn_3(HCit)_3 \cdot 14\ H_2O$ were recovered. The complex was analyzed by mass spectrometry, elemental analysis and X-ray crystallography. Complex **12**, is the same structure as that published by Wang et al. [57]

The published manganese citrate structure was synthesised over 72 hours, from the reaction between manganese acetate and citric acid at a high temperature and pressure in a basic aqueous solution. In this study, however, complex **12** was obtained from a solution of $MnCO_3$ and aqueous titanium citrate after refluxing for 24 hours. Manganese citrate is an example of a weak field case, with the Mn(II) having 5 d-electrons in a high spin configuration. As a result complex **12** is highly paramagnetic and no useful NMR data could be obtained.

Zhou et al also published two further manganese citrate structures, $Mn(HCit)_2^{4-}$ and $Mn(HCit)^-$, as well as isolating the corresponding Mn (III) complexes. [57, 58] Mass spectrometric analysis of an aqueous solution of complex **12** suggested that these three complexes are present in solution as well as a $Mn_2(H_2Cit)_2$ species.

On addition of calcium aceate to the titanium citrate solution a sparsely soluble white solid was recovered, complex **13**. The elemental data, melting point and ^1H NMR spectroscopy supported the formation of the hydrated $Ca_3(HCit)_2$ complex reported by Chatterjee et al. [10]

3.2.4 CATALYTIC ACTIVITY IN THE CONVERSION OF SOYBEAN OIL

The complexes **4-13** were then tested for their activity in the transesterification of virgin soybean oil. The starting materials used to form these complexes were also tested.

The following catalytic results were obtained at 195 ºC over 2 hours with a catalyst loading of 2.5 mol%. Soybean oil was used with a methanol ratio of 12:1. The same experimental procedure employed is detailed in Chapter 2, Section 2.2.2.

.

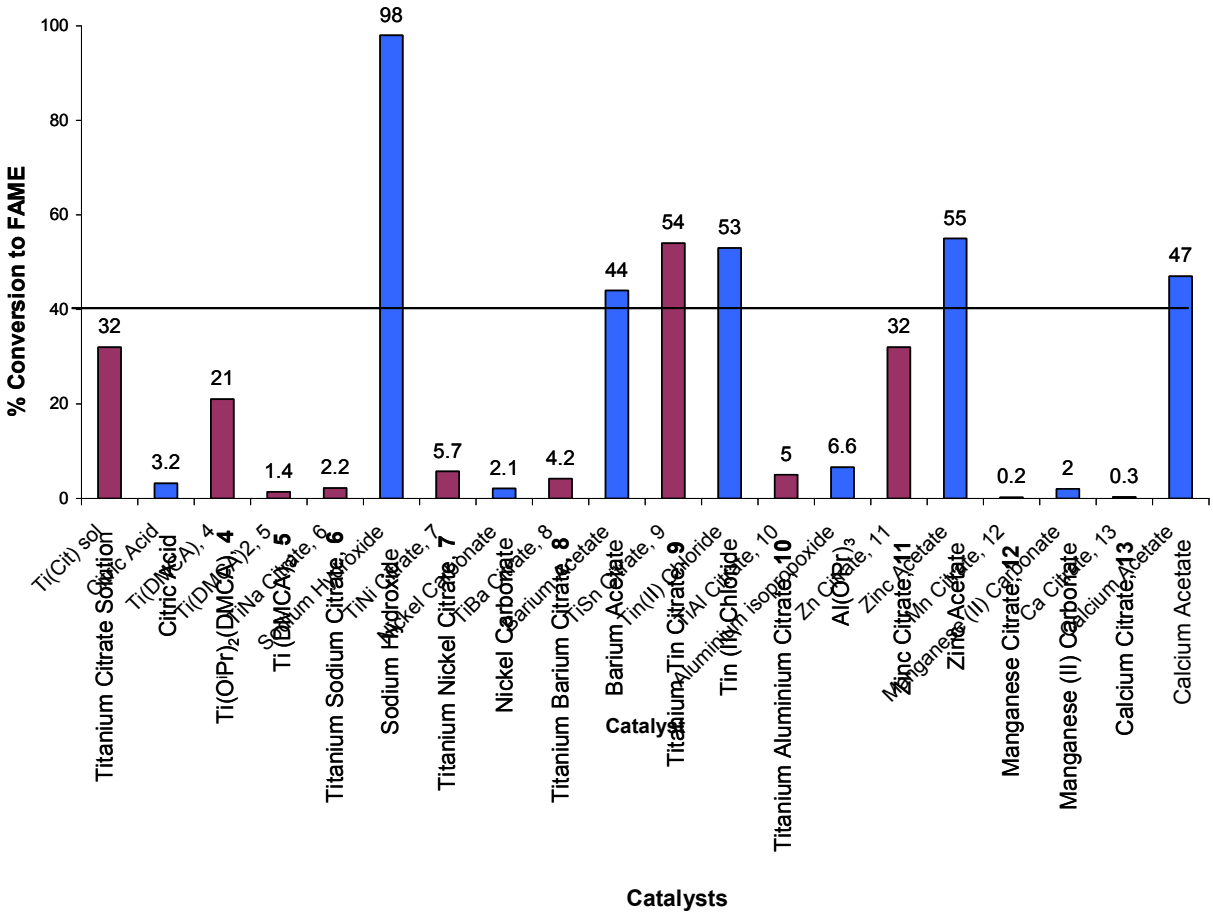

Figure 3.16 The catalytic activity of the synthesised citrate complexes, (purple) and the starting materials (blue) in the synthesis of FAME, the black line denotes the catalytic activity of $Ti(O^iPr)_4$.

In coordinating citric acid to titanium a series of methanol and water stable catalysts were created. The titanium citrate gel is heavily hydrated, despite the possibility of hydrolysis of the catalyst or the triglyceride, the catalyst still displays a degree of activity. However the yield of FAME is less than that obtained by using $Ti(O^iPr)_4$ as a catalyst. In using DMCA as a ligand instead of citric acid, two titanium species were synthesised. In comparison to the titanium citrate these complexes have less steric bulk around the titanium centre, with the titanium possessing labile ligands. In this way it was hoped to increase the activity of the homometallic citrate. Unfortunately this was not the case, with complexes **4** & **5** being too stable to affect the production of FAME.

When mixed metal titanium citrate complexes were screened in order to increase the activity through a cooperative effect, the catalytic activity was diminished even further. The homometallic citrates **11-13** were also inactive in the production of biodiesel, despite the simple salt starting materials being more active catalysts. With the exception of the titanium tin citrate species **9**, all the citrate complexes start to decompose at temperatures above 200 ºC. As titanium tin citrate is the only citrate catalyst that demonstrates a high degree of activity, the decomposition products of this reaction might be the catalytically active species. The original titanium sodium citrate screened at Johnson Matthey for the production of PET was only observed to be active at temperatures approaching 250 ºC, which is above its decomposition temperature. None of the titanium complexes, including complex **6**, showed any visible sign of saponification or the hydrolysis product TiO_2.

3.3 SUMMARY

Titanium citrates are highly variable species, taking many forms when in equilibrium in solution. The five membered ring formed between the titanium and citric acid ligand in the tris-citrate complex is highly stable. The binding modes of citric acid to other metals are also stable. This bonding motif means, along with their heavily hydrated character, that they are poor catalysts for the production of biodiesel.

In Chapter 2, the use of diol ligands as chelating agents were explored and found to protect the titanium centre from methanolysis but not hydrolysis. Using citric acid as a ligand, attractive as it is inexpensive and its complexes are considered to be environmentally benign, stabilises the titanium against hydrolysis. However, despite the increased water stability essential in converting waste oils to FAME, the loss in activity over using $Ti(O^{i}Pr)_4$, is too substantial for the catalysts to be considered industrially viable.

In the next chapter, naturally occurring amino acids are used as ligands, by changing the bonding motif it is hoped that the protection of the titanium centre will be somewhat moderated.

3.4 REFERENCES

1. J. McMurray, *Organic Chemistry*, 4th Edition, Brooks/Cole Publishing Company, 1996.
2. M. Matzapetakis, N. Karligiano, A. Bino, M. Dakanali, C.P. Raptopoulou, V. Tangoulis, A. Terzis, J. Giapintzakis and A. Salifoglou, *Inorganic Chemistry*, 2000, **39**, 4044-4051.
3. T. A. Hudson, K. J. Berry, B. Moubaraki, K. S. Murray and R. Robson, *Inorganic Chemistry*, 2006, **45**, 3549-3556.
4. T. Kemmitt, N. I. Al-Salim, G. J. Gainsford, A. Bubendorfer and M. Waterland, *Inorganic Chemistry*, 2004, **43**, 6300-6306.
5. E. N. Baker, H. M. Baker, B. F. Anderson and R. D. Reeves, *Inorganica Chimica Acta-Bioinorganic Chemistry*, 1983, **78**, 281-285.
6. R. Job, P. J. Kelleher, W. C. Stallings, C. T. Monti and J. P. Glusker, *Inorganic Chemistry*, 1982, **21**, 3760-3764.
7. J. P. Glusker, D. Van Der Helm, W. E. Love, M. Dornberg, J. A. Minkin, C. K. Johnson and A. L. Patterson, *Acta Crystallographica*, 1965, **19**, 561-574.
8. M. Rossi, L.F. Rickles and J. P. Glusker, *Acta Crystallographica C*, 1983, **39**, 987-990.
9. C. E. Nordman, A. S. Weldon and A. L. Patterson, *Acta Crystallographica*, 1960, **12**, 414-417.
10. K. P. Chatterjee and N. R. Dhar, *Journal of Physical Chemistry*, 1924, **28**, 1009-1028.
11. C. K. Johnson, *Acta Crystallographica*, 1965, **18**, 1004-1017.
12. B. Sheldric, *Acta Crystallographica Section B-Structural Science*, 1974, **B 30**, 2056-2057.
13. R. Baggio and M. Perec, *Inorganic Chemistry*, 2004, **43**, 6965-6968.
14. R. S. Dickins, S. Aime, A. S. Batsanov, A. Beeby, M. Botta, J. Bruce, J. A. K. Howard, C. S. Love, D. Parker, R. D. Peacock and H. Puschmann, *Journal of the American Chemical Society*, 2002, **124**, 12697-12705.

15. S. Bouhlassa, M. Petitramel and R. Guillaumont, *Bulletin De La Societe Chimique De France Partie I-Physicochimie Des Systemes Liquides Electrochimie Catalyse Genie Chimique*, 1984, 5-11.
16. O. Seiler, C. Burschka, D. Schwahn and R. Tacke, *Inorganic Chemistry*, 2005, **44**, 2318-2325.
17. P. R. Deacon, M. F. Mahon, K. C. Molloy and P. C. Waterfield, *Journal of the Chemical Society Dalton Transactions*, 1997, 3705-3712.
18. G. Q. Wu, L. Y. Wang, D. G. Evans and X. Duan, *European Journal of Inorganic Chemistry*, 2006, 3185-3196.
19. M. Murrie, S. J. Teat, H. Stoeckli-Evans and H. U. Gudel, *Angewandte Chemie-International Edition*, 2003, **42**, 4653-4656.
20. R. Zhao, Y. F. Deng, Z. H. Zhou and S. W. Ng, *Acta Crystallographica Section E-Structure Reports Online*, 2003, **59**, M666-M668.
21. M. Kaliva, E. Kyriakakis and A. Salifoglou, *Inorganic Chemistry*, 2002, **41**, 7015-7023.
22. M. Kaliva, T. Giannadaki, A. Salifoglou, C. P. Raptopoulou and A. Terzis, *Inorganic Chemistry*, 2002, **41**, 3850-3858.
23. J. Q. Xu, D. M. Li, Y. H. Xing, R. Z. Wang, S. Q. Liu, T. G. Wang, Y. Xing, Y. H. Lin and H. Q. Jia, *Journal of Coordination Chemistry*, 2001, **53**, 25-33.
24. Z. H. Zhou, H. L. Wan and K. R. Tsai, *Polyhedron*, 1997, **16**, 75-79.
25. C. Djordjevic, M. Lee and E. Sinn, *Inorganic Chemistry*, 1989, **28**, 719-723.
26. D. W. Hartley, G. Smith, D. S. Sagatys and C. H. L. Kennard, *Journal of the Chemical Society-Dalton Transactions*, 1991, 2735-2739.
27. G. Smith, D. S. Sagatys, R. C. Bott, D. E. Lynch and C. H. L. Kennard, *Polyhedron*, 1992, **11**, 631-634.
28. S. Senthilkumaar, K. Porkodi and R. Vidyalakshmi, *Journal of Photochemistry and Photobiology a-Chemistry*, 2005, **170**, 225-232.
29. M. P. Pechini, *United States Pat.*, US 3330697, 1966.
30. J. X. Li, Z. Y. Wen, X. X. Xu, Z. H. Gu and X. H. Xu, *Journal of Inorganic Materials*, 2007, **22**, 432-436.
31. X. X. Xu, Z. Y. Wen, J. G. Wu and X. L. Yang, *Solid State Ionics*, 2007, **178**, 29-34.

32. R. Mouazer, Y. Elmarraki, M. Persin, M. Cretin, J. Sarrazin and A. Larbot, *Colloids and Surfaces a-Physicochemical and Engineering Aspects*, 2003, **216**, 261-273.
33. W. J. Zheng, H. X. Zhao, M. M. Xu, D. K. Peng and G. Y. Meng, *Journal of Inorganic Materials*, 2000, **15**, 451-455.
34. R. B. J. Martin, *Inorganic Biochemistry*, 1986, **28**, 181-187.
35. H. Z. Sun, H. Y. Li, R. A. Weir and P. J. Sadler, *Angewandte Chemie-International Edition*, 1998, **37**, 1577-1579.
36. J. M. Fritsch and K. McNeill, *Inorganic Chemistry*, 2005, **44**, 4852-4861.
37. B. Rodriguez-Garrido, M. C. Arbestain, M. C. Monterroso and F. Macias, *Environmental Science & Technology*, 2004, **38**, 5046-5052.
38. M. Dakanali, E. T. Kefalas, C. P. Raptopoulou, A. Terzis, G. Voyiatzis, I. Kyrikou, T. Mavromoustakos and A. Salifoglou, *Inorganic Chemistry*, 2003, **42**, 4632-4639.
39. Y. F. Deng, Z. H. Zhou, H. L. Wan and K. R. Tsai, *Inorganic Chemistry Communications*, 2004, **7**, 169-172.
40. M. Kakihana, M. Tada, M. Shiro, V. Petrykin, M. Osada and Y. Nakamura, *Inorganic Chemistry*, 2001, **40**, 891-894.
41. T. Kemmitt, N. I. Al-Salim, G. J. Gainsford, A. Bubendorfer and M. Waterland, *Inorganic Chemistry*, 2004, **43**, 6300-6306.
42. J. M. Collins, R. Uppal, C. D. Incarvito and A. M. Valentine, *Inorganic Chemistry*, 2005, **44**, 3431-3440.
43. E. T. Kefalas, P. Panagiotidis, C. P. Raptopoulou, A. Terzis, T. Mavromoustakos and A. Salifoglou, *Inorganic Chemistry*, 2005, **44**, 2596-2605.
44. J. Paradies, J. Crudass, F. MacKay, L. J. Yellowlees, J. Montgomery, S. Parsons, L. Oswald, N. Robertson and P. J. Sadler, *Journal of Inorganic Biochemistry*, 2006, **100**, 1260-1264.
45. J. Tsay and T. Fang, *Journal of the American Ceramic Society*, 1999, **82**, 1409-1415.
46. Y. F. Deng, Z. H. Zhou and H. L. Wan, *Inorganic Chemistry*, 2004, **43**, 6266-6273.
47. Z. Zhou, Y. Deng, Y. Jiang, H. Wan and S. Ng, *Dalton Transactions*, 2003, 2636-2638.

48. C. W. Schwietert and J. P. McCue, *Co-ordination Chemistry Reviews*, 1999, **184**, 67-89.
49. M. Lunn and M. G. Davidson., *Personal Communication*, Johnson Matthey Catalysts 2004.
50. K. Tomita, V. Petrykin, M. Kobayashi, M. Shiro, M. Yoshimura and M. Kakihana, *Angewandte Chemie-International Edition*, 2006, **45**, 2378-2381.
51. R. Mahrwald and B. Ziemer, *Tetrahedron Letters*, 2002, **43**, 4459-4461.
52. C. Rennekamp, H. Wessel, H. W. Roesky, P. Muller, H. G. Schmidt, M. Noltemeyer, I. Uson and A. R. Barron, *Inorganic Chemistry*, 1999, **38**, 5235-5240.
53. G. A. Banta, S. J. Rettig, A. Storr and J. Trotter, *Canadian Journal of Chemistry-Revue Canadienne De Chimie*, 1985, **63**, 2545-2549.
54. M. Shibasaki, H. Sasai and T. Arai, *Angewandte Chemie-International Edition in English*, 1997, **36**, 1237-1256.
55. Y. Deng, Z. Zhou and H. Wan, *Inorganic Chemistry*, 2004, **43**, 6266-6273.
56. E.T. Kefalas, P. Panagiotidis, C.P. Raptopoulou, A. Terzis, T. Mavromoustakos and A. Salifoglou, *Inorganic Chemistry*, 2005, **44**, 2596-2605.
57. W. G. Wang, X. F. Zhang, F. Chen, C. B. Ma, C. N. Chen, Q. T. Liu, D. Z. Liao and L. C. Li, *Polyhedron*, 2005, **24**, 1656-1668.
58. H. L. Carrell and J. P. Glusker, *Acta Crystallographica B*, 1973, **29**, 638-639.
59. G. Knothe, *Journal of the American Oil Chemists Society*, 2000, **77**, 489-493.

CHAPTER 4

METAL COMPLEXES BASED ON α-AMINO ACIDS

This chapter describes the synthesis, structure and reactivity of a number of titanium and zinc α-amino acid complexes. A series of amino acid derived phenolate ligands have also been synthesised and their titanium and germanium adducts made. These complexes have been the investigated as Lewis acid catalysts for the transesterification of soybean oil to FAME.

4.1 INTRODUCTION

There are 20 standard naturally occurring α-amino acids, and one β-amino acid. In α-amino acids the carboxylic acid and amine are both situated on the same carbon, they have the general formula $HOOCCRHNH_2$. With the exception of glycine and β-alanine all of these amino acids are chiral, with both the L- and D- optical isomers being found in nature. A list of relevant naturally occurring amino acids explored in this study is given below in Fig 4.1. α-Amino acids are attractive ligands as they are inexpensive, readily available from a variety of sources and the decomposition products are generally non-toxic.

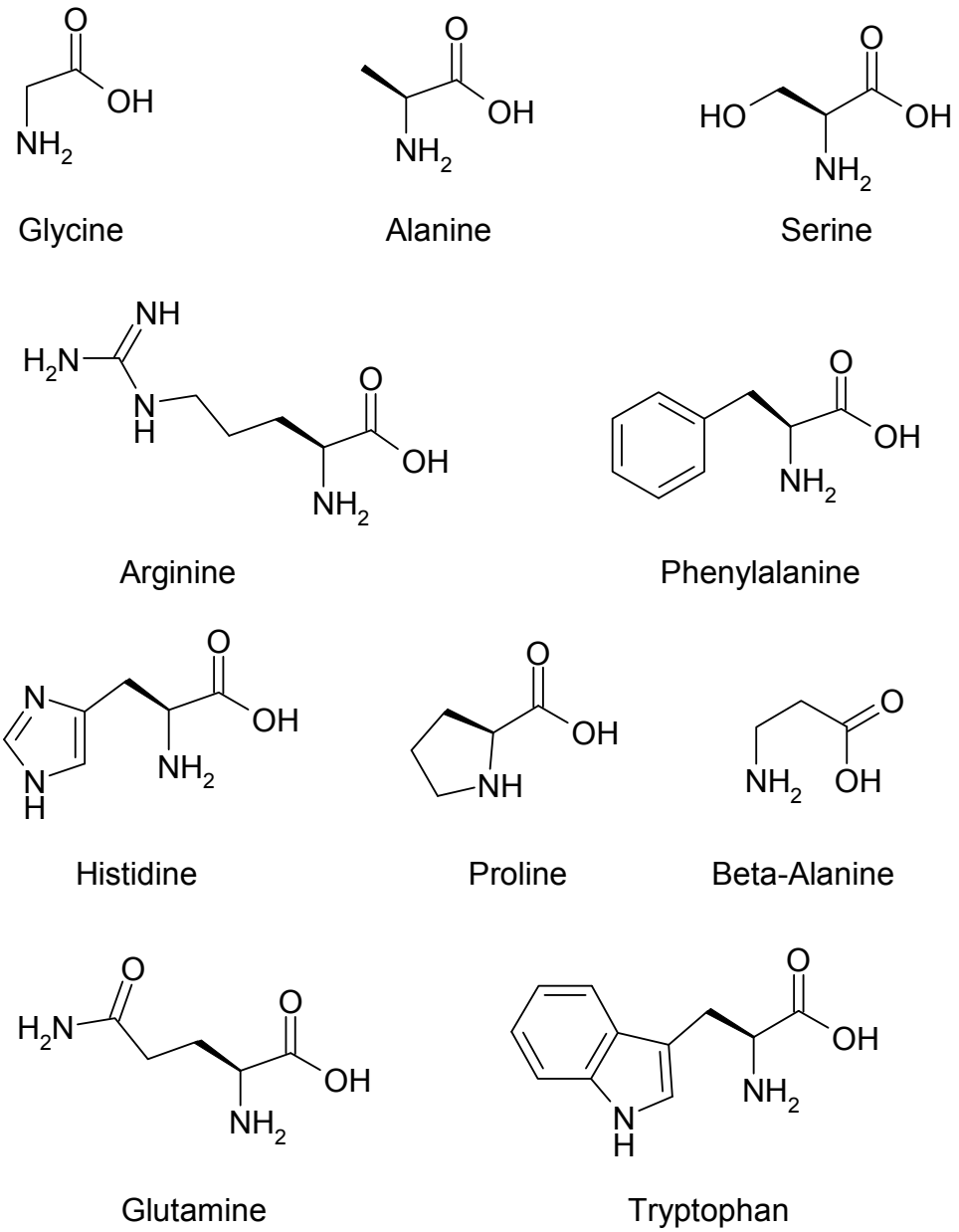

Figure 4.1 Naturally occurring amino acids employed as ligands in this chapter

The coordination chemistry of amino acids is well established, and has been extensively reviewed. [1-3] For example, transition metal complexes such as Cr, [4] Cu, [5-7] Pd, [7, 8] and Co [9] derivatives have been investigated, as have heavier metals such as Hg, [10] Pb, [11] Sn [12] and Cd [13].

Amino acids (as well as their synthetic counterparts such as EDTA and NTA) are excellent agents for metal complexation. A thermodynamically favoured, five membered, chelate ring between the amino and carboxylate acid groups is commonly observed, R- groups containing heteroatoms can also be involved in the binding motif.

This participation is dependent on the metal. For example tryptophan can complex to ruthenium through a η^6 interaction [14] and to mercury through the indole amine group. [15] However, no interaction with the indole group is observed in the tryptophan complexes of Cu (II) and Mn (II). [16, 17]

Amino acid complexes of titanium, in contrast to other metals, are rare. In the 1950s Lundgren et al. reported the titanium complexes of glycine, alanine and phenylalanine. All three complexes were formed in a 1:1 ratio with $Ti(O^nBu)_4$, however, no structural data was reported in this study. All the complexes formed were sensitive to hydrolysis and on standing at room temperature the formation of titanium dioxide and a cyclic anhydride derived from the amino acid were observed. [18]

More recently the solid state structure of a dimeric titanium glycine complex was reported by Schubert et al. [19] Bina et al. published the structures of a series of *N*-methyl amino acid titanocene complexes. In these complexes the titanium coordinated via the carboxylic acid arm only, the complexes of *N*-methyl-glycine, *N*-methyl-alanine and *N*-methyl-methinone have all been prepared by this method. [20-22] Both these structural types are shown in Fig. 4.2 below.

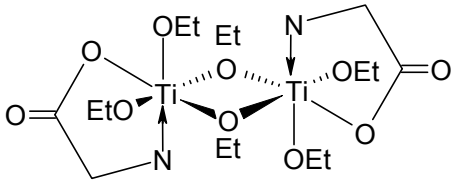

Titanium ethoxide glycinate

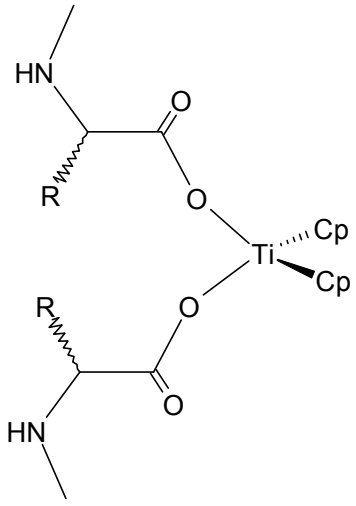

Titanium N-methyl-amino acid cyclopentadiene

Figure 4.2 Examples of amino acid complexes of titanium

Most synthetic amino acids used to chelate metals, such as EDTA and nitrilotriacetic acid (NTA), incorporate tertiary amine groups rather than the primary

amines found in α-amino acids. Titanium complexes of this sort are less sensitive to moisture with oxo- or hydroxy- species rather than TiO_2 being the normal hydrolysis products. [23] Titanium nitriloacetic acid can be hydrolysed to give a tetrameric oxo-complex, shown below in Fig. 4.3 (A). [24]

Ti(EDTA), shown below in Fig. 4.3 (B), is highly stable and in the structural investigation of this complex Fackler et al. observed that the complex would not hydrolyse in an aqueous solution yet water could bind through the oxygen atom to the metal centre without the formation of a hydroxide species. [25]

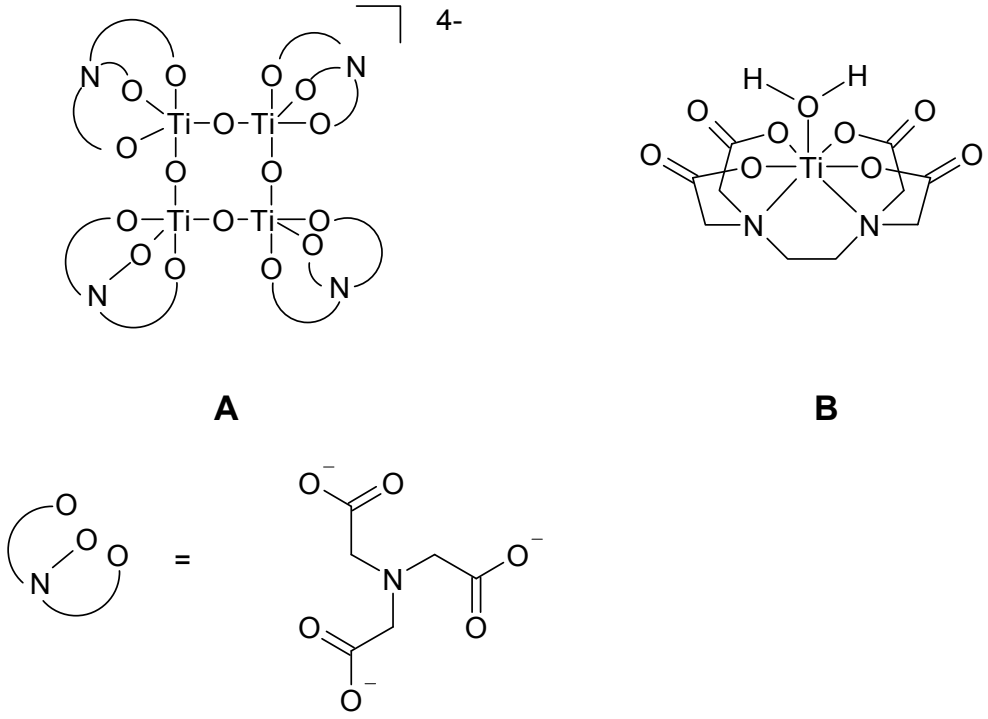

Figure 4.3 Titanium adducts of both NTA (A) and EDTA (B)

It is also possible to synthesise similar amino acid ligands from glycine. Shongwe et al. reacted glycine with a 2,4 disubstituted phenol substrate, shown in Fig. 4.4 (A, B). These glycine bisphenolate ligands were then used to chelate Fe(III). [26] Ceccato et al. also synthesised an amine bisphenolate ligand from glycine, shown below in Fig. 4.4 (C), this ligand was used to chelate vanadium.[27]

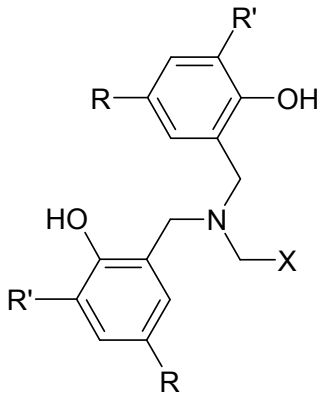

A : R = Br, R' = Br, X= COOH
B : R = Cl, R' = Me, X= COOH
C : R = H, R' = H, X= COOH
D : R = Me, R' = Me, X= CH_2OH
E : R = ^{t}Bu, R' = ^{t}Bu, X= CH_2Py
F : R = ^{t}Bu, R' = ^{t}Bu, X= CH_2OMe
G : R = Me, R' = Me, X= H
H : R = ^{t}Bu, R' = ^{t}Bu, X= $CH_2(C_{10}H_7)$

Figure 4.4 Examples of phenolic based ligands

Titanium has been coordinated to a number of other amine bisphenol ligands containing an amine,[28] pyridine,[29] ether,[30] alcohol,[31, 32] alkyl [33] or an aromatic group [34] side arm. These ligands are shown above in Fig 4.4 (D-H**).** All these titanium species tend to be monomeric with the exception of (D), which forms a dimer via the bridging alkoxide moiety.

Other tetravalent metals, such as Sn(IV) and Ge(IV), readily complex with amino acids and the resulting complexes have been extensively investigated. [35-39] Sn(IV) complexes, though highly active in many esterification and transesterification reactions, [40-42] are considerably more toxic than their Ge(IV) analogues. [43] Chemically, both metals are similar and readily form mixed metal complexes including clusters. [44, 45] Generally Ge(IV) is less reactive than Sn(IV) but the halides and alkoxides of germanium will readily hydrolyse to oxide species, despite this Ge(IV) organometallic complexes have been used as catalysts in a number of reactions.[46-48] Examples of amino acid binding to germanium are shown below in Fig. 4.5

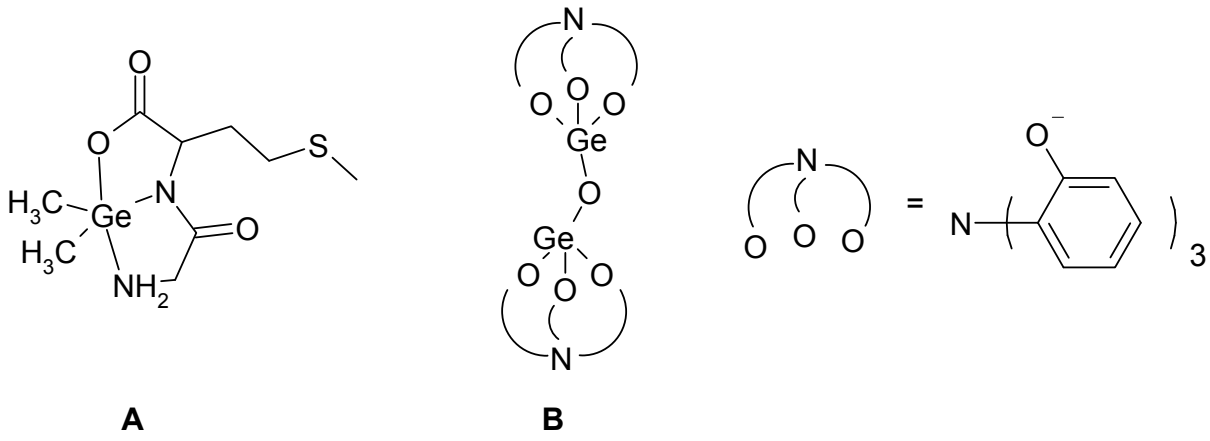

Figure 4.5 Typical germanium amino acid complex, (A), taken from Preut et al.[49] Typical germanium hydrolysis product, (B), taken from Livant et al. [50]

Germanium alkoxides also have the potential to undergo alcoholysis reactions and form germanium methoxide on reaction with an excess of methanol. Recently germanium alkoxides have been investigated as initiators and catalysts for the polymerisation of cyclic esters. In the production of polylactide many alternative metal systems have been investigated to replace the current tin based initiators. Germanium spirocyclic alkoxide complexes were found to be active in this reaction at high temperature. [51, 52] Kricheldorf et al. compared different derivatives of germanium in the polymerisation of ε-caprolactone. In this study he found that $Ge(OEt)_4$ was a more effective esterification catalyst than the germanium alkyl derivatives. [53]

Previously germanium metal and related complexes have been considered too expensive for wide scale industrial use. However, the price of germanium metal has more than halved in the last five years because of the increase in the mining of coal and zinc ore, where germanium is mainly found. [54]

In contrast to germanium, zinc complexes of α-amino acids have been extensively researched. The complexes generally consist of two N,O-chelating amino acid groups, shown above in Fig. 4.6 (A-C). The three common arrangements are for the zinc to form a square pyramidal, octahedral or trigonal bipyramidal structure. There are a few exceptions to this general rule such as zinc histidine, where the zinc is bound by the primary and tertiary amine groups, although both carboxylic acid arms are deprotonated they do not coordinate to the zinc centre. [55]

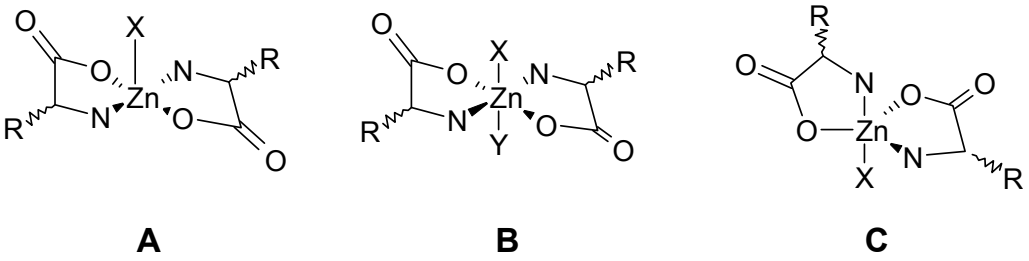

Figure 4.6 Normal bonding motifs for zinc α-amino acid complexes, X and Y can be solvent molecules or carboxylate moieties from other zinc amino acid units

Many different α-amino acid zinc complexes have been reported with the aim of exploring the rich biometallic chemistry present in most zinc enzymes and a large number of these have been structurally characterised. Generally these zinc salts are highly insoluble in common organic solvents. [56-63] Rombach et al. published the structure of zinc phenylalanine, an extremely distorted trigonal bipyramid. This complex took 12 months to crystallise from an aqueous solution and was subsequently insoluble. No NMR data was published in this report. [64]

Zinc salts of amino acids have been widely used in catalysis. Darbre et al. reported the zinc salts of proline and lysine were effective catalysts for the aldol addition of p-nitrobenzaldehyde and acetone. Zinc proline is highly water-soluble and as such the reaction was performed in an aqueous medium. [63, 65]

The researchers proposed that the zinc proline catalysis involves the coordination of the carbonyl oxygen of the ketone to the acidic zinc centre. Various reactions follow including deprotonation of the α-CH on the ketone by the now unbound secondary amine on the proline. [66]

It is not only the activity of these complexes that is beneficial, zinc amino acid complexes are considered resorbable (non-toxic because they are found in the human metabolism). This is an important factor when designing polymers (which will have the catalyst bound into the matrix) for biomedical and pharmaceutical applications. In this context Kricheldorf et al. examined a range of zinc amino acid salts including zinc proline for their activity in the polymerisation of L-lactide. In these studies they concluded that though the zinc amino acid salts were comparatively sluggish catalysts they were comparable to other zinc carboxylate salts such as zinc stearate. [67]

As discussed in Chapter 1, zinc complexes have been widely used as both a support and as catalysts for the transesterification of vegetable oils. Peters et al. tested zinc salts of amino acids in the conversion of triacylglycerides to FAME. In this study two basic amino acids with basic R- groups (arginine and histidine) were reacted with zinc to form two ill-defined heterogeneous catalysts. Both salts were active in the transesterification though the zinc arginine more so. They concluded that the R groups of the amino acid were highly important and that the more basic the R- group the higher the conversion of biodiesel. [68]

In the following section the synthesis and characterisation of a range of titanium, germanium and zinc complexes is presented followed by an investigation of their catalytic activity for the production of biodiesel from soybean and eventually waste oils.

4.2 RESULTS AND DISCUSSION

4.2.1 SYNTHESIS OF α-AMINO ACID TITANIUM COMPLEXES

Four titanium amino acid complexes of alanine, glycine, proline and tryptophan were formed by suspension of the amino acid in isopropyl alcohol followed by the slow addition of $Ti(O^iPr)_4$. The suspension was then refluxed for 24 hours. On reaction the resulting suspension was filtered and the product recrystallised from the filtrate. The crystalline solids were insoluble in all common organic solvents and as such the relative ratios of amino acid to titanium could only be determined by ^1H NMR after hydrolysing the species in D_2O. These compounds were synthesised in a moisture free environment as they readily hydrolyse, as well as in a methanol free environment to avoid the production of titanium methoxide.

4.2.1.1 Titanium Alanine, $[(Ala)Ti(O^iPr)_3]_2$, 14

Complex **14** was recovered as large colourless crystals from the solution on standing over 3 days. These crystals were suitable for X-ray crystallography analysis, the molecular structure is shown below in Fig. 4.7.

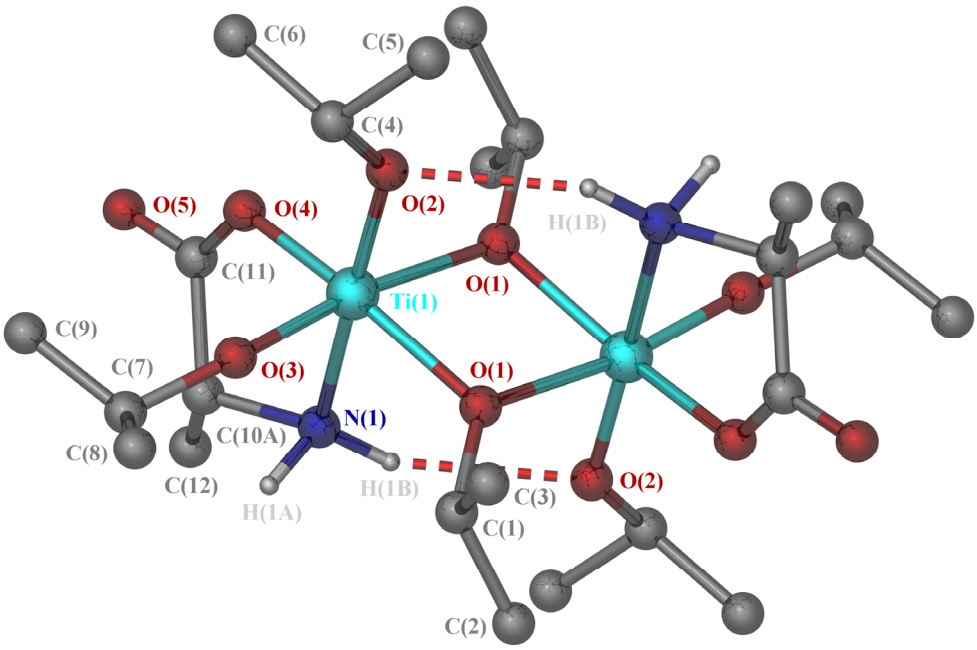

*Figure 4.7 Molecular structure of the titanium alanine species **14**, all hydrogen atoms, except H(1A) and H(1B), have been omitted for clarity*

X-ray structure analysis of **14**, showed that one isopropoxide substituent of the original titanium alkoxide was replaced by the alanine ligand. The amino acid chelates to titanium through the carboxylate and amine groups. Two of the remaining isopropoxide groups are terminal and one bridges to a second titanium atom. This results in a dimer in which the titanium atoms are in a *pseudo* octahedral coordination mode, as shown by the angles N(1)-Ti(1)-O(2) 171.36(11)° and O(3)-Ti(1)-O(4) 94.79(11)°. The bridging isopropoxide is asymmetric in nature, [Ti(1)-O(1) 1.974(2) Å and Ti(1)-O(1)# 2.091(2) Å], presumably as a result of the trans effect. The dimeric motif of **14** is further stabilised by a hydrogen bond between a terminal isopropoxide group on one titanium centre and the amine group bound to the other [N(1)···O(2)#, 3.111 Å, N(1)-H(1B)···O(2)# 153.55(1)°]

The binding mode of the amino acid in **14** forms a stable, thermodynamically favoured five-membered ring and this motif is commonly observed in other transition metal amino acid complexes. Many transition metal complexes of alanine having been reported, [7, 13, 56, 69] yet this is the first structural example of a titanium-alanine complex.

4.2.1.2 Titanium Glycine, $[(Gly)Ti(O^iPr)_3]_n$, 15

Using the general method described above, the filtrate obtained from the reaction between glycine and $Ti(O^iPr)_4$, yielded a microcrystalline solid on standing for 24 hours that was recovered in a 47% yield. The microcrystalline solid was not suitable for X-ray diffraction. ^1H and ^{13}C NMR spectroscopy of the hydrolysis products from complex **15,** as well as the elemental analysis of the solid, reveal a stoichiometry of 1 amino acid to 3 isopropoxide ligands consistent with a molecular formula of $(Gly)Ti(O^iPr)_3$. It is likely that the solid state structure is dimeric and analogous to both complex **14** and the titanium glycine ethoxide species reported by Schubert et al. [19]

4.2.1.3 Titanium Proline, $[(Pro)Ti(O^iPr)_3]_n$, 16

Following the same synthetic procedure, a microcrystalline solid was obtained from the filtrate of proline and $Ti(O^iPr)_4$. The crystalline solid, **16,** was also not suitable for X-ray diffraction studies. Elemental analysis of the crystalline solid, along with the NMR analysis of the hydrolysis products suggests a formula of $(Pro)Ti(O^iPr)_3$, it is also likely, analogous to **14**, that **16** is dimeric in nature.

4.2.1.4 Titanium Tryptophan, $[(Tryp)Ti(O^iPr)_3]_2$, 17

Using the general method described above, $Ti(O^iPr)_4$ and tryptophan were reacted together and the resulting filtrate yielded small, yellow crystals on standing for 7 days at room temperature. These crystals were analysed by melting point, elemental analysis and X-ray crystallography. The hydrolysis products were analyzed by ^1H and ^{13}C NMR spectroscopy. The analytical analysis confirms the formation of a dimeric complex analogous to complex **14.** The solid state structure of **17** is shown below in Fig. 4.8.

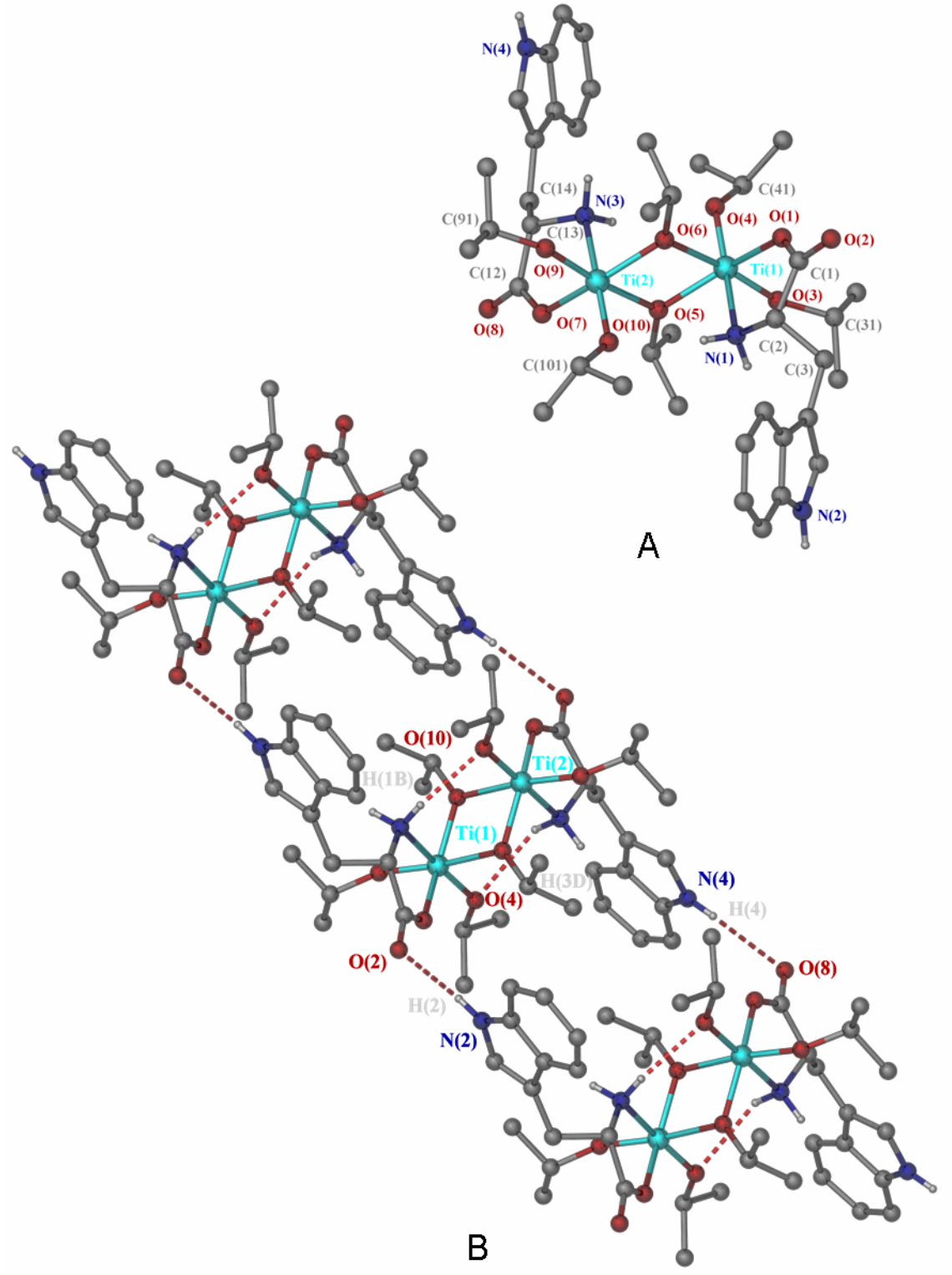

*Figure 4.8 Dimeric molecular unit of the titanium tryptophan complex **17**, **A**, and the supramolecular structure of **17**, **B**, all alkyl hydrogen atoms have been omitted for clarity*

On the molecular level, **17** is isostructual with complex **14**. Both titanium atoms have a *pseudo* octahedral coordination geometry involving an N, O- chelating amino acid group. The bridging isopropoxides are asymmetric and intramolecular N-H···O hydrogen bonding is observed.

However, in contrast to alanine, tryptophan possesses an additional N-H group as a potential H-bond donor. These groups participate in intermolecular H bond interactions with carboxylate groups of neighbouring dimers [N(2)···O(2), 3.370(1) Å, N(2)-H(2)···O(2) 134.01(1)°, N(4)···O(8), 3.368(1) Å, N(4)-H(4)···O(8) 134.04(1)°] resulting in a polymeric supramolecular chain, shown in Fig 4.8 (B).

The stability of complex **17** is similar to that of **14-16** in that it undergoes hydrolysis on exposure to air.

4.2.2 Catalytic Activity of 14-17 in the Conversion of Soybean Oil

The following catalytic results were obtained under the same conditions as previously described in Chapter 2 & 3 namely 195 ºC over 2 hours with a catalyst loading of 2.5 mol%. Soybean oil was used with a methanol ratio of 12:1. The detailed experimental procedure employed is reported in Chapter 6.

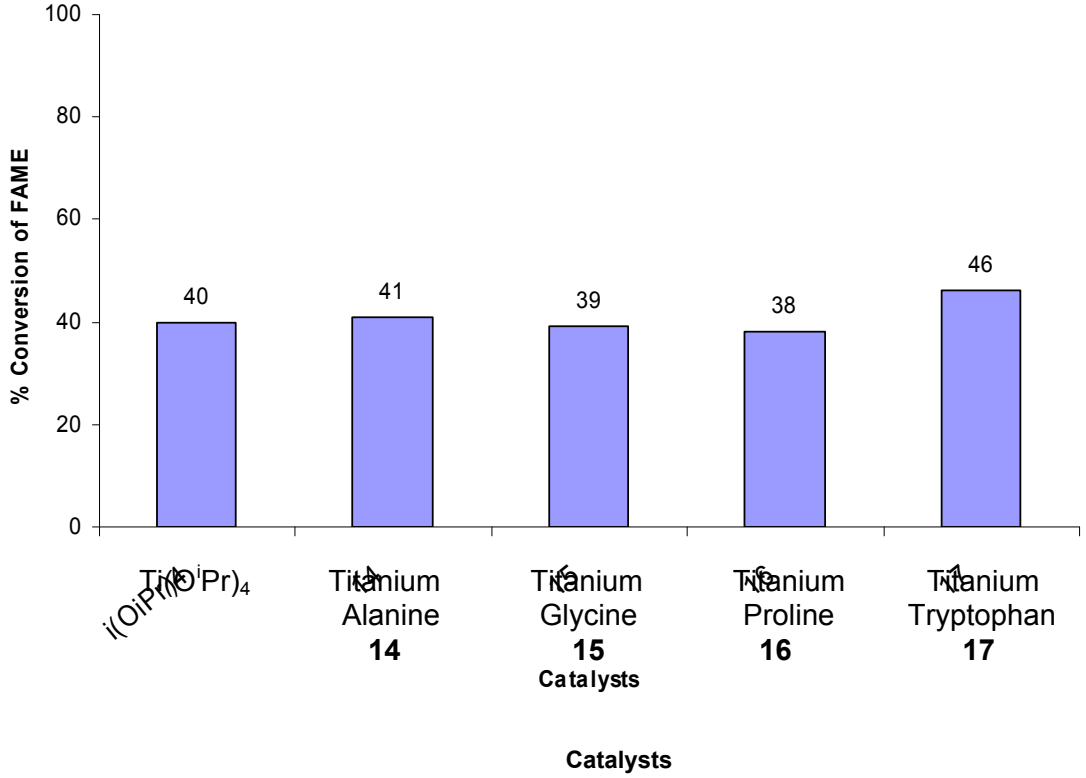

Figure 4.9 Catalytic activity of a range of titanium α-amino acid complexes

The catalytic activity of these complexes is presented in Fig.4.9. These results show that **14-17** are no more effective as transesterification catalysts than $Ti(O^iPr)_4$, suggesting that all are prone to methanolysis regardless of the identity of the amino acid substituent. This methanolysis reaction was confirmed by suspending complexes **14-17** in a methanol solution and analysing the resulting suspension by NMR. Due to the rapid formation of $Ti(OMe)_4$, titanium α-amino acid complexes are clearly unsuitable for the transesterification of vegetable oils without synthetic ligand modification to enhance the stability of the titanium centre.

4.2.3 Synthesis Of Amino Acid 2,4-Dimethyl Phenolates

4.2.3.1 Ligand H_3L1- H_3L3 Synthesis

From the catalytic results given above it is clear that the unmodified α-amino acids do not stabilise the titanium centre sufficiently to prevent methanolysis, presumably since no steric or electronic protection was afforded by the amino acid substituent. To provide

enhanced protection of the metal centre we reasoned that simple modification to functionalise the amine group would suffice.

The amino acids, glycine and β-alanine were reacted with formaldehyde and 2,4 dimethyl phenol in a modified Mannich reaction to yield ligands, H_3**L1** and H_3**L2**, (Fig. 4.10). Tris(3,5-dimethyl-2-hydroxybenzyl) amine, H_3**L3** a related, though non amino acid based ligand was also synthesised. The germanium and titanium complexes of H_3**L1-** H_3**L3** were then investigated.

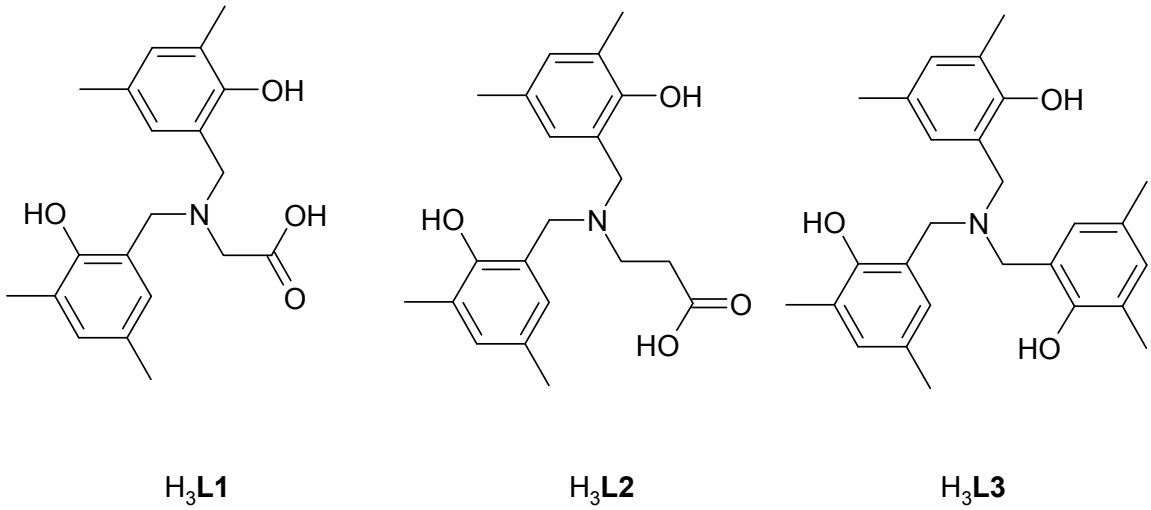

H_3**L1** H_3**L2** H_3**L3**

*Figure 4.10 The three amino phenolate based ligands, H_3**L1**-H_3**L3***

4.2.3.2 Titanium L1 Complex, [(L1)Ti(O^iPr)]$_3$, 18

Ti(O^iPr)$_4$ reacts rapidly with a suspended toluene solution of H_3**L1.** The resulting complex is highly soluble in most common organic solvents and can be recovered as a microcrystalline solid from a toluene : hexane solution. The resulting complex, **18,** was analysed by ^{1}H and ^{13}C NMR spectroscopy as well as mass spectrometry. In spite of only obtaining very small crystals an X-ray structure of **18** was obtained using a syncotron radiation source at Daresbury. The molecular structure of **18**, is shown in Fig. 4.11.

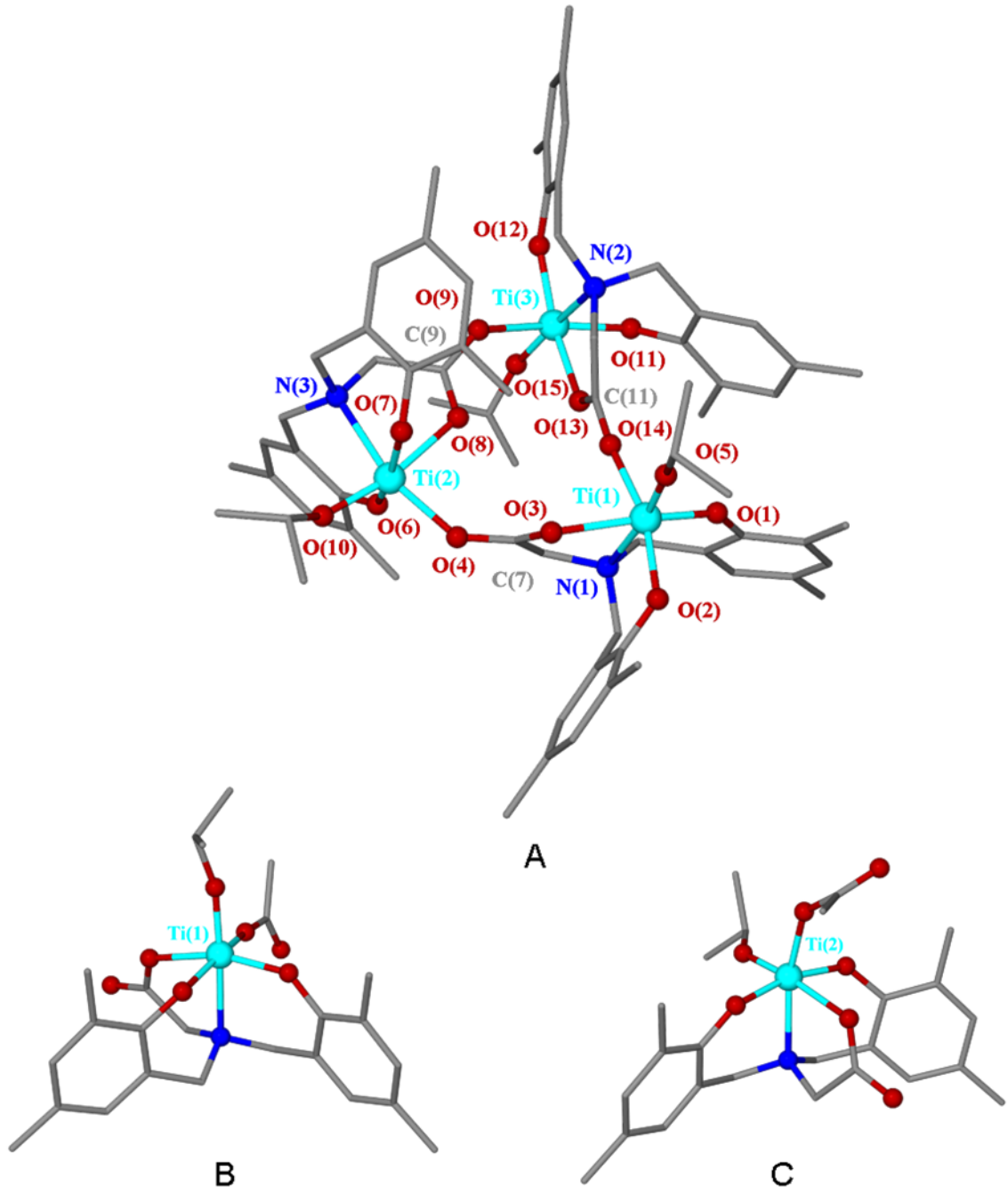

Figure 4.11 Molecular structure of the trimeric complex ***18****, (A), and the two coordination motifs of the titanium centres (B & C). All hydrogen atoms and solvent molecules have been omitted for clarity*

The crystallographic analysis indicates that **18** is trimeric and that each of the titanium centres are in a distorted octahedral geometry. The trimeric motif results from each of the carboxylate arms bridging two titanium atoms together. Each of the carboxylate groups appears to be delocalised exemplified by the bond lengths C(11)-

O(13) 1.258(6) Å and C(11)-O(14) 1.259(6) Å. The Ti-O bond length is therefore mostly influenced by the ligand in the trans position. For example, O(13) and O(3) are both trans to a phenoxide group and the bond lengths Ti(3)-O(13) and Ti(1)-O(3) are 2.066(3) Å and 2.082(3) Å respectively. O(4) and O(8) are trans to an amine and isopropoxide group and the bond lengths Ti(2)-O(4) and Ti(2)-O(8) are 1.985(3) Å and 2.136(3) Å respectively.

Each titanium centre is crystallographically unique, yet there are two general binding motifs. The amine group is trans to the isopropoxide ligand in the two titanium centres Ti(1) and Ti(3) (Fig. 4.11 B) whereas the amine and isopropoxide group bound to the Ti(2) lie cis to each other (Fig. 4.11 C). The titanium-phenoxide bond lengths are similar for all the titanium atoms and are on average 1.86 Å in length.

Ti(1) and Ti(3) have an average titanium-amine bond length of 2.32 Å. Both titanium atoms also have relatively short titanium-isopropoxide bond lengths of 1.773(4) Å and 1.783(4) Å respectively. The titanium-isopropoxide bond length for Ti(2) is 1.790(3) Å however, the titanium-amine bond length is significantly shorter at 2.259(4) Å. The bond lengths in complex **18**, are similar to the dimeric species reported by Nomura et al. [32]

Peaks assignable to every proton in the trimeric complex are found in the ^{1}H NMR spectrum suggesting that the complex retains its trimeric form in the solution state. Further evidence of this is found in the ^{13}C spectrum and also the ESI mass spectrum where the peak $[M+H]^{+}$ 1342.4682 m/z assignable to the trimer is observed, no peaks assignable to the monomer or dimer were identified.

4.2.3.3 Titanium L2 Complex, [(L2)Ti(O^{i}Pr)]$_3$, 19

Ti(O^{i}Pr)$_4$ was also reacted with H$_3$**L2** in a similar manner as described above. The resulting complex, [**L2**Ti(O^{i}Pr)]$_3$, complex **19,** forms a deep red solution when dissolved in toluene. An orange microcrystalline solid was recovered from a hexane and toluene solution. Complex **19** is highly soluble in most common organic solvents, the ^{1}H and ^{13}C NMR spectra as well as mass spectrometry suggest that the complex is trimeric in solution. The solid state structure is presumably analogous to complex **18**.

4.2.3.4 Germanium L2 Complex, [(L2)Ge(O^{i}Pr)]$_3$, 20

The synthesis of a germanium complex of **L1**, was attempted, however, the only recoverable compound was insoluble in all common solvents and microanalysis of the powder was inconclusive. The preparation of this compound was abandoned.

Ge(O^{i}Pr)$_4$ formed a soluble species on reaction with **L2**. The ligand was suspended in toluene and the germanium alkoxide added slowly. On refluxing for 72 hours, a clear solution was obtained. A microcrystalline solid was obtained from this solution on standing at room temperature. The mass spectroscopic, ^{1}H and ^{13}C NMR spectra indicate that the product formed is monomeric with the formula (**L2**)Ge(O^{i}Pr).

4.2.3.5 Titanium L3 Complex, [(L3)Ti(O^{i}Pr)]$_3$, 21

H$_3$**L3** was reacted with Ti(O^{i}Pr)$_4$, according to the literature preparation given by Kol et al. This complex, **21,** was recovered from ether in a 90% yield. Analysis of the yellow crystals confirmed the formation of the five coordinate monomeric titanium complex (**L3**)Ti(O^{i}Pr) reported therein. [70]

4.2.3.6 Germanium L3 Complex, (L3)Ge(O^{i}Pr) · HO^{i}Pr, 22

Reaction of ligand **L3** with Ge(O^{i}Pr)$_4$ in toluene yielded (**L3**)Ge(O^{i}Pr) · HO^{i}Pr, complex **22**. The molecular structure was determined by X-ray crystallography and is similar to the titanium structure of complex **21**, reported by Kol et al. The molecular structure of **22** is shown below in Fig 4.12.

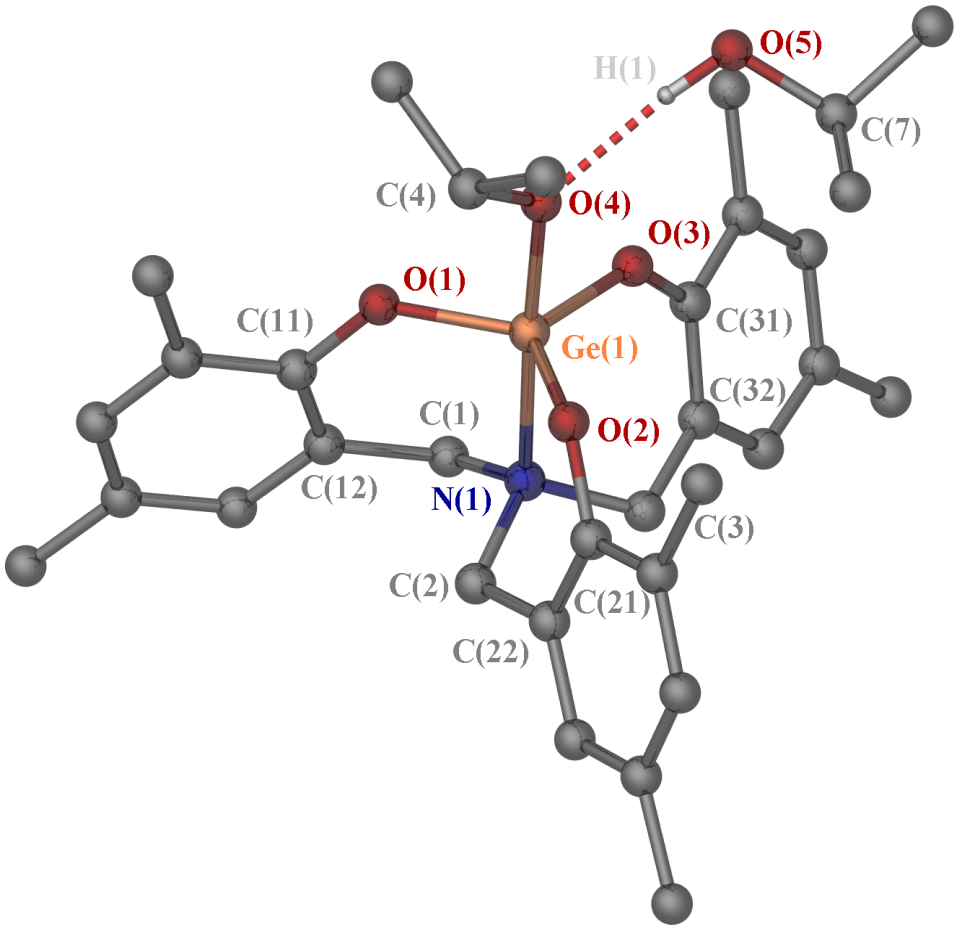

Figure 4.12 Molecular structure of the germanium trisphenolate complex ***22****. All hydrogen atoms not involved in hydrogen bonding and solvent molecules have been omitted for clarity*

The germanium centre is approximately trigonal bipyramidal. The ligand possesses C_3 symmetry and binds through the amino group as well as the three phenoxide arms. The lengths of these bonds, N(1)-Ge(1) 2.112(1) Å, and Ge(1)-(O2) 1.799(1) Å are normal for a germanium aryloxide. [71]

Complex **22** is the first example of a mixed alkoxide-aryloxide germanium crystal structure, as well as being one of the few germanium isopropoxide complexes to be structurally characterised. [72-75] Unlike the titanium complex **21** or the similar Si(**L3**)(OMe) structure, complex **22** contains an isopropanol in the secondary coordination sphere of the germanium, the isopropanol is hydrogen bonded to the isopropoxide ligand [O(4)···O(5) 2.810(1) Å, O(5)-(H1)···O(4) 169.59(1)°].

^{1}H NMR spectroscopy confirmed that the solid state structure was maintained in solution. At room temperature a broad singlet is observed for the methylene protons (Fig 4.13 D), on cooling to -30 °C an AX spin system is observed, (Fig 4.13 B and E) showing the retention of the C_3 symmetric structure. At room temperature there is a rapid inversion between the *P* and *M* enantiomers on the NMR timescale.

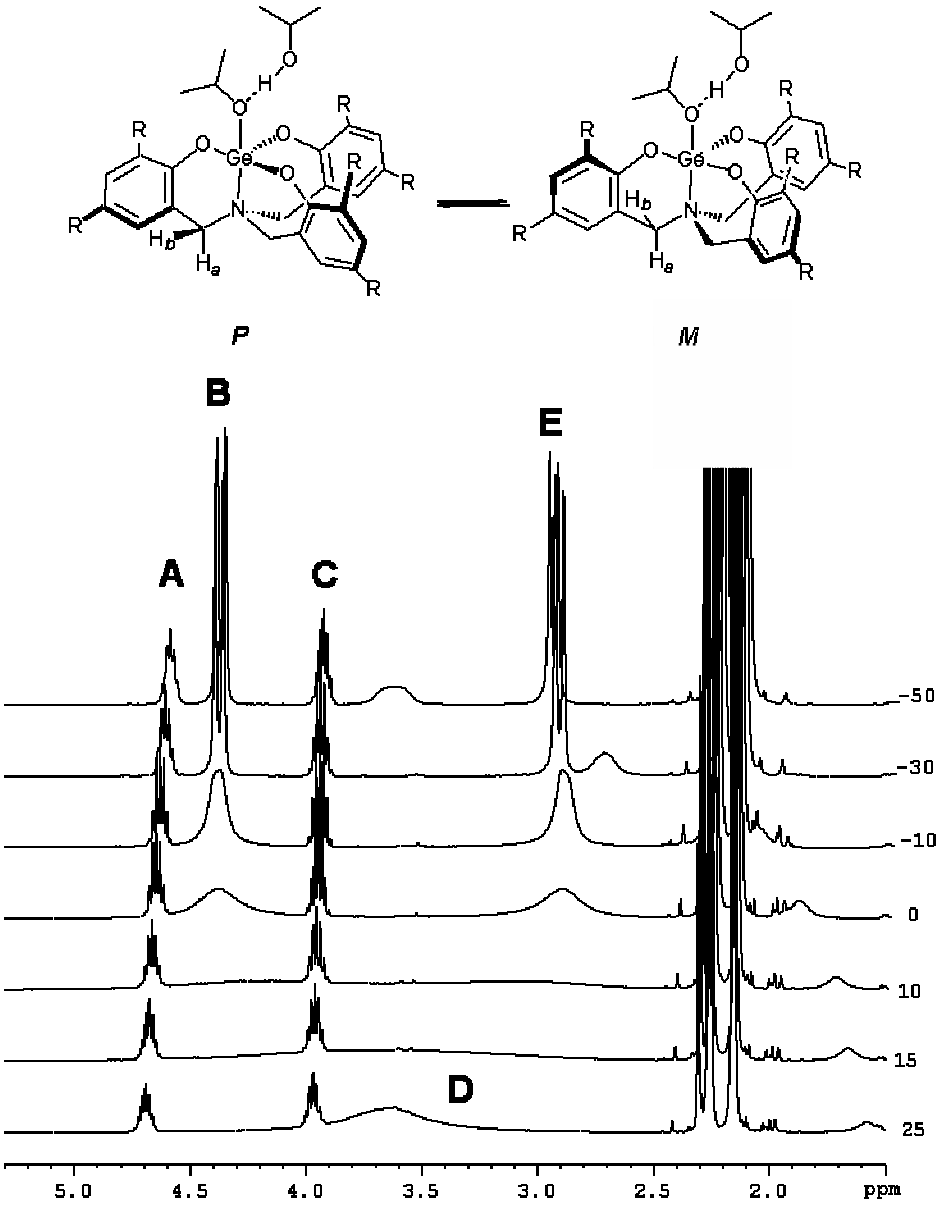

Figure 4.13 Variable Temperature ^{1}H NMR spectra ($CDCl_3$) of complex ***22***

Two 1:1 septets due to the methine protons of the isopropanol and isopropoxide moieties are observed in ^{1}H NMR spectra (Fig 4.13 A & C) even at elevated

temperatures (85 ºC), suggesting that rapid alcohol-alkoxide exchange does not take place.

4.2.4 Catalytic Activity of 18-22 in the Conversion of Soybean Oil

The following catalytic testing was undertaken using the same method detailed previously namely 195 ºC over 2 hours with a catalyst loading of 2.5 mol%. Soybean oil (36.8 ml) was used with a methanol ratio of 12:1. The same experimental procedure employed is detailed in Chapter 6. The catalytic activity of these complexes is presented below in Fig.4.14.

.

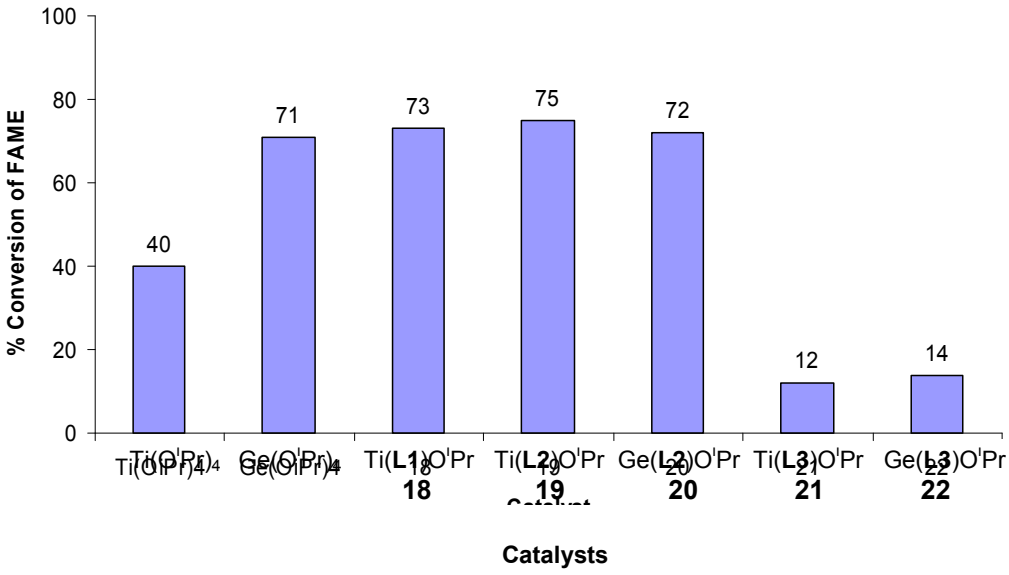

*Figure 4.14 Catalytic activity of the complexes **18-22***

In Section 4.2.2 it was shown that titanium complexes of α-amino acids, regardless of the amino acid, do not protect the titanium centre from methanolysis. On reaction with the bisphenolate ligands, **L1** and **L2,** titanium trimers are formed and in both cases demonstrate a much higher activity suggesting that modification of the amino acid ligand inhibits titanium methoxide formation.

All the complexes involving ligands **L1** or **L2** were active, in contrast to the complexes of **L3,** which were inactive for the transesterification reaction. Complexes **18**

and **19** are highly active in the transesterification of soybean oil. The six-coordinate titanium complexes contain two labile carboxylate groups and, in order for catalysis to proceed, it is likely that these are displaced by glyceride.

This mechanism was also suggested by Nomura et al. for the polymerisation of ethylene by an analogous titanium species. The titanium catalyst was a dimer with an alkoxide group (as opposed to the carboxylate of H_3**L1**). [32] It is plausible that complexes **18** and **19** form a similar catalytic species in the transesterification reaction as shown below in Fig. 4.15.

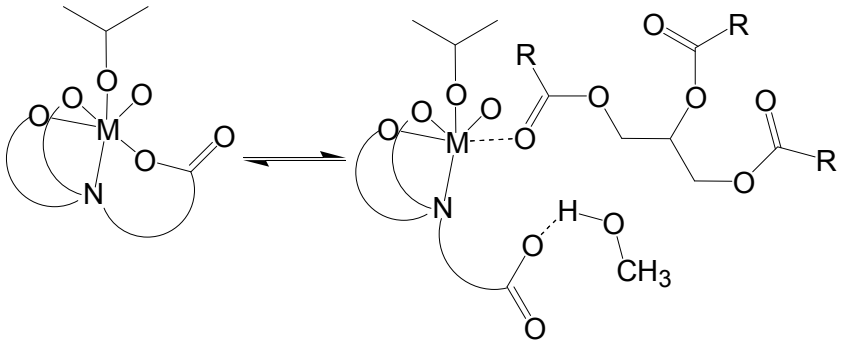

Figure 4.15 Possible catalytic species resulting in the transesterification of the triglyceride molecule

In contrast complexes **21** and **22** are poor Lewis acidic catalysts as the metal centre is presumably stabilised by the strong apical bonds. $Ge(O^iPr)_4$ forms $Ge(OMe)_4$ under the reaction conditions but this methoxide analogue is more active than the titanium species presumably due to a lack of aggregation and formation of an insoluble powder.

4.2.5 Synthesis of Zinc α-Amino Acid Complexes

The titanium complexes **18** and **19**, as well as the germanium alkoxides tested, demonstrated high levels of activity in the conversion of biodiesel. However, the cost of germanium or requirement to synthesise elaborate ligands make such catalysts uneconomically viable for the industrial conversion of biodiesel. In order to find an economically viable alternative, which did not require expensive ligand modification for stability, a number of zinc α-amino acid complexes were investigated.

The zinc complexes, **23**-**27**, were all formed by adding zinc acetate to a basic solution of two equivalents of amino acid in methanol. In all cases presented below, the zinc amino acid complex precipitates from solution and was then either recrystallised from water or used without further purification. These complexes are shown below in Fig. 4.16.

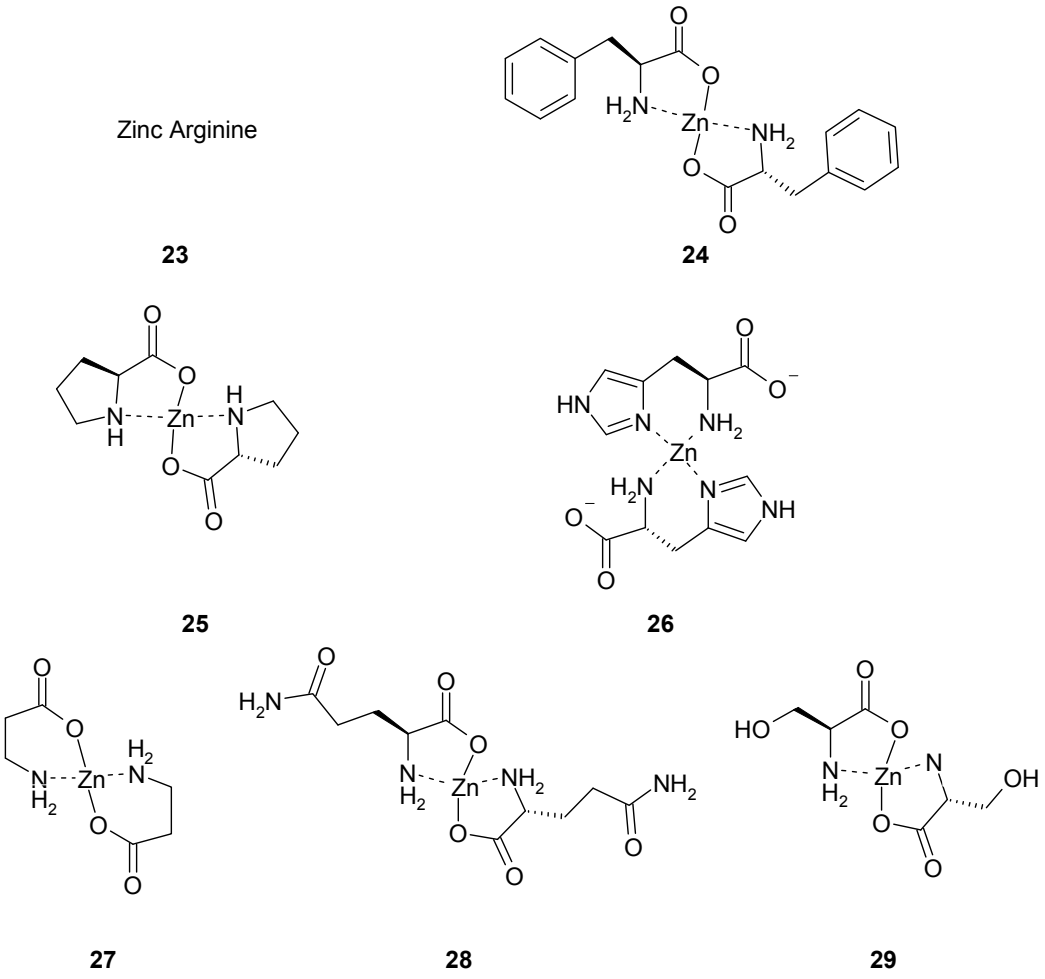

*Figure 4.16 A number of complexes, **23-29**, presented in Section 4.2.5*

4.2.5.1 Zinc Amino Acid Complexes, 23-27

The reaction between zinc acetate and arginine gave a high yield of fine white powder. This solid was insoluble in all common organic solvents. **23** is a non-stoichiometric solid containing 12.63% zinc which is both stable to hydrolysis and methanolysis. Peters et al. reported a similar ill defined solid for the production of biodiesel. [68]

Zinc phenylalanine, complex **24**, was also recovered in a high yield, this complex was sparsely soluble in boiling water. The ^{1}H NMR spectrum was obtained and the melting point and elemental analysis confirm the formation of the bis amino acid species detailed in Fig. 4.16 above. The solid state structure of **24** was published by Rombach et al.[64] The zinc atom is five coordinate and lies in a distorted trigonal bipyramidal arrangement. The chelating carboxylate oxygen atoms are bound in the apical positions. This structure was obtained by the slow evaporation of the aqueous solution over 12 months and was insoluble on formation.

Large clear crystals of zinc proline, **25,** were obtained from an aqueous solution on standing over 3 days. Complex **25** was analysed by elemental analysis, melting point and NMR spectroscopy, all these techniques confirmed the formation of the unhydrated bis-amino acid system reported by Ng et al. [76]

In complex **25** the secondary amine is bound to the zinc. In the zinc histidine complex, **26,** it is the primary and tertiary amines that bind to the metal centre. Both carboxylic acid groups are deprotonated but do not participate in the binding motif, zinc histidine is also heavily hydrated. Like most zinc amino acid complexes **26** is insoluble in other solvents and only sparingly soluble in boiling water. The elemental analysis, melting point and ^{1}H NMR spectra confirmed that this compound was the hydrated zinc bis-amino acid complex reported by Dalosto et al. [55]

The zinc species **27** recovered from the reaction mixture was also only sparingly soluble in boiling water. The elemental analysis, melting point and ^{1}H NMR spectroscopy confirm the formation of the bis-amino acid complex, presumably the β-alanine chelates to the zinc *via* the carboxylate and amine groups to form a six membered ring.

4.2.4.2 Complexes 28 & 29

Complex **28** and **29** were formed by dissolving the amino acid and zinc acetate in a basic aqueous solution. On reaction, after two hours at room temperature, the basic solution was reduced in volume and allowed to stand, small crystals were recovered from this solution. Both amino acid complexes crystallised out in the monoclinic space group $P2_1$. The molecular structure of complex **28** as well as the supramolecular structure is shown below in Fig. 4.17.

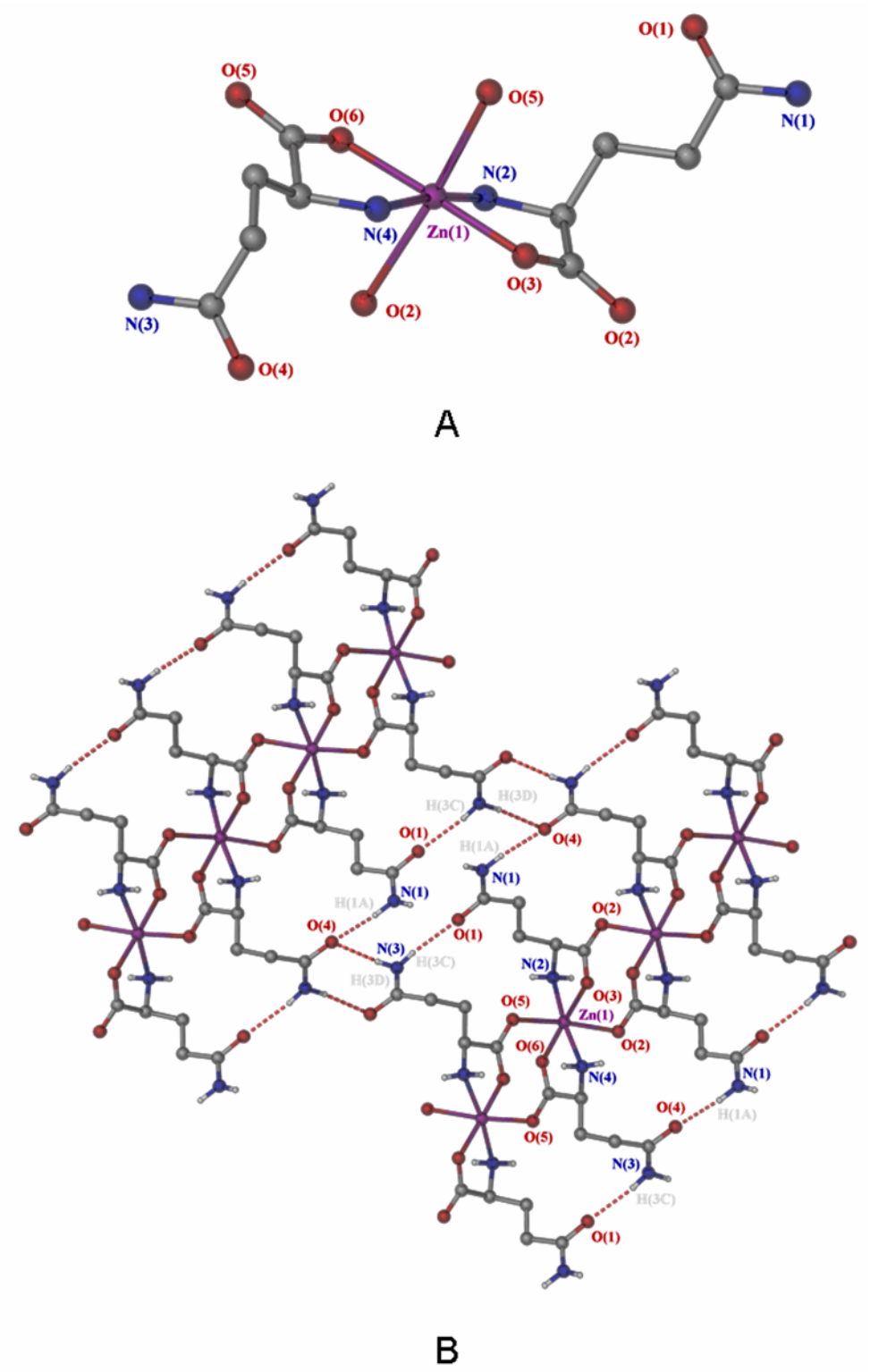

Figure 4.17 Coordination environment of zinc in ***28****, (A), and the supramolecular structure (B). All alkyl hydrogen atoms have been omitted for clarity*

The zinc glutaminate adopts the expected binding mode, with chelation *via* the amino and carboxylate groups. Like most other zinc amino acid complexes, **28** is polymeric in the solid state, however the zinc is in a 6 coordinate geometry with the carboxyl groups from two other units completing the octahedral array.

The binding mode of **28** is not unique, as the zinc structure of asparigine also forms this type of polymeric structure where the amine groups lie trans to one another.[57] The donating carbonyl-zinc bond lengths, Zn(1)-O(5) 2.299(2) Å and Zn(1)-O(2) 2.442 (2) Å, are significantly larger than the carboxylate-zinc bond lengths of Zn(1)-O(3) 2.051(2) Å and Zn(1)-O(6) 2.050(2) Å. This is also observed in other octahedral zinc amino acid complexes. The zinc coordination sphere bound to the amino acid is slightly distorted, typified by the angles N(4)-Zn(1)-N(2) 172.28(12)° and O(3)-Zn(1)-O(6) 178.27(9)°.

Each zinc based molecular unit is bound to another by the two covalent interactions discussed above, the amide substituent also participates in hydrogen bonding [N(1)···O(4), 2.914(1) Å, N(1)-H(1A)···O(4) 167.77(1)° and N(3)···O(1), 3.003(1) Å, N(3)-H(3C)···O(1) 169.44(1)°] stabilising this 1-D polymeric sheet. The amide also hydrogen bonds to other amide groups linking the 1-D chains together to form a polymeric 3-D array [N(3)···O(4), 2.239(1) Å, N(3)-H(3D)···O(4) 168.15(1)°]. Only one other metal complex of the free glutamine ligand has been reported, this is a Cu(II) species which forms a similar bis-amino acid complex to **28**. [77]

The structure of zinc serine was published by Van der Helm et al. in the 1970s.[62] The structure was obtained at 295 K and crystallised in the $P2_1$ space group. During the course of this investigation crystals suitable for X-ray diffraction were obtained, and the resulting structure was acquired at 150 K, the molecular structure is shown below in Fig. 4.18.

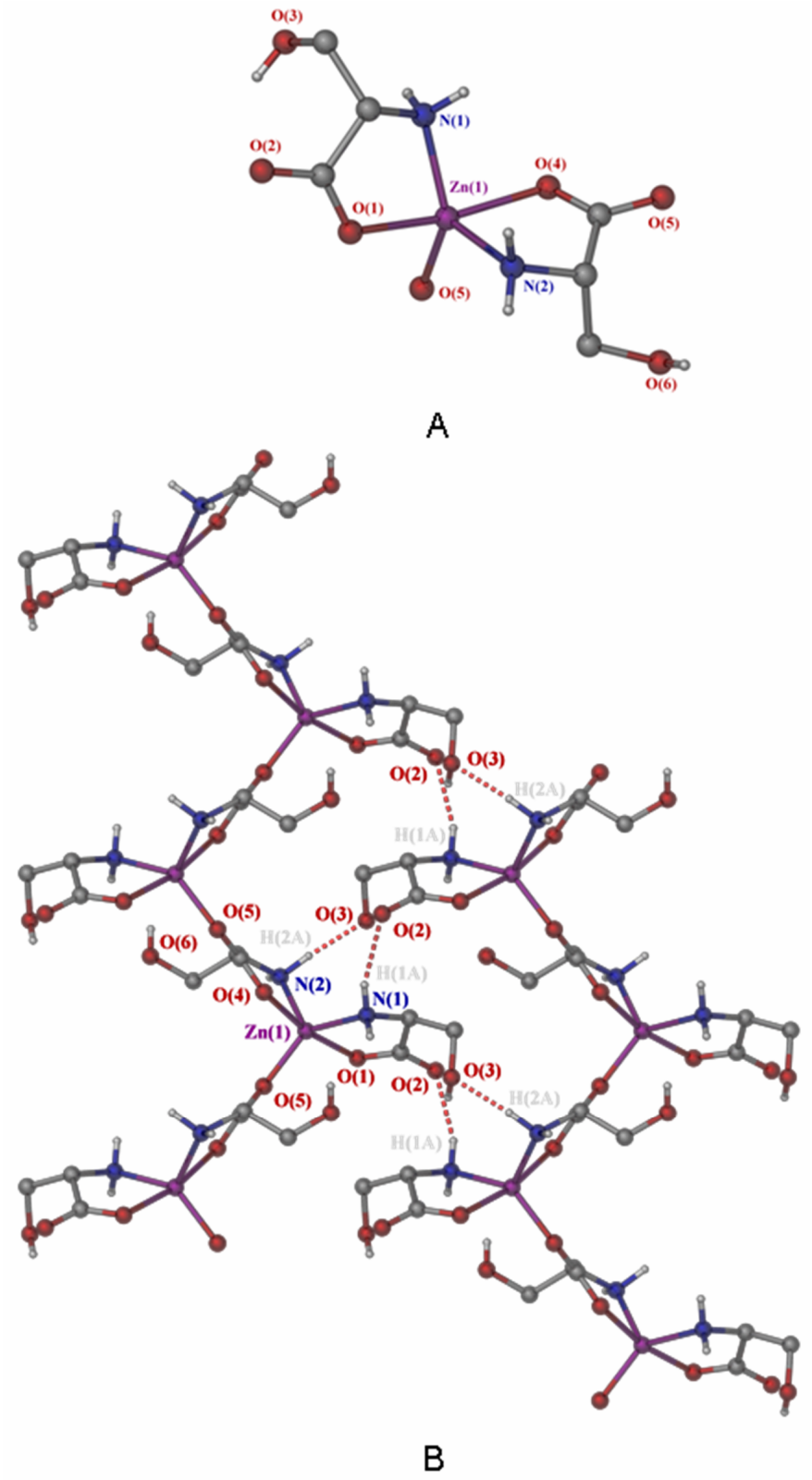

Figure 4.18 Molecular unit of complex ***29****, showing the metal coordination environment, (A), and the supramolecular structure, (B). All alkyl protons have been omitted for clarity*

The zinc atoms in **29** are five-coordinate where both amino acid ligands of the complex are bound to the zinc *via* the amine and carboxylic acid. However, only one of the amino acid ligands bridges to another zinc species via the carbonyl group. This is the most common binding mode in zinc amino acid complexes and the zinc salts of phenylalanine, leucine and proline all bind in this manner. [60, 64, 76]

The zinc ion itself is in a heavily distorted trigonal bipyramidal formation. This is exemplified by the angles N(1)-Zn(1)-N(2) 115.58(14)°, O(1)-Zn(1)-O(4) 168.72(12)° and N(1)-Zn(1)-O(1) 80.58(12)°. The bond lengths in the monomeric structure are similar to most amino acid complexes, however, the bond length O(5)-Zn(1) 1.973(3) Å is shorter than the zinc carboxylate bond lengths Zn(1)-O(1) 2.115 (3) Å and Zn(1)-O(4) 2.149(3) Å. This was also observed by Rombach et al in the structure of zinc phenylalanine. [64]

This bridging carboxylate forms a one dimensional coordination array. Each of these sheets hydrogen bonds extensively to the other sheets to create a 3-D arrangement, as shown in Fig. 4.17 (B). The structure contains three hydrogen atoms that form strong hydrogen bonds, two of which are displayed in Fig. 4.17 above. The distance of N(2) from O(3) is 2.894(1) Å where the angle N(2)-H(2A)-O(3) is 172.18(1)°. The other hydrogen bond displayed is slightly longer, N(1)···(O2) is 3.024(1) Å and the angle between the donor, proton and acceptor is 161.51(1)°.

4.2.6 Catalytic Activity of 23-29 in the Conversion of Soybean Oil

The following catalytic results were obtained at 195 ºC over 2 hours with a catalyst loading of 2.5 mol%. Soybean oil was used with a methanol ratio of 12:1. The same experimental procedure employed is detailed in Chapter 2, Section 2.2.2. The catalytic activity of complexes **23**-**29** is presented below in Fig. 4.19 as well as zinc acetate for comparison.

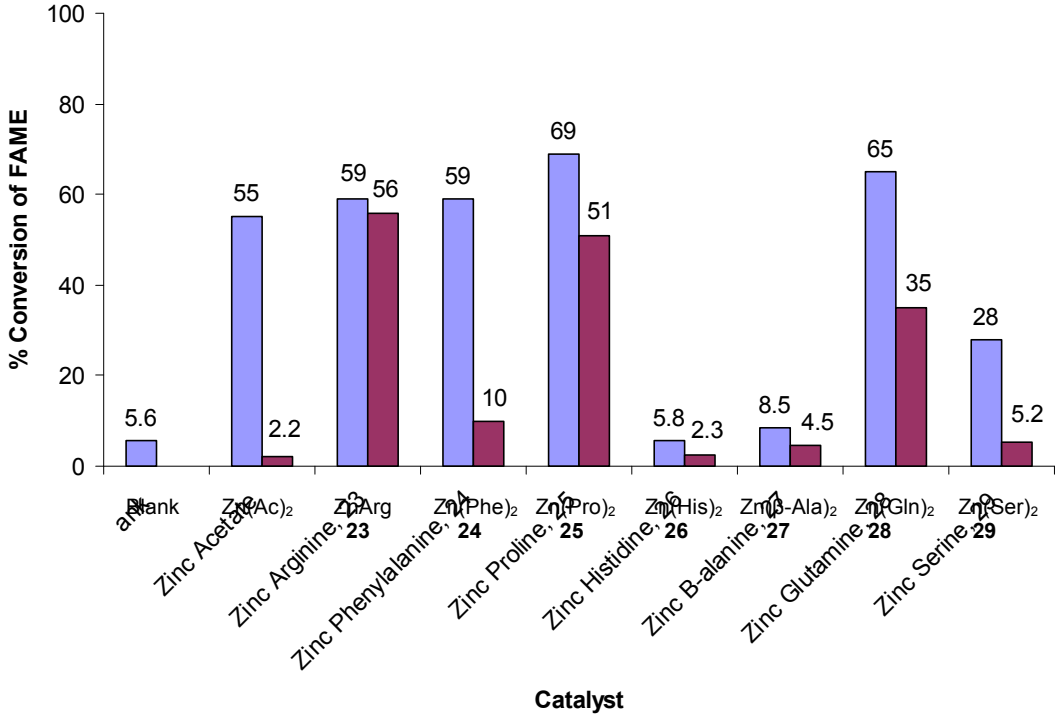

Figure 4.19 The catalytic activity of the zinc amino acid catalysts (blue) ***23-29****, compared to the corresponding free amino acids (purple) for the transesterification of soybean oil*

Zinc acetate, the starting material used in the zinc amino acid synthesis, was shown to be active in the conversion of soybean oil. Four of the zinc amino acid catalysts investigated were found to have a comparable or higher catalytic activity than this simple zinc salt.

There are three possible mechanisms by which these amino acid based catalysts can convert the glycerides to FAME. Firstly, if the amino acid constituent is basic then a Brønsted base catalysed reaction could proceed via generation of the methoxide anion. Secondly a Lewis acid catalysed mechanism is possible with the zinc activating the glyceride ester by an interaction with the ester linkage. Thirdly, a synergic effect is possible where the metal binds to the glyceride and the ligand has a positive cooperative effect in producing FAME.

Zinc acetate is a strong Lewis acid and presumably converts the soybean oil solely via the Lewis acid catalysed mechanism. Peters et al. tested a range of zinc based catalysts, including zinc arginate, for the production of FAME from rapeseed oil. In this study they concluded that only zinc salts of amino acids containing highly basic groups

would be active in the transesterification. [78] However, **23** converts a similar amount of FAME as the free arginine and it is likely that there is no synergic cooperation between the zinc and basic moiety which is beneficial to the conversion of FAME. **24** and **25** are both active catalysts and contain no basic constituent. The results collected in this study indicate that there is no correlation with bascity of the amino acid moiety and catalytic activity.

In **24** and **25** the zinc ion is five coordinate and both complexes are active for the transesterification. However, the zinc in complex **29** is in a five coordinate geometry and demonstrates a greatly reduced catalytic activity. Complex **28** is also highly active yet the zinc ion is in a stable octahedral array. It seems unlikely that there is a correlation between the coordination number of the zinc in the solid state and catalytic activity for the series of complexes tested.

Zinc proline, **25**, is the most active catalyst in the series under these reaction conditions and gives a significant increase on using either proline or zinc acetate as catalysts. The conversion of the FAME by zinc proline is presumably synergic, and further testing was undergone to examine this increase in activity.

4.2.7 Catalytic Activity of Various Zinc Based Systems on a Model Industrial Scale

To further examine the viability of **25** for the conversion of vegetable oils to FAME on an industrial scale, further experiments were undertaken on a scaled up process under industrial conditions.

The catalytic screening was performed using rapeseed oil with a FFA acid content of 0.56%, the catalyst (1 mol%) and methanol (6 equivalents), the reaction was performed at 200 °C. This testing was done on a scale over 10x larger than that of the laboratory testing so far described. The degree of transesterification was determined using HPLC, the chromatograph is shown in Chapter 6.

The catalytic activity of complex **25** under these more exacting conditions was compared to other zinc complexes, which had been shown to have a similar catalytic activity under the laboratory testing conditions. The yields of the separate glycerides can then be extrapolated from the plot. This technique allows a further insight into the activity of the various catalysts.

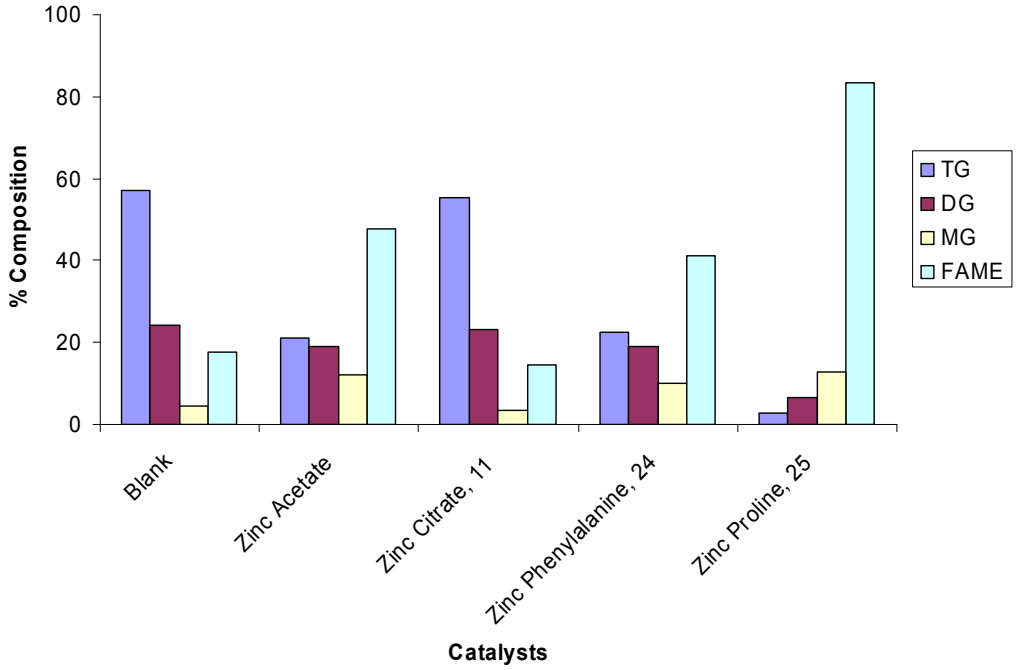

Figure 4.20 Percentage composition of the reaction mixture containing tri-, di- and and monoglyceride as well as FAME, catalysed by various zinc complexes

Catalyst	% TG	% DG	% MG	% Yield of FAME
Blank	57.1	24.1	4.5	17.6
Zinc Acetate	21.2	19	12	47.8
Zinc Citrate, **11**	55.3	23.2	3.4	14.7
Zinc Phenylalanine, **24**	22.6	19.1	10	41.1
Zinc Proline, **25**	2.6	6.6	12.8	83.3

Table 4.1 Conversion of rapeseed oil by various zinc based catalysts

Under these testing conditions there is no improvement in conversion on using the zinc citrate than using no catalyst at all. Zinc acetate and **24** both produce similar results and there would seem to be little advantage in using **24** over zinc acetate in the biodiesel reaction**.**

The zinc proline catalyst converts almost all of the triglycerides to FAME as well as a significant proportion of the other glycerides. Although testing on a laboratory

scale can distinguish between the catalysts the results show the importance of a pilot scale for a full evaluation of catalytic potential.

In light of these results **25** was deemed to be a potential industrial catalyst for the conversion of vegetable oil to biodiesel. However, as previously discussed in Chapter 1, few potential biodiesel catalysts for the conversion of waste oils have been reported. Further testing was done on a laboratory scale to evaluate the activity of **25** in converting model waste oils.

4.2.8 CATALYTIC CONVERSION OF MODEL WASTE OILS

Having demonstrated that zinc proline is a viable catalyst for the production of FAME from virgin vegetable oils on both a laboratory and larger scale process we investigated the activity of the zinc proline for converting waste oils.

Measured amounts of stearic acid (as a model for the various FFA present in waste oils) and water were added to the vegetable oil to simulate a lower quality feedstock.

The following catalytic testing was done on the smaller laboratory scale at 195 ºC over 2 hours with a catalyst loading of 2.5 mol%. Soybean oil was used with a methanol ratio of 12:1. The same experimental procedure employed is detailed in Chapter 6. The catalytic activity of these complexes is present below in Fig. 4.21 and Fig. 4.22.

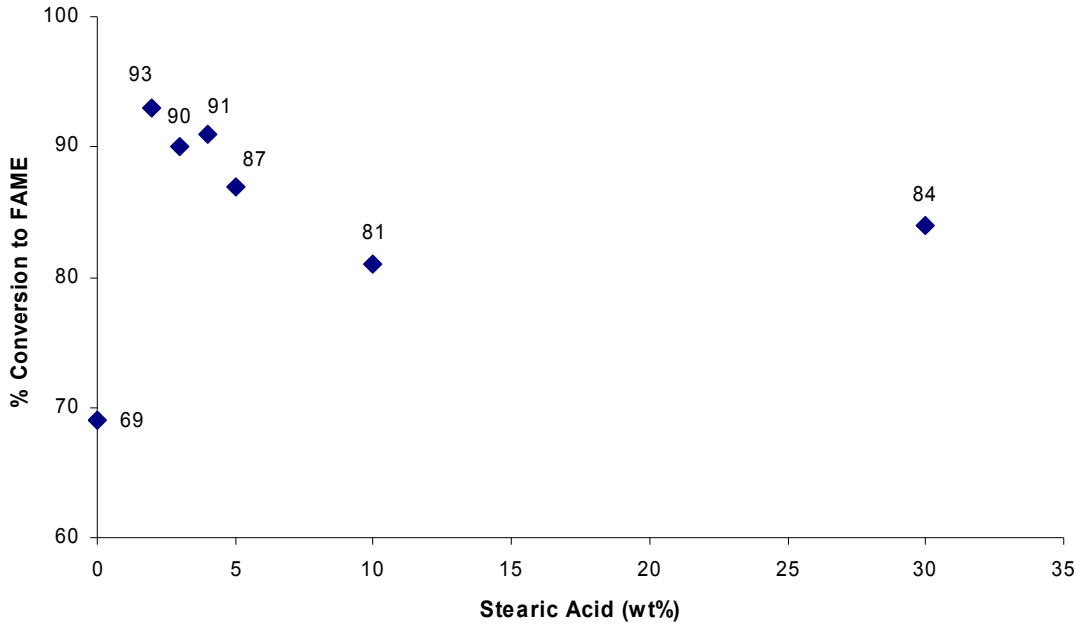

Figure 4.21 The effect of FFA concentration on the conversion of glycerides to FAME catalysed by zinc proline complex ***25***

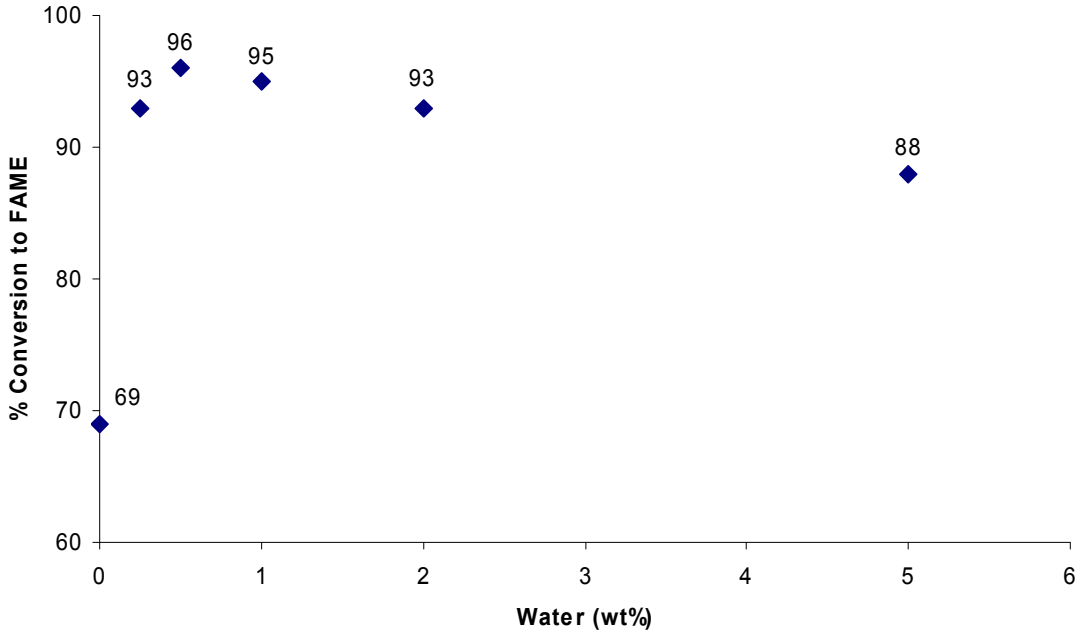

Figure 4.22 The effect of water on the zinc proline catalysed transesterification of soybean oil

Remarkably on addition of stearic acid to the soybean oil the activity of the zinc proline catalyst increases dramatically. This activity is reduced slightly at high FFA concentrations, yet is still significantly higher than in the conversion of virgin soybean oil.

Zinc carboxylate catalysts are widely used in esterification reactions, and have been shown to convert FFA to FAME. [79] Zinc proline is presumably catalysing the esterification of the stearic acid, producing FAME and water. There is not a high enough FFA content to explain the large rise in activity and so it is likely that the water is increasing the activity of the zinc proline catalyst. This trend is also observed on the addition of water alone to the reaction. If all the stearic acid (2 wt%) was esterified it would produce 2.5 mmol of water.

Water has a large effect on the activity of the zinc proline catalyst. Counter intuitively an increase in water increases the activity of the catalyst. Just a 0.25 wt% (~5 mmol) amount of water increases the activity of the zinc proline catalyst. This reactivity is slightly diminished on addition of larger volumes but is still far greater than in the absence of water.

This effect was also observed for the enzymatic catalysis of waste oils, where it is assumed that the water is helping to solubilise the catalyst into the reactants. [80, 81] Zinc proline is soluble in aqueous solutions yet the activity of the catalyst is at its highest at low concentrations of water, this suggests that the competing hydrolysis reaction is also favoured and that the increase in solubility is not the sole factor determining the higher activity of the zinc proline.

Di Serio et al. reported that on the addition of water to vegetable oil, the activity of zinc acetate was greatly reduced. This was explained by the formation of zinc hydroxide and the resulting reduction in Lewis acidity. However, a series of amine stabilised zinc hydroxide complexes have been reported, [82] these complexes have also been shown to be active in the transesterification reaction where the hydroxide ligands are displaced by methoxide groups and this reactive species catalyses the transformation. [83] It is possible that a similar species is being formed in the transesterification reaction under these conditions and is more active in the conversion of triglcyerides to FAME than the zinc carboxylate alone.

4.3 SUMMARY

Amino acids are excellent chelating ligands, however the titanium derived species are prone to hydrolysis and methanolysis when used in the biodiesel reaction. The stability of these complexes can be increased dramatically by chelation of the metal to an amino acid bisphenolate derivative. The titanium complexes of these ligands were more active than the free amino acid complexes and the trisphenolate derivatives. Germanium was also shown to be active in the transesterification of vegetable oils. However, the cost of germanium and the cost of the bisphenolate ligand synthesis are prohibitive for the use of these catalyst types in industry.

A range of moisture stable zinc amino acids were synthesised, and zinc proline was found to be highly active on both a laboratory scale process and model industrial process. The activity of the zinc proline catalyst could be improved by the addition of water or FFA and indicates that zinc proline is a potential industrial catalyst for the transesterification of waste oils to FAME.

It is clear that zinc carboxylates are active in the transesterification of vegetable oils and the zinc being bound to an amine group can increase the activity over that of the simple carboxylate. None of the zinc amino acid catalysts are soluble in methanol, which would be advantageous for the activity and also the ease of delivery into the reactor itself. In the next chapter other zinc carboxylate systems will be further investigated for the activity in the biodiesel reaction.

4.4 REFERENCES

1. C. Kremer, J. Torres, S. Dominguez and A. Mederos, *Coordination Chemistry Reviews*, 2005, **249**, 567-590.
2. A. Iakovidis and N. Hadjiliadis, *Coordination Chemistry Reviews*, 1994, **135**, 17-63.
3. B. Gyurcsik and L. Nagy, *Coordination Chemistry Reviews*, 2000, **203**, 81-149.
4. K. Madafiglio, T. M. Manning, C. M. Murdoch, W. R. Tulip, M. K. Cooper, T. W. Hambley and H. C. Freeman, *Acta Crystallographica Section C-Crystal Structure Communications*, 1990, **46**, 554-561.
5. O. Yamauchi, A. Odani, T. Kohzuma, H. Masuda, K. Toriumi and K. Saito, *Inorganic Chemistry*, 1989, **28**, 4066-4068.
6. N. Ohata, H. Masunda and O. Yamauchi, *Inorganica Chimica Acta*, 1999, **286**, 37-45.
7. O. Yamauchi, A. Odani and M. Takani, *Journal of the Chemical Society Dalton Transactions*, 2002, 3411-3421.
8. O. Yamauchi and A. Odani, *Journal of the American Chemical Society*, 1981, **103**, 391-398.
9. A. C. Rizzi, C. D. Brondino, R. Calvo, R. Baggio, M. T. Garland and R. E. Rapp, *Inorganic Chemistry*, 2003, **42**, 4409-4416.
10. N. J. Taylor and A. J. Carty, *Journal of the American Chemical Society*, 1977, **99**, 6143-6145.
11. N. Burford, M. D. Eelman, W. G. LeBlanc, T. S. Cameron and K. N. Robertson, *Chemical Communications*, 2004, 332-333.
12. J. E. Anderson, S. M. Sawtelle, J. S. Thompson, S. A. K. Nguyen and J. Calabrese, *Inorganic Chemistry*, 1992, **31**, 2778-2785.
13. A. Demaret and F. Abraham, *Acta Crystallographica Section C-Crystal Structure Communications*, 1987, **43**, 2067-2069.
14. A.Schluter, K.Bieber and W.S.Sheldrick, *Inorganica Chimica Acta*, 2002, **340**, 35-43.
15. M.-C.Corbeil and A. L. Beauchamp, *Canadian Journal of Chemistry*, 1988, **66**, 2458-2464.

16. T.Yajima, R.Takamido, Y.Shimazaki, A.Odani, Y.Nakabayashi and O.Yamauchi, *Dalton Transactions*, 2007, 299-307.
17. Yu Xie, Hao-Han Wu, Guo-Ping Yong and Z.-Y. Wang, *Acta Crystallographica Section E-Structure Reports Online*, 2006, **62**, m2089.
18. H. P. Lundgren, W. G. Rose and M. K. Walden, *Journal of Organic Chemistry*, 1961, **26**, 1487-1491.
19. U. Schubert, S. Tewinkel and F. Moller, *Inorganic Chemistry*, 1995, **34**, 995-997.
20. R. Bina, M. Pavlista, Z. Cernosek, I. Cisarova and I. Pavlik, *Applied Organometallic Chemistry*, 2005, **19**, 701-710.
21. R. Bina, I. Cisarova and I. Pavlik, *Applied Organometallic Chemistry*, 2004, **18**, 71-72.
22. R. Bina, I. Cisarova, M. Pavlista and I. Pavlik, *Applied Organometallic Chemistry*, 2004, **18**, 262-263.
23. H. Mimoun, M. Postel, F. Casabianca, J. Fischer and A. Mitschler, *Inorganic Chemistry*, 1982, **21**, 1303-1306.
24. K. Wieghardt, U. Quilitzsch, J. Weiss and B. Nuber, *Inorganic Chemistry*, 1980, **19**, 2514-2519.
25. J. P. Fackler, F. J. Kristine, A. M. Mazany, T. J. Moyer and R. E. Shepherd, *Inorganic Chemistry*, 1985, **24**, 1857-1860.
26. M. S. Shongwe, C. H. Kaschula, M. S. Adsetts, E. W. Ainscough, A. M. Brodie and M. J. Morris, *Inorganic Chemistry*, 2005, **44**, 3070-3079.
27. A. S. Ceccato, A. Neves, M. A. de Brito, S. M. Drechsel, A. S. Mangrich, R. Werner, W. Haase and A. J. Bortoluzzi, *Journal of the Chemical Society-Dalton Transactions*, 2000, **10**, 1573-1577.
28. E. Y. Tshuva and M. Versano, *Inorganic Chemistry Communications*, 1999, **2**, 371-373.
29. C. L. Boyd, T. Toupance, B. R. Tyrrell, B. D. Ward, C. R. Wilson, A. R. Cowley and P. Mountford, *Organometallics*, 2005, **24**, 309-330.
30. S. Groysman, I. Goldberg, M. Kol, E. Genizi and Z. Goldschmidt, *Inorganica Chimica Acta*, 2003, **345**, 137-144.
31. Y. Kim and J. G. Verkade, *Organometallics*, 2002, **21**, 2395-2399.
32. S.Padmanabhan, S.Katao and K.Nomura, *Organometallics*, 2007, **26**, 1616-1626.

33. E. Y. Tshuva, I. Goldberg, M. Kol and Z. Goldschmidt, *Inorganic Chemistry*, 2001, **40**, 4263-4270.
34. A. J. Chmura, M. G. Davidson, M. D. Jones, M. D. Lunn and M. F. Mahon, *Dalton Transactions*, 2006, 887-889.
35. H. C. Freeman, G. N. Stevens and I. F. Taylor, *Chemical Communications*, 1974, 366-368.
36. H. I. Beltran, L. S. Zamudio-Rivera, T. Mancilla, R. Santillan and N. Farfan, *Chemistry-a European Journal*, 2003, **9**, 2291-2306.
37. N. K. Goh, C. K. Chu, L. E. Khoo, D. Whalen, G. Eng, F. E. Smith and R. C. Hynes, *Applied Organometallic Chemistry*, 1998, **12**, 457-466.
38. F. L. Lee, E. J. Gabe, L. E. Khoo, W. H. Leong, G. Eng and F. E. Smith, *Inorganica Chimica Acta*, 1989, **166**, 257-261.
39. R. K. Iyer, S. G. Deshpande and V. Amirthalingam, *Polyhedron*, 1984, **3**, 1099-1104.
40. J. Otera, *Chemical Reviews*, 1993, 1449-1470.
41. B. Jousseaume, C. Laporte, M. Rascle and T. Toupance, *Chemical Communications*, 2003, **12**, 1428-1429.
42. F. R. Abreu, D. G. Lima, E. H. Hamu, S. Einloft, J. C. Rubim and P. A. Z. Suarez, *Journal of the American Oil Chemists Society*, 2003, **80**, 601-604.
43. A. M. Florea and D. Busselberg, *Biometals*, 2006, **19**, 419-427.
44. V. Krishnan, S. Gross, S. Muller, L. Armelao, E. Tondello and H. Bertagnolli, *Journal of Physical Chemistry B*, 2007, **111**, 7519-7528.
45. M. Veith, C. Mathur and V. Huch, *Phosphorus, Sulfur and Silicon and the Related Elements*, 1997, **125**, 489-492.
46. Y. Lee, H. Terashima, Y. Shimodaira, K. Teramura, M. Hara, H. Kobayashi, K. Domen and M. Yashima, *Journal of Physical Chemistry C*, 2007, **111**, 1042-1048.
47. T. Ekou, A. Vicente, G. Lafaye, C. Especel and P. Marecot, *Applied Catalysis a-General*, 2006, **314**, 64-72.
48. M. Boutzeloit, V. M. Benitez, V. A. Mazzieri, C. Especel, F. Epron, C. R. Vera, C. L. Pieck and P. Marecot, *Catalysis Communications*, 2006, **7**, 627-632.
49. H. Preut, M. Vornefeld and F. Huber, *Acta Crystallographica Section C-Crystal Structure Communications*, 1989, **45**, 1504-1506.

50. P. Livant, J. Northcott and T. R. Webb, *Journal of Organometallic Chemistry*, 2001, **620**, 133-138.
51. A. Finne, Reema and A. C. Albertsson, *Journal of Polymer Science Part A-Polymer Chemistry*, 2003, **41**, 3074-3082.
52. H. R. Kricheldorf and S. Rost, *Macromolecular Chemistry and Physics*, 2004, **205**, 1031-1038.
53. H. R. Kricheldorf and D. Langanke, *Polymer*, 2002, **43**, 1973-1977.
54. *United States Geological Survey, http://www.usgs.gov/*, Accessed August, 2007.
55. S. D. Dalosto and R. Calvo, *Journal of Physical Chemistry*, 2001, **105**, 1074-1085.
56. S. D. Dalosto, M. G. Ferreyra, R. Calvo, O. E. Piro and E. E. Castellano, *Journal of Inorganic Biochemistry*, 1999, **73**, 151-155.
57. F. S. Stephens, R. S. Vagg and P. A. Williams, *Acta Crystallographica Section B-Structural Science*, 1977, **33**, 433-437.
58. L. Kryger and S. E. Rasmussen, *Acta Chemica Scandinavica* 1973, **27**, 2674-2676.
59. J. M. Newman, C. A. Bear, T. W. Hambley and H. C. Freeman, *Acta Crystallographica Section C-Crystal Structure Communications*, 1990, **46**, 44-48.
60. C. A. Steren, R. Calvo, O. E. Piro and B. E. Rivero, *Inorganic Chemistry*, 1989, **28**, 1933-1938.
61. R. B. Wilson, P. de Meester and D. J. Hodgson, *Inorganic Chemistry*, 1977, **16**, 1498-1502.
62. D. van der Helm, A. F. Nicholas and C. G. Fisher, *Acta Crystallographica Section B-Structural Science*, 1970, **26**, 1172-1174.
63. T. Dabre and M. Machuqueiro, *Chemical Communications*, 2003, 1090-1091.
64. M. Rombach, M. Gelinsky and H. Vahrenkamp, *Inorganica Chimica Acta*, 2002, **334**, 25-33.
65. M. A. Calter and R. K. Orr, *Tetrahedron Letters*, 2003, **44**, 5699-5701.
66. J. Kofoed, T. Darbre and J. L. Reymond, *Chemical Communications*, 2006, 1482-1484.
67. H. R. Kricheldorf and D. O. Damrau, *Macromolecular Chemistry and Physics*, 1998, **199**, 1747-1752.

68. S. K. F. Peter, R. Ganswindt, H. Neuner and E. Weidner, *European Journal of Lipid Science and Technology*, 2002, **104**, 324-330.
69. A. Dijkstra, *Acta Crystallographica* 1966, **20**, 588-590.
70. M. Kol, M. Shamis, I. Goldberg, Z. Goldschmidt, S. Alfi and E. Hayut-Salant, *Inorganic Chemistry Communications*, 2001, **4**, 177-179.
71. J. Wagler, U. Bohme, E. Brendler, B. Thomas, S. Goutal, H. Mayr, B. Kempf, G. Remennikov and G. Roewer, *Inorganica Chimica Acta*, 2005, **358**, 4270-4286.
72. *Search of the Cambridge Structural Database version 5.27.*
73. F. H. Allen, *Acta Crystallographica Section B-Structural Science*, 2002, **58**, 380-388.
74. P. Jutzi, S. Keitemeyer, B. Neumann and H. G. Stammler, *Organometallics*, 1999, **18**, 4778-4784.
75. N. W. Mitzel and K. Vojinovic, *Journal of the Chemical Society-Dalton Transactions*, 2002, 2341-2343.
76. Chew-Hee Ng, Hoong-Kun Fun, Soon-Beng Teo, Siang-Guan Teoh and K.Chinnakali, *Acta Crystallographica Section C-Crystal Structure Communications*, 1995, **51**, 244-245.
77. J. M. Schveigkardt, A. C. Rizzi, O. E. Piro, E. E. Castellano, R. C. de Santana, R. Calvo and C. D. Brondino, *European Journal of Inorganic Chemistry*, 2002, 2913-2919.
78. U. Schuchardt, R. R. Sercheli and M. Vargas, *The Journal of Brazilian Chemical Society*, 1998, **9**, 199-210.
79. M. Di Serio, R. Tesser, M. Dimiccoli, F. Cammarota, M. Nastasi and E. Santacesaria, *Journal of Molecular Catalysis a-Chemical*, 2005, **239**, 111-115.
80. T. W. Tan, K. L. Nie and F. Wang, *Applied Biochemistry and Biotechnology*, 2006, **128**, 109-116.
81. R. Brenneis, B. Baeck and G. Kley, *European Journal of Lipid Science and Technology*, 2004, **106**, 809-814.
82. G. Parkin, *Chemical Communications*, 2000, 1971-1985.
83. R. A. Allred, K. Doyle, A. M. Arif and L. M. Berreau, *Inorganic Chemistry*, 2006, **45**, 4097-4108.

CHAPTER 5

HOMOGENEOUS ZINC CARBOXYLATE CATALYSTS

In the following chapter the suitability of zinc carboxylate systems as catalysts for the transesterification of vegetable and waste oils is further examined. The activity of a number of simple zinc carboxylate salts has been determined, as well as that of various zinc carboxylate amine systems. The transesterification reactions were undertaken on both a laboratory scale and on the pilot industrial scale described in Chapter 4.

5.1 INTRODUCTION

Zinc carboxylates have been widely used as catalysts in various esterification reactions [1-3] and ester polymerisations [4] as well as in the production of biodiesel. [5-7] The complexes are highly Lewis acidic, inexpensive and, depending on the carboxylate moiety, generally non-toxic.

Zinc salts of smaller carboxylic acids are generally soluble in methanol whereas the longer chain carboxylates, such as zinc stearate, are soluble in aliphatic solvents and lipids. Both of these attributes have advantages in the production of biodiesel, as a methanolic catalyst solution is easier to deliver to the reactor and work up after but a catalyst soluble in the lipid layer will tend to have a higher activity.

In the solid state, the anhydrous saturated zinc carboxylates form 2-D sheets as shown in Fig. 5.1. The structural characterisation has been reported for zinc acetate, [8] propionoate, [9] butanoate, [10] hexanoate [11] and octanoate. [12]

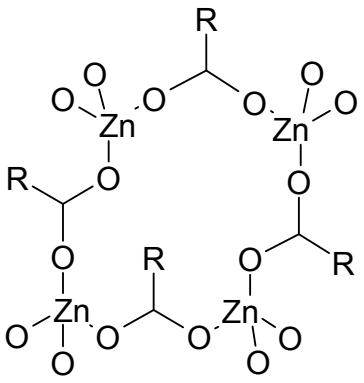

Figure 5.1 Solid state structure of saturated zinc carboxylates where R = CH_3, C_3H_7, C_4H_9, C_6H_{13} and C_8H_{17}

Each zinc atom is coordinated to four oxygen centres from four different carboxylate groups in a tetrahedral fashion. Although this structural motif was observed for all the saturated zinc carboxylates, the unsaturated zinc crotonate (CH_3CH=$CHCOOH$) forms a different structure, shown below in Fig. 5.2. [13]

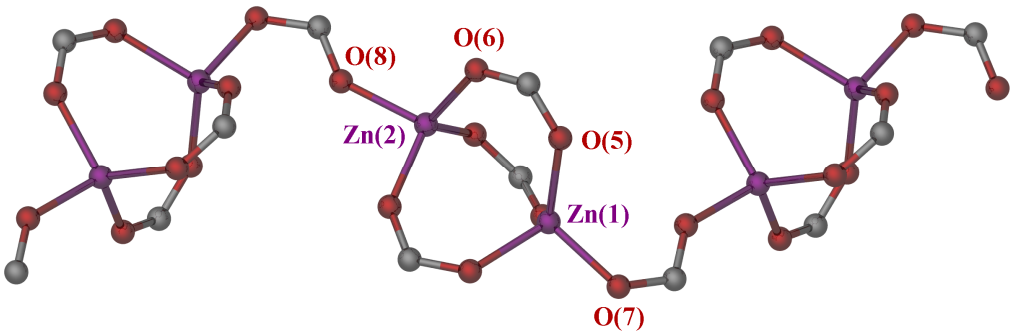

Figure 5.2 Structural motif of zinc crotonate, taken from Clegg et al.

In this structure, the repeat unit consists of two zinc atoms being bridged by three crotonate ligands in a 'paddle' motif, a fourth crotonate ligand bridges two units together to give a 1-D chain.

Clegg et al. also reported that a homometallic zinc structure could be isolated on addition of quinoline to zinc crotonate in ethanol. By reducing the amount of quinoline in the solution a homometallic trimer was also recovered. Heterometallic zinc trimers

were also formed when another metal crotonate was present in solution, these structures are shown below in Fig. 5.3. [14, 15]

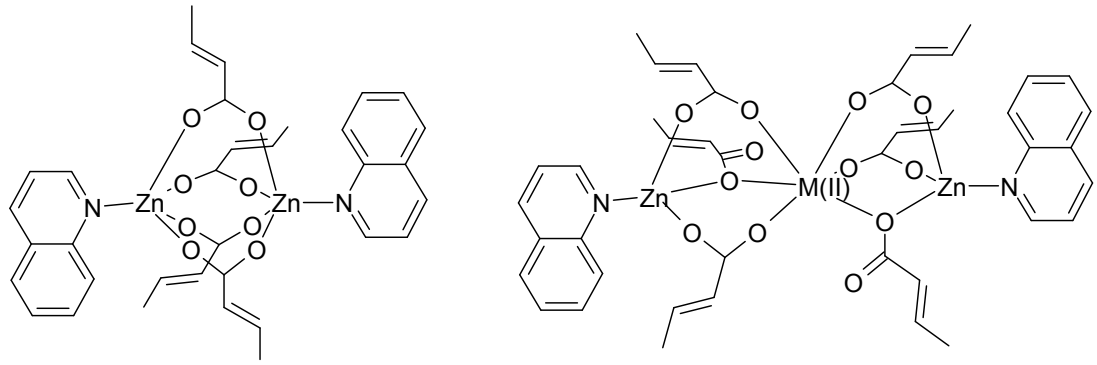

Figure 5.3 Zinc crotonate structures where M(II) = Zn, Co, Ni, Cd, Mg, Ca, Sr and Mn

There are no other structural examples of zinc carboxylate-quinoline complexes in the literature. However, with the similar ligands NPBA (*N*-(4-pyridyl)benzamide), NPA (*N*-(2-pyridine)-7-azaindole), azaindole, imidazole and pyridine, the zinc carboxylates remain monomeric with the ligands bound to the metal centre along with the original carboxylate groups. [16-19]

Triethylamine can also act as a Lewis base and coordinates to a range of metal carboxylates. Solid state structural information has been published on a range of triethylamine metal carboxylate compounds (Fig. 5.4). [20-23]

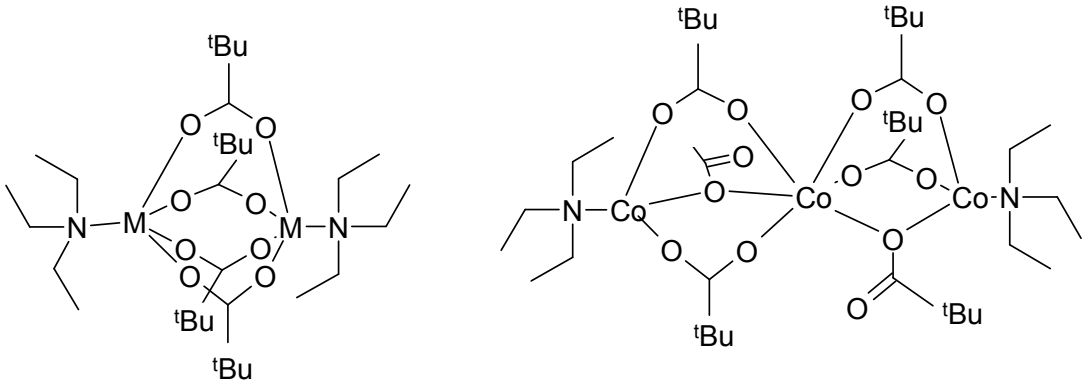

Figure 5.4 Examples of triethylamine metal complexes, where M = Ni, Co, Rh or Co

To the best of our knowledge none of the previously mentioned complexes have been used as catalysts in any type of esterification reaction. However, Di Serio et al tested a range of divalent metal acetates and stearates in the transesterification of rapeseed oil to FAME (Table 5.1). In this study they found that the stearate salts, regardless of the identity of the metal, were more active than the acetate salts of the same metal. Although the relative degree of enhancement varied from metal to metal the general increase in activity was attributed to the solubility of the stearate salts in the oil layer. [6]

Catalyst (ºC)	Ba	Ca	Mg	Cd	Mn	Pb	Zn	Co	Ni
Acetate (150)	2	4	10	40	15	43	28	6	-
Acetate (200)	11	31	39	85	67	81	67	20	7
Stearate (200)	73	73	72	89	62	58	64	81	7

Table 5.1 Percentage conversions of FAME achieved by a range of divalent metal catalysts using a standard 600:100:1 loading of methanol, soybean oil and catalyst over 2 hours, reported by Di Serio et al. [6]

This study also highlights that a significant factor in the catalytic production of biodiesel using metal carboxylates is the identity of the metal itself. Ni carboxylates were inactive regardless of the temperature or carboxylate moiety. Ba, Ca, Co and Mg stearates were all active at 200 °C, though the acetates were much less active. The most active catalysts were the stearate and acetate salts of Zn, Cd, Mn and Pb, which were all highly active at 200 °C. This trend in activity follows the Lewis acidity of the metal ion, with the more acidic complex giving a higher conversion of FAME. It is worth noting that when the temperature is raised to over 215 °C, the acetate salts of Ba and Ca also become highly active. [24]

Di Serio et al. also examined the effect of FFA and water on these carboxylate salts. On the addition of FFA, the competitive esterification reaction was observed. The resulting water from this reaction reacted with the carboxylate salts to form the metal hydroxide. These hydroxide species are insoluble and markedly less Lewis acidic than the carboxylate salts, a large decrease in the catalytic activity is therefore observed. This deactivation was also observed on addition of water to the reaction. Lowering the

catalyst loading, raising the reaction temperature or increasing the time of reaction can reduce these competitive side reactions. [6]

The highest conversions of FAME were achieved when Pb (II) or Cd (II) were used, although surprisingly Sn (II) acetate was not examined in this study, Sn(II) complexes are also highly active. [25, 26] Despite the high activity of these metals in the transesterification toxicity issues make them unattractive as commercial catalysts. [27, 28]

The manganese and zinc carboxylate salts gave only slightly lower yields of FAME and because of their inexpense, low toxicity and comparably high activity are promising candidates as industrial catalysts.

5.2 RESULTS AND DISCUSSION

A range of simple metal carboxylate salts and a number of zinc crotonate complexes discussed above were synthesised according to literature preparations. These were then tested for their activity in the transesterification of soybean oil, rapeseed oil and model waste oils.

5.2.1 CATALYTIC CONVERSION OF SOYBEAN OIL

The following catalytic results were obtained as detailed in the previous chapters namely at 195 ºC over 2 hours with a metal loading of 2.5 mol%. Soybean oil, 36.8 ml, was used with a methanol ratio of 12:1.

5.2.1.1 Carboxylate Complex Activity

A range of metal carboxylate catalysts were examined for their activity in the conversion of virgin soybean oil (Fig. 5.5.)

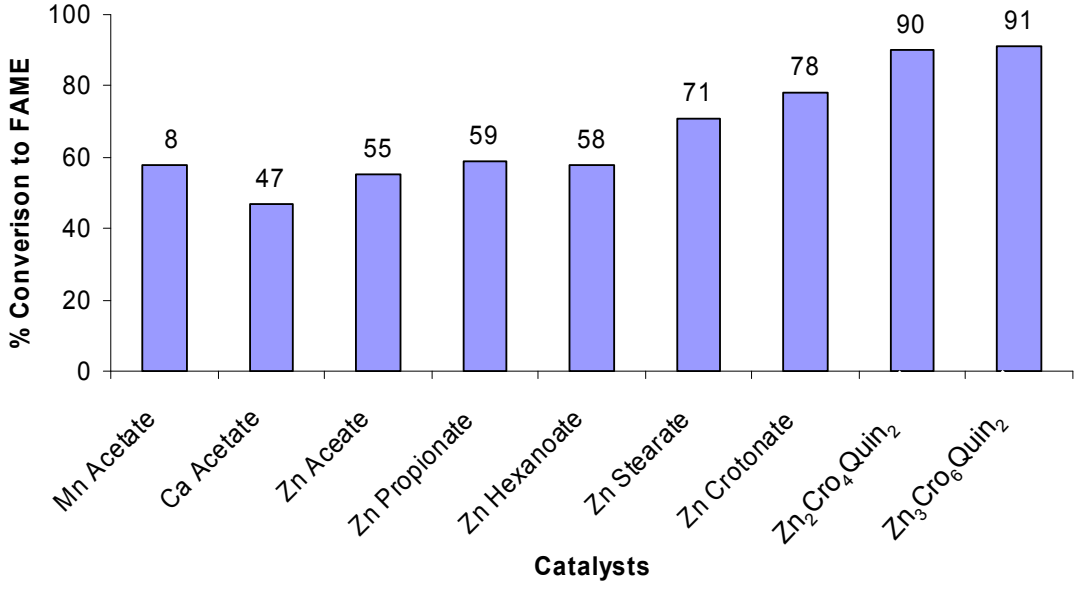

Figure 5.5 Catalytic activity of the various carboxylate catalysts

In contrast to the results presented by Di Serio et al. (Table 5.1) calcium, zinc and manganese acetates were all found to have a similar activity under the reaction conditions. The zinc salts of longer chain carboxylates were also examined. While the activity of the zinc propionate and zinc hexanoate is similar to that of the zinc acetate, zinc stearate shows a large increase in activity. Given that this elevated activity is solely due to the solubility in the oil layer it is surprising that zinc crotonate was more active than the stearate salt, converting 78% of the glycerides to FAME over the two hours.

The $Zn_2(Cro)_4Quin_2$ demonstrates a higher activity in the conversion of soybean oil than any of the other carboxylate salts. $Zn_3(Cro)_6Quin_2$, is as active as the bimetallic complex despite one of the three zinc centres being an octahedral co-ordinately saturated metal centre. This suggests that the zinc crotonate structure is not maintained in solution and the active catalytic species, while dependent on the amine base, is not the same as the solid state structure.

5.2.1.2 Methanolic Catalyst Solutions

An important consideration for a viable biodiesel catalyst is the cost of production and the ease of delivery to the reactor. A catalyst formed *in situ* in methanol could be used instead of the isolated solid. This approach, as long as the activity of the catalyst is undiminished, would prove to be more efficient.

A solution of zinc crotonate was dissolved in methanol and quinoline added. This stock solution of methanol and catalyst was used *insitu* as opposed to isolated solids $Zn_2(Cro)_4Quin_2$ and $Zn_3(Cro)_6Quin_2$. The total metal content was kept at 2.5 mol% for all transesterification reactions. Results for the conversion of soybean oil to FAME are given in Table 5.2.

Catalyst	% Conversion to FAME
Quinoline	29
$ZnCro_2$	78
$Zn_2Cro_4Quin_2$	91
$Zn_3Cro_6Quin_2$	90
'$Zn_2Cro_4Quin_2$' [a]	88
'$Zn_3Cro_6Quin_2$' [a]	87

Table 5.2 Conversion of FAME using various methanolic catalyst solutions

A methanolic solution of zinc crotonate and quinoline converts the same amount of glycerides prepared in this manner than by crystallisation of the solid complexes. Two further solutions were made by adding manganese crotonate and calcium crotonate to the zinc crotonate quinoline solution, the total metal content was kept at 2.5 mol%, the results are given below in Table 5.3.

Catalyst	% Conversion to FAME
'$Zn_2Cro_4Quin_2$'	88
'$ZnMnCro_4Quin_2$'	43
'$ZnCaCro_4Quin_2$'	83

Table 5.3 Conversion of FAME using various methanolic catalyst solutions [a]

In the synthesis of *insitu* methanolic solutions, the presence of another metal crotonate to a solution of zinc crotonate and quinoline reduces the amount of FAME produced compared to using the zinc crotonate solution alone.

Despite numerous attempts no heterometallic zinc dimer complexes were isolated from the reaction in alcohol. For example the attempted synthesis of $ZnM(II)Cro_4Quin_2$, (where M = Ba, Ca or Mn) was unsuccessful however where M(II) = Zn the product was isolated in high yield.

[a] *insitu* methanolic solution

5.2.1.3 Temperature Dependence

The $Zn_2(Cro)_4Quin_2$ and $Zn(Cro)_2$ showed a higher activity than the other metal carboxylate complexes presented in the literature. These two complexes were then examined for the optimum operating temperature, the results are shown below in Fig. 5.6.

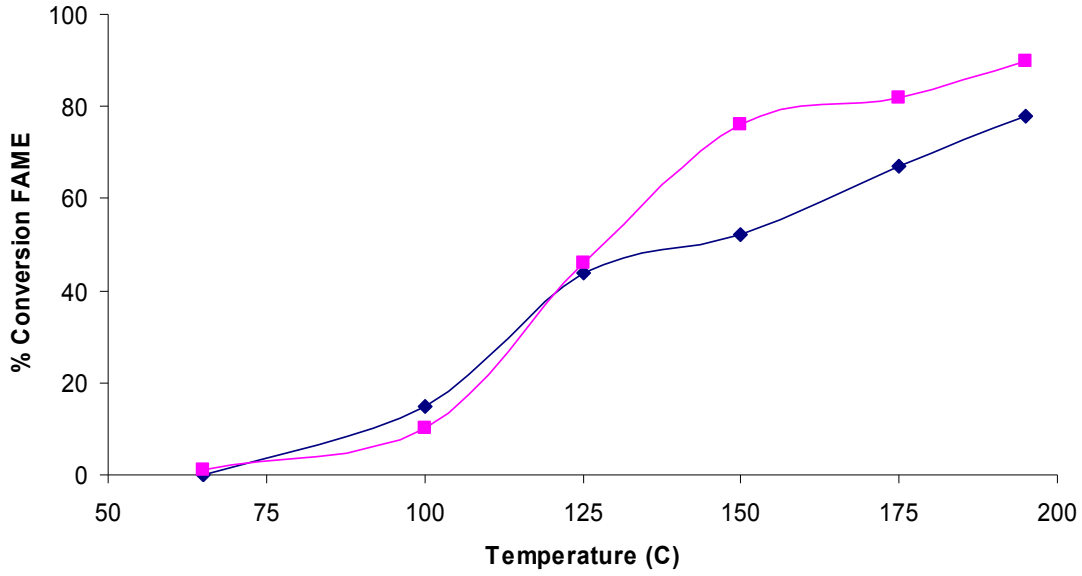

*Figure 5.6 Temperature dependence of the conversion of FAME while using $Zn(Cro)_2$ (blue) and complex **30**, $Zn_2(Cro)_4Quin_2$, (pink)*

Both of the catalysts are inactive at the reflux temperature of methanol, and only convert small amounts of the glyceride to FAME at 100 °C. Both complexes convert similar amounts of glycerides until the temperature reaches 125 °C. After 125 °C the production of FAME retains a roughly linear relationship with temperature for the $Zn(Cro)_2$ catalysed reaction. $Zn_2(Cro)_4Quin_2$ becomes highly active after this temperature and is a more effective catalyst than the $Zn(Cro)_2$ alone. At temperatures over 150 °C the activity of the $Zn_2(Cro)_4Quin_2$ system only increases marginally with an increase in temperature. This is presumably due to the system reaching equilibrium. For a more effective comparison of the zinc crotonate systems a temperature of 150 °C is optimum.

5.2.1.4 The Effect of Quinoline on Differing Zinc Carboxylates

As shown above the formation of the catalyst *in situ* is as effective as using the isolated solids as catalysts (Table 5.2). In Fig. 5.6 it was shown that 150 °C was the optimum temperature to observe catalytic potential. In all subsequent testing of the catalysts these conditions were employed. The effect of quinoline on the catalytic activity of the range of zinc carboxylates was then examined (Fig. 5.7).

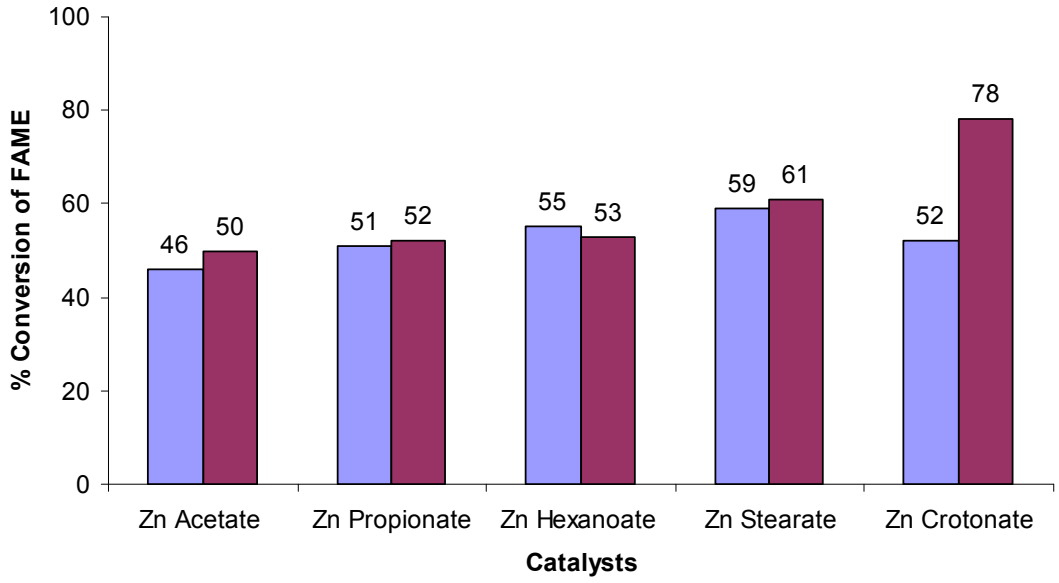

Figure 5.7 Conversion of glycerides to FAME using homogeneous mixtures of zinc carboxylates, with (purple) and without (blue) quinoline

At 150 °C all the zinc carboxylates demonstrate a similar activity in the conversion of soybean oil. Where the addition of quinoline to the zinc crotonate solution forms a highly active species, it has no discernable effect on the activity of any of the saturated carboxylate catalysts.

Despite exhaustive attempts no products were isolated from the reaction of the simple zinc carboxylate salts and quinoline in alcohol and it seems likely that the interaction between the zinc crotonate and quinoline base is vital to produce an active species.

5.2.1.5 The Variation of the Base with Zinc Crotonate

In order to further investigate the effect of quinoline on the zinc crotonate catalyst, a series of related bases were used in conjunction with zinc crotonate in the conversion of soybean oil. The results are shown below in Fig. 5.8.

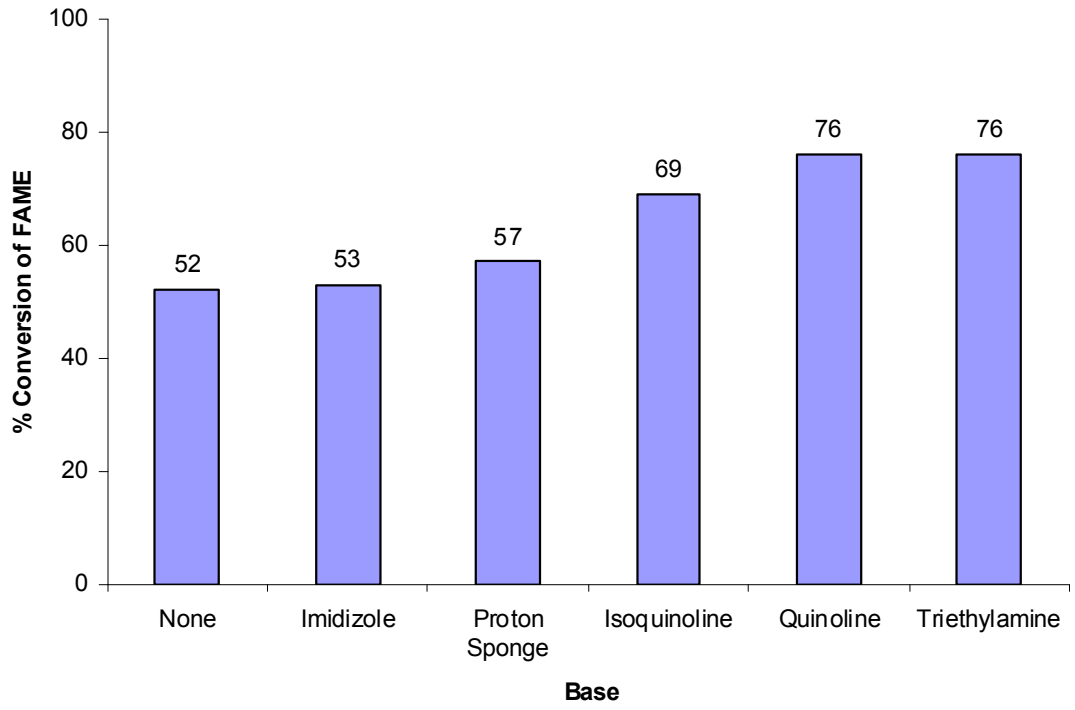

Figure 5.8 The effect of different bases on the zinc crotonate catalysed conversion of FAME

1,8-bis(dimethylamino)naphthalene (proton sponge) is a strong Brønsted base, but as the amine groups are sterically inaccessible, it is a very poor ligand. The addition of this base to the zinc crotonate solution does not increase the yield of FAME significantly.

Using isoquinoline in place of the quinoline gives a similarly high conversion of FAME. Triethylamine also increases the activity of the zinc crotonate. As discussed in the introduction, triethylamine can act as a Lewis base on addition to metal carboxylates.

Addition of imidazole did not increase the activity of the zinc crotonate. However, zinc crotonate complexes of imidazole are known to be monomeric, regardless of the concentration of base. [19]

While it is difficult to speculate as to the exact structural nature of the catalytic active species the identity of the neutral ligand has structural consequences. From the data presented above it seems likely that to enhance the activity of the zinc crotonate centre further, a coordinating amine base that does not form monomeric complexes in solution is necessary. Furthermore the observation that the proton sponge did not significantly increase the yield of FAME suggests that there is no simple synergic effect between the Lewis acid and the Brønsted base.

5.2.1.6 Effect of Sub-Stoichiometric Addition of Quinoline

As previously shown the activity of the zinc crotonate solution containing 1 equivalent and 0.67 equivalents are almost identical. Further experiments into the effect of quinoline concentration were undertaken; the results are shown below in Fig. 5.9

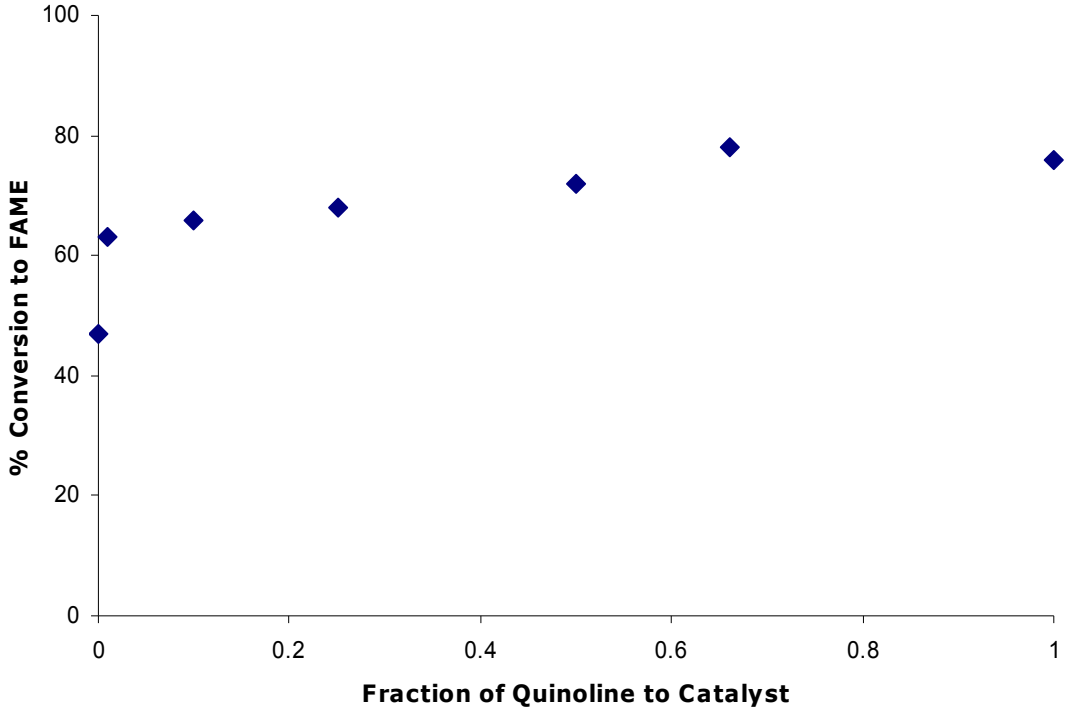

Figure 5.9 Effect of the concentration of quinoline on the zinc crotonate catalysed conversion of FAME

The addition of just 1 mol % of quinoline relative to the zinc crotonate is enough to raise the conversion of glyceride to FAME significantly. The activity increases roughly linearly until reaching the maximum at between 67 and 100 mol %.

In an attempt to further understand the effect that quinoline has, and therefore to propose a model to explain the behaviour of these homogeneous zinc carboxylate catalysts, zinc crotonate systems were used as catalysts on a pilot industrial scale equipped with a sampling port.

5.2.2 Catalytic Conversion on a Pilot Industrial Scale

The catalytic screening was performed using rapeseed oil with a FFA acid content of 0.56%, the catalyst (1 mol%) and methanol (6 equivalents). This testing was done on a scale over 10x larger than that of the laboratory testing so far described. The reactor contained a sampling port and measurements of the levels of the tri-, di- and monoglycerides as well as the FAME produced could be examined over time. The degree of transesterification was determined using HPLC.

The first set of reactions were undertaken at 150 °C. For the first run the zinc crotonate was suspended in the vegetable oil, this was then heated to the reaction temperature and the methanol added via a Gilson pump. The second and third catalytic runs were undertaken under the same conditions, except with triethylamine and quinoline added to the vegetable oil prior to heating. The fourth run was undertaken by dissolving zinc crotonate and quinoline in methanol and adding this solution to the vegetable oil, when the oil had reached the reaction temperature. The results are shown below in Fig. 5.10.

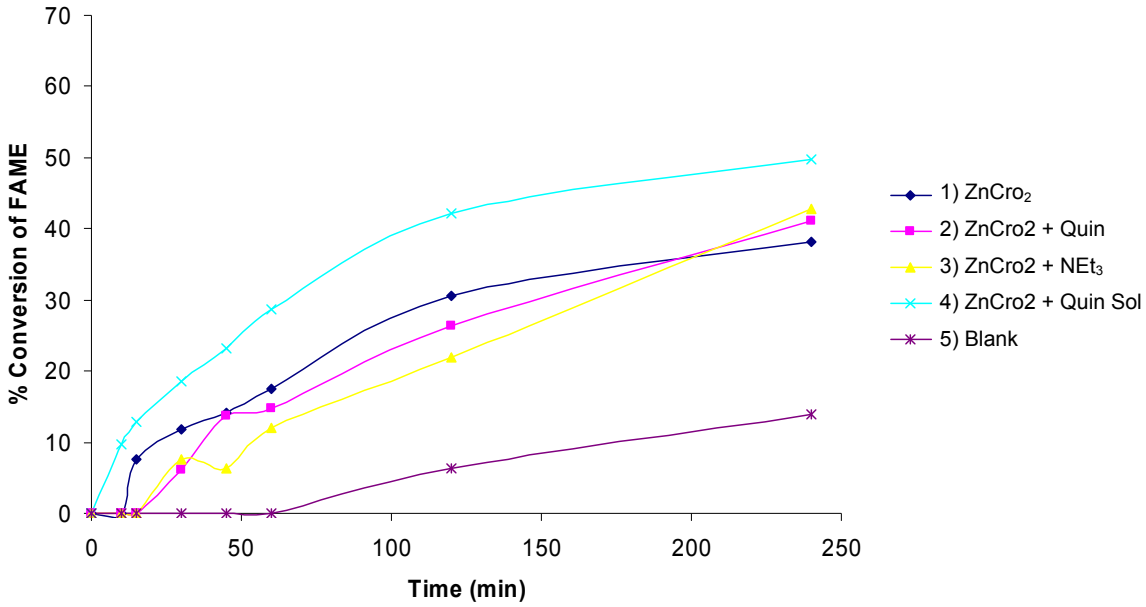

Figure 5.10 Catalytic results for the conversion of rapeseed oil to FAME using various zinc crotonate catalysts

An increase in the activity of the catalyst is observed when using an amine base originally dissolved in the alcohol. This rise in activity over zinc crotonate is not observed when the catalyst and the amine are added to the oil prior to heating.

In the second series of testing, the zinc crotonate was dissolved in the methanol before the reaction. A series of tests were untaken to examine the catalytic activity of the zinc crotonate when different concentrations of quinoline were used, these reactions were run at 200 °C (Fig. 5.11).

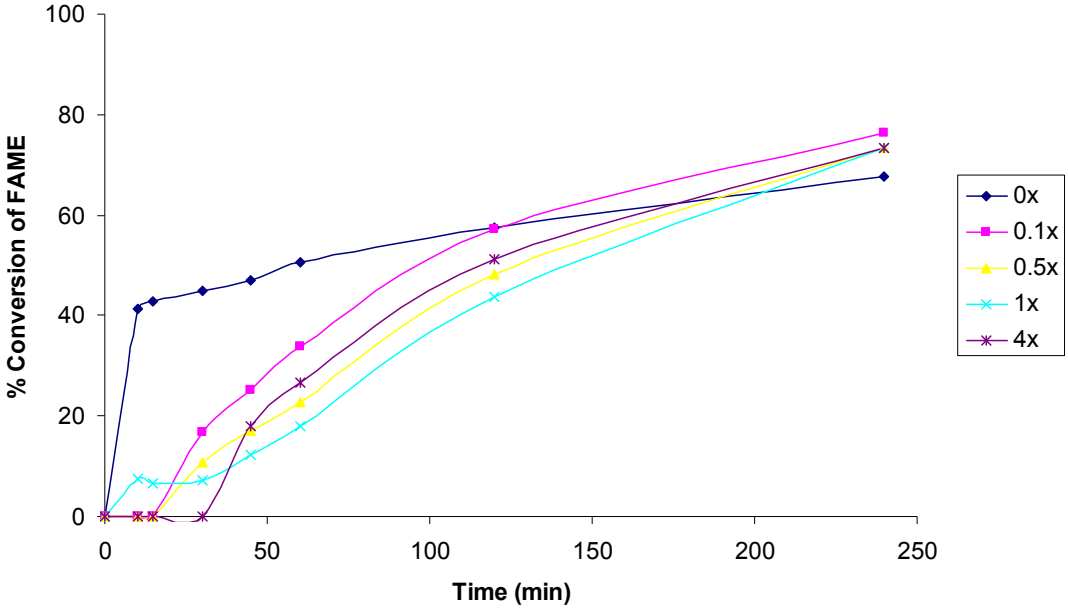

Figure 5.11 FAME yields for zinc crotonate catalysed conversion of rapeseed oil, using differing concentrations of quinoline (molar equiv. to the catalyst)

The overall conversion of rapeseed oil over four hours is lower for the zinc crotonate catalysed reaction where quinoline is not used. However, if quinoline is added to the reaction mixture then the final yield of FAME is higher, irrespective of the volume of quinoline. More detailed plots of the zinc crotonate catalysed reaction with and without quinoline are given below in Fig. 5.12 and 5.13.

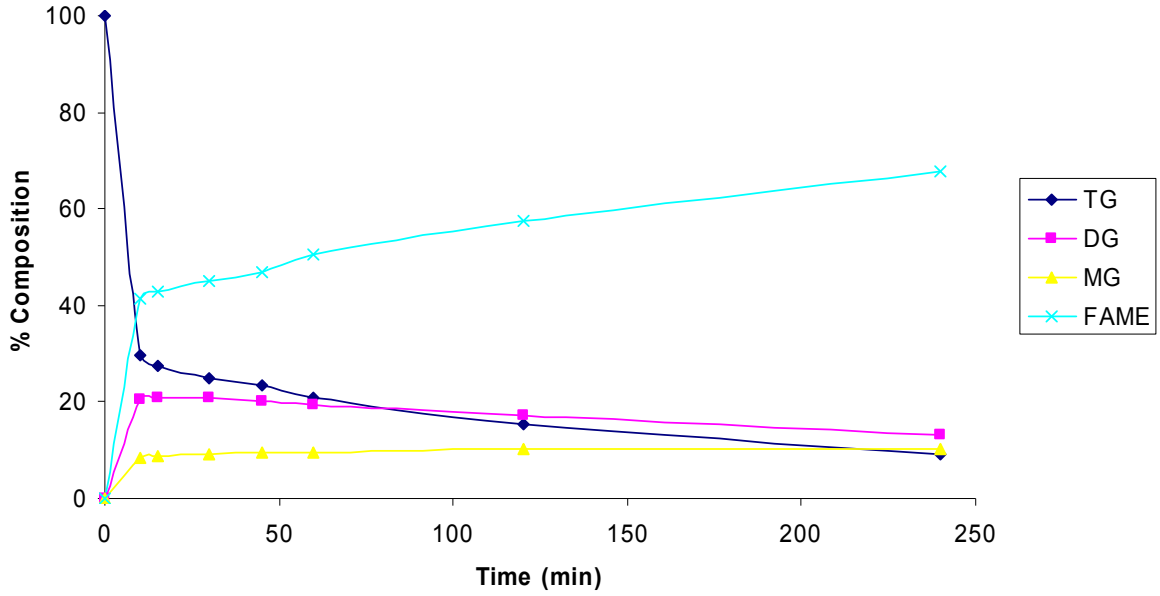

Figure 5.12 Yield of the glycerides and FAME produced in the zinc crotonate catalysed conversion of rapeseed oil.

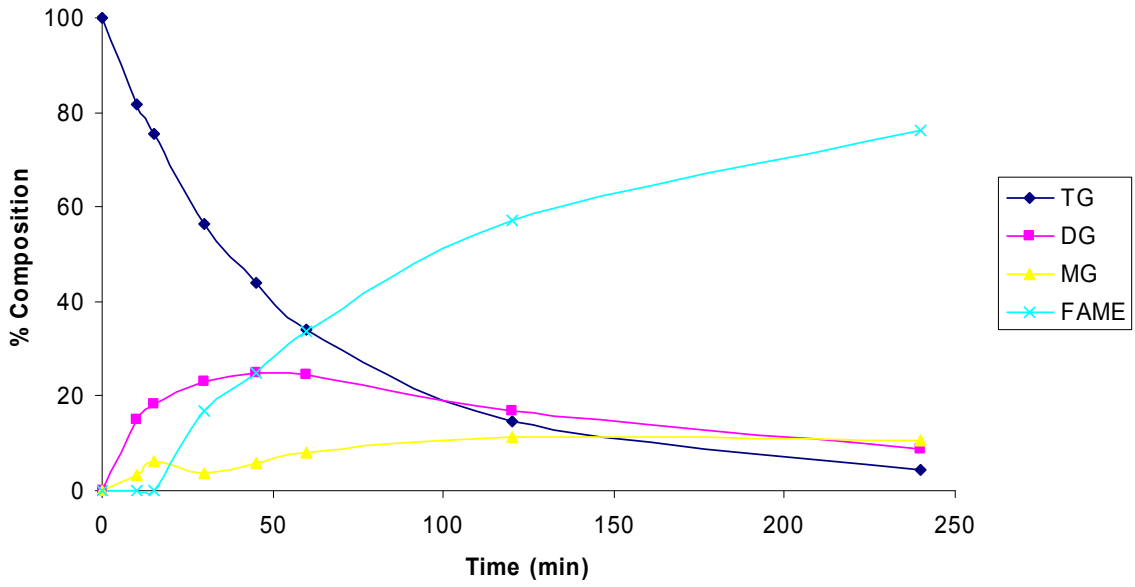

Figure 5.13 Yield of the glycerides and FAME produced for the zinc crotonate catalysed conversion of rapeseed oil after the addition of 0.1 molar equivalents of quinoline

In the zinc crotonate catalysed transesterification a large initial rate of reaction was observed. After ten minutes over 70% of the triglycerides have been converted, however the zinc crotonate is deactivated to some extent and the conversion of di- and monoglyceride molecules decreases only slightly. The monoglyceride concentration rises slightly during this time. After a further 3 hours and 50 minutes reaction time the FAME concentration has risen by a half of the concentration achieved in the first ten minutes.

On the addition of quinoline to the catalyst-methanol solution the conversion of FAME is markedly different. The triglyceride concentration is reduced gently and steadily throughout the reaction time. However, the di- and monoglyceride are also steadily converted and the eventual yield of FAME is significantly higher when using quinoline along side the carboxylate catalyst.

The zinc crotonate catalyst is selective for the conversion of triglycerides to FAME. When quinoline is added to the methanol catalyst solution the rate of this reaction is significantly slowed. The base seems to inhibit the formation of FAME from triglycerides to some extent, yet also inhibits the formation of an inactive glyceride zinc system. In this manner the judicious use of quinoline under these reaction conditions allows the controlled conversion of rapeseed oil and the eventual overall yield of FAME is higher than that of using zinc crotonate alone.

In light of these results the zinc crotonate-quinoline system was deemed to be a potential industrial catalyst for the conversion of vegetable oil to biodiesel. However, as previously discussed in Chapter 1, few potential biodiesel catalysts for the conversion of waste oils have been reported. Further testing was done on a laboratory scale to evaluate the activity of the catalyst in converting model waste oils.

5.2.3 Catalytic Conversion of Model Waste Oil

Measured amounts of stearic acid (as a model for the various FFA present in waste oils) and water were added to the vegetable oil to simulate a lower quality feedstock. The following catalytic results were obtained at 195 ºC over 2 hours with a catalyst loading of 2.5 mol%. Soybean oil was used with a methanol ratio of 12:1. The same experimental procedure employed is detailed in Chapter 2, Section 2.2.2.

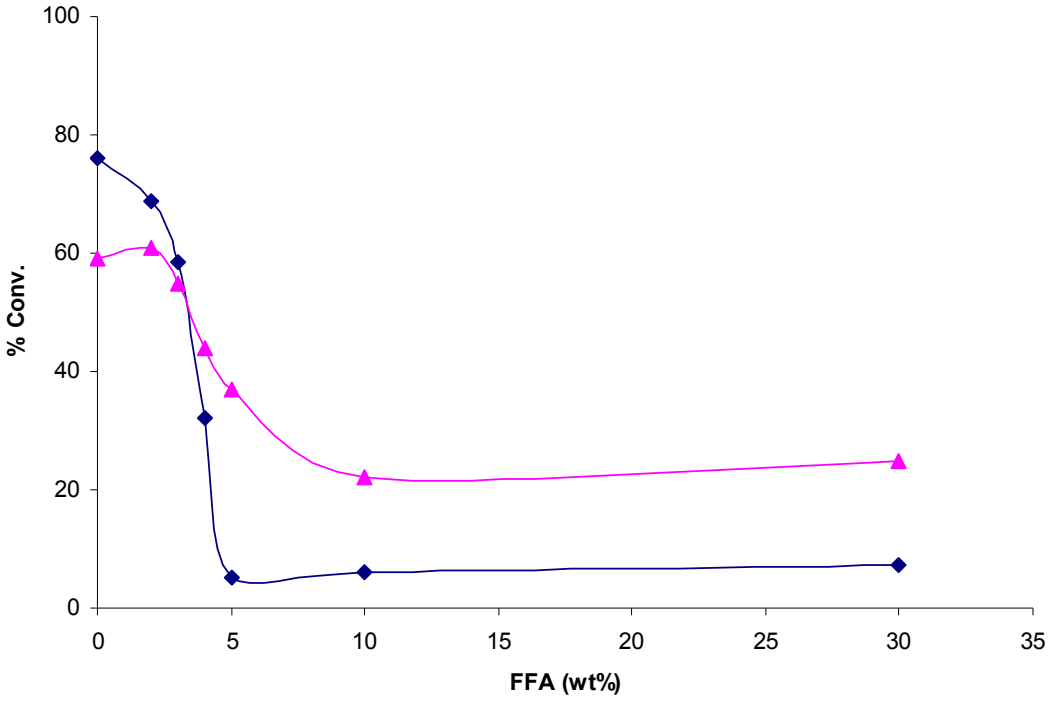

Figure 5.14 The effect of FFA concentration on the zinc crotonate quinoline (blue) and zinc stearate (pink) catalysed conversion of FAME

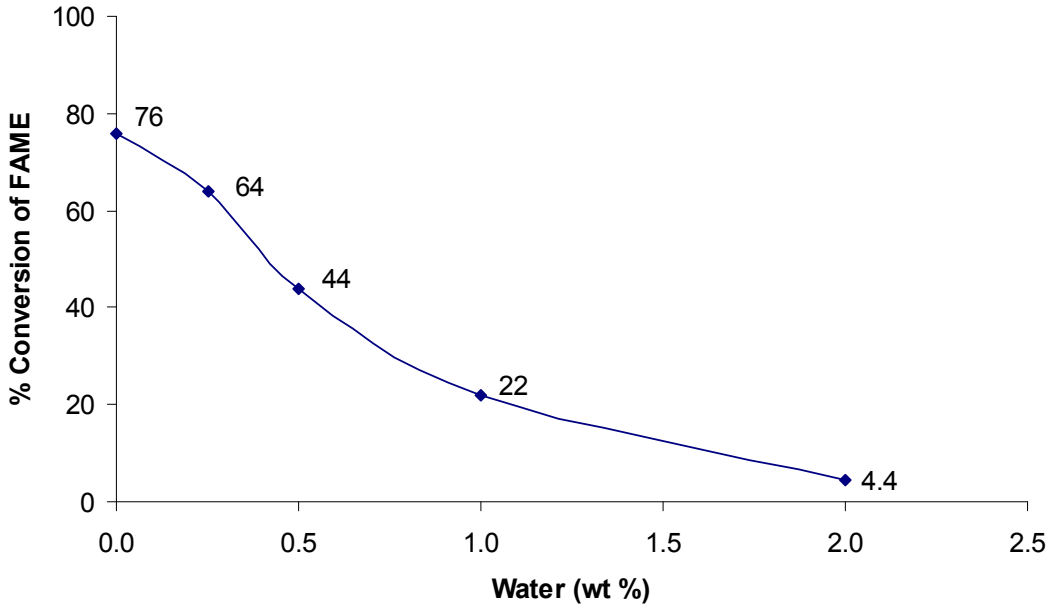

Figure 5.15 The effect of water on the conversion of FAME while using zinc crotonate quinoline as a catalyst

The addition of FFA to the biodiesel reaction deactivates the zinc crotonate catalyst. When 5 wt% (6 mmol) FFA has been added the catalyst is almost completely deactivated. Di Serio et al. observed a similar result on using metal acetates. Reasoning that the esterification reaction of the FFA is preferential and the resulting water deactivates the catalyst due to the formation of zinc hydroxide.

The activity of the two catalysts does not follow the same reaction path on addition of FFA to the vegetable oil. And it is therefore unlikely that the stearic acid is reacting with the zinc crotonate to form zinc stearate.

The additional water clearly affects the conversion of FAME, with up to 2 wt% (~40 mmol) being enough to completely deactivate the catalyst system. The additional FFA and water, either generated by the esterification, or inherent in the oil itself is enough to completely deactivate the zinc crotonate quinoline catalyst.

5.2.4 Proposed Model For Vegetable Oil Transesterification Using Zinc Crotonate

In this section a mechanism is proposed for the zinc crotonate catalysed reaction based on the results presented above. The general physical conditions in the biodiesel reaction are described in more detail in Chapter 1, Section 1.4.

For the zinc crotonate catalysed reaction, prior to the onset of catalysis, the reaction mixture is biphasic with a hydrophobic layer containing the triglyceride and a hydrophilic layer containing the methanol and catalyst (Fig. 5.16). Assuming the catalyst is not present in the triglyceride layer, as unlike zinc stearate the zinc crotonate is highly soluble in methanol but not soluble in vegetable oil, the initial rate of reaction will be slow. However, on reaction of the triglyceride, one equivalent of FAME and diglyceride are formed. Diglyceride has been shown to form a *pseudo* homogeneous layer with the methanol. [29, 30] An additional factor to consider here is potential ligand exchange between diglyceride and carboxylate (Fig. 5.16 A).

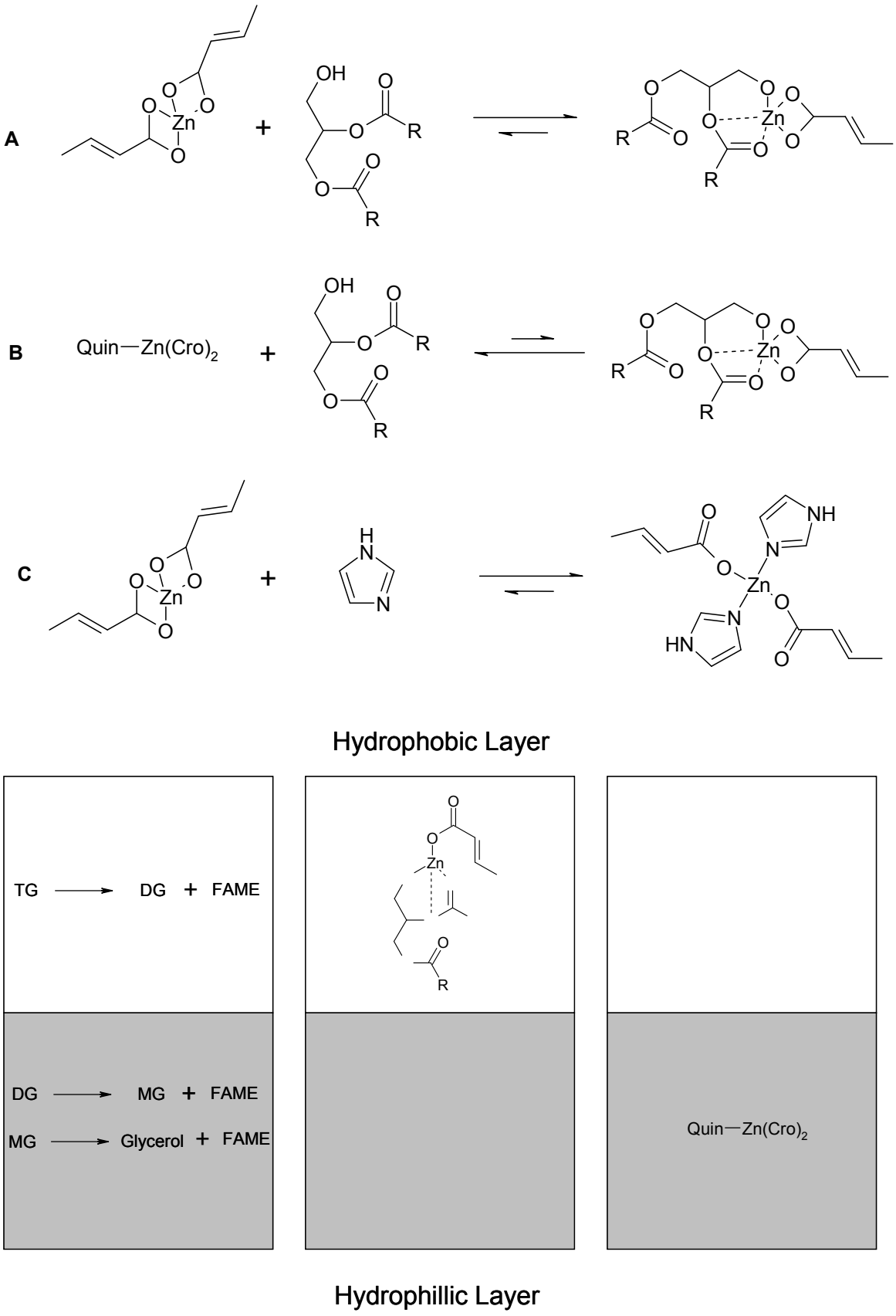

Figure 5.16 Possible equilibrium reactions involved in the zinc crotonate catalysed conversion of vegetable oils in both the lipid (white) and methanol soluble (grey) phases

If such a ligand exchange takes place it would partition the metal into the triglyceride layer, enhancing the transesterification of the triglyceride. This would explain the similar conversions of FAME from the zinc stearate and zinc crotonate catalysed reactions (Fig. 5.5). Once the triglyceride content has been depleted, the conversion of FAME will slow considerably as the catalyst will not be in contact with the other glyceride species. This selectivity to converting triglycerides over the di- and monoglycerides is observed for the zinc crotonate catalysed reaction (Fig 5.12).

On addition of quinoline to the reaction the equilibrium is shifted to the production of the zinc carboxylate-quinoline species, which is highly soluble in methanol (Fig. 5.16 B). Therefore the rate of reaction for the conversion of triglyceride is reduced, however, the conversion of di- and monoglyceride is now favoured. The slow conversion of the triglyceride was observed on the pilot scale testing rig (Fig 5.13).

Chisholm et al. reported an analogous effect in the copolymerisation of propylene oxide and carbon dioxide. A mechanistic study of the insertion of CO_2 into the aluminium alkoxide (TPP)Al-O$(CH_2)_9CH_3$ was undertaken. On addition of DMAP, the equilibrium is shifted markedly to the right. At high concentrations of base, the carbonate was almost completely formed. [31]

In Section 5.1.3, water (either generated from FFA esterification or present in the feedstock), was shown to deactivate the zinc crotonate quinoline system. A similar level of deactivation was not observed when using zinc stearate. The zinc stearate is presumably in the hydrophobic layer and therefore is not as prone to hydrolysis as the zinc crotonate quinoline complex, which is in the hydrophilic layer.

As the zinc crotonate-quinoline complex is not the active species, and only drives the equilibrium towards the creation of the zinc carboxylate, only a sub-stoichiometric amount of Lewis base is needed. This was observed on both the laboratory and pilot scale testing. However, if a stable zinc amine complex is produced instead of the seemingly active paddle like structure, then the activity would also be diminished (Fig. 5.16 C).

5.3 SUMMARY

In this chapter a number of zinc carboxylates were investigated as catalysts in the transesterification of vegetable and waste oils. Zinc crotonate was found to be the most active catalyst in the series, under the reaction conditions, converting over 78% of the glycerides to FAME over two hours. Judicious use of quinoline in a methanolic solution of zinc crotonate enhanced this activity further.

On further experimentation it was revealed that the initial rate of conversion when using zinc crotonate as a catalyst is very high and most of the triglyceride is converted to the diglyceride and FAME in the first minutes of the reaction. The production of these glycerides deactivates the catalyst and the rate of reaction slows dramatically. On addition of quinoline to the zinc crotonate the initial rate of reaction is much slower but the production of di and mono-glycerides has no noticeable effect on the initial rate.

A tentative model was put forward in an attempt to explain this difference in activity. The reaction of zinc crotonate with the partially reacted glycerides would form a highly hydrophobic species. This would therefore be active towards conversion of the triglyceride yet show a greatly reduced activity in converting the di and mono-glycerides to FAME. On addition of base, the formation of the zinc-glyceride species becomes unfavourable and as the catalyst is no longer in the lipid layer, the rate of the triglyceride conversion is dramatically slowed, the conversion of di- and monoglycerides is now favoured.

None of the catalysts tested were resistant to FFA or water in the reaction medium and unlike zinc proline, would not be suitable for the production of FAME from lower quality feedstocks.

5.4 REFERENCES

1. G. W. Parshall and S. D. Ittel, *Homogeneous Catalysis: The Applications and Chemistry of Catalysis by Soluble Transition Metal Complexes*, Wiley, 1992.
2. G. Bartoli, M. Bosco, A. Carlone, R. Dalpozzo, M. Locatelli, P. Melchiorre, P. Palazzi and L. Sambri, *Synthetic Letters*, 2006, 2104-2108.
3. A. Macierzanka and H. Szelag, *Industrial & Engineering Chemistry Research*, 2004, **43**, 7744-7753.
4. V. Vargha and P. Truter, *European Polymer Journal*, 2005, **41**, 715-726.
5. S. Bhatia, A. L. Ahmad, A. R. Mohamed and S. Y. Chin, *Chemical Engineering Science*, 2006, **61**, 7436-7447.
6. M. Di Serio, R. Tesser, M. Dimiccoli, F. Cammarota, M. Nastasi and E. Santacesaria, *Journal of Molecular Catalysis A-Chemical*, 2005, **239**, 111-115.
7. S. Y. Chin, A. L. Ahmad, A. R. Mohamed and S. Bhatia, *Applied Catalysis A-General*, 2006, **297**, 8-17.
8. W. Clegg, I. R. Little and B. R. Straughan, *Acta Crystallographica Section C-Crystal Structure Communications*, 1987, **43**, 456-457.
9. W. Clegg, I. R. Little and B. R. Straughan, *Acta Crystallographica Section C-Crystal Structure Communications*, 1986, **42**, 1701-1703.
10. J. Blair, R. A. Howie and J. L. Wardell, *Acta Crystallographica Section C-Crystal Structure Communications*, 1993, **49**, 219-221.
11. P. Segedin, N. Lah, M. Zefran, I. Leban and L. Golic, *Acta Chimica*, 1999, **46**, 172-184.
12. F. Lacouture, J. Peultier, M. Francois and J. Steinmetz, *Acta Crystallographica Section C-Crystal Structure Communications*, 2000, **56**, 556-557.
13. W. Clegg, I. R. Little and B. P. Straughan, *Acta Crystallographica Section C-Crystal Structure Communications*, 1986, **42**, 919-920.
14. W. Clegg, I. R. Little and B. P. Straughan, *Inorganic Chemistry*, 1988, **27**, 1916-1923.
15. W. Clegg, I. R. Little and B. P. Straughan, *Journal of the Chemical Society-Dalton Transactions*, 1986, 1283-1288.

16. J. C. Noveron, M. Soo Lah, R. E. Del Sesto, A. M. Arif, J. S. Miller and P. J. Stang, *Journal of the American Chemical Society*, 2002, **124**, 6613-6625.
17. Q. Wu, J. A. Lavigne, Y. Tao, M. D'Iorio. and S. Wang, *Inorganic Chemistry*, 2000, **39**, 5248-5254.
18. W. D. Horrocks, J. N. Ishley and R. R. Whittle, *Inorganic Chemistry*, 1982, **21**, 3265-3269.
19. D. A. Brown, N. J. Fitzpatrick, H. Muller-Bunz and A. T. Ryan, *Inorganic Chemistry*, 2006, **45**, 4497-4507.
20. S. E. Nefedov, *Russian Chemical Bulletin*, 2004, **53**, 259-261.
21. I. L. Eremenko, S. E. Nefedov, A. A. Sidorov, M. A. Golubnichaya, P. V. Danilov, V. N. Ikorskii, Y. G. Shvedenkov, V. M. Novotortsev and I. I. Moiseev, *Inorganic Chemistry*, 1999, **38**, 3764-3773.
22. M. Mikuriya, H. Azuma, R. Nukada and M. Handa, *Chemistry Letters*, 1999, 57-58.
23. M. Ebihara, M. Nomura, S. Sakai and T. Kawamura, *Inorganica Chimica Acta*, 2007, **360**, 2345-2352.
24. H. N. Basu, M. E. Norris, *United States Pat.*, US 5525126, 1996.
25. M. Di Serio, E. Santacesaria, *Italian Pat.*, ITMI2004A001323, 2004.
26. F. R. Abreu, D. G. Lima, E. H. Hamu, S. Einloft, J. C. Rubim and P. A. Z. Suarez, *Journal of the American Oil Chemists Society*, 2003, **80**, 601-604.
27. M. Lunn and B. Zwinjenburg, *Personal Communication*, Johnson Matthey Catalysts, 2004.
28. A. M. Florea and D. Busselberg, *Biometals*, 2006, **19**, 419-427.
29. G. Vicente, M. Martinez, J. Aracil and A. Esteban, *Industrial & Engineering Chemistry Research*, 2005, **44**, 5447-5454.
30. S. Gryglewicz, *Bioresource Technology*, 1999, **70**, 249-253.
31. M. H. Chisholm and Z. Zhou, *Journal of the American Chemical Society*, 2004, **126**, 11030-11039.

CHAPTER 6

CONCLUSIONS AND FURTHER RESEARCH

In the following chapter the work presented in the body of the thesis is summarised and some conclusions presented. Possible further research to supplement this investigation is also suggested

6.1 CONCLUSIONS

In this body of work a range of potential Lewis acid transesterification catalysts have been synthesised and characterised. These catalysts were then tested for their activity in the conversion of soybean oil and model waste oils into biodiesel.

It was found that homoleptic titanium alkoxides are possible catalysts in the conversion of soybean oil with methanol. However, on addition of the catalyst to the methanol, titanium methoxide is irreversibly formed; this complex has a greatly reduced activity than the original titanium species. The titanium alkoxide can be stabilised against this by the judicious use of a diol ligand to give a heteroleptic titanium species. This titanium species, though highly active in the conversion of virgin soybean oil, is not stable to titanium carboxylate or titanium dioxide formation on the addition of FFA or water respectively.

Further stability of the titanium alkoxide centre was sort and a range of homo- and heterometallic titanium citrate complexes were synthesised. These complexes were highly variable species and were all stable to hydrolysis. This increased stability was in part due to the creation of three five membered rings and a large increase in steric bulk around the titanium centre. All the complexes formed were heavily hydrated and coupled with the stable bonding motif meant that they are not suitable as catalysts in the industrial production of biodiesel.

Amino acids are also excellent chelating ligands and a range of titanium derived species were synthesised. All of these species formed were prone to hydrolysis and methanolysis and are not industrially suitable for the conversion of vegetable oil.

However, the stability of these complexes was enhanced by modification of the amino acid ligand to form an amino acid bisphenolate derivative. The titanium as well as germanium adducts of these ligands were shown to be highly active in the conversion of vegetable oil but it was thought that the cost of the ligand synthesis was prohibitive for these complexes to be industrially viable.

A range of moisture stable zinc amino acids were also synthesised from a range of amino acids and zinc acetate. All of these complexes were insoluble in both methanol and vegetable oil. However, zinc proline was found to be highly active in the conversion of soybean oil on both a laboratory scale process and pilot industrial process. The activity of the zinc proline catalyst could be improved by the addition of water or FFA and demonstrates that zinc proline is a potential precatalyst for the industrial conversion of waste oils to FAME.

Zinc acetate and stearate have been investigated previously as possible biodiesel catalysts. However, in this study zinc crotonate was shown to be more active, the use of quinoline in a methanolic solution of zinc crotonate enhanced this activity even further. Testing carried out on an industrial pilot scale suggested that the quinoline binds to the zinc crotonate making the zinc species soluble in the partially esterified glyceride layer. This reduces the initial rate of reaction, however, over a period of four hours the overall yield of FAME is higher. None of the homogeneous zinc carboxylate catalysts tested continued to be as active in the presence of FFA or water in the reaction medium and unlike zinc proline, would not be suitable for the production of FAME from lower quality feedstocks.

6.2 FURTHER WORK

In this body of work titanium alkoxides were shown to have potential in the transesterification of vegetable oils, however, without expensive ligand modification there seems little hope of the titanium catalyst being robust enough to convert waste oils at an industrially acceptable temperature and pressure.

The zinc catalysts presented in both Chapters 4 and 5, on the other hand, are highly active in the conversion of vegetable oil and in the case of zinc proline demonstrate an increased water and FFA stability. A further study in to the optimisation of the conditions would be vital before this catalyst could be used for the industrial

synthesis of biodiesel. It is also remarkable that the catalytic activity of the zinc proline catalyst is increased on addition (or generation) of water. An attempt to isolate any intermediate species would give a unique insight into the activity of zinc carboxylates in the transesterification reaction.

A tentative model for the conversion of biodiesel by homogeneous Lewis acid catalysts was presented at the end of Chapter 5. This model, if validated with further experimental evidence, would provide an unprecedented insight into the conversion of vegetable oils, paving the way to new catalyst design.

CHAPTER 7

EXPERIMENTAL

7.1 GENERAL EXPERIMENTAL TECHNIQUES

7.1.1 GENERAL PROCEDURES

All starting materials except where otherwise stated were purchased from Aldrich, Lancaster, Fisher or Strem and were used without further purification. The vegetable oil used was Soyola soybean oil and was used with no pre-treatment with reagent grade methanol. Where appropriate the reactions and manipulations were carried out under a dry, oxygen free argon atmosphere using standard Schlenk line techniques.

7.1.2 NMR SPECTROSCOPY

Standard ^{1}H NMR spectra were recorded using a Bruker 250, Bruker Advance 300 NMR or Bruker 400 NMR spectrometer. ^{13}C NMR spectra were recorded on the same spectrometers. NMR samples were prepared by using 20+ mg of sample dissolved in a suitable deuterated solvent and referenced to the appropriate residual solvent peak.

7.1.3 FT-IR SPECTROSCOPY

The IR spectra were either collected using KBr plates with nujol mull or KBr pressed discs were made where appropriate, the data were collected on a Nicolet-Nexus FT-IR spectrometer.

7.1.4 Mass Spectrometry

For aqueous or methanol soluble solutions a micrOTOF electrospray time-of-flight (ESI-TOF) mass spectrometer was used; this was coupled to an Agilent 1200 LC system as an autosampler. 10 μL of sample was injected into a 30:70 flow of water:acetonitrile at 0.3 mL/min to the mass spectrometer. 10 uL of 5 mM sodium formate was injected after the sample. This acted as a calibrant over the mass range 50-1500 m/z. The observed mass and isotope pattern perfectly matched the corresponding theoretical values as calculated from the expected elemental formula.

For air sensitive samples solubilised in DCM, a micrOTOFQ electrospray quadrupole time-of-flight (ESI-QTOF) mass spectrometer was used; this was coupled to a syringe driver situated inside a glove box under Argon. An opening through the side of the glove box allows for the PEEK tubing from the syringe pump to pass through to the mass spectrometer without any interaction with air or moisture. The sample was infused at a rate of 10 uL/min. The instrument was calibrated using a range of tertiary ammonium bromine salts to achieve accurate mass. The observed mass and isotope pattern perfectly matched the corresponding theoretical values as calculated from the expected elemental formula.

7.1.5 Microanalysis

All CHN elemental analysis was performed by Alan Carver at the Department of Chemistry, University of Bath on a CE-440 Elemental Analyser. The ICP-OES measurements were completed by Medac Ltd.

7.1.6 Melting Point

The samples were analyzed using a Griffin variable heat melting point machine, capable of recording temperatures of up to 250 °C.

7.1.7 X-RAY DIFFRACTOMETRY

X-ray crystallography data was obtained using the Nornius 3-circle diffractometer with a xyz area detector using graphite monochromated kappa CCD Mo-Kα radiation (λ=0.71073) at 150K unless otherwise stated. Suitable single crystals (from 0.1x 0.1x 0.1mm^3 to 0.5x 0.5x 0.5mm^3) were coated with a perfluorinated ether oil. This is inert to air and the crystals were mounted onto the goniometer by using a glass fibre. This was frozen by a stream of cold nitrogen gas to prevent decomposition and to fix the orientation of crystal. The refinement method used was Full-matrix least-squares on F^2.

The solid state structure of complex **18** was obtained as Daresbury using a Synchrotron X-ray radiation source (λ=0.69070). The crystal was cooled to 28K using a Helix cryostream prior to the experiment.

7.1.8 POWDER X-RAY DIFFRACTOMETRY

pXRD measurements were performed on a Bruker DX axes diffractometer, with a step of 0.050 ° and step time of 5 s.

7.1.9 EXPERIMENTAL PROCEDURES FOR CATALYST TESTING

7.1.9.1 Small Scale Catalytic Testing, Analyzed by ^{1}H NMR

Soybean Oil (36.8 ml, 40 mmol) and MeOH (19.5 ml, 480 mmol) were placed in a 120 ml autoclave. The catalyst (2.5 mol %) was added, the autoclave sealed and placed in a graphite bath, the mixture was then heated to temperature, t=0 was taken when the graphite bath had reached that. The mixture was mechanically stirred throughout the experiment. After 120 minutes the autoclave was submerged in water and opened when the pressure had reached atmospheric. The reaction mixture was added to water and shaken vigorously. The top layer (FAME and remaining vegetable oil) was dissolved in $CDCl_3$ and analysed by ^{1}H NMR spectroscopy. The yield of FAME was calculated by taking the integral value of the methoxy group of the FAME against the remaining proton signals adjacent to the glycerol backbone of the triglyceride. This method was

first reported by G. Knothe. [1] The yields calculated by ^{1}H NMR showed a deviation from the values calculated by HPLC of 3%. An example of a vegetable oil, FAME NMR spectrum is shown below in figure 6.1.

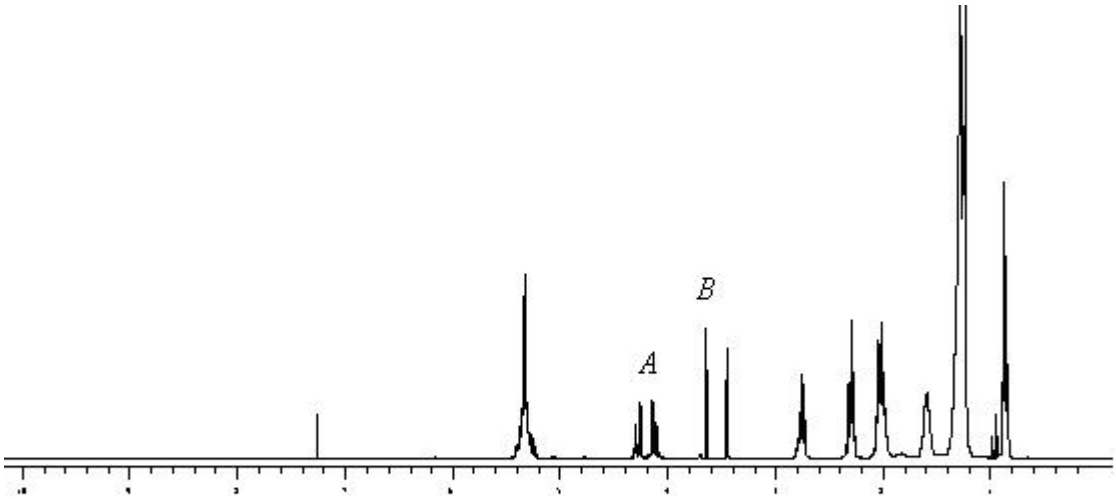

Figure 6.1, ^{1}H NMR spectra of the partially transesterified soybean oil. The plot shows the glyceride (A) and FAME (B) peaks

7.1.9.2 Large Scale Catalytic Testing, Analysis by HPLC

The catalytic screening was performed in a large glass vial inside a stainless steel reactor equipped with an automatic stirrer set to 300 rpm. The reaction was carried out using rapeseed oil (330g, 0.375 mols) with a FFA acid content of 0.56%. The reactor was then sealed and purged three times with N_2 gas, after this the vessel was left with an internal pressure of 10 bar. The temperature was raised to 20 °C above the starting temperature and the methanol (72g, 2.25 mols) was added automatically over two minutes via a Gilson pump. The temperature was steadied at the set temperature. The point at which the Gilson pump was started was taken as t=0. The temperature and pressure were recorded at regular intervals. The FAME yields, in the catalytic tests, were determined using HPLC.

The FAME yields, in the catalytic tests, were determined using HPLC. The samples were diluted to 100 mL with THF (HPLC grade). A 1 ml aliquot was then transferred through a filter into a HPLC vial. The following samples were then analyzed over 45 minutes on a Waters HPLC 2690 HPLC machine and the data analyzed using

Run Samples version 3.20. An example of the HPLC chromatograph is shown below in Fig. 6.2.

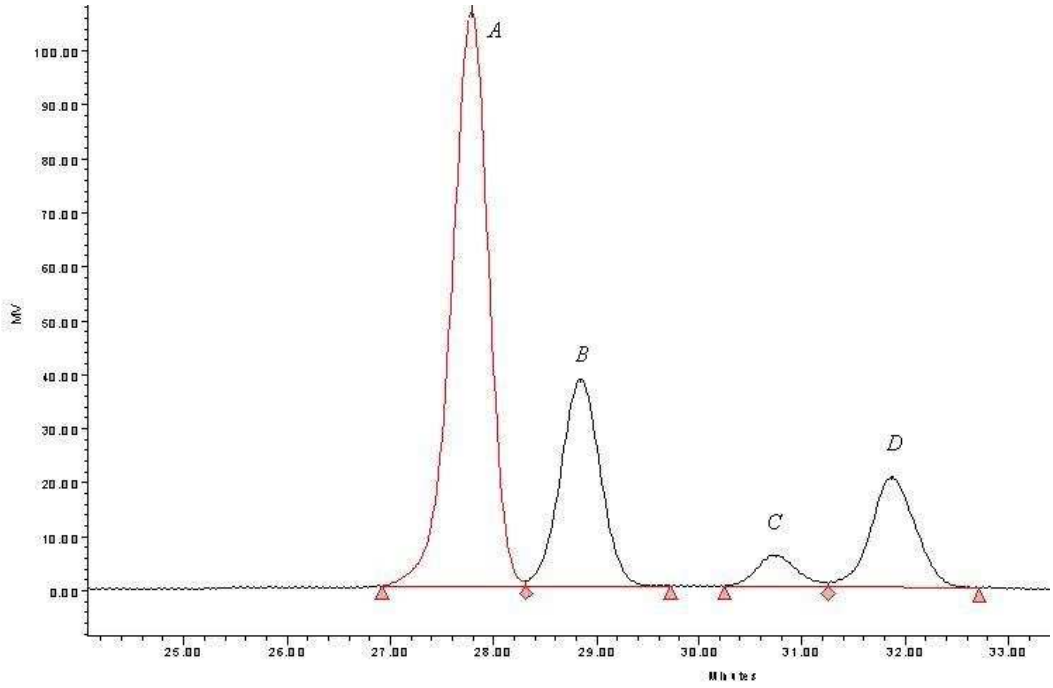

Figure 6.2 HPLC chromatogragh of the partially transesterified rapeseed oil. The plot shows the triglyceride (A), diglyceride (B), monoglyceride (C) and FAME (D)

The peaks were calibrated against known concentrations of trioleate, dioleate and monoleate as well as oleic acid methyl ester. A UV detector was used in this HPLC experiment.

7.2 EXPERIMENTAL PROCEDURES FOR CHAPTER 2

7.2.1 Complex Synthesis and Characterisation

Titanium 1,4 Butanediol, $Ti_2(C_4H_8O_2)_3(C_4H_9O_2)_2$, (1)

1,4-butanediol (2.4 ml, 26.2 mmol) was added to $Ti(O^iPr)_4$ (2 ml, 6.6 mmol) in hexane (20 ml). CH_2Cl_2 (2 ml) was added and the solution stirred for 1 hr. After three days standing, clear crystals were obtained.

Yield 1.70 g, (96%). M.pt. 128-134 °C. Elemental analysis: Calcd for $C_{20}H_{42}O_{10}Ti_2$: C, 44.6; H, 7.86. Found: C, 44.6; H, 8.21. ^{1}H NMR (300 MHz, $CDCl_3$): 1.68 (4H, m, C$\underline{H}_2$), 3.70 (4H, m, C$\underline{H}_2$O). ^{13}C NMR (400 MHz, $CDCl_3$) 29.8 ($\underline{C}H_2$), 62.9 (O$\underline{C}H_2$).

Titanium (2*R*, 3*R*)-2,3-Butanediol, $Ti_3(C_4H_8O_2)_4(C_4H_9O_2)_4$, (2)

(2*R*,3*R*)-2,3-butanediol (0.48 ml, 5.24 mmol) was added to $Ti(O^iPr)_4$ (0.4 ml, 1.22 mmol) in hexane (5 ml). The solution was stirred for 1 hr and the volatiles removed. The product was recrystallised from hexane over 7 days at -4 °C yielding small cubic crystals suitable for X-ray diffraction, yield 0.263 g (70%).

Elemental analysis: Calcd for $C_{32}H_{68}O_{16}Ti_3$: C, 45.1; H, 8.04. Found: C, 44.0; H, 7.86. ^{1}H NMR (300 MHz, $CDCl_3$): 1.02 (18H, m, C$\underline{H}_3$), 1.09 (6H, d, J = 6.0 Hz, C$\underline{H}_3$), 1.16 (6H, d J = 6.0 Hz, C$\underline{H}_3$), 1.23 (6H, d, J = 6.0 Hz, C$\underline{H}_3$), 1.42 (6H, d J = 6.0 Hz, C$\underline{H}_3$),1.52 (6H, d, J = 6.0 Hz, C$\underline{H}_3$), 3.66 (4H, m, C$\underline{H}$O), 4.2 (4H, m, C$\underline{H}$O), 4.50 (8H, m, C$\underline{H}$O). ^{13}C NMR (300 MHz, $CDCl_3$) 19.3, 19.5, 19.6, 19.7 (two overlapping peaks), 20.1, 20.2, 20.5 ($\underline{C}H_3$), 75.7, 77.3, 82.3, 85.0, 86.7, 88.8, 90.4. 91.0 ($\underline{C}$HO).

Titanium 1,3-Propanediol, $Ti_4(C_3H_6O_2)_3(C_3H_7O)_{10}$, (3)

1,3-Propanediol (5.4 ml, 75 mmol) was added to a stirred solution of $Ti(O^iPr)_4$ (30 ml, 100 mmol) the mixture was stirred for 30 minutes and left to stand. After 2 hrs large, clear cubic crystals were observed.

Elemental analysis: Calcd for $C_{39}H_{88}O_{16}Ti_4$: C, 46.6; H, 8.83. Found: C, 46.0; H, 8.72. ^{1}H NMR (500 MHz, $CDCl_3$): 1.20-1.26 (60H, m, C<u>H</u>$_3$), 1.82-2.07 (6H, m, $CH_2C\underline{H}_2CH_2$), 4.04-5.16 (22H, m, C<u>H</u>, C<u>H</u>$_2$). ^{13}C NMR (300 MHz, $CDCl_3$) 26.4, 26.6, 26.9 (CH_3) 35.1, 35.4 (<u>C</u>H_2), 72.4, 73.4, 76.6, 77.9, 79.0 (<u>C</u>H_2OH).

Titanium 1,3-Propanediol THF Solutions

$Ti(O^iPr)_4$ (0.3 ml, 1 mmol) was added to THF (1 ml) and agitated, a variable amount of 1,3 propanediol was added followed by MeOH (19.5 ml). This solution was then added to the vegetable oil in the reaction vessel.

7.2.2 CRYSTAL DATA AND STRUCTURE REFINEMENTS FOR 1-3

Complex	**1**	**2**	**3**
Empirical formula	C_{20} H_{40} O_{10} Ti_2	C_{32} H_{68} O_{16} Ti_3	C_{39} H_{88} O_{16} Ti_4
Formula weight	536.32	852.56	1004.69
Temperature, K	150(2)	150(2)	173(2)
Crystal system	monoclinic	orthorhombic,	triclinic
Space group	$P2_1/n$	$P2_12_12_1$	P-1
Unit cell:			
a, Å	10.9910(2)	9.14900(10)	16.7670(2)
b, Å	9.2710(2)	16.13900(10)	18.8700(2)
c, Å	12.3350(2)	29.0140(3)	19.3650(2)
α, °	90	90	70.6300(10)
β, °	100.976(1)	90	70.3030(10)
γ, °	90	90	81.6900(1)
Volume, Å^3	1233.91(4)	4284.08(7)	5438.26(10)
Z	2	4	4
Calc. density, mg/m^3	1.444	1.322	1.227
Abs. coeff. mm^{-1}	0.697	0.608	0.623
F(000)	568	1816	2152
Crystal size, mm	0.25 x 0.25 x 0.13	0.22 x 0.15 x 0.10	
θ range, °	3.36 to 27.48	3.58 to 27.48	3.52 to 27.52
Limiting indices	-11<=h<=14, -11<=k<=12, -15<=l<=15	-11<=h<=11, -20<=k<=20, -37<=l<=36	21<=h<=21, -24<=k<=24, -25<=l<=23
Reflections collected / unique	11202 / 2803 [R(int) = 0.0329]	68883 / 9766 [R(int) = 0.0572]	95969 / 24760 [R(int) = 0.0347]
Completeness to θ	= 27.48, 99.4 %	= 27.48 , 99.4 %	= 27.52, 99.0 %
Max. and min. transmission	0.9149 and 0.8450	0.9417 and 0.8754	
Data / restraints / parameters	2803 / 0 / 145	9766 / 4 / 492	24760 / 0 / 1103
Goodness-of-fit on F^2	1.092	1.049	1.021
Final R indices [I>2σ(I)]	R_1 = 0.0307	R_1 = 0.0346	R_1 = 0.0437
	wR_2 = 0.0822	wR_2 = 0.0771	wR_2 = 0.1058
R indices (all data)	R_1 = 0.0351	R_1 = 0.0480	R_1 = 0.0598
	wR_2 = 0.0850	wR_2 = 0.0834	wR_2 = 0.1179
Largest diff. peak and hole, e/ Å^3	0.713 and -0.429	0.334 and -0.418	1.055 and -1.095

7.3 EXPERIMENTAL PROCEDURES FOR CHAPTER 3

7.3.1 Complex Synthesis and Characterisation

Titanium Citrate Solution

$Ti(O^iPr)_4$ (2.5 ml, 8 mmol) was added to an aqueous solution of citric acid (4.61 g, 24 mmol). This solution was refluxed for 24 hrs and the volatiles reduced. The solution was left to stir overnight.

^1H NMR (300 MHz, D_2O): 2.85 (2H, d, ^2J = 16.5 Hz, α,γ, C<u>H</u>), 2.99 (2H, d, ^2J = 16.5 Hz, α',γ', C<u>H</u>). HRMS (EI, m/z) calc for $C_6H_8O_7$ $[M-H]^-$ 191.0192; found 191.0197. Calc for $[Ti(C_6H_4O_7)(H_2O)]$ $[M-H]^-$ 252.9469; found 252.9464. Calc for $[Ti(C_6H_6O_7)_2]$ $[M-H]^-$ 426.9634; found 426.9634. Calc for $[Ti(C_6H_7O_7)_2(C_6H_6O_7)]$ $(M-H^+)$ 618.9904; found 618.9902.

1,5-Dimethyl Citrate Monohydrate, $C_8H_{12}O_8$, (DMCA)

This ligand was prepared using a modified literature procedure.[2] Citric acid (20.00 g, 104 mmol) was dissolved in methanol (200 mL) and conc. sulphuric acid added (3 ml). The mixture was refluxed for 2 hrs and then H_2O (200 mL) was added. An excess of calcium hydroxide was added and the solution filtered. The volatiles were removed and the solid recrystallised from a minimum amount of methanol yielding large rectangular, clear crystals. Yield 16.03 g (55%).

M.pt. 119-121°C. Elemental Analysis : Calcd for $C_8H_{12}O_8$: C, 40.3; H, 5.93. Found C, 40.3; H, 5.59. ^1H NMR (300 MHz, $CDCl_3$): 2.82 (2H, d, ^2J = 16.0 Hz, C<u>H</u>$_2$), 2.95 (2H, d, ^2J = 16.0 Hz, C<u>H</u>$_2$) 3.66 (6H, s, C<u>H</u>$_3$), 5.07 (br s, <u>H</u>$_2$O). ^{13}C NMR (300 MHz, D_2O): 43.8 (<u>C</u>H_2), 52.8 (^{t}<u>C</u>), 74.0 (O<u>C</u>H_3), 172.5 (H_3CO_2<u>C</u>), 177.2 (HOO<u>C</u>).

Titanium Dimethyl Citrate, $Ti(DMCA)(O^iPr)_2$, (4)

$Ti(O^iPr)_4$ (3 mL, 10 mmol) was added drop wise under argon to a solution of 1,4 dimethylcitrate monohydrate (2.85 g, 10 mmol) dissolved in 20 ml of dry toluene. The

reaction was stirred at RT for 2 hrs after which all the solvents were removed. The product was then recrystallised from a toluene and hexane mixture to yield 2.48 g (68%) of small, clear crystals.

Elemental analysis : Calcd for $C_{14}H_{24}O_9Ti$: C, 42.3; H, 5.70. Found C, 41.3; H, 5.94. ^{1}H NMR (300 MHz, $CDCl_3$): 3.03 (2H, d, ^2J = 16.0 Hz, C$\underline{H}_2$), 3.13 (2H, d, ^2J = 16.0 Hz, C$\underline{H}_2$) 3.67 (6H, s, C$\underline{H}_3$), 4.91 (2H, m, O^{i}Pr, C$\underline{H}$). ^{13}C NMR (300 MHz, D_2O): 24.2, 24.3, 25.1 (O^{i}Pr, $\underline{C}H_3$), 41.3 ($\underline{C}H_2$), 52.0 ($^t\underline{C}$), 64.3 (O^{i}Pr, O$\underline{C}$) 81.1 (O$\underline{C}H_3$), 172.0 ($H_3CO_2\underline{C}$), 177.7 (HOO$\underline{C}$).

Titanium Dimethyl Citrate, Ti(DMCA)$_2$, (5)

$Ti(O^iPr)_4$ (1.5 mL, 5 mmol) was added drop wise under argon to a solution of 1,4 dimethylcitrate hydrate (2.85 g, 10 mmol) dissolved in 20 ml of dry toluene. The reaction was stirred at RT for 2 hrs after which all the solvents were removed. The product was recovered from toluene and washed with hexane (20 mL) to give a fine white powder, 1.42 g (46%).

Elemental Analysis : Calcd for $C_{16}H_{20}O_{14}Ti$: C, 39.7; H, 4.16. Found C, 41.0; H, 4.87. ^{1}H NMR (300 MHz, MeOD): 2.85 (8H, m, C$\underline{H}_2$) 3.62 (12H, s, C$\underline{H}_3$). ^{13}C NMR (300 MHz, D_2O): 44.3 ($\underline{C}H_2$), 52.7 (^{t}C), 75.1 (O$\underline{C}H_3$), 172.1 ($H_3CO_2\underline{C}$), 175.6 (HOO$\underline{C}$). HRMS (EI, m/z) calc for $C_{16}H_{22}O_{14}Ti$ $[M+H]^+$ 485.0407; found 485.0404.

Titanium Sodium Citrate, $TiNa_2(C_6H_6O_7)_3 \cdot 10\ H_2O$, (6)

1 molar NaOH solution (24 ml, 24 mmol) was added to an aqueous solution of titanium citrate (8 mmol). The solution was stirred for 1 hr and the volatiles reduced. On standing over 48 hrs large, clear crystals formed.

Yield 4.02 g (60%), M.pt. 111-114°C (dec.). Elemental analysis : Calcd for $C_{36}H_{56}O_{63}Na_4Ti_2$: C, 25.5; H, 3.92. Found: C, 25.9; H, 3.78. ^{1}H NMR (300 MHz, D_2O): 2.60-2.88 (4H, m, α,γ,α',γ', C$\underline{H}$). ^{13}C NMR (300 MHz, D_2O): 43.9, 44.0 (-$\underline{C}H_2$), 88.9 (O-$\underline{C}$), 174.9 ($\underline{C}O_2$), 175.1 ($\underline{C}O_2$), 179.0 ($\underline{C}O_2$). HRMS (EI, m/z) calc for $TiNa_2(C_6H_6O_7)_3$ $[M-H]^-$ 618.9904; found 618.9902.

Titanium Nickel Citrate. $Ti_2Ni(C_6O_7H_{6.66})_6 \cdot 14\ H_2O$, (7)

Nickel Carbonate (1.00 g, 8 mmol) was added to the titanium citrate solutions (8 mmol) and refluxed over 24 hrs. The solution went emerald green on addition of the $NiCO_3$ complex, which when dissolved left a dark green, gelatinous solution. The product was left to crystallise, affording small cubic crystals.

Yield 0.64 g (12%) M.pt. 168 °C (dec.). Elemental analysis : Calcd for $C_{36}H_{68}O_{56}Ti_2Ni$: C, 27.9; H, 4.42. Found: C, 27.7; H, 4.53. ^{1}H NMR (300 MHz, D_2O): 2.45-3.22 (4H, m, C<u>H</u>).

Titanium Barium Citrate, $TiBa(C_6H_6O_7)_3$, (8)

Barium acetate (2.05 g, 8 mmol) was added to a solution of titanium citrate (8 mmol) and the solution was refluxed for 2 hrs until the barium acetate had been dissolved. A fine microcrystalline powder crashed out of solution on cooling.

Yield 3.23 g (44.2%), M.pt. 215 °C (dec.). Elemental analysis : Calcd for $C_{18}H_{28}O_{28}TiBa$: C, 25.5; H, 3.31. Found: C, 25.6; H, 3.31. ^{1}H NMR (300 MHz, D_2O): 2.58-2.89 (4H, m, α,γ,α',γ', C<u>H</u>). FT-IR: 3547 cm^{-1} (υ O-H, H_2O) 2921, 2854 cm^{-1} (υ C-H, CH_2), 1719 cm^{-1}, 1652 cm^{-1} (υ C=O). 1199 cm^{-1} (υ C-OH).

Titanium Tin Citrate, $TiSn(C_6H_6O_7)_3 \cdot 2HCl \cdot 3H_2O$, (9)

Sn(II)Cl_2 (1.52 g, 8 mmol) was added to the solution of titanium and citric acid and a dark, swamp green colour was observed. The mixture was stirred for a further 24 hrs and on evaporation of the solvent a green hydrated gel was left. The gel was found to have a pH between 0 and 1.

Yield 3.01g, M.pt. 149 °C (dec.). Elemental analysis : Calcd for $C_{18}H_{26}O_{24}Cl_2TiSn$: C, 25.0; H, 3.03. Found: C, 24.8; H, 2.78. ^{1}H NMR (300 MHz, D_2O): 2.56 (2H, d, ^2J = 16.0 Hz, C<u>H</u>$_2$), 2.74 (2H, d, ^2J = 16.0 Hz, C<u>H</u>$_2$). ^{13}C NMR (300 MHz, D_2O): 43.5 (-<u>C</u>H_2), 73.5 (<u>C</u>O), 173.6 (HOO<u>C</u>), 177.1 (O_2<u>C</u>). ^{119}Sn NMR (400 MHz, D_2O): -696.9 (Sn(II)). HRMS (EI, m/z) calc for $C_6H_8O_7$ $[M-H]^-$ 191.0192; found 191.0191. Calc for $[Sn(C_6H_6O_7)]$ $[M-H]^-$ 308.9047; found 308.9047. Calc for

$[Ti(C_6H_6O_7)_2]$ $[M-H]^-$ 426.9634; found 426.9632. Calc for $[Ti(C_6H_7O_7)_2(C_6H_6O_7)]$ $[M-H]^-$ 618.9904; found 618.9907. Calc for $[TiSn(C_6H_6O_7)_3]$ $[M-H]^-$ 736.8783; found 736.8784.

Titanium Aluminium Citrate glass, $TiAl(C_6H_6O_7)_2(C_6H_5O_7) \cdot 8H_2O$, (10)

Anhydrous Citric acid (4.61 g, 24 mmol) was dissolved in H_2O (30 ml). $Ti(O^iPr)_4$ (2.5 ml, 8 mmol) was added over the course of 10 min. with constant stirring. This solution was refluxed until all the precipitate had dissolved. The solvent was reduced by 75 % under vacuum, and the resulting viscous solution was left to stir overnight. Aluminium isopropoxide (8 mmol) was dissolved into the solution on stirring and turned the solution gunmetal blue. On slow evaporation of the solvent, a gel was formed of the same colour.

Yield 3.41 g (86%). Elemental analysis: Calcd for $C_{18}H_{33}O_{29}AlTi$: C, 27.4; H, 4.21. Found: C, 27.2; H, 3.74. ^{1}H NMR (300 MHz, D_2O): 2.42-2.79 (4H, m, C<u>H</u>). ^{13}C NMR (300 MHz, D_2O): 41.8, 42.6, 43.1, 43.6 (<u>C</u>H_2), 73.6, 73.7 (<u>C</u>O), 173.7, 174.0 (O_2<u>C</u>), 177.6, 179.3 (O(O)<u>C</u>). ^{27}Al NMR (400 MHz, D_2O): -0.52 (AlX_6/ sym.), 6.03 (AlX_6 / unsym.). HRMS (EI, m/z) calc for $[Al(C_6H_7O_7)(C_6H_6O_7)]$ $[M-H]^-$ 407.0043; found 407.0048. Calc for $[Ti(C_6H_6O_7)_2]$ $[M-H]^-$ 426.9634; found 426.9644. Calc for $[Al(C_6H_7O_7)_3]$ $[M-H]^-$ 599.0313; found 599.0318. Calc for $[Ti(C_6H_7O_7)_2(C_6H_6O_7)]$ $[M-H]^-$ 618.9904; found 618.9904.

Zinc Citrate, $Zn_3(C_6H_5O_7)_2 \cdot 14H_2O$, (11)

Zinc acetate dihydrate (4.39 g, 24 mmol) was added to the solution of titanium and citric acid and the mixture was refluxed for 48 hrs on which the solution had become clear. Standing for three days yielded small, cubic crystals 3.54 g (43%).

M.pt. 239 °C (dec.). Elemental analysis : Calcd for $C_{12}H_{34}Zn_3O_{25}$: C, 18.7; H, 4.18. Found: C, 19.1; H, 3.95. ^{1}H NMR (300 MHz, D_2O): 2.50 (2H, d, ^{2}J = 17.0 Hz, C<u>H</u>$_2$), 2.67 (2H, d, ^{2}J = 17.0 Hz, C<u>H</u>$_2$). ^{13}C NMR (300 MHz, D_2O): 44.1 (<u>C</u>H_2), 74.7 (^{t}<u>C</u>), 177.3, 177.7 (OO<u>C</u>), 180.7 (<u>C</u>OOH).

Manganese Citrate, $Mn_3(C_6H_5O_7)_2 \cdot 14H_2O$, (12)

Manganese carbonate (2.76 g, 24 mmol) was added to the solution of titanium citrate and the resulting bimetallic solution was refluxed for 48 hrs, yielding a clear orange/ yellow solution. Large pink crystals 2.70 g (34%) were formed on standing.

M.pt. 247 °C (dec.). Elemental analysis : Calcd for $C_{12}H_{38}Mn_3O_{28}$: C, 18.1; H, 4.81. Found: C, 18.2; H, 4.84. HRMS (EI, m/z) calc for $C_6H_7O_7$ ($M\text{-}H^+$) 191.0192; found 191.0198. Calc for $[Mn(C_6H_5O_7)]$ ($M\text{-}H^+$) 243.9416; found 243.9419. Calc for $[Mn(C_6H_7O_7)(C_6H_6O_7)]$ ($M\text{-}H^+$) 435.9686; found 435.9691. Calc for $[Mn_2(C_6H_6O_7)(C_6H_5O_7)]$ ($M\text{-}H^+$) 488.8910; found 488.8924. Calc for $[Mn_3(C_6H_4O_7)(C_6H_5O_7)]$ ($M\text{-}H^+$) 541.8134; found 541.8157.

Calcium Citrate, $Ca_3(C_6H_5O_7)_2 \cdot 9H_2O$, (13)

Calcium acetate was added to the titanium citrate solution and dissolved instantly. The solution was refluxed for 1 hr. On standing a sparsely soluble, fine, white powder crashed out.

Yield 5.01g (94 %), M.pt. 234 °C (dec.). Elemental analysis : Calcd for $C_{36}H_{88}O_{71}Ca_9$: C, 21.4; H, 4.39. Found: C, 21.0; H, 4.24. ^{1}H NMR (300 MHz, D_2O): 2.48 (2H, d, ^2J = 16.4 Hz, α,γ, C<u>H</u>), 2.66 (2H, d, ^2J = 16.4 Hz, α',γ', C<u>H</u>).

7.3.2 CRYSTAL DATA AND STRUCTURE REFINEMENTS

Complex	**DMCA**	**4**	**6**
Empirical formula	C_8 H_{14} O_8	C_{14} H_{24} O_9 Ti	C_{36} H_{56} Na_4 $O_{63.04}$ Ti_2
Formula weight	238.19	384.23	1685.17
Temperature, K	150(2)	150(2)	150(2)
Crystal system	triclinic	monoclinic	monoclinic
Space group	*P*-1	$P2_1/n$	*C*2/c
Unit cell:			
a, Å	7.8290 (3)	10.55600(10)	18.8770(2)
b, Å	8.0800 (3)	15.6210(3)	10.91100(10)
c, Å	9.4480 (5)	10.8620(2)	31.5760(4)
α, °	95.300 (2)	90	90
β, °	109.770 (2)	95.522 (1)	97.2740(10)
γ, °	106.784 (2)	90	90
Volume, Å^3	526.36(4)	1782.78(5)	6451.27(12)
Z	2	4	4
Calc. density, mg/m^3	1.503	1.432	1.735
Abs. coeff. mm^{-1}	0.137	0.522	0.414
F(000)	252	808	3457
Crystal size, mm	0.25 x 0.20 x 0.10	0.30 x 0.25 x 0.25	0.20 x 0.10 x 0.10
θ range, °	3.93 to 27.46	3.66 to 27.49°.	3.60 to 28.28
Limiting indices	-10<=h<=8, -10<=k<=10, -12<=l<=12	-13<=h<=13, -20<=k<=20, -14<=l<=14	-25<=h<=24, -14<=k<=14, - 41<=l<=41
Reflections collected / unique	6205 / 2386 [R(int) = 0.0435]	30551 / 4081 [R(int) = 0.0392]	34441 / 6998 [R(int) = 0.0516]
Completeness to θ	= 27.46, 99.4 %	= 27.49, 99.7 %	= 28.28, 87.2 %
Max. and min. transmission	0.9864 and 0.9665	0.8805 and 0.8590	0.9597 and 0.9217
Data / restraints / parameters	2386 / 0 / 145	4081 / 0 / 243	6998 / 0 / 431
Goodness-of-fit on F^2	1.099	1.058	1.037
Final R indices [I>2σ(*I*)]	R_1 = 0.0455 wR_2 = 0.1125	R_1 = 0.0491 wR_2 = 0.1368	R_1 = 0.0764 wR_2 = 0.2059
R indices (all data)	R_1 = 0.0653 wR_2 = 0.1229	R_1 = 0.0562 wR_2 = 0.1426	R_1 = 0.0945 wR_2 = 0.2172
Largest diff. peak and hole, e/ Å^3	0.256 and -0.367	1.331 and -0.609	1.511 and -1.812

Complex	**7**	**11**	**12**
Empirical formula	C_{36} H_{68} Ni O_{56} Ti_2	C_{12} H_{38} O_{28} Zn_3	C_{12} H_{38} Mn_3 O_{28}
Formula weight	1551.41	826.53	795.24
Temperature, K	150(2)	150(2)	150(2)
Crystal system	monoclinic	monoclinic	monoclinic
Space group	*P*-3	$P2_1/n$	$P2_1/n$
Unit cell:			
a, Å	15.43800(10)	11.1320 (1)	11.2340 (1)
b, Å	15.43800(10)	11.9050 (1)	12.0160 (1)
c, Å	7.68000(10)	11.9420(1)	12.0920 (1)
α, °	90	90	90
β, °	90	116.208(1)	115.74 (1)
γ, °	120	90	90
Volume, Å^3	1585.16(3)	1419.93(2)	1470.26(2)
Z	1	2	2
Calc. density, mg/m^3	1.625	1.933	1.796
Abs. coeff. mm^{-1}	0.667	2.627	1.378
F(000)	804	848	818
Crystal size, mm	0.38 x 0.35 x 0.35	0.20 x 0.20 x 0.20	0.20 x 0.20 x 0.20
θ range, °	3.74 to 28.27	3.76 to 28.30	3.70 to 27.53
Limiting indices	-18<=h<=20, -20<=k<=20, -10<=l<=10	-14<=h<=14, -15<=k<=15, -15<=l<=15	-14<=h<=14, -15<=k<=15, -15<=l<=15
Reflections collected / unique	25063 / 2611 [R(int) = 0.0400]	26470 / 3513 [R(int) = 0.0677]	25199 / 3376 [R(int) = 0.0582]
Completeness to θ	= 28.27, 99.7 %	= 28.30, 99.3 %	= 27.53, 99.5 %
Max. and min. transmission	0.8002 and 0.7858	0.6216 and 0.6216	0.7701 and 0.7701
Data / restraints / parameters	2611 / 0 / 174	3513 / 0 / 270	3376 / 0 / 270
Goodness-of-fit on F^2	1.077	1.118	1.089
Final R indices [I>2σ(*I*)]	R_1 = 0.0287 wR_2 = 0.0735	R_1 = 0.0289 wR_2 = 0.0731	R_1 = 0.0266 wR_2 = 0.0629
R indices (all data)	R_1 = 0.0312 wR_2 = 0.0750	R_1 = 0.0372 wR_2 = 0.0773	R_1 = 0.0325 wR_2 = 0.0658
Largest diff. peak and hole, e/ Å^3	0.384 and -0.719	0.774 and -1.750	0.489 and -0.818

7.4 EXPERIMENTAL PROCEDURES FOR CHAPTER 4

Complexes 14-17

These amino acid complexes were synthesised by adapting a similar literature preparation described by Schubert et al. [3] The amino acid (10 mmol) was dried under vacuum for 1 hrs. Dry ^{i}PrOH (60ml) and Ti($O^{i}Pr$)$_4$ (3 ml, 10 mmol) were added and the suspension was refluxed overnight. The suspension was filtered hot removing any resulting white, insoluble precipitate.

Titanium Alanine, Ti($C_3H_6NO_2$)($O^{i}Pr$)$_3$, (14)

After 24 hrs little precipitate was left and the mixture was filtered and then reduced until a minimum amount of solvent remained. After 3 days large clear crystals were obtained at -4 ° C, yield 2.41 g (91%).

Elemental analysis : Calcd for $C_{12}H_{21}NO_5Ti$: C, 46.1; H, 8.39; N, 4.41. Found: C, 45.7; H, 8.40; N, 4.50. ^{1}H NMR (300 MHz, D_2O): 1.17 (18H, d, ^{3}J = 6.0 Hz, $O^{i}Pr$, C$\underline{H}_3$), 1.48 (3H, d, ^{3}J = 7.0 Hz, C$\underline{H}_3$), 3.78 (1H, q, ^{3}J = 7.0 Hz, NC$\underline{H}$), 4.02 (1H, sept, ^{3}J = 6.0 Hz, $O^{i}Pr$, C$\underline{H}$). ^{13}C NMR (300 MHz, D_2O): 16.4 ($\underline{C}H_3$), 24.0 ($O^{i}Pr$, $\underline{C}H_3$), 50.8 (N$\underline{C}$H), 64.6 ($O^{i}Pr$, $\underline{C}$H) 176.1 ($\underline{C}O_2$).

Titanium Glycine, Ti($C_2H_5NO_2$)($O^{i}Pr$)$_3$, (15)

A microcrystalline solid crashed out of solution after standing for 24 hrs. Yield 1.40 g (47%).

Elemental analysis : Calcd for $C_{12}H_{21}NO_5Ti$: C, 46.1; H, 8.39; N, 4.41. Found: C, 45.7; H, 8.40; N, 4.50. ^{1}H NMR (300 MHz, D_2O): 1.03 (6H, d, ^{3}J = 6.0 Hz, $O^{i}Pr$, C$\underline{H}_3$), 3.78 (1H, sept., ^{3}J = 6.0 Hz, $O^{i}Pr$, C$\underline{H}$), 4.29 (2H, s, NC$\underline{H}$). 4.02 (1H, sept, ^{3}J = 6.0 Hz, $O^{i}Pr$, C$\underline{H}$). ^{13}C NMR (300 MHz, D_2O): 24.1 ($O^{i}Pr$, $\underline{C}H_3$), 41.4 ($\underline{C}H_2$), 64.0 ($O^{i}Pr$, $\underline{C}$H) 172.3 ($\underline{C}O_2$).

Titanium Proline, $Ti(C_5H_8NO_2)(O^iPr)_3$, (16)

On standing over 3 days a microcrystalline powder was recovered, yield 0.97 g, (29%).

M.pt. 169 °C (dec). Elemental analysis : Calcd for $C_{14}H_{28}NO_5Ti$: C, 49.7; H, 8.34; N, 4.14. Found: C, 49.2; H, 8.33; N, 3.98. ^{1}H NMR (300 MHz, CD_3OD): 1.13 (6H, d, ^{3}J = 6.0 Hz, O^{i}Pr, C$\underline{H}_3$), 1.69-2.29 (4H, m, C$\underline{H}_2$), 3.10-3.40 (2H, m, NC$\underline{H}_2$), 3.92 (1H, sept, ^{3}J = 6.0 Hz, O^{i}Pr, C$\underline{H}$), 4.01 (1H, m, C$\underline{H}$). ^{13}C NMR (300 MHz, CD_3OD): 25.2 (O^{i}Pr, $\underline{C}H_3$), 25.3, 30.4 ($\underline{C}H_2$), 47.7 (N$\underline{C}H_2$), 62.7 (N$\underline{C}$H), 64.8 (O^{i}Pr, $\underline{C}$H) 173.1 ($\underline{C}O_2$).

Titanium Tryptophan, $Ti(C_{11}H_{10}N_2O_2)(C_3H_7O)_3$, (17)

The titanium tryptophan complex fully dissolved overnight and on standing over 7 days yielded large clear cubic crystals, yield 2.74 g (64%).

M.pt. 146 °C (dec). Elemental analysis : Calcd for $C_{40}H_{64}N_4O_{10}Ti_2$: C, 56.2; H, 7.31; N, 6.44. Found: C, 56.2; H, 7.47; N, 6.60. ^{1}H NMR (300 MHz, D_2O): 1.17 (6H, d, ^{3}J = 6.0 Hz, O^{i}Pr, C$\underline{H}_3$), 3.17-3.96 (3H, m, C$\underline{H}_2$, NC$\underline{H}$), 4.07 (1H, sept, ^{3}J = 6.0 Hz, O^{i}Pr, C$\underline{H}$), 7.17-7.33 (2H, m, C$\underline{H}$), 7.52 (1H, d, ^{3}J = 6.0 Hz, C$\underline{H}$), 7.74 (1H, d, ^{3}J = 6.0 Hz, C$\underline{H}$).

N,N-bis(2-hydroxy 3,5 dimethyl benzyl)glycine, H_3L1

Glycine (3.00 g, 40 mmol) was added to mixture of 2,4 dimethylphenol (10 ml, 80 mmol) and paraformaldehyde (3.00 g, 100 mmol) in methanol (100 mL). The mixture was then stirred at reflux for 4 days. The product was filtered off and washed with cold methanol to yield 11.67 g (85%)**.**

Elemental Analysis: Calcd for $C_{20}H_{25}NO_4$: C, 70.0; H, 7.34, N 4.08. Found C, 69.1; H, 7.44; N, 3.98. ^{1}H NMR (300 MHz, DMSO): 2.15 (6H, s, C$\underline{H}_3$), 2.18 (6H, s, C$\underline{H}_3$) 3.18 (2H, s, C$\underline{H}_2$) 3.67 (2H, s, C$\underline{H}_2$), 6.80 (2H, s, ^{Ar}C$\underline{H}$), 6.90 (2H, s, ^{Ar}C$\underline{H}$). HRMS (EI, m/z) calc for $C_{21}H_{27}NO_4$ (M-H$^+$) 343.1708; found 343.1711.

N,N-bis(2-hydroxy 3,5 dimethyl benzyl)β-Alanine, H_3L2

Ligand **B** was synthesised via the same method used to synthesise ligand H_3**L1.**

Yield 9.99 g (70%), M.pt. 178 °C. Elemental Analysis : Calcd for $C_{21}H_{27}NO_4$: C, 70.6; H, 7.61, N 3.92. Found C, 70.8; H, 7.59; N, 3.31. ^{1}H NMR (300 MHz, DMSO): 2.17 (6H, s, C$\underline{H}_3$), 2.21 (6H, s, C$\underline{H}_3$) 2.60 (2H, t, ^{3}J = 6 Hz, C$\underline{H}_2$) 3.21 (2H, t, ^{3}J = 6 Hz, C$\underline{H}_2$), 4.18 (4H, m, C$\underline{H}_2$), 6.87 (2H, s, ^{Ar}C$\underline{H}$), 6.93 (2H, s, ^{Ar}C$\underline{H}$). HRMS (EI, m/z) calc for $C_{21}H_{27}NO_4$ ($M+H^+$) 358.2013; found 358.2017.

Tris(3,5-dimethyl-2hydroxybenzyl) Amine, H_3**L3**

Ligand H_3**L3** was synthesised in an adapted preparation to that given by Kol et al. [4] Hexamethylenetetramine (0.94 g, 6.66 mmol) was added to mixture of 2,4 dimethylphenol (10 ml, 80 mmol) and paraformaldehyde (3.00 g, 100 mmol). The solution was refluxed for 48 hrs and the resulting white powder recrystallised from methanol and ether.

M.pt. 187 °C. Elemental Analysis : Calcd for $C_{21}H_{27}NO_4$: C, 70.6; H, 7.61, N 3.31. Found C, 70.2; H, 8.56; N, 3.22. ^{1}H NMR (300 MHz, $CDCl_3$): 2.18 (9H, s, C$\underline{H}_3$), 2.21 (9H, s, C$\underline{H}_3$) 3.61 (6H, s, C$\underline{H}_2$) 6.72 (3H, s, ^{Ar}C$\underline{H}$), 6.85 (3H, s, ^{Ar}C$\underline{H}$).

Titanium L1, [Ti(L1)(O^{i}Pr)]$_3$, (18)

Ti(O^{i}Pr)$_4$ (0.6 ml, 2 mmol) was added to **L1** (2 mmol) in a suspension of toluene using standard schlenk techniques. The mixture was refluxed for 1 hr resulting in a deep red solution. The volatiles were removed and the resulting product redissolved in toluene and hexane. On standing at room temperature for 3 days small cubic crystals were formed.

Yield 0.55 g (61%), Mpt. 248 °C (dec.). ^{1}H NMR (300 MHz, $CDCl_3$) 0.92-1.13 (5H, m, hex). 1.34-1.64 (15H, m, hex, C$\underline{H}_3$ O^{i}Pr), 1.84 (3H, br s, C$\underline{H}_3$), 2.02 (6H, d, ^{3}J = 6 Hz, O^{i}Pr, C$\underline{H}_3$), 2.08-2.36 (34.5H, m, phenolate, tol, C$\underline{H}_x$), 2.63-2.76 (3H, m, C$\underline{H}_2$) 3.11-3.34 (6H, m, C$\underline{H}_2$), 3.64-3.89 (5H, m, C$\underline{H}_2$), 4.14 (1H, d, ^{2}J = 18 Hz, C$\underline{H}_2$), 4.29-4.61 (4H, m, C$\underline{H}_2$), 4.76 (1H, sept, J = 6.0 Hz, OiPr, C$\underline{H}$), 5.01 (1H, sept, J = 6.0 Hz,

OiPr, CH), 5.16 (1H, sept, J = 6.0 Hz, OiPr, CH), 6.49-7.03 (14.5H, m, tol, phenolate, CH). ^{13}C NMR (300 MHz, $CDCl_3$) 14.1, 15.8, 16.1, 16.1, 16.2, 16.5, 16.6 (two peaks overlapping), 16.7, 16.9, 17.2, 19.7, 20.6 (two peaks overlapping), 20.9, 24.7, 25.0, 25.4 (CH_3) 29.7, 31.6, 60.0, 60.1, 61.3, 62.9, 63.4, 63.5, 64.4 (CH_2) 77.2, 79.1, 80.0 (O^iPr, CH) 123.1, 123.2, 123.9, 124.0, 124.0, 124.1, 124.5, 124.5, 124.5, 124.6, 125.0, 125.2, 127.1, 127.3, 127.3, 127.4, 127.6, 127.6, 127.7, 128.2, 128.3 (two peaks overlapping), 129.0, 129.1, 129.2, 130.4, 130.5, 131.3, 131.4, 131.4, (Ar) 156.8, 157.6, 158.6, 161.0, 162.7, 163.0 (Ar-O) 178.9, 181.6, 182.7 (COO). HRMS (ESI, m/z) calc for $C_{69}H_{87}N_3O_{15}Ti_3$ $[M+H]^+$ 1342.4672; found 1342.4682.

Titanium L2, $[Ti(L2)(O^iPr)]_3$, (19)

A similar technique in synthesising complex **19** was used. A fine orange solid formed after 7 days at -8 °C from the bright red mixture.

Yield 0.21 g (61%), Mpt. 246 °C (dec.). Elemental Analysis : Calcd for $C_{24}H_{30}NO_5Ti$: C, 62.3; H, 6.98, N 3.03. Found C, 61.6; H, 6.83; N, 3.08. ^{1}H NMR (300 MHz, $CDCl_3$): 1.31-1.38 (6H, m, O^iPr, CH_3). 1.42 (3H, d, ^3J = 6 Hz, O^iPr, CH_3), 1.46 (3H, d, ^3J = 6 Hz, O^iPr, CH_3), 1.54 (3H, d, ^3J = 6 Hz, O^iPr, CH_3), 1.64 (3H, d, ^3J = 6 Hz, O^iPr, CH_3), 1.76 (3H, s, phenolate, CH_3), 2.02 (3H, s, phenolate, CH_3), 2.08-2.27 (30H, m, phenolate, CH_3), 2.29-2.52 (5H, m, CH_2) 2.53-2.80 (6H, m, CH_2), 2.81-3.13 (4H, m, CH_2), 3.15-3.28 (1H, m, CH_2), 3.30-3.46 (1H, m, CH_2), 3.52-3.79 (3H, m, CH_2), 3.99 (1H, d, ^2J = 14 Hz, CH_2), 4.03 (1H, d, ^2J = 14 Hz, CH_2), 4.40 (1H, d, ^2J = 14 Hz, CH_2), 4.82 (1H, d, ^2J = 14 Hz, CH_2), 5.18-5.29 (2H, m, O^iPr, CH), 5.35 (1H, sept, J = 6.0 Hz, O^iPr, CH), 6.27 (1H, s, phenolate CH), 6.48 (1H, s, phenolate CH), 6.53-6.62 (4H, m, phenolate CH), 6.66-6.70 (2H, m, phenolate, CH) 6.75 (1H, s, phenolate CH), 6.79 (1H, s, phenolate CH), 6.82 (1H, s, phenolate CH), 6.90 (1H, s, phenolate CH). ^{13}C NMR (300 MHz, $CDCl_3$) 15.9, 16.4, 16.5, 16.5, 16.7, 17.2, 20.4, 20.5, 20.5, 20.6, 20.6, 21.6, 22.7, 24.7, 25.1, 25.2, 25.2, 25.4 (CH_3) 31.4, 31.6, 32.2 (two peaks overlapping), 53.8, 54.3, 55.7, 59.5, 60.2, 61.5, 61.9, 63.5 (CH_2) 80.0, 80.7, 82.3 (O^iPr, CH) 124.1, 124.1, 124.2, 124.3, 124.5, 124.8, 124.8, 124.9, 125.0, 125.0, 125.2, 126.0, 126.6, 127.0, 127.2, 127.5, 127.8, 128.2, 128.3, 128.5, 128.7, 129.0, 130.2, 130.5, 130.6, 130.7, 130.8, 130.8, (Ar) 157.5, 158.0, 159.4, 159.5, 159.9, 159.9 (Ar-O) 179.9, 181.0, 182.4 (COO). HRMS (EI, m/z) calc for $C_{72}H_{93}N_3O_{15}Ti_3$ $[M+H]^+$ 1384.5142; found 1384.5154.

Germanium L2, Ge(L2)(O^iPr), (20)

H_3**L2** (0.49g, 1.35 mmol) was suspended in toluene and $Ge(O^iPr)_4$ (0.4 ml, 1.35 mmol) was added slowly. The reaction mixture was held at reflux for 72 hrs, by which time the solution was clear. The solution was reduced by half and a fine white solid formed after standing overnight at room temperature.

Yield 0.52 g (80%). Elemental Analysis : Calcd for $C_{38}H_{46}NO_5Ge$: C, 67.7; H, 6.91, N 2.13. Found C, 67.9; H, 7.29; N, 2.26. ^{1}H NMR (300 MHz, $CDCl_3$): 1.07-1.13 (6H, m, O^iPr, C$\underline{H}_3$). 1.33 (3H, s, phenolate, C$\underline{H}_3$), 2.17 (6H, s, phenolate, C$\underline{H}_3$), 2.21 (3H, s, phenolate, C$\underline{H}_3$), 2.21 (6H, s, tol, C$\underline{H}_3$), 2.45-2.73 (2H, m, C$\underline{H}_2$), 3.40-3.73 (4H, m, C$\underline{H}_2$), 4.87 (1H, sept, J = 6.0 Hz, O^iPr, C$\underline{H}$), 5.18 (1H, d, ^{2}J = 14 Hz, C$\underline{H}_2$), 5.49 (1H, d, ^{2}J = 14 Hz, C$\underline{H}_2$), 6.58 (1H, s, phenolate, C$\underline{H}$), 6.72 (1H, s, phenolate, C$\underline{H}$), 6.78 (1H, s, phenolate, C$\underline{H}$), 6.81 (1H, s, phenolate, C$\underline{H}$), 7.15-7.27 (10H, m, tol, C$\underline{H}$). ^{13}C NMR (300 MHz, $CDCl_3$): 16.7, 17.7, 20.3, 21.6, 21.6, 21.7 ($\underline{C}H_3$) 20.4 (tol, $\underline{C}H_3$) 26.9, 47.2, 57.4, 58.4 ($\underline{C}H_2$) 68.2 (O^iPr, $\underline{C}H$) 125.3 128.2 129.0 137.9 (tol, $\underline{C}H$) 118.3, 120.7, 126.3, 126.3, 126.6, 127.0 127.1 128.5, 131.3, 132.0 (Ar) 156.2, 155.5 (Ar-O) 170.4 (COO).

Titanium L3, Ti(L3)(O^iPr), (21)

21 was synthesised by the same method given by Kol et al. [4]

Yield 0.89 g (86%). Elemental analysis: Calc for $C_{30}H_{37}NO_4Ti$ C, 68.8; H, 7.12; N, 2.68. Found C, 67.8; H, 7.17; N, 2.52. ^{1}H NMR (400 MHz, $CDCl_3$) 1.44 (6H, d, J = 6.0 Hz O^iPr, C$\underline{H}_3$). 2.12 (9H, s, phenolate, C$\underline{H}_3$), 2.15 (9H, s, phenolate, C$\underline{H}_3$), 2.73 (3H, m, NC$\underline{H}_2$), 3.88 (3H, m, NC$\underline{H}_2$) 5.12 (1H, sept, J = 6.0 Hz, O^iPr, C$\underline{H}$), 6.61 (3H, s, phenolate, C$\underline{H}$), 6.76 (3H, s, phenolate, C$\underline{H}$). ^{13}C NMR (300 MHz, $CDCl_3$) 16.6, 20.9 ($\underline{C}H_3$) 26.0 (O^iPr, $\underline{C}H_3$) 58.7 (O^iPr, $\underline{C}H$) 79.8 (O^iPr, $\underline{C}H$), 123.9, 124.6, 127.8, 129.6, 130.9, 169.9 (Ar).

Germanium L3, Ge(L3)(O^iPr)(HO^iPr), (22)

H_3**L3** (0.84 g, 2 mmol) was dissolved in toluene (20 ml) and $Ge(O^iPr)_4$ (0.62 g, 2 mmol) was added under dry argon. The reaction mixture stirred at room temperature for 2 hr before the volatiles were removed under vacuum and the product recrystallised from the minimum amount of toluene at 4 °C yielding 0.79 g, (65 %) clear crystals.

M.pt. 223-225 °C. Elemental analysis: Calc for $C_{36.5}H_{49}NO_5Ge$ C, 67.0; H, 7.55; N, 2.14. Found C, 66.7; H, 7.59; N, 2.31. ^{1}H NMR (400 MHz, $CDCl_3$) 1.21 (6H, d, J = 6.0 Hz O^{i}Pr, C$\underline{H}_3$). 1.41 (6H, d J = 6.0 Hz, O^{i}Pr, C$\underline{H}_3$), 1.60 (1H, br s, O$\underline{H}$), 2.21 (9H, s, phenolate, C$\underline{H}_3$), 2.30 (9H, s, phenolate, C$\underline{H}_3$), 2.36 (1.5H, s, tol, C$\underline{H}_3$), 3.64 (6H, br s, NC$\underline{H}_2$) 3.95 (1H, sept, J = 6.0 Hz, HO^{i}Pr, C$\underline{H}$), 4.73 (1H, sept, J = 6.0 Hz, O^{i}Pr, C$\underline{H}$), 6.57 (3H, s, phenolate, C$\underline{H}$), 6.93 (3H, s, phenolate, C$\underline{H}$), 7.10-7.30 (2.5H, m, tol, C$\underline{H}$). ^{13}C NMR (300 MHz, $CDCl_3$) 16.5, 20.3 (Ar-$\underline{C}H_3$), 25.3 (tol), 25.3 (HOCH($\underline{C}H_3$)$_2$), 26.4 (OCH($\underline{C}H_3$)$_2$), 59.3 (N-CH_2), 64.2 (HO$\underline{C}$H(CH_3)$_2$), 65.7 (O$\underline{C}$H(CH_3)$_2$), 119.1 (Ar), 125.2 (tol), 126.4 (Ar), 128.1 (tol), 128.6 (Ar), 129.0 (tol), 129.4, 131.9 (Ar), 137.8 (tol), 152.0 (O-Ar). HRMS (FAB, m/z) calc for $C_{30}H_{37}N_1O_4Ge$ $[M+H]^+$ 549.1929; found 549.1931.

Complexes 23-29

Amino acid complexes **23-27** were synthesised in an adapted literature preparation given by Dabre et al. [5] The amino acid (40 mmol) was added to MeOH (50 ml) and stirred, triethylamine (5.5 ml, 40 mmol) was added and the mixture was left to stir at room temperature for 2 hrs. Zinc acetate dihydrate (4.39g, 20 mmol) was added after this time and the mixture was left to stir overnight. Complexes **28** & **29** were synthesised in an identical manner except in an aqueous solution (50 ml)

Zinc Arginine, (23)

Zinc arginine was filtered off as an insoluble white powder (2.84g, 91% yield) and washed with MeOH (200 ml) and H_2O (200 ml). Mpt: 250+ Elemental Analysis: Found C, 32.8; H, 6.45; N, 19.5. ICP-OES metal analysis: Zn, 12.63.

Zinc Phenylalanine, $Zn(C_9H_8NO_2)_2$, (24)

Zinc phenylalanine was filtered off and washed with MeOH (200 ml). M.pt: 194 ºC (dec.)**;** ^{1}H NMR (300 MHz, D_2O): δ= 2.69-2.80 (m, 1H), 2.88-2.96 (m, 1H), 3.55-3.65 (m, 1H), 6.94-7.08 (m, 5H) Elemental Analysis: Calcd for $C_{18}H_{20}N_2O_4Zn$: C, 54.9; H, 5.12; N, 7.11. Found C, 54.4; H, 4.96; N, 7.98.

Zinc Proline, $Zn(C_5H_8NO_2)_2$, (25)

Zinc proline was filtered off and washed with MeOH (200 ml). M.pt. 250+ ºC**;** ^{1}H NMR (300 MHz, D_2O): δ= 1.85 (m, 3H), 2.17 (m, 1H), 3.18 (m, 2H), 3.96 (m, 1H), 4.69 (s, $\underline{H}_2O$). ^{13}C NMR (300 MHz, D_2O): 25.9 ($\underline{C}H_2$), 30.1 ($\underline{C}H_2$), 47.6 (N$\underline{C}$H), 60.9 (N$\underline{C}H_2$). Elemental Analysis: Calcd for $C_{10}H_{16}N_2O_4Zn$: C, 40.9; H, 5.49; N, 9.54. Found C, 40.8; H, 5.44; N, 9.62.

Zinc Histidine, $Zn(C_6H_8N_3O_2)_2 \cdot 3H_2O$, (26)

The product was filtered off and washed with H_2O (1 l) and MeOH (200 ml). This afforded a solid, fine white powder (6.74 g, 79 %) this was sparsely soluble in boiling H_2O. M.pt. 250+ °C**;** ^{1}H NMR (300 MHz, D_2O): δ= 3.02 (m, 2H), 3.83 (s, 1H), 4.65 (m, $\underline{H}_2O$), 6.85 (s, 1H), 7.55 (s, 1H); Elemental Analysis: Calcd for $C_{12}H_{22}N_6O_7Zn$: C, 33.7; H, 5.18; N, 19.7. Found C, 34.3; H, 5.17; N, 19.8.

Zinc β-Alanine, $Zn(C_3H_6NO_2)_2$, (27)

Zinc β-alanine was filtered off and washed with MeOH (200 ml). This afforded a fine, white powder which was sparingly soluble in boiling H_2O. M.pt. 250+**;** ^{1}H NMR (300 MHz, D_2O): δ= 3.02 (m, 2H), 3.83 (s, 1H), 4.65 (m, $\underline{H}_2O$), 6.85 (s, 1H), 7.55 (s, 1H); Elemental Analysis: Calcd for $C_6H_{12}N_2O_4Zn$: C, 29.8; H, 5.02; N, 11.6. Found C, 29.8; H, 4.84; N, 11.0.

Zinc Glutamine, $Zn(C_5H_9N_2O_3)_2$, (28)

Zinc glutamine was redissolved in 200 ml of H_2O and stored at 4 °C where small cubic crystals had formed after 5 days, (4.54 g, 64 %). M.pt. 219 (dec.); ^{1}H NMR (300 MHz, D_2O): δ= 1.55 (m, 1H), 1.72 (m, 1H), 2.04 (t, 2H, ^3J = 7.0 Hz), 3.07 (dd, 1H, ^3J = 5.0 Hz), 4.65 (s, $\underline{H}_2O$). Elemental Analysis: Calcd for $C_{10}H_{18}N_4O_6Zn$: C, 33.8; H, 5.10; N, 15.7. Found C, 34.0; H, 5.11; N, 15.6.

Zinc Serine, $Zn(C_3H_6NO_3)_2$, (29)

Zinc serine was dissolved in H_2O (100 ml) and stored at 4 °C where hard, rectangular crystals formed after 5 days, (2.29 g, 42%). ^1H NMR (300 MHz, D_2O): δ= 3.39 (s, 1H), 3.74 (s, 2H), 4.69 (m, $\underline{H_2}O$). ^{13}C NMR (300 MHz, D_2O): 55.8 (N$\underline{C}$H), 62.7 (HO$\underline{C}H_2$), 178.8 (COO). Elemental Analysis: Calcd for $C_6H_{12}N_2O_6Zn$: C, 26.3; H, 4.42; N, 10.2. Found C, 26.5; H, 4.32; N, 10.4.

7.3.2 CRYSTAL DATA AND STRUCTURE REFINEMENTS

Complex	**15**	**17**	**18**
Empirical formula	$C_{24}H_{54}N_2O_{10}Ti_2$	$C_{40}H_{64}N_4O_{10}Ti_2$	$C_{41.25}H_{47.50}N_{1.50}O_{7.50}Ti_{1.50}$
Formula weight	626.49	856.75	756.16
Temperature, K	150(2) K	150(2)	296(2)
Crystal system	monoclinic	monoclinic	triclinic
Space group	$P2_1/c$	$P2_1$	P-1
Unit cell:			
a, Å	10.0920(1)	10.5960(2)	12.6472(11)
b, Å	15.9640(2)	9.6040(1)	18.1058(16)
c, Å	11.0990(2)	21.8520(3)	19.0066(17)
α, °	90	90	96.1780(10)
β, °	108.526(1)	99.2640(10)	103.7850(10)
γ, °	90	90	106.7680(10)
Volume, Å^3	1695.48(4)	2194.74(6)	3973.7(6)
Z	2	2	4,
Calc. density, mg/m^3	1.227	1.296	1.264
Abs. coeff. mm^{-1}	0.518	0.421	0.359
F(000)	672	912	1594
Crystal size, mm	0.30 x 0.30 x 0.10	0.35 x 0.30 x 0.15	
θ range, °	3.54 to 27.55	3.17 to 27.52	3.30 to 24.86
Limiting indices	-13<=h<=13; -20<=k<=20; -14<=l<=14	-13<=h<=13, -12<=k<=12, -28<=l<=28	-15<=h<=15, -22<=k<=22, -23<=l<=23
Reflections collected / unique	30474 / 3896 [R(int) = 0.0371]	34957 / 9828 [R(int) = 0.0339]	32420/ 14882 [R(int) = 0.0549]
Completeness to θ	99.3 %	= 27.52, 99.0 %	= 24.86, 99.2 %
Max. and min. transmission	0.86 and 0.81	0.9395 and 0.8666	
Data / restraints / parameters	3896 / 0 / 210	9828 / 1 / 521	14882 / 5 / 927
Goodness-of-fit on F^2	1.265	1.050	1.033
Final R indices [I>2σ(I)]	R_1 = 0.0616 wR_2 = 0.1481	R_1 = 0.0308 wR_2 = 0.0761	R_1 = 0.0753 wR_2 = 0.1963
R indices (all data)	R_1 = 0.0654 wR_2 = 0.1495	R_1 = 0.0333 wR_2 = 0.0774	R_1 = 0.1213 wR_2 = 0.2249
Largest diff. peak and hole, e/ Å^3	0.584 and -0.393	0.302 and -0.470	1.422 and -1.101

Complex	**28**	**29**
Empirical formula	$C_{10}H_{18}N_4O_6Zn$	$C_6H_{12}N_2O_6Zn$
Formula weight	355.65	273.55
Temperature, K	150(2)	150(2)
Crystal system	monoclinic	monoclinic
Space group	$P2_1$	$P2_1/n$
Unit cell:		
a, Å	9.4080(1)	5.6440(2)
b, Å	5.0150(3)	8.8120(3)
c, Å	14.4480(4)	9.4730(3)
α, °	90	90
β, °	105.008(2)	95.853(2)
γ, °	90	90
Volume, Å^3	658.42(4)	468.68(3)
Z	2	2
Calc. density, mg/m^3	1.794	1.938
Abs. coeff. mm^{-1}	1.901	2.633
F(000)	368	280
Crystal size, mm	0.35 x 0.13 x 0.05	0.20 x 0.15 x 0.10
θ range, °	4.12 to 27.50	4.03 to 27.37
Limiting indices	-12<=h<=12, -6<=k<=6, -18<=l<=18	-7<=h<=7, -11<=k<=11, -11<=l<=12
Reflections collected / unique	11867 / 3007 [R(int) = 0.0663]	3347 / 1734 [R(int) = 0.0530]
Completeness to θ	= 27.50, 99.6 %	= 27.37, 95.4 %
Max. and min. transmission	0.9109 and 0.5558	0.7787 and 0.6210
Data / restraints / parameters	3007 / 1 / 223	1734 / 5 / 152
Goodness-of-fit on F^2	0.992	1.119
Final R indices [I>2σ(I)]	R_1 = 0.0351 wR_2 = 0.0697	R_1 = 0.0352 wR_2 = 0.0884
R indices (all data)	R_1 = 0.0498 wR_2 = 0.0740	R_1 = 0.0376 wR_2 = 0.0895
Largest diff. peak and hole, e/ Å^3	0.326 and -0.757	0.610 and -1.219

7.5 EXPERIMENTAL PROCEDURES FOR CHAPTER 5

Zinc Carboxylate Compounds

The carboxylic acid (200 mmol) was added to the hydrated metal acetate (100mmol) in H_2O (200 ml). This was then refluxed for 2 hrs and the resulting compound reduced to dryness using a rotary evaporator.

Zinc Propionoate, $Zn(C_3H_5O_2)_2$

Zinc propianoate was redissolved in a minimum amount of H_2O and yielded large clear crystals, yield 15.6 g (74%) on standing over 24 hrs. M.pt. 182-185 °C, ^{1}H NMR (300 MHz, D_2O): δ= 0.90 (3H, t, J = 6.0 Hz, C$\underline{H}_3$), 2.06 (2H, q, J = 6 Hz, C$\underline{H}_2$). ^{13}C NMR (300 MHz, $CDCl_3$) 10.2 (C$\underline{H}_3$), 30.0 (C$\underline{H}_2$), 185.5 (C$\underline{O}_2$).

Zinc Crotonate, $Zn(C_4H_5O_2)_2$

Zinc crotonate was recrystallised from a H_2O/ MeOH mixture to yield 15.1 g (64%), a microcrystalline powder. M.pt. 201-204 °C; ^{1}H NMR (300 MHz, D_2O): δ= 1.78 (3H, d, J = 6.5 Hz, C$\underline{H}_3$), 5.86 (1H, d, J = 15.5 Hz, C$\underline{H}$), 6.95 (1H, sept, J = 6.5 Hz, C$\underline{H}$). ^{13}C NMR (300 MHz, $CDCl_3$) 19.3 (C$\underline{H}_3$), 126.4 (C$\underline{H}$CH$_3$), 146.2 (C$\underline{H}$CH), 175.5 (C$\underline{O}_2$).

Zinc Hexanoate $Zn(C_6H_{11}O_2)_2$

The complex was recrystallised from H_2O and was recovered as a fine off white powder, yield 18.6 g (63%). M.pt. 131-134 °C; ^{1}H NMR (300 MHz, D_2O): 0.70 (6H, t, J = 6 Hz, C$\underline{H}_3$), 1.13 (8H, m, C$\underline{H}_2$), 1.42 (4H, quin, C$\underline{H}_2$), 2.05 (4H, t, J = 6 Hz, OCC$\underline{H}_2$) ^{13}C NMR (300 MHz, D_2O): 13.7 (C$\underline{H}_3$), 22.2, 25.9, 31.4, 37.8 (C$\underline{H}_2$) 178.0 (COO).

Manganese Crotonate $Zn(C_4H_5O_2)_2$

Manganese crotonate was recovered as a fine, light pink powder, yield 13.5 g (60%). Mpt. 186 °C (dec.). HRMS (EI, m/z) calc for $MnC_8H_{11}O_2$ ($M+H^+$) 226.0032; found 226.0031.

Calcium Crotonate $Ca(C_4H_5O_2)_2$

Calcium crotonate was recovered as an off-white powder, yield 15.1 g (72%). ^{1}H NMR (300 MHz, D_2O): δ= 1.80 (3H, d, J = 6.5 Hz, C<u>H</u>$_3$), 5.81 (1H, d, J = 15.5 Hz, C<u>H</u>), 6.64 (1H, sept, J = 6.5 Hz, C<u>H</u>). ^{13}C NMR (300 MHz, $CDCl_3$) 17.4 (<u>C</u>H$_3$), 126.3 (<u>C</u>HCH$_3$), 143.4 (<u>C</u>HCH). HRMS (EI, m/z) calc for $CaC_8H_{11}O_2$ ($M+H^+$) 211.0283; found 211.0282.

Zinc Crotonate Quinoline, $Zn(C_4H_5O_2)_2$Quin

An adapted literature preparation taken from Clegg et al. was used to synthesise the following zinc complexes. The analytical data collected is in agreement with the published results. [6, 7]

Zinc crotonate (2.35 g, 10 mmol) and quinoline (1.2 ml, 10 mmol) were refluxed in methanol for 2 hrs. The solution was then concentrated on a rotary evaporator, small white crystals were formed over 72 hrs at -4 °C**.**

Elemental Analysis: Calcd for $C_{17}H_{17}NO_4Zn$: C, 55.9; H, 4.70; N, 3.84. Found: C, 55.1; H, 4.66; N, 3.89. ^{1}H NMR (300 MHz, MeOD): 1.71 (12H, d, J = 6 Hz, C<u>H</u>$_3$), 5.81 (4H, d, J = 16 Hz, C<u>H</u>), 6.79 (4H, sept, J = 6 Hz, C<u>H</u>) 7.52 (4H, m, ^{Ar}<u>C</u>H), 7.71 (2H, m, ^{Ar}<u>C</u>H), 7.88 (2H, d, J = 8 Hz. ^{Ar}<u>C</u>H) 8.08(2H, d, J = 8 Hz. ^{Ar}<u>C</u>H) 8.34 (2H, d, J = 8 Hz. ^{Ar}<u>C</u>H) 8.83 (2H, d, J = 8 Hz. ^{Ar}<u>C</u>H). ^{13}C NMR (300 MHz, $CDCl_3$) 18.1 (<u>C</u>H$_3$), 126.1 144.5 (<u>C</u>H), 121.7 127.7 128.5, 128.6, 129.1, 131.0, 138.8, 147.3, 151.3 (^{Ar}<u>C</u>), 174.9 (<u>C</u>OO).

Zinc Crotonate Quinoline, $Zn_3(C_4H_5O_2)_6Quin_2$

The trinuclear complex was prepared by the same method as the binuclear zinc crotonate except for the amount of quinoline (0.8 ml, 6.66mmol) used.

^{1}H NMR (300 MHz, MeOD): 1.73 (18H, d, J = 6 Hz, C$\underline{H}_3$), 5.79 (6H, d, J = 16 Hz, C$\underline{H}$), 6.78 (6H, sept, J = 6 Hz, C$\underline{H}$) 7.48 (4H, m, $^{Ar}\underline{C}$H), 7.71 (2H, m, $^{Ar}\underline{C}$H), 7.89 (2H, d, J = 8 Hz. $^{Ar}\underline{C}$H), 8.02 (2H, d, J = 8 Hz. $^{Ar}\underline{C}$H) 8.34 (2H, d, J = 8 Hz. $^{Ar}\underline{C}$H) 8.87 (2H, d, J = 8 Hz. ^{Ar}CH). ^{13}C NMR (300 MHz, CD_3OD) 18.4 (CH_3), 127.4 144.6 (CH), 123.2 127.5 128.9, 129.4, 130.0, 130.7, 139.9, 148.9, 152.2 (^{Ar}C), 176.6 (COO).

7.6 REFERENCES

1. G. Knothe, *Journal of the American Oil Chemists Society*, 2000, **77**, 489-493.
2. P. R. Deacon, M. F. Mahon, K. C. Molloy and P. C. Waterfield, *Journal of the Chemical Society Dalton Transactions*, 1997, 3705-3712.
3. U. Schubert, S. Tewinkel and F. Moller, *Inorganic Chemistry*, 1995, **34**, 995-997.
4. M. Kol, M. Shamis, I. Goldberg, Z. Goldschmidt, S. Alfi and E. Hayut-Salant, *Inorganic Chemistry Communications*, 2001, **4**, 177-179.
5. T. Dabre and M. Machuqueiro, *Chemical Communications*, 2003, 1090-1091.
6. W. Clegg, I. R. Little and B. P. Straughton., *Dalton Transactions*, 1986, 1283-1288.
7. W. Clegg, I. R. Little and B. P. Straughan, *Inorganic Chemistry*, 1988, **27**, 1916-1923.

APPENDIX I

TABULATED CATALYSIS RESULTS

Catalyst	Temperature (ºC)	FFA (Wt%)	Water (Wt%)	Chapter	Yield of FAME
Blank	195	0	0	2	5.6
Ti(1,4 BD), **1**	195	0	0	2	6.4
Ti(2,3 BD), **2**	195	0	0	2	12
Ti(1,3 PD), **3**	195	0	0	2	76
$Ti(O^iPr)_4$	195	0	0	2	40
$Ti(O^iPr)_4$, THF	195	0	0	2	47
$Ti(O^iPr)_4$, THF	195	0	0.5	2	1.5
$Ti(O^iPr)_4$, 0.5x 1,3 PD, THF	195	0	0	2	49
$Ti(O^iPr)_4$, 0.5x 1,3 PD, THF	195	0	0.5	2	6.0
$Ti(O^iPr)_4$, 0.67x 1,3 PD, THF	195	0	0	2	58
$Ti(O^iPr)_4$, 0.67x 1,3 PD, THF	195	0	0.5	2	4.2
$Ti(O^iPr)_4$, 0.75x 1,3 PD, THF	195	0	0	2	84
$Ti(O^iPr)_4$, 0.75x 1,3 PD, THF	195	2	0	2	84
$Ti(O^iPr)_4$, 0.75x 1,3 PD, THF	195	3	0	2	75
$Ti(O^iPr)_4$, 0.75x 1,3 PD, THF	195	4	0	2	56
$Ti(O^iPr)_4$, 0.75x 1,3 PD, THF	195	10	0	2	54
$Ti(O^iPr)_4$, 0.75x 1,3 PD, THF	195	30	0	2	46
$Ti(O^iPr)_4$, 0.75x 1,3 PD, THF	195	5	0	2	42
$Ti(O^iPr)_4$, 0.75x 1,3 PD, THF	195	0	0.5	2	7.2
$Ti(O^iPr)_4$, 1.25x 1,3 PD, THF	195	0	0	2	74
$Ti(O^iPr)_4$, 1.25x 1,3 PD, THF	195	0	0.5	2	5.4
$Ti(O^iPr)_4$, 1.5x 1,3 PD, THF	195	0	0	2	64
$Ti(O^iPr)_4$, 1.5x 1,3 PD, THF	195	0	0.5	2	4.6
$Ti(O^iPr)_4$, 1x 1,3 PD, THF	195	0	0	2	76
$Ti(O^iPr)_4$, 1x 1,3 PD, THF	195	0	0.5	2	1.4

Catalyst	Temperature (ºC)	FFA (Wt%)	Water (Wt%)	Chapter	Yield of FAME
$Ti(O^iPr)_4$, 2x 1,3 PD, THF	195	0	0	2	55
$Ti(O^iPr)_4$, 2x 1,3 PD, THF	195	0	0.5	2	8.2
$Ti(O^iPr)_4$, 4x 1,3 PD, THF	195	0	0	2	59
$Ti(O^iPr)_4$, 4x 1,3 PD, THF	195	0	0.5	2	13
$Ti(O^iPr)_4$, 0.75x 1,3 PD, THF	175	0	0	2	64
$Ti(O^iPr)_4$, 0.75x 1,3 PD, THF	150	0	0	2	56
$Ti(O^iPr)_4$, 0.75x 1,3 PD, THF	100	0	0	2	4.3
$Ti(O^iPr)_4$, 0.75x 1,3 PD, THF	65	0	0	2	0.56
$Ti(O^iPr)_4$, 0.75x 1,3 PD, THF	25	0	0	2	0
Citric acid	195	0	0	3	3.2
Titanium Citrate Solution	195	0	0	3	32
Ti DMCA, **4**	195	0	0	3	21
Ti $DMCA_2$, **5**	195	0	0	3	1.4
DMCA	195	0	0	3	4.0
Titanium Sodium Citrate, **6**	195	0	0	3	2.2
Sodium Hydroxide	195	0	0	3	98
Titanium Nickel Citrate, **7**	195	0	0	3	5.7
Nickel Carbonate	195	0	0	3	2.1
Titanium Barium Citrate, **8**	195	0	0	3	4.2
Barium Acetate	195	0	0	3	44
Titanium Tin Citrate, **9**	195	0	0	3	51
Tin Chloride	195	0	0	3	53
Titanium Aluminium Citrate **10**	195	0	0	3	5.0
Aluminium Isopropoxide	195	0	0	3	6.6
Zinc Citrate, **11**	195	0	0	3	28
Zinc Acetate	195	0	0	3	55
Manganese Citrate, **12**	195	0	0	3	0.2
Manganese Carbonate	195	0	0	3	2.0
Calcium Citrate, **13**	195	0	0	3	0.3
Calcium Acetate	195	0	0	3	47

Catalyst	Temperature (ºC)	FFA (Wt%)	Water (Wt%)	Chapter	Yield of FAME
Titanium Alanine, **15**	195	0	0	4	39
Titanium Glycine, **14**	195	0	0	4	41
Titanium Proline, **16**	195	0	0	4	38
Titanium Tryptophan, **17**	195	0	0	4	46
Ti(L1)O^{i}Pr, **18**	195	0	0	4	73
Ti(L2)O^{i}Pr, **19**	195	0	0	4	75
Ge(L2)O^{i}Pr, **20**	195	0	0	4	72
Ti(L3)O^{i}Pr, **21**	195	0	0	4	12
Ge(L3)O^{i}Pr, **22**	195	0	0	4	14
Ge(O^{i}Pr)$_4$	195	0	0	4	71
Zinc Acetate	195	0	0	4	55
Acetic acid	195	0	0	4	2.2
Zinc Arginine, **23**	195	0	0	4	59
Arginine	195	0	0	4	56
Zinc Phenylalanine, **24**	195	0	0	4	59
Phenylalanine	195	0	0	4	10
Zinc Proline, **25**	195	0	0	4	69
Proline	195	0	0	4	51
Zinc Histidine, **26**	195	0	0	4	5.8
Histidine	195	0	0	4	2.3
Zinc β-alanine, **27**	195	0	0	4	8.5
β-alanine	195	0	0	4	4.5
Zinc Glutamine, **28**	195	0	0	4	65
Glutamine	195	0	0	4	35
Zinc Serine, **29**	195	0	0	4	28
Serine	195	0	0	4	5.2
Zinc Proline, **25**	195	0	0	4	69
Zinc Proline, **25**	195	0	0.25	4	93
Zinc Proline, **25**	195	0	0.5	4	96
Zinc Proline, **25**	195	0	1	4	95
Zinc Proline, **25**	195	0	2	4	93

Catalyst	Temperature (ºC)	FFA (Wt%)	Water (Wt%)	Chapter	Yield of FAME
Zinc Proline, **25**	195	0	5	4	88
Zinc Proline, **25**	195	2	0	4	93
Zinc Proline, **25**	195	3	0	4	90
Zinc Proline, **25**	195	4	0	4	91
Zinc Proline, **25**	195	5	0	4	87
Zinc Proline, **25**	195	10	0	4	81
Zinc Proline, **25**	195	30	0	4	84
Calcium Acetate	195	0	0	5	47
Manganese Acetate	195	0	0	5	58
Zinc Acetate	195	0	0	5	55
Zinc Propionate	195	0	0	5	51
Zinc Hexanoate	195	0	0	5	55
Zinc Stearate	195	0	0	5	71
Zinc Crotonate	195	0	0	5	78
$Zn_2(Cro)_4Quin_2$,	195	0	0	5	90
$Zn_3(Cro)_6Quin_2$,	195	0	0	5	91
Quinoline	195	0	0	5	29
‘$Zn_2(Cro)_4Quin_2$’ *insitu*	195	0	0	5	88
‘$Zn_3(Cro)_6Quin_2$’ *insitu*	195	0	0	5	89
‘$ZnCa(Cro)_4Quin_2$’ *insitu*	195	0	0	5	83
‘$ZnMn(Cro)_4Quin_2$’ *insitu*	195	0	0	5	43
$Zn(Cro)_2$	195	0	0	5	78
$Zn(Cro)_2$	175	0	0	5	67
$Zn(Cro)_2$	150	0	0	5	52
$Zn(Cro)_2$	125	0	0	5	44
$Zn(Cro)_2$	100	0	0	5	15
$Zn(Cro)_2$	65	0	0	5	0
$Zn_2(Cro)_4Quin_2$,	195	0	0	5	90
$Zn_2(Cro)_4Quin_2$	175	0	0	5	82
$Zn_2(Cro)_4Quin_2$	150	0	0	5	76

Catalyst	Temperature (ºC)	FFA (Wt%)	Water (Wt%)	Chapter	Yield of FAME
$Zn_2(Cro)_4Quin_2$	125	0	0	5	46
$Zn_2(Cro)_4Quin_2$	100	0	0	5	10
$Zn_2(Cro)_4Quin_2$	65	0	0	5	1
Zn Acetate, Quin	150	0	0	5	50
Zn Propionate, Quin	150	0	0	5	52
Zn Hexanoate, Quin	150	0	0	5	53
Zn Stearate, Quin	150	0	0	5	61
$Zn(Cro)_2$, Dioctadecylmethylamine	150	0	0	5	65
$Zn(Cro)_2$, Imidizole	150	0	0	5	53
$Zn(Cro)_2$, Isoquinoline	150	0	0	5	69
$Zn(Cro)_2$, Proton Sponge	150	0	0	5	57
Zn(Cro)2, Triethylamine	150	0	0	5	76
$Zn(Cro)_2$, 0.01x Quin	150	0	0	5	63
$Zn(Cro)_2$, 0.1x Quin	150	0	0	5	66
$Zn(Cro)_2$, 0.25x Quin	150	0	0	5	68
$Zn(Cro)_2$, 0.5x Quin	150	0	0	5	72
$Zn(Cro)_2$, 0.66x Quin	150	0	0	5	78
$Zn(Cro)_2$, 2x Quin	150	0	0	5	20
$Zn(Cro)_2$, 4x Quin	150	0	0	5	25
Zn Stearate	150	2	0	5	61
Zn Stearate	150	3	0	5	55
Zn Stearate	150	4	0	5	44
Zn Stearate	150	5	0	5	37
Zn Stearate	150	30	0	5	25
Zn Stearate	150	10	0	5	22
$Zn(Cro)_2$, Quin	150	0	0	5	76
$Zn(Cro)_2$, Quin	150	0	0.25	5	64
$Zn(Cro)_2$, Quin	150	0	0.50	5	44
$Zn(Cro)_2$, Quin	150	0	1	5	22
$Zn(Cro)_2$, Quin	150	0	2	5	4.4

Catalyst	Temperature (ºC)	FFA (Wt%)	Water (Wt%)	Chapter	Yield of FAME
$Zn(Cro)_2$, Quin	150	2	0	5	69
$Zn(Cro)_2$, Quin	150	3	0	5	59
$Zn(Cro)_2$, Quin	150	4	0	5	32
$Zn(Cro)_2$, Quin	150	5	0	5	5.1
$Zn(Cro)_2$, Quin	150	10	0	5	6.0
$Zn(Cro)_2$, Quin	150	30	0	5	7.4

Table A1 Catalytic results for the conversion of soybean oil to FAME using the various catalysts reported, on the laboratory scale over 2 hours, with a methanol to soybean oil ratio of 12:1 and a catalyst loading of 2.5 mol%

Catalyst	Temp. (ºC)	Time (min)	% TG	% DG	% MG	% FAME
Blank	200	120	57.1	24.1	4.5	17.6
Zinc Acetate	200	120	21.2	19	12	47.8
Zinc Citrate, **11**	200	120	55.3	23.2	3.4	14.7
Zinc Phenylalanine, **24**	200	120	22.6	19.1	10	41.1
Zinc Proline, **25**	200	120	2.6	6.6	12.8	83.3
$Zn(Cro)_2$ in RSO	150	0	100	0	0	0
$Zn(Cro)_2$ in RSO	150	10	79.6	14.8	5.7	0
$Zn(Cro)_2$ in RSO	150	15	73.7	17.3	1.5	7.5
$Zn(Cro)_2$ in RSO	150	30	61.8	23.1	3.3	11.8
$Zn(Cro)_2$ in RSO	150	45	58.0	24.8	3.1	14.1
$Zn(Cro)_2$ in RSO	150	60	53.2	25.7	3.6	17.4
$Zn(Cro)_2$ in RSO	150	120	37.5	25.5	6.4	30.6
$Zn(Cro)_2$ in RSO	150	240	30.1	23.9	7.8	38.1
$Zn(Cro)_2$, Quin, in RSO	150	0	100	0	0	0
$Zn(Cro)_2$, Quin, in RSO	150	10	79.9	16.2	3.9	0
$Zn(Cro)_2$, Quin, in RSO	150	15	76.9	17.4	5.8	0
$Zn(Cro)_2$, Quin, in RSO	150	30	71.5	21.1	1.3	6.1

Catalyst	Temp. (ºC)	Time (min)	% TG	% DG	% MG	% FAME
$Zn(Cro)_2$, Quin, in RSO	150	45	60.7	24.2	1.4	13.7
$Zn(Cro)_2$, Quin, in RSO	150	60	57.9	24.3	3.0	14.8
$Zn(Cro)_2$, Quin, in RSO	150	120	42.7	25.4	5.6	26.3
$Zn(Cro)_2$, Quin, in RSO	150	240	26.9	22.6	9.3	41.2
$Zn(Cro)_2$, Quin, MeOH	150	0	100	0	0	0
$Zn(Cro)_2$, Quin, MeOH	150	10	68.5	19.0	2.9	9.6
$Zn(Cro)_2$, Quin, MeOH	150	15	63.1	21.3	2.8	12.9
$Zn(Cro)_2$, Quin, MeOH	150	30	53.6	23.8	4.0	18.6
$Zn(Cro)_2$, Quin, MeOH	150	45	46.4	24.7	5.6	23.2
$Zn(Cro)_2$, Quin, MeOH	150	60	39.8	24.7	6.8	28.7
$Zn(Cro)_2$, Quin, MeOH	150	120	24.2	18.8	7.4	42.1
$Zn(Cro)_2$, Quin, MeOH	150	240	26.2	22.4	9.3	49.7
Blank	150	0	100	0	0	0
Blank	150	10	91.3	6.5	2.2	0
Blank	150	15	90.	7.5	2.4	0
Blank	150	30	86.1	10.4	3.5	0
Blank	150	45	84.1	11.8	4.1	0
Blank	150	60	81.6	13.2	5.2	0
Blank	150	120	73.3	18.4	2.0	6.3
Blank	150	240	61.8	21.2	3.1	13.9
$Zn(Cro)_2$, NEt_3, in RSO	150	0	100	0	0	0
$Zn(Cro)_2$, NEt_3, in RSO	150	10	84.4	7.2	8.4	0
$Zn(Cro)_2$, NEt_3, in RSO	150	15	80.8	13.7	5.5	0
$Zn(Cro)_2$, NEt_3, in RSO	150	30	72.7	18.0	1.7	7.5
$Zn(Cro)_2$, NEt_3, in RSO	150	45	65.7	24.6	3.3	6.4
$Zn(Cro)_2$, NEt_3, in RSO	150	60	60.8	23.6	3.4	12.1
$Zn(Cro)_2$, NEt_3, in RSO	150	120	44.7	28.1	5.3	22
$Zn(Cro)_2$, NEt_3, in RSO	150	240	25.5	22.8	8.7	42.9
$Zn(Cro)_2$	200	0	100	0	0	0
$Zn(Cro)_2$	200	10	29.6	20.6	8.3	41.4
$Zn(Cro)_2$	200	15	27.3	20.9	8.8	42.9

Catalyst	Temp. (ºC)	Time (min)	% TG	% DG	% MG	% FAME
$Zn(Cro)_2$	200	30	25.1	20.9	9.0	44.9
$Zn(Cro)_2$	200	45	23.5	20.2	9.4	46.9
$Zn(Cro)_2$	200	60	20.7	19.3	9.5	50.4
$Zn(Cro)_2$	200	120	15.3	17.0	10.2	57.4
$Zn(Cro)_2$	200	240	9.1	13.0	10.1	67.7
$Zn(Cro)_2$, 0.1x Quin, MeOH	200	0	100	0	0	0
$Zn(Cro)_2$, 0.1x Quin, MeOH	200	10	81.8	14.9	3.2	0
$Zn(Cro)_2$, 0.1x Quin, MeOH	200	15	75.4	18.3	6.2	0
$Zn(Cro)_2$, 0.1x Quin, MeOH	200	30	56.4	23.1	3.6	16.7
$Zn(Cro)_2$, 0.1x Quin, MeOH	200	45	44.0	25.0	5.8	25.1
$Zn(Cro)_2$, 0.1x Quin, MeOH	200	60	33.8	24.4	7.9	33.7
$Zn(Cro)_2$, 0.1x Quin, MeOH	200	120	14.5	16.8	11.3	57.2
$Zn(Cro)_2$, 0.1x Quin, MeOH	200	240	4.4	8.6	10.5	76.3
$Zn(Cro)_2$, 0.5x Quin, MeOH	200	0	100	0	0	0
$Zn(Cro)_2$, 0.5x Quin, MeOH	200	10	85.9	10.1	4.0	0
$Zn(Cro)_2$, 0.5x Quin, MeOH	200	15	80.7	13.6	5.7	0
$Zn(Cro)_2$, 0.5x Quin, MeOH	200	30	66. 7	20.1	2.4	10.8
$Zn(Cro)_2$, 0.5x Quin, MeOH	200	45	54.9	24.0	4.1	16.9
$Zn(Cro)_2$, 0.5x Quin, MeOH	200	60	45.7	25.3	6.2	22.8
$Zn(Cro)_2$, 0.5x Quin, MeOH	200	120	20.1	20.7	10.9	48.3
$Zn(Cro)_2$, 0.5x Quin, MeOH	200	240	5.2	9.9	11.5	73.4
$Zn(Cro)_2$, Quin, MeOH	200	0	100.0	0.0	0.0	0
$Zn(Cro)_2$, Quin, MeOH	200	10	82.0	8.4	2.1	7.5
$Zn(Cro)_2$, Quin, MeOH	200	15	79.8	10.5	3.2	6.4
$Zn(Cro)_2$, Quin, MeOH	200	30	73.1	17.7	1.9	7.3
$Zn(Cro)_2$, Quin, MeOH	200	45	63.0	22.0	2.9	12.1
$Zn(Cro)_2$, Quin, MeOH	200	60	52.1	25.4	4.5	17.9
$Zn(Cro)_2$, Quin, MeOH	200	120	23.5	22.5	10.3	43.7
$Zn(Cro)_2$, Quin, MeOH	200	240	5.1	9.7	11.9	73.4
$Zn(Cro)_2$, 4x Quin, MeOH	200	0	100.0	0.0	0.0	0
$Zn(Cro)_2$, 4x Quin, MeOH	200	10	81.6	10.6	7.8	0

Catalyst	Temp. (ºC)	Time (min)	% TG	% DG	% MG	% FAME
$Zn(Cro)_2$, 4x Quin, MeOH	200	15	81.4	13.5	5.2	0
$Zn(Cro)_2$, 4x Quin, MeOH	200	30	67.5	21.5	11.0	0
$Zn(Cro)_2$, 4x Quin, MeOH	200	45	52.9	24.9	4.2	18.1
$Zn(Cro)_2$, 4x Quin, MeOH	200	60	41.5	26.1	5.8	26.6
$Zn(Cro)_2$, 4x Quin, MeOH	200	120	18.4	19.9	10.6	51.2
$Zn(Cro)_2$, 4x Quin, MeOH	200	240	5.3	9.8	11.5	73.4

Table A2 Catalytic results for the conversion of rapeseed oil to FAME using the various catalysts reported on the model pilot scale, with a methanol to oil ratio of 6:1 and a catalyst loading of 1 mol%